ANALYSIS OF GRID BEAM BRIDGES
BY
ANISOTROPIC PLATE THEORY

A THESIS
Submitted in partial fulfilment of the
requirements for the degree of
MASTER OF ENGINEERING
IN
STRUCTRURAL ENGINEERING INCLUDING
CONCRETE TECHNOLOGY

by
GYAN CHANDRA NAYAK

DEPARTMENT OF CIVIL ENGINEERING
UNIVERSITY OF ROORKEE
ROORKEE
May, 1964

CERTIFICATE

CERTIFIED that the dissertation entitled ANALYSIS OF GRID BEAM BRIDGES BY ANISOTROPIC PLATE THEORY which is being submitted by Sri G.C.Nayak in partial fulfilment for the award of the Degree of Master of Engineering in Structural Engineering including Concrete Technology of University of Roorkee is a record of student's own work carried out by him under my supervision and guidance. The matter embodied in this dissertation has not been submitted for the award of any other Degree or Diploma.

This is further to certify that he has worked for a period of 12 months from June '62 to May '64 for preparing dissertation for Master of Engineering Degree at the University.

(O.P. JAIN)
Professor and Head of Structural Engineering Section.
University of Roorkee, Roorkee.

Dated May 31, 1964.

ACKNOWLEDGEMENT

The author wishes to acknowledge his deep sense of gratitude to Dr. O.P.Jain, Professor and Head of Structural Engineering Section for planning and guiding the work.

The author also gratefully acknowledges the kind help rendered by Dr. A.S.Arya, Reader in Civil Engineering and Sri M.D.Kanchi, Reader in Civil Engineering from time to time.

Sincere thanks are due to the staff of Concrete Laboratory and Model Fabrication Workshop for their assistance.

CONTENTS

PART II

EXPERIMENTAL WORK

SYNOPSIS

An attempt is made here to present the load distribution analysis based on the Anisotropic Plate Theory as applied to modern grid beam bridges, with special reference to edge stiffened and continuous bridges.

As a basis for the subsequent work the basic analytic theory as applied to simply supported grid beam bridges has been briefly indicated. Analytical approach as extended to edge stiffened and continuous bridges has been presented. Approximate methods for continuous bridges based on Equivalent Stiffness and assumed deflected shapes have been developed. At all places the results have been compared with those obtained by other standard load distribution theories.

The analytical results have also been supplemented by suitable model tests.

The model test results have been found to agree fairly well with the approximate solutions presented for the edge stiffened and continuous bridges. It is felt that these approximate solutions can be safely used for design purposes, while at the same time making the analysis within easy reachof the Design Engineers.

CHAPTER 1

INTRODUCTION.

The magnitude of concentrated loads of road vehicles increased continuously and considering these loading changes, it is necessary to consider how these changes affect the approach to the analysis and design problems. These days in many countries the heaviest vehicles are permitted only on separate or on particular lane and attempts are made by structural designers to distribute these heavy loads in a bridge with several girders to all the girders in order to achieve an economical structure.

Rigid transverse framing of girders helps in the distribution of loads placed at this framed system, called a grid and thus a grid beam bridge is invariably adopted. In general a grid beam bridge consists of several parallel longitudinal beams, connected, if necessary, from place to place by cross beams and in addition, solidarised by the roadway generally made of reinforced concrete slab.

The longitudinal and transverse systems may have negligible torsional resistance or they may exert considerable torsional resistance. The beams are ordinarily equidistant but not always identical. Often it happens that the edge beams are stronger than the others. Besides, the beams can be prismatic or of variable moment of inertia. As regards to their mode of support, the most frequent case is that of a simple support at the two ends but the cases of cantilever and continuous beams on several supports are also found. Some-times the supporting abutments are inclined to the perpendicular at the longitudinal beams and the longitudinal and cross beams are not at right angles. This gives rise to the problem of skew.

The importance of these usually statically indeterminate systems of high degree, can be recognised by the fact that between the first ideas of ENGESSER (1880) on the subject and the present day, an extensive amount of literature has been published, out of which only a few important works are listed at the end. However, in many of these methods the amount of calculation is so much, that a structural designer hesitates to use them. For this reason the structures which can be easily analysed, though not always economical, are often used.

It is hardly necessary to say that the best method has nothing more than the merit of simplicity. The simple methods are usually very optimistic but very dangerous and errors committed can be considerable. As such it has been all the time felt that a method of analysis which is simple in use for design and analysis and considers the actual behaviour of the structure to the close, should be evolved.

1.1 BASIS AND SCOPE OF VARIOUS THEORIES.

Basis of various methods of elastic analysis of grid beam bridges can be conveniently studied according to assumptions made as regards to its construction. So far mainly four types of equivalent constructions have been considered by the various research workers of this field for the analysis of this problem. These are-

(i) Open grid work method,
(ii) Central diaphram method,
(iii) Continuous slab method, and
(iv) Plate Theory.

(i) Open Grid Work Method.

In this method the bridge structure is divided into individual longitudinal and transverse members each possessing appropriate flexural and torsional stiffness. The problem is then solved either by flexibility method or by stiffness method. Using flexibility method for each point of intersection of the members, equations of deflection and slope compatibility are written in terms of unknown forces and moments and finally a set of governing simultaneous equations are solved to obtain the forces and moments directly. LAZARIDES[1] (1952) has adopted a method of this type using flexibility coefficients. He has further made use of symmetry and antisymmetry of loading and deformations and clearly shows the typical nature of compatibility equations for bridge grillages.

If the torsion of members is not considered, there are in general, as many equations as there are beam intersections; if torsion is considered, the equations are three times of the equations for without torsion. By using symmetry and antisymmetry of loading and deformations the number of simultaneous equations is reduced to less than half in many cases.

Using the stiffness method, the " slope deflection gyration" equations for all the members are written; equilibrium equations are then set up in terms of deformations and slopes and finally solved. LIGHTFOOT AND SAWKO[2] (1960), MARTIN AND HERNADEZ[3] (1960) have adopted this method of analysis and with the help of electronic digital computers, they have solved the problems of grid works eliminating a large amount of arithmetic work. JANSSONIUS[4] (1948) has developed a relaxation approach for solving these equations. EWELL, OKUBO AND ABRAM[5] (1952) employ an auxiliary force system for controlling vertical displacements of the joints and use a moment and torque distribution process for transmission of the displacement effects. They also show that a horizontal gridwork of beams intersecting at right angles to one another yields a deflected surface similar to that of a slab when analysed under normal loads, and thus a transformation of the slab into comparable gridwork is possible. BEER AND RESINGER[6] (1954) have also adopted moment torque distribution process for the solution of gridworks.

RAY[11] (1960) has divided the analysis of grid floors into two stages. Firstly, the joint displacements are worked out by considering the floor as an anisotropic plate; the formulae for which are very simple to apply. In the second stage moment torque distribution is applied to find out (1) moments and torques in each member on consideration of no joint displacement and (2) the sway each joint amounting to values obtained as for an equivalent anisotropic plate. A comparison of results obtained by treating the floor as a pure plate and by considering it partly as a plate and partly as an open grid work, show interesting accord; the difference in the average bending moment and twisting moment at different joints being very insignificant.

The open gridwork solutions though appear to be very elegant but involve a large number of variables to start with and are extremely cumbersome. Further this method can not be generalised especially for the moving load problems. Hence, it is difficult to produce a simple design procedure for the solution of grid beam bridges, based on this approach.

(3) <u>Central Diaphram Method.</u>

This method assumes that the entire transverse system whether continuous in the form of slab, or consisting of distinct cross beams can be replaced by a single equivalent member at mid-span. The problem is then solved as an open gridwork, the solutions of which are easier and the distribution factors can be easily derived. LEONHARDT[8] (1938) replaces the transverse medium by a single member at mid span with zero torsional rigidity. With the further development of this method LEONHARDT AND ANDRA[9] (1950) have presented this method in a comprehensive manner in their book "The calculation of grillage beams".

ENGESSER (1889) replaces the transverse medium by an infinitely rigid central diaphram; thus the transverse diaphram always remains straight and the distribution factors can be obtained in the form of simple algebraic expressions of number of longitudinal beams and their spacing.

MALTER[10] (1958) replaces the transverse medium by three concentrated diaphrams, one at the centre and one each at the ends. He takes the stiffness of central diaphram as half of the total transverse medium and solves the two and four girder cases with girders having infinite torsional rigidity, using numerical solutions.

From this approach it is obvious that the location of the cross beam is most effective at the mid-span for distributing the loads to different girders. The greatest defect of this method is as regards to its basic assumptions. Most of these assumptions are invalid in practical bridge structures where the torsional stiffness of diaphram, particularly in reinforced and prestressed concrete bridges, may be considerable. Extensions of this method for edge stiffening girder case and other support conditions like cantilever and continuous beams on several supports are possible, through extensions for skew systems may present some difficulty.

(3) Continuous Slab Method.

In this method the transverse system is replaced by uniformly spread equivalent slab, which may or may not cover the full length of the span. PIPPARD AND deWAELE[11] (1938) have used this idea replacing the actual transverse system by a continuous transverse medium of equal stiffness, extending over the entire length. They further assume that the floor system prevents the girders from twisting and calculate the shearing forces per unit length of the girder in terms of the deflection of the girder; formulate certain differential equations which on solution give the deflections, bending moments and shearing forces at any section of the girder due to a given position of load. In the derivation, use of symmetry and antisymmetry of loads and deformations is made and cases of three and four girder are solved. HETENYI[12] (1938) assumes the grid deflections in such a manner that there is no rotation of individual members at their intersections with other members and with this assumption he obtains a solution by using sine series to represent load and deflection of the structure in the direction of the longitudinals. This approach is commonly known as 'Harmonic Analysis'.

PIPPARD'S approach is tedious and cumbersome and superposition in case of number of loads is tough in calculation. The assumptions require longitudinals of infinite torsional rigidity and these should be prevented from rigid body rotations at their ends. Moreover the approach is no more general. HETENYI's work is valuable for his harmonic analysis approach but again the defect is as regards to its basic assumption.

HENDRY & JAEGER[13] (1958) have used this method in most general form replacing transverse members by a uniform continuous medium of equivalent stiffness. Their approach is to write down differential equation for the loading on each longitudinal member including, where necessary, the effects of rotation and twisting; harmonic analysis is then used to derive the amplitudes of deflection and bending moment for each longitudinal member. Thus, distribution coefficients applicable to many practical cases are deduced; the coefficients have been derived for bridges with various number of girders. This particular approach is a considerable advance on the previous methods in this category and can be applied to various types of boundary condition generally met in bridge design.

HENDRY AND JAEGER's approach does not consider suitably the torsional stiffness of the transverse system and for each bridge having some definite number of girders a set of distribution coefficient curves are required. But using this approach the edge stiffening effects can be easily considered for the general case including the torsional stiffness.

(4) Plate Theory.

The last method covers those approaches which are based on anisotropic plate theory. In this analysis the actual bridge structure is replaced by an equivalent anisotropic plate which is then treated according to classical theory of plate. GUYON[14] (1946) is the first to develop this approach for grillages with members of negligible torsional stiffness and subsequently he has given a similar analysis for isotropic slabs[15] (1949). This approach is then generalised by MASSONNET[16] (1950) to include the effects of torsion. Extensions and developments of GUYON's and MASSONNET's work have been produced by many others. These generalise the use of this method and thus a simple design procedure has been formulated. The development of this method is discussed in Section 1.2 as it has been taken as a basic theme of this dissertation work.

Plate theory approach has the merit that a single set of distribution coefficients for the two extreme cases of no torsion grillage and a full torsion slab enable the distribution behaviour of any type of bridge structure to be found. Further the implications of the analysis can be easily seen by the designer and hence calculations do not merely become a set of mathematical formulae with no apparent physical meaning.

Further it is also important that the results obtained by this approach and the harmonic analysis approach or any other suitable method will be virtually identical provided that the assumptions are approximately valid for the structure considered. This has been clearly shown in the work of BALOG[17] (1957) and GUPTA[18] (1962); they have solved a simply supported bridge problem by various methods and have given this comparison. However, it is felt that the design procedure derived by plate theory is more easily applicable than by any other approaches.

After considering the methods based on elastic theory it should be pointed out that the plastic theory approach is also made for the analysis of grid beam bridges. HEYMAN[19] (1953) has given the plastic analysis of steel grillages. REYNOLDS[20] (1957) has given the ultimate load of prestressed concrete grillage bridges. GRANHOLM and ROWE[21] have considered the ultimate load problem of skew slab bridges.

There are at present very few works available on ultimate load analysis and this analysis is of little use as distribution properties of a bridge beyond elastic range are still unknown. Hence, there is lot of difficulty in developing a proper design procedure and suitable load factors. Although it is not possible at this stage to design a bridge structure on the ultimate load theory but it is useful to assess ultimate load for the following reasons:-

(i) to give true safety of bridge under known loads.

(ii) to enable safe designs to be prepared for bridges where no rigorous and easily applied design procedure is available e.g. skew bridges.

(iii) to eliminate overdesign due to conservative assumptions and,

(iv) toimprove the economy of the bridge design through proper appreciation of the behaviour of bridge under load.

1.2 DEVELOPMENT AND SCOPE OF ANISOTROPIC PLATE THEORY.

GUYON[14] (1946) is the first to conceive the idea of replacing a bridge structure by an anisotropic plate and has solved a case of simply supported grillage beams with negligible torsion. He has given the solution in terms of Fourier series and with the same analytical approach he has given another solution for an isotropic plate[15] (1949). MASSONNET[16] (1950) examined the possibilities of extending GUYON's work and thus has succeeded in giving the general approach by considering the problem with torsion. He has also given the interpolation formulae for the distribution coefficients for any particular value of torsional parameter. Due to the chaos and troubles of the post-war period, these works did not find the consideration due to them.

It must be taken as a contribution of MORICE and LITTLE[22] (1954) that they adopted the method of GUYON and MASSONNET. A considerable amount of work has been done at the Research Station of the Cement and Concrete Association of England by MORICE, LITTLE and ROWE[23 to 36]. The works have thus confirmed the applicability of the method to a wide range of bridge types and have indicated a high degree of accuracy. In original papers of GUYON and MASSONNET[14,15,16] a limited number of values for distribution coefficients are derived. However, in a later publication MASSONNET[37] (1954) has presented some comprehensive tables giving the values of the distribution coefficients for wide ranges. Thus, this is the first phase of development, from which the development of solutions, statements on assumptions and susceptibility to errors etc. can be obtained. Work of HOFFMAN and VLUGT[38] (1956) shows the applicability of this theory to analysis and design.

SATTLER[39] (1955) has presented the work of GUYON and MASSONNET in a comprehensive manner with graphs and shows the extension of this method for statically indeterminate systems. He also shows that there is a good agreement in analytical and test results of models of many girder, multispan balanced cantilever bridge and simply supported bridge. ROWE[23] (1955) considers the effect of Poisson's ratio on the load distribution. MASSONNET[40] (1958) introduces a new coefficient for calculation of the torsional moments and suggests an interpolation formula for this coefficient for any value of torsional parameter. He also extends this theory to edge stiffened bridge without considering any torsional stiffness. The calculations for edge stiffened girder bridges is also dealt by LITTLE and ROWE[24] (1957). In this work they have plotted the curves for different distribution coefficients due to edge moments acting on an anisotropic plate and have given the theoretical solution to the problem. ROWE[25,26] (1957) has further given the load distribution theory for no torsion bridges with various support conditions using Basic functions. SATTLER[41] (1959) points out that interpolation formula for coefficient of transverse distribution given by MASSONNET[16] is not valid and recommends two different interpolation formulae of distribution coefficients for different values of flexural parameter in two ranges. He further suggests an approximate method of calculation of bridges with edge stiffened beams by using combination of symmetry and antisymmetry components of distribution coefficients.

Taking as a point of departure in this theory NARUOKA AND OMURA[42,43] (1959) have given the classical

PART I.

ANALYSIS OF GRID BEAM BRIDGES BY ANISOTROPIC PLATE THEORY.

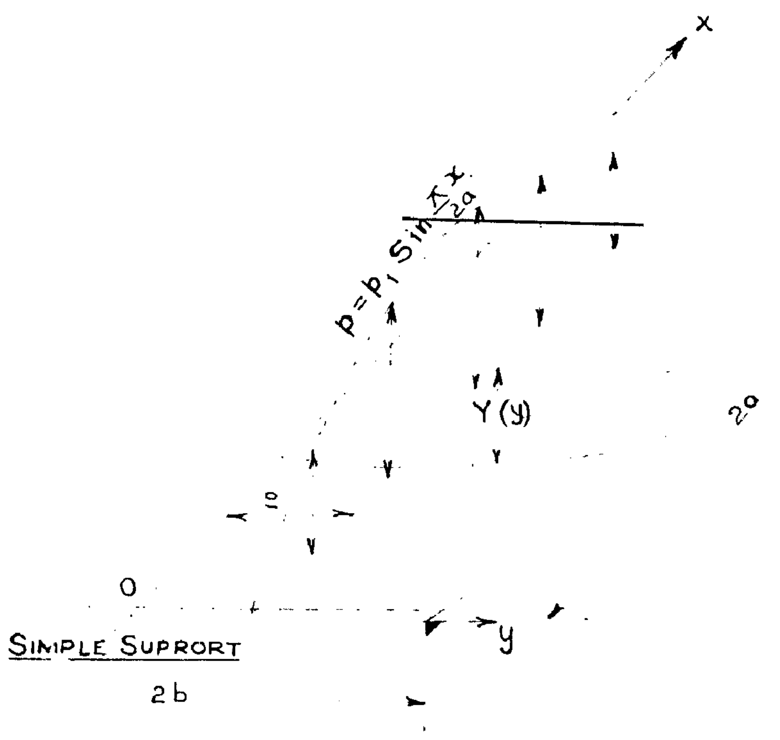

$\omega(x, y) = Y(y) \sin \frac{\pi x}{2a}$

FIG. 2·1

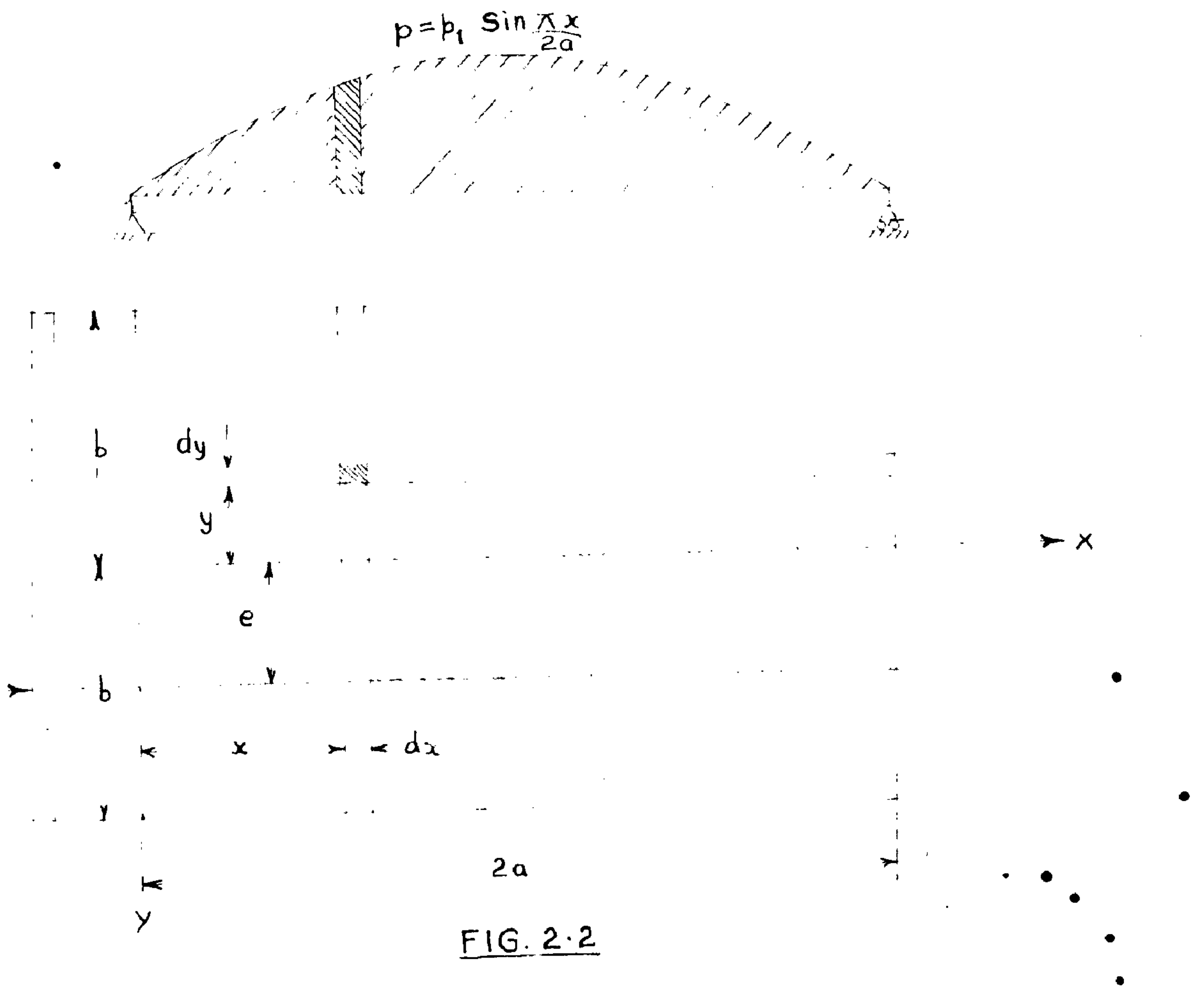

FIG. 2·2

CHAPTER 2.

ANALYSIS OF GRID BEAM BRIDGES BY ANISOTROPIC PLATE THEORY.

Ordinary flexibility and stiffness methods of analysis of the system called "open grillage" become more complicated if the number of beams is more. Additionally these methods become more and more difficult when torsional rigidity of the elements is considered. Further in the analysis of the bridge, a bridge is never an open grillage, because there is always a rolling slab. Therefore, it is better to abandon the concept of a construction of a bridge as discontinuous one and to consider it as a practically equivalent continuous structure which will obey the laws of differential calculus. In section 2.1 the basic expressions derived from the theory of anisotropic plate are given.

2.1 BASIC EXPRESSIONS OF THE ANISOTROPIC PLATE THEORY

2.1.1 Grid Beam Bridge without Torsional Rigidity.

(a) General equation of deformation due to sinusoidal load.

Replace a real bridge by continuous grillage formed by an infinite number of longitudinal and cross beams both not possessing any torsional rigidity (Fig.2.1).

Let,

ρ_P = flexural rigidity of longitudinal beams per unit width.

and ρ_E = flexural rigidity of cross beams per unit width.

The bridge is simply supported at its two edge parallel to y axis and its other two edges are free.

When the bridge is subjected to a sinusoidal load $p = p_1 \sin \pi \frac{x}{2a}$ (see fig.2.1), all the longitudinal beams will undergo a sinusoidal deformation and the deflection at any point (x,y) can be written as

$$w(x,y) = Y(y) \sin \frac{\pi x}{2a} \qquad \ldots\ldots (2.1)$$

where, Y(y) is the transverse deformation satisfying all conditions of equilibrium of longitudinal and cross beams. This transverse deformation Y(y) can be derived from the theory of beams on elastic foundation[46] where-as GUYON[14] determines the function Y(y) by Fourier Series.

Let q be the intensity of interacting forces at point (x,y) exerted by cross beams on longitudinal beam and vice-versa. Consider elementary longitudinal beam of width dy and flexural rigidity $EI = \rho_P\, dy$ (Fig.2.2) and elementary cross beam of width dx and flexural rigidity $EI = \rho_E\, dx$ and calculate intensity q by elementary theory of bending. Thus,

$$q\,dy = \rho_P \frac{\partial^4 w}{\partial x^4}\, dy \quad \text{and} \quad -q\,dx = \rho_E \frac{\partial^4 w}{\partial^4 y}\, dx \qquad \ldots\ldots (2.2)$$

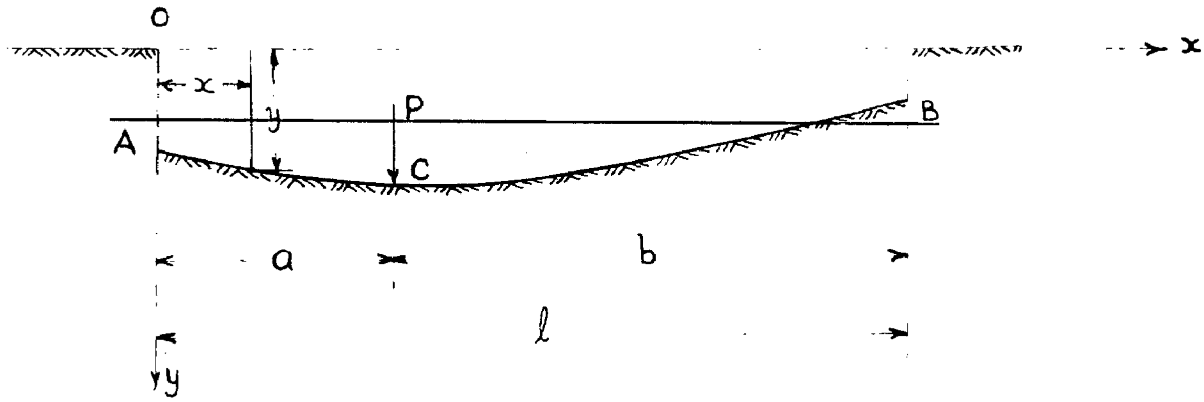

FIG. 2·3

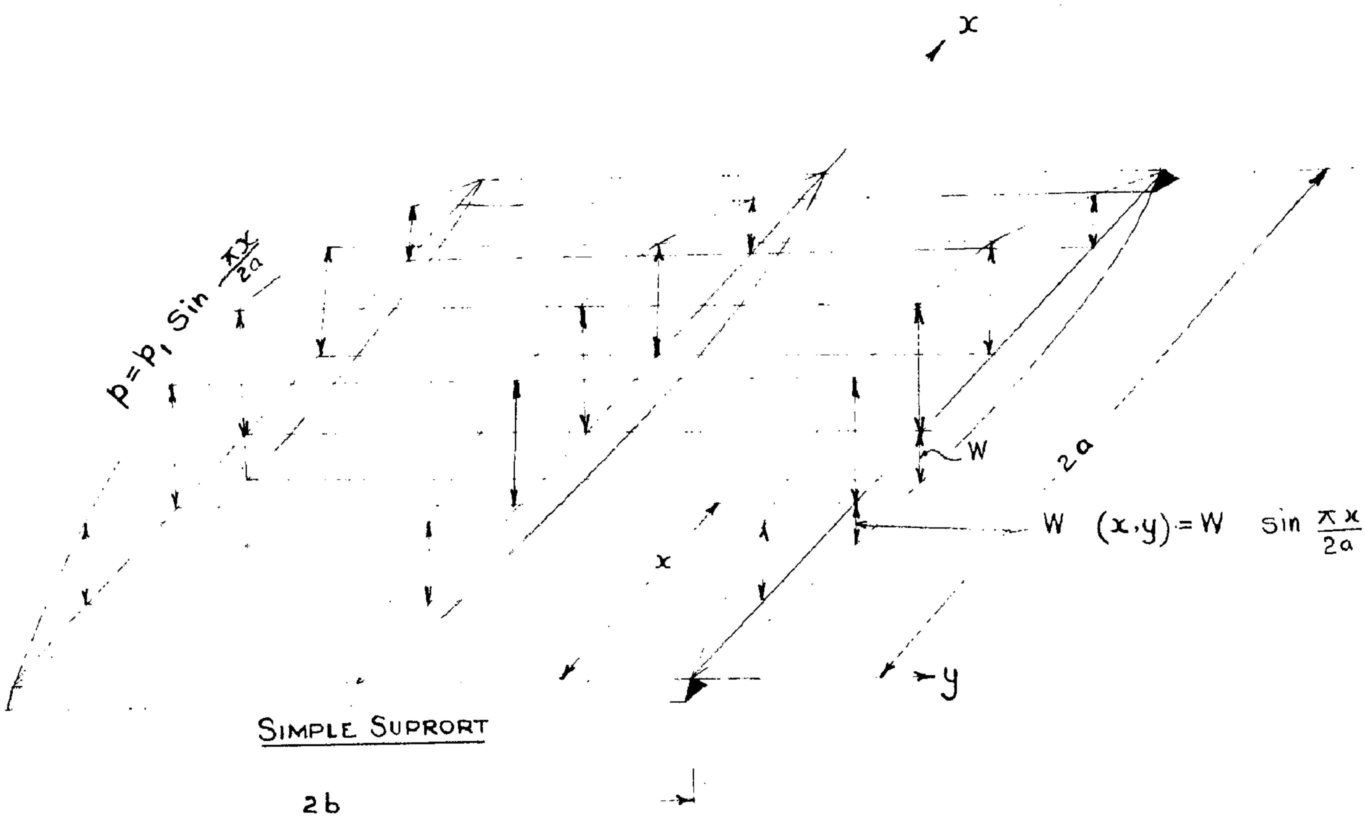

FIG. 2·5

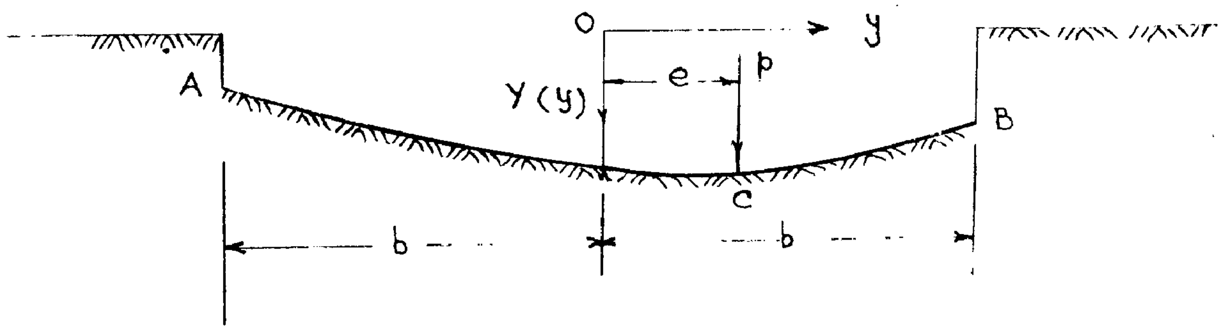

FIG. 2.4

Equating the values of ϕ from eqs. (2.2) we obtain the differential equation of no-torsion anisotropic plate in the unloaded portion as

$$\rho_P \frac{\partial^4 w}{\partial x^4} + \rho_E \frac{\partial^4 w}{\partial y^4} = 0 \qquad \text{... (2.3)}$$

Equation (2.3) admits solution (2.1) and Y(y) must satisfy the differential equation

$$\frac{d^4 Y}{dy^4} + \frac{\rho_P}{\rho_E} \frac{\pi^4}{16 a^4} Y = 0 \qquad \text{... (2.4)}$$

Equation (2.4) is similar to that of a prismatic beam of width B, resting on an elastic foundation (Fig.2.3) whose modulus of foundation is K

$$\frac{d^4 y}{dx^4} + \frac{BK}{EI} y = 0 \qquad \text{... (2.5)}$$

The deformation of the finite beam shown in Fig.2.3 is derived in the book, "Beams of Elastic Foundation" by HETENYI (46) p.p. 54-56. The following formulae for the deflection and bending moment curves are for the portion AC of the beam, where $x < a$. The same formulae can be used for the portion BC where $x < b$, by measuring x from end B and replacing a by b and b by a.

$$y = \frac{P\lambda}{KB} \frac{1}{\sinh^2 \lambda L - \sin^2 \lambda L} \Big\{ 2 \cosh \lambda x \cos \lambda x \, (\sinh \lambda l \cos \lambda a \cosh \lambda b$$

$$- \sin \lambda l \cosh \lambda a \cos \lambda b) + (\cosh \lambda x \sin \lambda x + \sinh \lambda x \cos \lambda x)$$

$$\Big[\sinh \lambda l \, (\sin \lambda a \cosh \lambda b - \cos \lambda a \sinh \lambda b) + \sin \lambda l \, (\sinh \lambda a \cos \lambda b - \cosh \lambda a \sin \lambda b) \Big] \Big\} \qquad \text{....(2.6)}$$

$$M = \frac{P}{2\lambda} \frac{1}{\sinh^2 \lambda l - \sin^2 \lambda l} \Big\{ 2 \sinh \lambda x \sin \lambda x \, (\sinh \lambda l \cos \lambda a \cosh \lambda b - \sin \lambda l \cosh \lambda a$$

$$\cos \lambda b) + (\cosh \lambda x \sin \lambda x - \sinh \lambda x \cos \lambda x) \Big[\sinh \lambda l \, (\sin \lambda a \cosh \lambda b - \cos \lambda a \sinh \lambda b) +$$

$$\sin \lambda l \, (\sinh \lambda a \cos \lambda b - \cosh \lambda a \sin \lambda b) \Big] \Big\} \qquad \text{....(2.7)}$$

where

$$\lambda = \sqrt[4]{\frac{BK}{4EI}}$$

Comparing equations (2.4) and (2.5)

$$\lambda = \frac{\pi}{2\sqrt{2}\,a} \sqrt[4]{\frac{\rho_P}{\rho_E}} \qquad \text{....(2.8)}$$

The elementary cross beam is identical to that of the prismatic beam of width $B = dx$, $EI = \rho_E \, dx$ and loaded with a concentrated load $p = p_1 \sin \frac{x}{2a} \, dx$ and placed on an elastic foundation of modulus $K = \rho_P \frac{\pi^4}{16a^4}$. Transforming equations (2.6) and (2.7), for the case shown in Fig. (2.4) in which span $l = 2b$ and the origin is at midpoint O; making suitable substitutions of above comparison and introducing $\phi = \lambda b$, the general equation of deformation $w(x,y)$ and transverse bending moment M_y for the portion, where $y<e$ is obtained. The same formula can be used for the portion where $y>e$, by replacing b by $-b$. Thus,

$$w(x,y) = \frac{p_1 \sin\frac{\pi x}{2a}}{2b} \cdot \frac{16a^4}{\rho_p \pi^4} \cdot \frac{2\phi}{\sinh^2 2\phi - \sin^2 2\phi} \Big\{ 2\cosh\phi\left(1+\tfrac{y}{b}\right)\cos\phi\left(1+\tfrac{y}{b}\right) \left(\sinh 2\phi \cos\phi\left(1+\tfrac{e}{b}\right)\cosh\phi\left(1-\tfrac{e}{b}\right) - \sin 2\phi \cosh\phi\left(1+\tfrac{e}{b}\right)\cos\phi\left(1-\tfrac{e}{b}\right)\right)$$
$$+ \left(\cosh\phi\left(1+\tfrac{y}{b}\right)\sin\phi\left(1+\tfrac{y}{b}\right) + \sinh\phi\left(1+\tfrac{y}{b}\right)\cos\phi\left(1+\tfrac{y}{b}\right)\right)\Big[\sinh 2\phi \left(\sin\phi\left(1+\tfrac{e}{b}\right)\cosh\phi\left(1-\tfrac{e}{b}\right) - \cos\phi\left(1+\tfrac{e}{b}\right)\sinh\phi\left(1-\tfrac{e}{b}\right)\right) +$$
$$\sin 2\phi\left(\sinh\phi\left(1+\tfrac{e}{b}\right)\cos\phi\left(1-\tfrac{e}{b}\right) - \cosh\phi\left(1+\tfrac{e}{b}\right)\sin\phi\left(1-\tfrac{e}{b}\right)\right)\Big]\Big\} \qquad \text{....(2.9)}$$

$$M_y = p_1 b \sin\frac{\pi x}{2a} \cdot \frac{1}{2\phi\left(\sinh^2 2\phi - \sin^2 2\phi\right)} \Big\{ 2\sinh\phi\left(1+\tfrac{y}{b}\right)\sin\phi\left(1+\tfrac{y}{b}\right) \left(\sinh 2\phi \cos\phi\left(1+\tfrac{e}{b}\right)\cosh\phi\left(1-\tfrac{e}{b}\right) - \sin 2\phi \cosh\phi\left(1+\tfrac{e}{b}\right)\cos\phi\left(1-\tfrac{e}{b}\right)\right)$$
$$+ \left(\cosh\phi\left(1+\tfrac{y}{b}\right)\sin\phi\left(1+\tfrac{y}{b}\right) - \sinh\phi\left(1+\tfrac{y}{b}\right)\cos\phi\left(1+\tfrac{y}{b}\right)\right)\Big[\sinh 2\phi \left(\sin\phi\left(1+\tfrac{e}{b}\right)\cosh\phi\left(1-\tfrac{e}{b}\right) - \cos\phi\left(1+\tfrac{e}{b}\right)\sinh\phi\left(1-\tfrac{e}{b}\right)\right) + \sin 2\phi$$
$$\left(\sinh\phi\left(1+\tfrac{e}{b}\right)\cos\phi\left(1-\tfrac{e}{b}\right) - \cosh\phi\left(1+\tfrac{e}{b}\right)\sin\phi\left(1-\tfrac{e}{b}\right)\right)\Big]\Big\} \qquad \text{.....(2.10)}$$

Guyon has used in place ϕ, the "flexural parameter"

$$\theta = \frac{b}{2a}\sqrt[4]{\frac{\rho_P}{\rho_E}} \qquad \text{....(2.11)}$$

Thus ϕ, λ and θ can be related by simple relation

$$\phi = \lambda b = \frac{\pi\theta}{\sqrt{2}} \qquad (2.12)$$

b. <u>The coefficient of transverse distribution K_o and transverse bending moment coefficient μ_o</u>.

Considering the practical side of the results obtained in equations (2.9) and (2.10), it is useful to compare the actual deflection w with the mean deflection W, when the load p is spread uniformly on the entire width $2b$ of the bridge (Fig.2.5), while remaining sinusoidal along longitudinal direction. The bridge will then undergo a cylindrical deformation given by

$$W = \frac{p_1}{2b} \; \frac{16\,a^4}{\rho_p \pi^4} \; \sin \frac{\pi x}{2a} \qquad \ldots (2.13)$$

Introducing $K_o \doteq \frac{w}{W}$ as the dimensionless ratio, and from equations (2.9) and (2.13) the coefficient of transverse distribution K_o can be written as

$$\begin{aligned} K_o = \frac{2\phi}{\sinh^2 2\phi - \sin^2 2\phi} \Big\{ & 2\cosh\phi\left(1+\tfrac{y}{b}\right)\cos\phi\left(1+\tfrac{y}{b}\right)\Big(\sinh 2\phi\cos\phi\left(1+\tfrac{e}{b}\right) \\ & \cosh\phi\left(1-\tfrac{e}{b}\right) - \sin 2\phi\cosh\phi\left(1+\tfrac{e}{b}\right)\cos\phi\left(1-\tfrac{e}{b}\right)\Big) + \Big\{\cosh\phi\left(1+\tfrac{y}{b}\right)\sin\phi \\ & \left(1+\tfrac{y}{b}\right) + \sinh\phi\left(1+\tfrac{y}{b}\right)\cos\phi\left(1+\tfrac{y}{b}\right)\Big)\Big[\sinh 2\phi\Big(\sin\phi\left(1+\tfrac{e}{b}\right)\cosh\phi\left(1-\tfrac{e}{b}\right) \\ & - \cos\phi\left(1+\tfrac{e}{b}\right)\sinh\phi\left(1-\tfrac{e}{b}\right)\Big) + \sin 2\phi\Big(\sinh\phi\left(1+\tfrac{e}{b}\right)\cos\phi\left(1-\tfrac{e}{b}\right) - \\ & \cosh\phi\left(1+\tfrac{e}{b}\right)\sin\phi\left(1-\tfrac{e}{b}\right)\Big)\Big]\Big\} \end{aligned}$$

$$\ldots (2.14)$$

Thus coefficient K_o depends on the value of flexural parameter θ or ϕ, the relative eccentricity $\frac{e}{b}$ of linear load $p = p_1 \sin\frac{\pi x}{2a}$ and the relative ordinate $\frac{y}{b}$ of the point under consideration. In short $K_0 = K_0(\theta, \frac{e}{b}, \frac{y}{b})$. The further interest of taking into consideration K_0 comes from the fact that the longitudinal bending moment M_x at any point can be written as $M_x = K_0 M_m$, where M_m is the mean bending moment produced in the transverse section at x of the bridge due to uniformly spread sinusoidal load $p = p_1 \sin \frac{\pi x}{2a}$ across the width of the bridge. This can be derived as

$$M_x = -\rho_p \frac{\partial^2 w}{\partial x^2} = \rho_p \frac{\partial^2 (K_0 W)}{\partial x^2} = K_0 \left(-\rho_p \frac{\partial^2 W}{\partial x^2}\right) = K_0 M_m \qquad \text{.... (2.15)}$$

Thus, knowing K_0, one can find out the deflection and longitudinal bending moment in the given bridge.

For the transverse bending moment M_y, the elementary cross beam behaves like a beam on elastic foundation and M_y can be easily expressed as

$$M_y = \mu_0 \, p_1 \, b \, \sin \frac{\pi x}{2a} \qquad \text{.... (2.16)}$$

where, μ_0 is a dimensionless transverse bending moment coefficient which depends on θ, $\frac{e}{b}$, $\frac{y}{b}$ and by comparing eq. (2.16) and (2.10) it can be obtained as

$$\mu_0 = \frac{1}{2\phi(\sinh^2 2\phi - \sin^2 2\phi)} \Big\{ 2 \sinh\phi\left(1+\tfrac{y}{b}\right) \sin\phi\left(1+\tfrac{y}{b}\right) \Big(\sinh 2\phi \cos\phi\left(1+\tfrac{e}{b}\right) \cosh\phi \cdot \left(1-\tfrac{e}{b}\right) - \sin 2\phi \cosh\phi\left(1+\tfrac{e}{b}\right) \cos\phi\left(1-\tfrac{e}{b}\right) \Big) + \Big(\cosh\phi\left(1+\tfrac{y}{b}\right) \sin\phi\left(1+\tfrac{y}{b}\right) - \sinh\phi\left(1+\tfrac{y}{b}\right) \cos\phi\left(1+\tfrac{y}{b}\right) \Big) \Big[\sinh 2\phi \Big(\sin\phi\left(1+\tfrac{e}{b}\right) \cosh\phi\left(1-\tfrac{e}{b}\right) - \cos\phi\left(1+\tfrac{e}{b}\right) \sinh\phi\left(1-\tfrac{e}{b}\right) \Big) + \sin 2\phi \Big(\sinh\phi\left(1+\tfrac{e}{b}\right) \cos\phi\left(1-\tfrac{e}{b}\right) - \cosh\phi\left(1+\tfrac{e}{b}\right) \sin\phi\left(1-\tfrac{e}{b}\right) \Big) \Big] \Big\} \qquad \text{.... (2.17)}$$

2.1.2 Torsionally Resistant Grid Beam Bridges.

As majority of bridges with several longitudinal beams have a slab flooring of reinforced concrete in which the torsional stresses play a predominant role, the theory developed in section 2.1.1 is, therefore, scarcely justified by reality. If one could practically neglect the effect of torsion in bridges with steel grillage beams, it is scarcely permissible to do so in the case of monolithic bridges ribbed with reinforced concrete and still less in the case of bridges reinforced or prestressed slabs, the use of which is more and more wide-spread.

Any structure with several longitudinal and cross beams forming a system of gridwork and the solid slab forming the flooring, is a construction intermediary between the anisotropic plate and the open grid. The relative importance of two elements, grid beams and solid slab, varies according to the plan of construction adopted: the behaviour could be that of a continuous series of grid beams to a thin slab flooring of constant thickness. To assimilate the fundamental approach to the problem and implications of solution, it is briefly recollected from (48), the equations which govern the deformations of an anisotropic plate and grid beam system.

a. Differential equations.

(1) Anisotropic Plates:

The stress-strain relationships of an anisotropic plate having xy plane as middle plane, can be written in general form.

$$\sigma_x = E_x' \epsilon_x + E'' \epsilon_y \; ; \qquad \sigma_y = E_y' \epsilon_y + E'' \epsilon_x$$

$$\tau_{xy} = G \gamma_{xy} \qquad \text{....(2.18)}$$

where,

$$E_x' = \frac{E_x}{1 - \nu_x \nu_y} \; ; \qquad E_y' = \frac{E_y}{1 - \nu_y \nu_x} \; ; \qquad E'' = \frac{\nu_x E_y}{1 - \nu_x \nu_y} = \frac{\nu_y E_x}{1 - \nu_x \nu_y}$$

ν_x and ν_y are the values of Poisson's ratio for the induced strains ϵ_x and ϵ_y in the anisotropic material. From the classical theory of bending of plates, the strain components and stress components can be written as

$$\epsilon_x = -z \frac{\partial^2 w}{\partial x^2} \; ; \qquad \epsilon_y = -z \frac{\partial^2 w}{\partial y^2} \qquad \text{and} \qquad \gamma_{xy} = -2z \frac{\partial^2 w}{\partial x \partial y}$$

$$\left.\begin{aligned} \sigma_x &= -z \left[E_x' \frac{\partial^2 w}{\partial x^2} + E'' \frac{\partial^2 w}{\partial y^2} \right] \\ \sigma_y &= -z \left[E_y' \frac{\partial^2 w}{\partial y^2} + E'' \frac{\partial^2 w}{\partial x^2} \right] \\ \tau_{xy} &= -2Gz \frac{\partial^2 w}{\partial x \partial y} \end{aligned}\right\} \qquad \text{... (2.19)}$$

Hence, the various bending and twisting moments have the

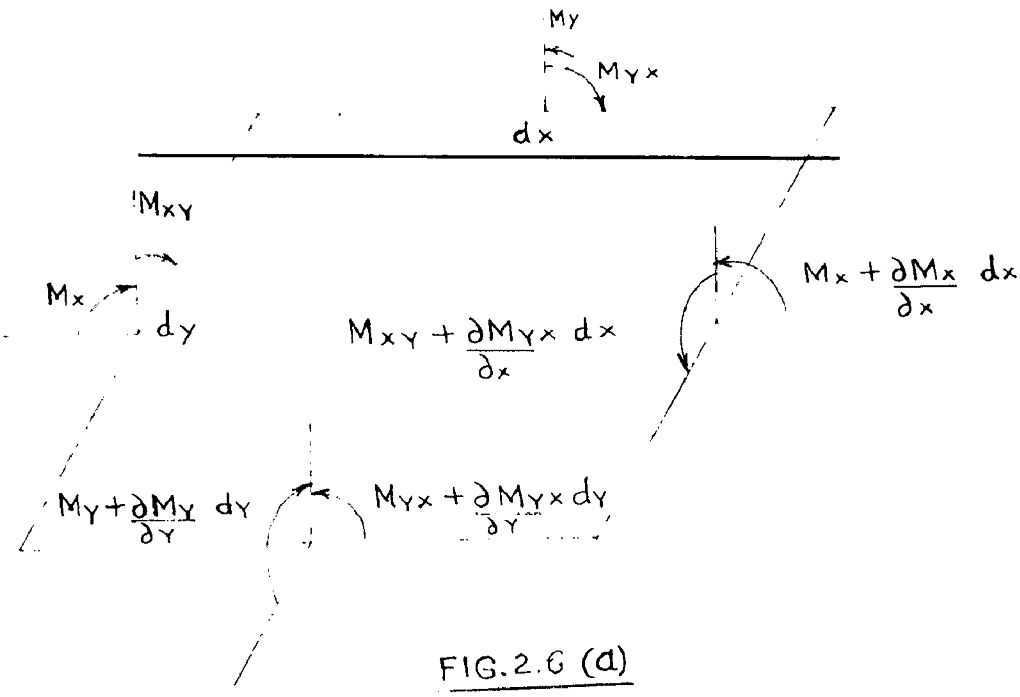

FIG. 2.6 (a)

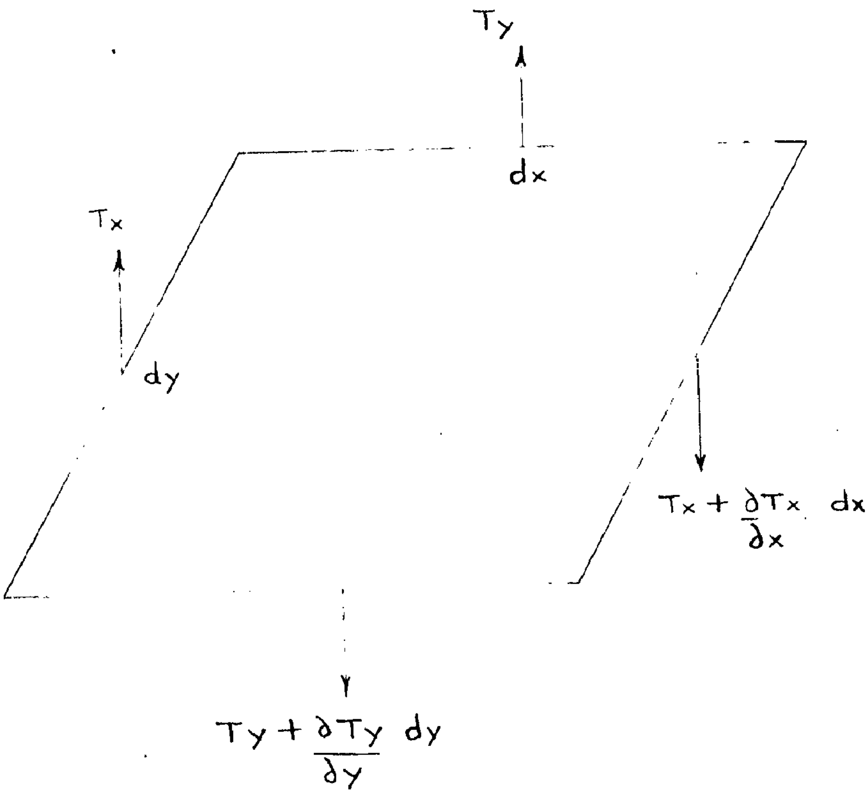

FIG. 2.6 (b)

values

$$M_x = \int_{-h/2}^{h/2} \sigma_x z\,dz = -\left(\rho_P \frac{\partial^2 w}{\partial x^2} + \rho_t \frac{\partial^2 w}{\partial y^2}\right)$$

$$M_y = \int_{-h/2}^{h/2} \sigma_y z\,dz = -\left(\rho_E \frac{\partial^2 w}{\partial y^2} + \rho_t \frac{\partial^2 w}{\partial x^2}\right)$$

$$M_{xy} = \int_{-h/2}^{+h/2} \tau_{xy}\, z\,dz = 2\gamma \frac{\partial^2 w}{\partial x \partial y} \quad ; \qquad \text{where.} \qquad \ldots.(2.20)$$

$$\rho_P = \frac{E_x' h^3}{12}; \qquad \rho_E = \frac{E_y' h^3}{12}; \qquad \rho_t = \frac{E'' h^3}{12}; \qquad \gamma = \frac{G h^3}{12}$$

and h = thickness of the plate.

Equilibrium equations of an element dx, dy of the plate lead to equations (2.21 and 2.22)- (See Fig. 2.6(a) and 2.6(b)

(1) Vertical equilibrium of forces gives

$$\frac{\partial T_x}{\partial x} + \frac{\partial T_y}{\partial y} = -p(x,y) \qquad \ldots.(2.21)$$

(2) Moments about x and y axes give (neglecting higher order quantities)

$$T_x = \frac{\partial M_x}{\partial x} + \frac{\partial M_{yx}}{\partial y}$$

$$T_y = \frac{\partial M_y}{\partial y} + \frac{\partial M_{xy}}{\partial x} \qquad \ldots.(2.22)$$

Combining equations (2.21) and (2.22) and substituting the values of M_x, M_y and M_{xy} from eq.(2.20) the general equation of deformation is obtained. Thus,

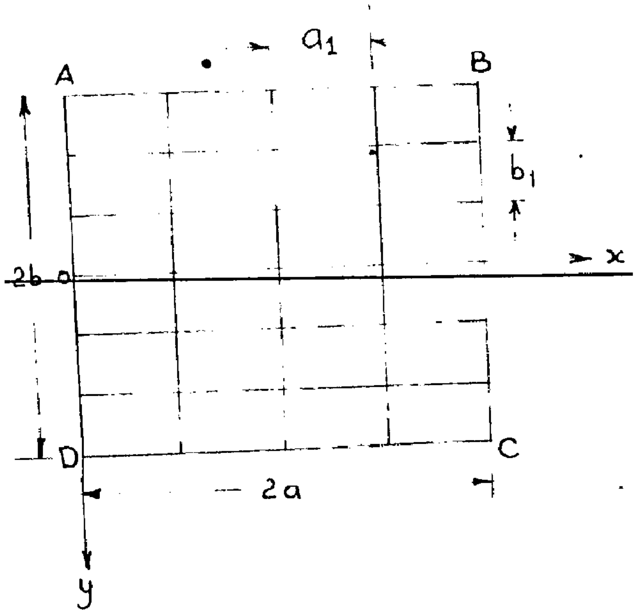

FIG. 2.7 (a)

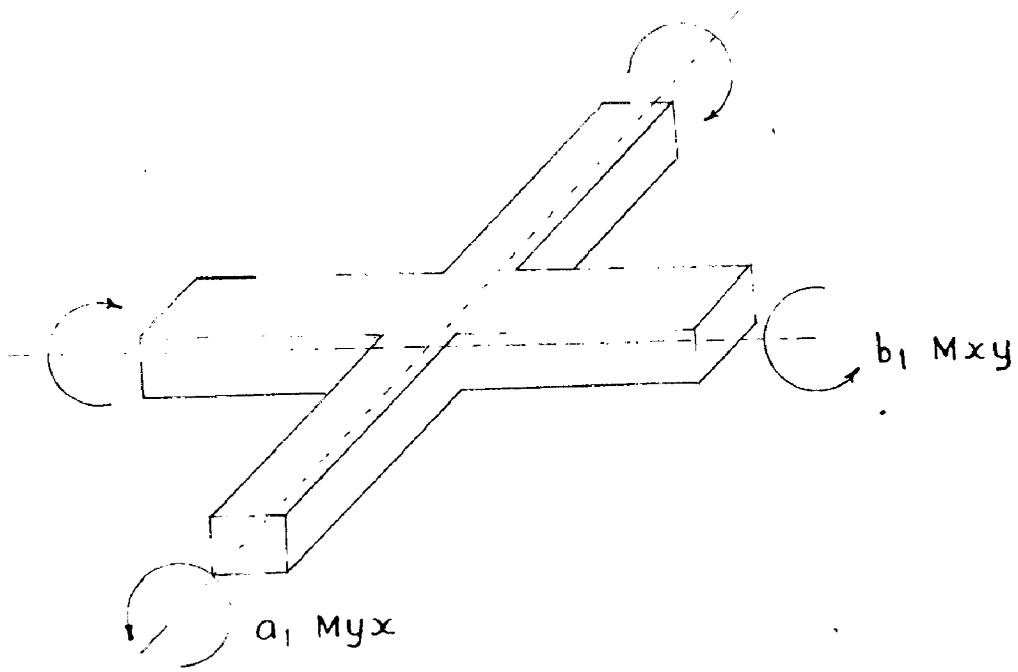

FIG. 2.7 (b)

equilibrium and deformation equations are

$$\frac{\partial^2 M_x}{\partial x^2} + \frac{\partial^2 M_{yx}}{\partial x \partial y} + \frac{\partial^2 M_y}{\partial y^2} - \frac{\partial^2 M_{xy}}{\partial x \partial y} = -p(x,y)$$

...(2.23)

$$\rho_P \frac{\partial^4 \omega}{\partial x^4} + 2H \frac{\partial^4 \omega}{\partial x^2 \partial y^2} + \rho_E \frac{\partial^4 w}{\partial y^4} = p(x,y) \qquad ...(2.24)$$

where, $H = \rho_t + 2\gamma$ and the equations of shear forces T_x and T_y can also be written from eqs. (2.22) and (2.20) as

$$T_x = -\left(\rho_P \frac{\partial^3 \omega}{\partial x^3} + H \frac{\partial^3 \omega}{\partial y^2 \partial x}\right) \quad \text{and.}$$

$$T_y = -\left(\rho_E \frac{\partial^3 w}{\partial y^3} + H \frac{\partial^3 w}{\partial x^2 \partial y}\right).$$

...(2.25)

(ii) <u>Grid Works.</u>

Consider the gridwork shown in Fig.(2.7a) the longitudinal beams parallel to x and cross beams parallel to y axis are rigidly connected at their points of intersection and resistant to torsion. Let I and I_T, and J and J_T be the moment of inertias and torsional inertias of longitudinal and cross beams spaced at b_1 and a_1 respectively. The equivalent continuous grid having infinite number of beams in both directions will have flexural rigidities per unit width in longitudinal and transverse directions as $\rho_P = \frac{EI}{b_1}$ and $\rho_E = \frac{EI_T}{a_1}$

respectively so that the unitary flexural moments produced are

$$M_x = -\rho_P \frac{\partial^2 w}{\partial x^2} \quad ; \qquad M_y = -\rho_E \frac{\partial^2 w}{\partial y^2} \qquad \ldots(226)$$

Similarly the equivalent continuous grid will have torsional rigidities per unit width in longitudinal and transverse direction as $\gamma_P = \frac{GJ}{b_1}$ and $\gamma_E = \frac{GJ_1}{a_1}$ respectively and the unitary torsional moments produced are

$$M_{xy} = \gamma_P \frac{\partial^2 w}{\partial x \partial y} \quad ; \qquad M_{yx} = -\gamma_E \frac{\partial^2 w}{\partial x \partial y} \qquad \ldots(2.27)$$

Substituting the equivalent values of M_x, M_y, M_{xy} and in the equilibrium equations (2.23) and (2.22), the governing differential equation för deflection and vertical shearing of gridworks, when treated as anisotropic plate, are obtained as

$$\rho_P \frac{\partial^4 w}{\partial x^4} + (\gamma_P + \gamma_E) \frac{\partial^4 w}{\partial x^2 \partial y^2} + \rho_E \frac{\partial^4 w}{\partial y^4} = p(x, y)$$

$$T_x = -\rho_P \frac{\partial^3 w}{\partial x^3} - \gamma_E \frac{\partial^3 w}{\partial x \partial y^2} \qquad \ldots(2.28)$$

$$T_y = -\rho_E \frac{\partial^3 w}{\partial y^3} - \gamma_P \frac{\partial^3 w}{\partial x^2 \partial y} \qquad \ldots(2.29)$$

(iii) <u>Comparison.</u>

Equation (2.28) is of the same form as equation (2.24). Introducing the notation

$$2H = 2\left(\rho_t + 2\gamma\right) = \left(\gamma_P + \gamma_E\right) = 2\alpha\sqrt{\rho_P \rho_E}$$

... (2.30a)

the equations (2.28) and (2.24) take the form

$$\rho_P \frac{\partial^4 w}{\partial x^4} + 2\alpha\sqrt{\rho_P \rho_E}\,\frac{\partial^4 w}{\partial x^2 \partial y^2} + \rho_E \frac{\partial^4 w}{\partial y^4} = p(x,y)$$

...(2.30)

where coefficient α is known as the torsional parameter and is given by

$$\alpha = \frac{\gamma_P + \gamma_E}{2\sqrt{\rho_P \rho_E}} = \frac{G\left(\frac{J}{b_1} + \frac{J_T}{a_1}\right)}{2E\sqrt{\frac{I}{b_1} \cdot \frac{I_T}{a_1}}}$$

...(2.31)

and varies between 0. to 1.

In the equivalent grid the Poisson's ratio has been neglected and thus this leads to E'' = 0 and corresponding rigidity $\rho_t = 0$

when $\alpha = 0$ and $\alpha = 1$ the eq. (2.30) reduces to

$$\rho_P \frac{\partial^4 w}{\partial x^4} + \rho_E \frac{\partial^4 w}{\partial y^4} = p(x,y)$$

...(2.30a)

$$\rho_P \frac{\partial^4 w}{\partial x^4} + 2\sqrt{\rho_P \rho_E}\,\frac{\partial^4 w}{\partial x^2 \partial y^2} + \rho_E \frac{\partial^4 w}{\partial y^4} = p(x,y).$$

...(2.30b)

For isotropic plate $\rho_P = \rho_E$ and $\alpha = 1$ then the equation (2.30) becomes Lang-range equation

$$\frac{\partial^4 w}{\partial x^4} + \frac{2\,\partial^4 w}{\partial x^2 \partial y^2} + \frac{\partial^4 w}{\partial y^4} = \frac{p(x,y)}{\rho_P}$$

...(2.30c)

For an isotropic plate, $\alpha = 1$ is irrespective of the value of Poisson's ratio. For an actual bridge, α has always a value intermediary between 0 and 1. Hence, the study of Eq.(2.30) for entire range between 0 to 1 is necessary.

Further it must be noted that the twisting moments M_{xy} and M_{yx} are equal and opposite in the case of anisotropic plate theory and these generally differ in equivalent continuous grid theory. Hence, the expressions of the vertical shear forces T_x and T_y i.e. Eq.(2.25) and (2.29), are slightly different in two theories. Equation (2.25) of anisotropic plate can be adopted without much error for the calculation of shear forces in bridges and eq.(2.25) can be re-written, after putting $H = \alpha\sqrt{\rho_P \rho_E}$ as

$$T_x = -\rho_P \frac{\partial^3 w}{\partial x^3} - \alpha\sqrt{\rho_P \rho_E}\,\frac{\partial^3 w}{\partial x \partial y^2} \qquad \text{and}$$

$$T_y = -\rho_E \frac{\partial^3 w}{\partial y^3} - \alpha\sqrt{\rho_P \rho_E}\,\frac{\partial^3 w}{\partial y \partial x^2} \qquad \ldots(2.29a)$$

Eq. (2.29a) is valid for all practical purposes as a large resistance due to torsion is met with only by slab in reinforced concrete bridges due to its plate effect. Thus, this leads to adopt $\gamma_P = \gamma_E$ and hence eq.(2.29a), without much error.

b. **Boundary Conditions.**

Referring to Fig.(2.7a) and recollecting that $\rho_t = 0$ for simplification, the boundary conditions can be written as

Along the simply supported edges (AD and BC)

(1) The deflection, w, is zero, i.e.

$$w = 0 \qquad \text{at} \quad x = 0 \quad \& \quad x = 2a \qquad \ldots (2.32a)$$

(2) The bending moment M_x, is zero i.e.

$$\frac{\partial^2 w}{\partial x^2} = 0 \qquad \text{at} \quad x = 0 \quad \& \quad x = 2a \qquad \ldots (2.32b)$$

Along the free edge (AB & AD)

(3) The bending moment, M_y, is zero i.e.,

$$\frac{\partial^2 w}{\partial y^2} = 0 \qquad \text{at} \quad y = \pm b \qquad \ldots (2.32c)$$

(4) The reaction at the free edges is zero, i.e.

$$R_y = T_y + \frac{\partial M_{yx}}{\partial x} = 0 \quad \text{at} \quad y = \pm b$$

From equations (2.29) and (2.27)

$$\frac{\partial^3 w}{\partial y^3} + 2\alpha\sqrt{\frac{\rho_P}{\rho_E}}\,\frac{\partial^3 w}{\partial x^2 \partial y} = 0 \quad \text{at} \quad y = \pm b \ldots (2.32d)$$

c. <u>General equation of deformation of a simply supported bridge in the unloaded region.</u>

Employing the Levy series for deflections,

$$w = \sum Y_m(y) \sin \frac{m\pi x}{2a} \qquad \ldots (2.33)$$

the solution for homogeneous differential equation (2.30) for $p(xy) = 0$ can be obtained. Where Y_m is a function of y only. Each term of the series satisfies boundary conditions (2.32a) and (2.32b) along the simply supported edges. Substituting the expression (2.33) for w in the equation (2.30) for the unloaded portion, Y_m must satisfy the equation

$$Y_m'''' - 2\alpha m^2 \lambda^2 Y_m'' + m^4 \lambda^4 Y_m = 0 \qquad \ldots (2.34)$$

where,

$$\lambda = \frac{\pi}{2a} \sqrt[4]{\frac{\rho_P}{\rho_E}} \qquad \ldots (2.35)$$

The general solution of the equation (2.34) to include all cases from $\alpha = 0$ to $\alpha = 1$, is given by

$$Y_m = e^{m\lambda\sqrt{\frac{1+\alpha}{2}}\,y} \left\{ A_m \cos\left(m\lambda\sqrt{\tfrac{1-\alpha}{2}}\right)y + \frac{B_m}{\sqrt{\frac{1-\alpha}{2}}} \sin\left(m\lambda\sqrt{\tfrac{1-\alpha}{2}}\right)y \right\}$$

$$+ e^{-m\lambda\sqrt{\frac{1+\alpha}{2}}\,y} \left\{ C_m \cos\left(m\lambda\sqrt{\tfrac{1-\alpha}{2}}\right)y + \frac{D_m}{\sqrt{\frac{1-\alpha}{2}}} \sin\left(m\lambda\sqrt{\tfrac{1-\alpha}{2}}\right)y \right\}$$

$$\ldots (2.35)$$

where Am, Bm, Cm & Dm are arbitrary constants.

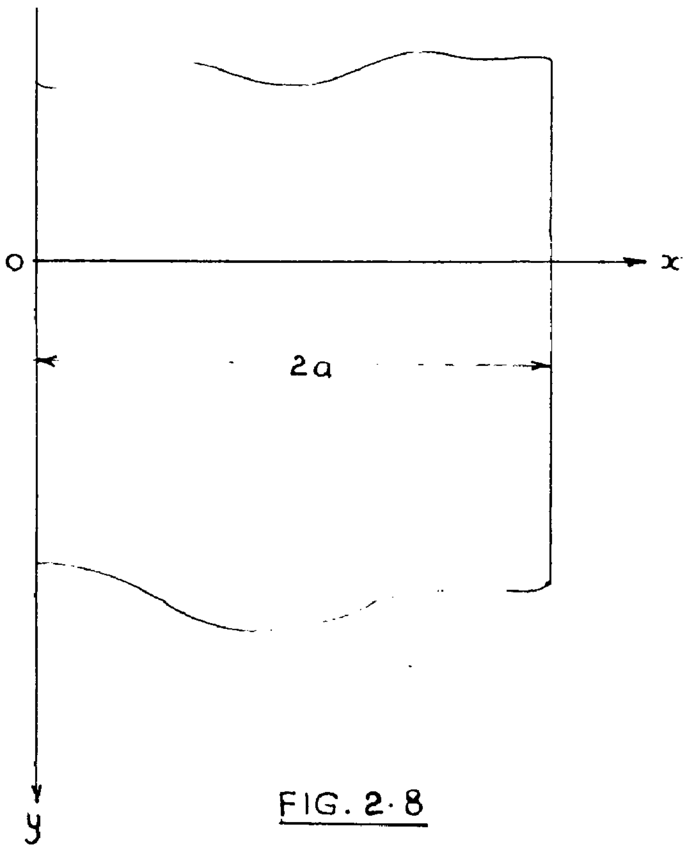

FIG. 2·8

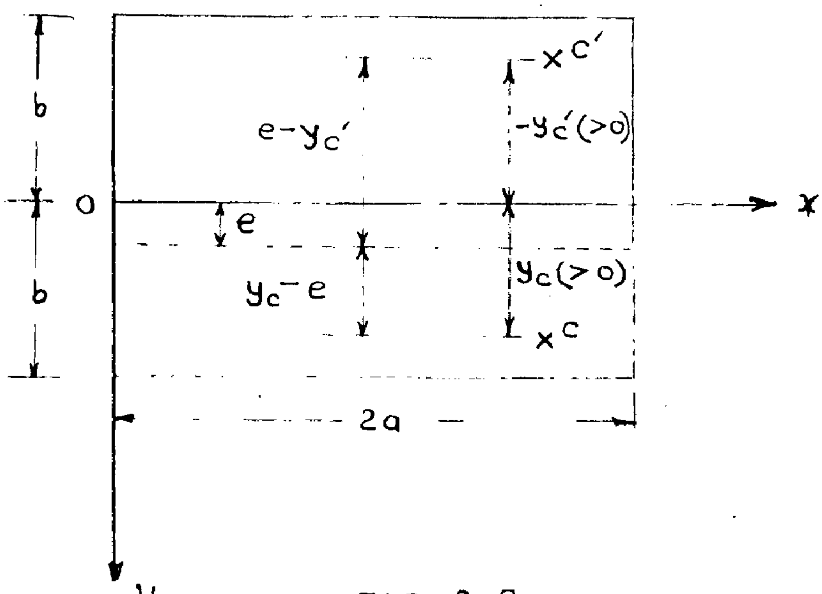

FIG. 2.9

d. <u>General equation of deformation of an infinitely wide simply supported bridge with a sinusoidal load along x axis.</u>

Consider an infinitely wide bridge of span with a load $p = p_m \sin\frac{m\pi x}{2a}$ acting along OX (Fig. 2.8). For large values of y, and considering only positive values of y of the portion, the equation (2.35) will apply for unloaded region. However, it is obvious that the deflections, w and slopes $\frac{\partial w}{\partial y}$ tend to zero as $y \to \infty$ and hence equation (2.35) must be reduced to

$$Y_m = e^{-m\lambda\sqrt{\frac{1+\alpha}{2}}\,y}\left\{C_m \cos\left(m\lambda\sqrt{\tfrac{1-\alpha}{2}}\right)y + \frac{d_m}{\sqrt{\frac{1-\alpha}{2}}}\sin\left(m\lambda\sqrt{\tfrac{1-\alpha}{2}}\right)y\right\}$$

$$\text{for } y \geq 0 \qquad \ldots\ldots(2.36)$$

and the deflection of the bridge is expressed by

$$\omega_m = e^{-m\lambda\sqrt{\frac{1+\alpha}{2}}\,y}\left\{c_m \cos\left(m\lambda\sqrt{\tfrac{1-\alpha}{2}}\right)y + \frac{d_m}{\sqrt{\frac{1-\alpha}{2}}}\sin\left(m\lambda\sqrt{\tfrac{1-\alpha}{2}}\right)y\right\}\sin\frac{m\pi x}{2a}$$

Considering the symmetry of the deflection of the bridge it is obvious that the slope along x axis,

$$\left[\frac{\partial \omega_m}{\partial y}\right]_{y=0} = 0 \qquad \text{which gives on simplification}$$

$$d_m = c_m\sqrt{\frac{(1+\alpha)}{2}}$$

Again, considering symmetry, C_m is determined from the condition that the shearing force, T_y, along x axis is equivalent to half the load i.e. from eq.(2.29a)

$$-\rho_E \frac{\partial^3 w_m}{\partial y^3} - \alpha\sqrt{\rho_P \rho_E}\ \frac{\partial^3 w_m}{\partial x^2 \partial y} = -\frac{p_m}{2}\ \sin\frac{m\pi x}{2a}$$

Substituting the value of w_m and solving for c_m, it is obtained as

$$c_m = \frac{p_m}{2\sqrt{2(1+\alpha)}\ \ \rho_E\ m^3 \lambda^3} \qquad \text{....(2.37)}$$

When the load $p = p_m \sin\frac{m\pi x}{2a}$ acts on a line parallel and eccentric, e, from the x axis, the equation for w_m is obtained by replacing y by $|y-e|$. The modulus value is used to ensure symmetry of deflection for both positive and negative values of e. Thus the equation for w_m becomes,

$$w_m = c_m\ e^{-m\lambda\sqrt{\frac{1+\alpha}{2}}|y-e|}\left\{\cos\left(m\lambda\sqrt{\tfrac{1-\alpha}{2}}|y-e|\right)+\sqrt{\tfrac{1+\alpha}{1-\alpha}}\ \sin\left(m\lambda\sqrt{\tfrac{1-\alpha}{2}}|y-e|\right)\right\}$$

$$\times \sin\frac{m\pi x}{2a} \qquad \text{.... (2.38)}$$

e. __General equation of deformation of a simply supported bridge of finite width 2b with a sinusoidal load__ $p = p_m \sin\frac{m\pi x}{2a}$ __acting along a line parallel to - - - - - - - and eccentric, e, from x axis.__

For the bridge of finite width (fig. 2.9) the general equation may be found by superposing solutions to the two cases (c and d) i.e. combining equations (2.35) and (2.38). The equation thus obtained can be more conveniently written in terms of hyperbolic functions i.e.

$$w_m = \Big[A'_m \cosh\left(m\lambda\sqrt{\tfrac{1+\alpha}{2}}\right)y \cos\left(m\lambda\sqrt{\tfrac{1-\alpha}{2}}\right)y + B'_m \sinh\left(m\lambda\sqrt{\tfrac{1+\alpha}{2}}\right)y$$

$$\cos\left(m\lambda\sqrt{\tfrac{1-\alpha}{2}}\right)y + \frac{C'_m}{\sqrt{\frac{1-\alpha}{2}}} \cosh\left(m\lambda\sqrt{\tfrac{1+\alpha}{2}}\right)y \sin\left(m\lambda\sqrt{\tfrac{1-\alpha}{2}}\right)y$$

$$+\frac{D'_m}{\sqrt{\frac{1-\alpha}{2}}} \sinh\left(m\lambda\sqrt{\tfrac{1+\alpha}{2}}\right)y \sin\left(m\lambda\sqrt{\tfrac{1-\alpha}{2}}\right)y + C_m\, e^{-m\lambda\sqrt{\frac{1+\alpha}{2}}\,|y-e|}$$

$$\left(\cos\left(m\lambda\sqrt{\tfrac{1-\alpha}{2}}\,|y-e|\right) + \sqrt{\tfrac{1+\alpha}{1-\alpha}}\,\sin\left(m\lambda\sqrt{\tfrac{1-\alpha}{2}}\,|y-e|\right)\right)\Big] \sin\frac{m\pi x}{2a} \quad \text{....(2.39)}$$

The four unknown constants A'_m, B'_m, C'_m and D'_m can be determined from the boundary conditions (2.32c) and (2.32d) along the two free edges. For simplification, let

$$\frac{\pi y}{b} = \beta \; ; \qquad \frac{\pi e}{b} = \psi$$

where, and represent radian measure of the section and load eccentricities respectively. As the flexural parameter or parameter of transverse beam $\theta = \frac{b}{2a}\sqrt[4]{\frac{\rho_P}{\rho_E}}$ λ could be expressed in the form $\lambda = \frac{\pi\theta}{b}$ and

$$\lambda\,(b+e) = \theta\,(\pi+\psi) \quad \text{and} \quad \pi\,(b-e) = \theta\,(\pi-\psi)$$

Further introducing,

$$\phi = \pi\theta\sqrt{\tfrac{1+\alpha}{2}} \; ; \qquad \eta = \pi\theta\sqrt{\tfrac{1-\alpha}{2}}$$

$$\gamma = \theta\sqrt{\tfrac{1+\alpha}{2}} \; ; \qquad \delta = \theta\sqrt{\tfrac{1-\alpha}{2}}$$

and solving for the constants A'_m, B'_m, C'_m and D'_m from boundary conditions, it is obtained that

$$A'_m = \frac{c_m}{M}(\cosh\phi - \sinh\phi)\Big\{\Big[\cosh\gamma\psi\Big(\sqrt{\tfrac{1+\alpha}{2}}\ \sin\eta - \sqrt{\tfrac{1-\alpha}{2}}\ \cos\eta\Big)$$

$$-\sinh\gamma\psi\ \sin\delta\psi\Big(\sqrt{\tfrac{1+\alpha}{2}}\cos\eta + \sqrt{\tfrac{1-\alpha}{2}}\sin\eta\Big)\Big]\times\Big[-\sinh\phi\cos\eta$$

$$+\sqrt{\tfrac{1+\alpha}{2}}\cosh\phi\sin\eta\Big] + \Big[\cosh\gamma\psi\ \cos\delta\psi(\alpha\sin\eta + \sqrt{1-\alpha^2}\cos\eta)$$

$$-\sinh\gamma\psi\ \sin\delta\psi(\alpha\cos\eta - \sqrt{1-\alpha^2}\ \sin\eta)\Big]\times\Big[\sqrt{2(1+\alpha)}\cosh\phi\cos\eta$$

$$+\frac{2\alpha}{\sqrt{2(1-\alpha)}}\ \sinh\phi\ \sin\eta\Big]\Big\} \qquad \ldots (3.40a)$$

$$B'_m = \frac{c_m}{N}(\cosh\phi - \sinh\phi)\Big\{\Big[\sinh\gamma\psi\ \cos\delta\psi\Big(\sqrt{\tfrac{1+\alpha}{2}}\ \sin\eta - \sqrt{\tfrac{1-\alpha}{2}}\cos\eta\Big)$$

$$-\cosh\gamma\psi\ \sin\delta\psi\Big(\sqrt{\tfrac{1+\alpha}{2}}\cos\eta + \sqrt{\tfrac{1-\alpha}{2}}\ \sin\eta\Big)\Big]\times\Big[-\cosh\phi\cos\eta + \sqrt{\tfrac{1+\alpha}{1-\alpha}}\sinh\phi\sin\eta\Big]$$

$$+\Big[\sinh\gamma\psi\cos\delta\psi(\alpha\sin\eta + \sqrt{1-\alpha^2}\cos\eta) - \cosh\gamma\psi\ \sin\delta\psi\ (\alpha\cos\eta - \sqrt{1-\alpha^2}\sin\eta)\Big]$$

$$\times\Big[\sqrt{2(1+\alpha)}\sinh\phi\cos\eta + \frac{2\alpha}{\sqrt{2(1-\alpha)}}\cosh\phi\sin\eta\Big]\Big\}$$

$$\ldots (3.40b)$$

$$C'_m = -\frac{c_m}{N}\sqrt{\frac{1-\alpha}{2}}(\cosh\phi - \sinh\phi)\Big\{\Big[\sinh\gamma\psi\cos\delta\psi\Big(\sqrt{\tfrac{1+\alpha}{2}}\sin\eta - \sqrt{\tfrac{1-\alpha}{2}}\cos\eta\Big)$$

$$-\cosh\gamma\psi\sin\delta\psi\Big(\sqrt{\tfrac{1+\alpha}{2}}\cos\eta + \sqrt{\tfrac{1-\alpha}{2}}\ \sin\eta\Big)\Big]\times\Big[\sinh\phi\sin\eta + \sqrt{\tfrac{1+\alpha}{1-\alpha}}\cosh\phi\cos\eta\Big]$$

$$+\Big[\sinh\gamma\psi\cos\delta\psi(\alpha\sin\eta + \sqrt{1-\alpha^2}\cos\eta) - \cosh\gamma\psi\sin\delta\psi(\alpha\cos\eta - \sqrt{1-\alpha^2}\sin\eta)\Big]$$

$$\times\Big[-\sqrt{2(1+\alpha)}\cosh\phi\sin\eta + \frac{2\alpha}{\sqrt{2(1-\alpha)}}\sinh\phi\cos\eta\Big]\Big\}$$

$$\ldots (3.40c)$$

$$D'_m = -\frac{c_m}{M}\sqrt{\frac{1-\alpha}{2}}\,(\cosh\phi - \sinh\phi)\Bigg\{\Bigg[\cosh\gamma\psi\cos\delta\psi\left(\sqrt{\frac{1+\alpha}{2}}\,\sin\eta - \sqrt{\frac{1-\alpha}{2}}\,\cos\eta\right)$$

$$-\sinh\gamma\psi\sin\delta\psi\left(\sqrt{\frac{1+\alpha}{2}}\,\cos\eta + \sqrt{\frac{1-\alpha}{2}}\,\sin\eta\right)\Bigg]\times\left[\cosh\phi\sin\eta + \sqrt{\frac{1+\alpha}{1-\alpha}}\,\sinh\phi\cos\eta\right]$$

$$+\left[\cosh\gamma\psi\cos\delta\psi\left(\alpha\sin\eta + \sqrt{1-\alpha^2}\cos\eta\right) - \sinh\gamma\psi\sin\delta\psi\left(\alpha\cos\eta - \sqrt{1-\alpha^2}\sin\eta\right)\right]$$

$$\times\left[-\sqrt{2(1+\alpha)}\,\sinh\phi\sin\eta + \frac{2\alpha}{\sqrt{2(1-\alpha)}}\cosh\phi\cos\eta\right]\Bigg\}$$

...(2.40d)

where,

$$M = (2\alpha+1)\sqrt{\frac{1-\alpha}{2}}\,\sinh\phi\cosh\phi - (2\alpha-1)\sqrt{\frac{1+\alpha}{2}}\,\sin\eta\cos\eta$$

$$N = (2\alpha+1)\sqrt{\frac{1-\alpha}{2}}\,\sinh\phi\cosh\phi + (2\alpha-1)\sqrt{\frac{1+\alpha}{2}}\,\sin\eta\cos\eta .$$

The complete expression for w_n may now be obtained by substituting the expressions for four constants in the equation (2.39).

2.2 APPLICATION OF ANISOTROPIC PLATE THEORY TO SIMPLY SUPPORTED GRID BEAM BRIDGES.

From the theory developed in Section 2.1 it is possible to calculate thoroughly the forces in a bridge for any distribution of load but the exact method leads to impracticable calculations. It is for this reason that an approximate method of calculation which is sufficiently accurate for practical application is developed. Under this for any case of definite loading it is sufficient to make $m = 1$ in all the formulae derived in section 2.1.

2.2.1 Distribution Coefficients.

a. Coefficient of transverse distribution K.

It is useful to introduce the relationship between the actual deflection, w_m and the mean deflection, W_m , i.e. the deflection produced if the applied loads are uniformly spread over the entire width as it has been done for the case in section 2.1.1 for $\alpha=0$. The mean deflection W_m is then written as

$$W_m = \frac{p_m}{2b} \frac{16a^4}{\rho_p m^4 \pi^4} \sin\frac{m\pi x}{2a} \qquad \text{.....(2.41a)}$$

and if it is assumed that

$$\omega_m = K_{\alpha m} W_m \qquad \text{.... (2.41b)}$$

where $K_{\alpha m}$ is known as a transverse distribution coefficient, then $K_{\alpha m}$ is obtained from equations (2.39) and (2.40) as

$$K_{\alpha m} = \frac{2b\rho_p m^4\pi^4}{p_m\, 16a^4}\Big\{A_m' \cosh m\gamma\beta \cos m\delta\beta + B_m' \sinh m\gamma\beta \cos m\delta\beta + \frac{C_m'}{\sqrt{\frac{1-\alpha}{2}}}\cosh m\gamma\beta \sin m\delta\beta + \frac{D_m'}{\sqrt{\frac{1-\alpha}{2}}}\sinh m\gamma\beta \sin m\delta\beta + C_m\left[\cosh m\gamma|\beta-\psi| - \sinh m\gamma|\beta-\psi|\right]\left[\cos m\delta|\beta-\psi| + \sqrt{\frac{1+\alpha}{1-\alpha}}\sin m\delta|\beta-\psi|\right]\Big\} \qquad \text{.... (2.42)}$$

Hence $K_{\alpha m}$ is dependent on m, α, θ, β and ψ or in short $K_{\alpha m} = K\,(m, \alpha, \theta, \frac{e}{b}, \frac{y}{b})$

So far only the mth term in the Fourier series of the load has been considered, and therefore, the complete expression for the deflection of the bridge is a Fourier series, namely

$$w = K_{\alpha 1} W_1 + K_{\alpha 2} W_2 + K_{\alpha 3} W_3 + \cdots\cdots + K_{\alpha m} W_m + \cdots \qquad \ldots (2.43a)$$

and the actual 'mean' deflection is

$$W = W_1 + W_2 + W_3 + \cdots\cdots + W_m + \cdots\cdots \qquad \ldots (2.43b)$$

The true distribution coefficient, K_α is therefore, given by

$$K_\alpha = \frac{w}{W} = \frac{K_{\alpha 1} W_1 + K_{\alpha 2} W_2 + \cdots\cdots + K_{\alpha m} W_m + \cdots}{W_1 + W_2 + \cdots\cdots + W_m + \cdots} \qquad \ldots (2.44)$$

Since W_m is inversely proportional to m^4, both expressions (2.43a and 2.43b) are rapidly convergent, and for all practical applications it is sufficiently accurate to consider the first term only; thus $K_\alpha \simeq K_{\alpha 1}$

The longitudinal bending moment M_x is given by (while neglecting ρ_t)

$$M_x = -\rho_p \frac{\partial^2 w}{\partial x^2}$$

Considering the mth term of the series i.e. $w_m = K_m W_m$

$$M_{xm} = - D_p \frac{\partial^2 w_m}{\partial x^2}$$

$$= K_{\alpha m} \frac{p_m}{2b} \frac{4a^2}{m^2 \pi^2} \sin \frac{m\pi x}{2a}$$

.... (2.45a)

The mean longitudinal moment M_m is obtained by using equation (2.41a). Thus,

$$M_m = \frac{p_m}{2b} \frac{4a^2}{m^2 \pi^2} \sin \frac{m\pi x}{2a} \quad \text{.... (2.45b)}$$

From equations (2.45a) and (2.45b)

$$M_{xm} = K_{\alpha m} M_m.$$

Considering all terms,

$$M_x = K_{\alpha 1} M_1 + K_{\alpha 2} M_2 + \cdots\cdots + K_{\alpha m} M_m.$$

.... (2.45c)

and

$$M_{mean} = M_1 + M_2 + M_3 + \cdots\cdots + M_m + \cdots \quad \text{.... (2.45d)}$$

Thus the true distribution coefficient K_α', for longitudinal bending moments is obviously

$$K_\alpha' = \frac{M_x}{M_{mean}} = \frac{K_{\alpha 1} M_1 + K_{\alpha 2} M_2 + \cdots\cdots + K_{\alpha m} M_m.}{M_1 + M_2 + \cdots\cdots + M_m + \cdots}$$

.... (2.46)

Since M_m is inversely proportional to m^2, both series in equations (2.45c) and (2.45d) are convergent though not so rapidly as series in equation (2.44). However, for all practical applications it will be sufficiently accurate to consider the first term only of each series. Thus $K'_{\alpha} \simeq K_{\alpha_1}$ provided some increase in bending moment so derived is assumed. For all design purposes equation (2.47) is usually adopted.

$$M_x = 1{\cdot}1 \; K_{\alpha_1} M_1 \qquad \ldots (2.47)$$

Hence a single set of distribution coefficient is sufficient to determine both the deflections and longitudinal moments in the bridge structure and it is common to denote K_{α_1} by K_{α}.

From equation (2.42) K_{α} can be determined for any values of the torsional parameter. In the two limiting cases i.e. $\alpha = 0$ and $\alpha = 1$, the values of K_0 and K_1 can be calculated. The value of K_0 has already been obtained (eq. 2.14) and the value of K_1 is given by

$$\begin{aligned} K_1 = \frac{\sigma}{2\sinh^2\sigma} \Big\{ & (\sigma\cosh\sigma + \sinh\sigma)\cosh\theta\chi - \sinh\sigma\,\theta\chi\,\sinh\theta\chi \\ & + \frac{[(\sigma\cosh\sigma - \sinh\sigma)\cosh\theta\beta - \sinh\sigma\,\theta\beta\,\sinh\theta\beta]}{3\sinh\sigma\cosh\sigma - \sigma} \times \\ & \times [(\sigma\cosh\sigma - \sinh\sigma)\cosh\theta\psi - \sinh\sigma\,\theta\psi + \sinh\theta\psi] \\ & + \frac{[(2\sinh\sigma + \sigma\cosh\sigma)\sinh\theta\beta - \sinh\sigma\,\theta\beta\cdot\cosh\theta\beta]}{3\sinh\sigma\cosh\sigma + \sigma} \times \\ & [(2\sinh\sigma + \sigma\cosh\sigma)\sin\theta\psi - \sinh\sigma\cdot\theta\psi\,\cosh\theta\psi] \Big\} \end{aligned}$$

$$\ldots (2{\cdot}48).$$

where $\chi = \pi - |\beta - \psi|$ and $\sigma = \pi\theta$

Further it has been shown by MASSONNET[16] that distribution coefficient for any intermediate value of α can be determined with sufficient accuracy from the interpolation formula

$$K_\alpha = K_0 + (K_1 - K_0)\sqrt{\alpha} \qquad \ldots.(2.49)$$

SATTLER[41] has later found that under certain conditions, by using equation (2.49) very large errors can crop up. Therefore, the following interpolation formulae are recommended by him for the case of

$$0 < \theta < 0.1 \qquad K_\alpha = K_0 + (K_1 - K_0)\,\alpha^{0.05}$$

$$0.1 < \theta < 1 \qquad K_\alpha = K_0 + (K_1 - K_0)\,\alpha^{1 - e^{\left(\frac{0.065 - \theta}{0.663}\right)}} \qquad \ldots (2.50)$$

b. <u>Coefficient of transverse bending moment</u> μ :

The transverse bending moment, M_y , is given by $M_y = -\rho_E \frac{\partial^2 w}{\partial y^2}$ and by substituting the value of w from (2.39) it can be shown that

$$M_y = \sum_{m=1}^{\infty} \mu_{\alpha m} \cdot b \, p_m \sin\frac{m\pi x}{2a} \qquad \ldots (2.51)$$

where is dependent on θ , α , $\frac{y}{b}$ and $\frac{e}{b}$ and p_m is the load amplitude of the mth term in Fourier series.

Also μ_α is known as coefficient of transverse bending moment and in the two limiting cases the value of for has already been obtained (equation 2.17) and for

$$\mu_1 = \frac{1}{4\sigma \sinh^2\sigma}\left\{\frac{[(\sigma\cosh\sigma - \sinh\sigma)\cosh\theta\psi - \sinh\sigma\,\theta\psi\,\sinh\theta\psi]}{3\sinh\sigma\cosh\sigma - \sigma}\right.$$

$$\times\left[(\sigma\cosh\sigma - 3\sinh\sigma)\cosh\theta\beta - \sinh\sigma\,\theta\beta\sinh\theta\beta\right]$$

$$+\frac{[(\sigma\cosh\sigma + 2\sinh\sigma)\sinh\theta\psi - \sinh\sigma\,\theta\psi\,\cosh\theta\psi]}{3\sinh\sigma\,\cosh\sigma + \sigma}$$

$$[\sigma\cosh\sigma\,\sinh\theta\beta - \sinh\sigma\,\theta\beta\,\cosh\theta\beta]$$

$$\left. + (\sigma\cosh\sigma - \sinh\sigma)\cosh\theta\chi - \sinh\sigma\,\theta\chi\,\sinh\theta\chi\right\}$$

.... (2.52)

In this case also it has been shown by MASSONNET[16] that for any value of α the coefficient μ_α can be obtained from the interpolation formula.

$$\mu_\alpha = \mu_0 + (\mu_1 - \mu_0)\sqrt{\alpha}$$

... (2.53)

c. <u>Coefficient of torsional moment τ.</u>

The torsional moments in the longitudinal and cross beams can be calculated by the formula

$$M_{xy} = \frac{2\gamma_P}{\gamma_P+\gamma_E}\,\tau_\alpha\, b p \cos\frac{\pi x}{2a}$$

$$M_{xy} = -\frac{2\gamma_E}{\gamma_P+\gamma_E}\,\tau_\alpha\, b p \cos\frac{\pi x}{2a}$$ ... (2.54)

where τ_α is the coefficient of torsional moment and depends on θ , α , $\frac{y}{b}$ and $\frac{e}{b}$. The calculations carried out by MASSONNET[37] show that the coefficient τ_α is represented with a sufficient precision by the interpolation formula

$$\tau_\alpha = \tau_1 \sqrt{\alpha} \qquad \text{.... (2.55)}$$

where the value τ_1, corresponds to the particular case of an isotropic slab.

d. <u>Rigorous method of calculation.</u>

To find the influence surfaces, consider a concentrated load P of coordinates x = o, y = e. The problem of finding different stresses due to any load system in a bridge, then can be completely solved by making use of the principle of superposition. The force P can be replaced by a Fourier series

$$q = \frac{P}{a} \sum_{m=1}^{\infty} \sin \frac{m\pi e}{2a} \sin \frac{m\pi x}{2a} \qquad \text{...(2.55a)}$$

at an eccentricity e. In this series considering the mth term $p = p_m \sin \frac{m\pi x}{2a}$, where

$$p_m = \frac{P}{a} \sin \frac{m\pi e}{2a} \qquad \text{..(2.55 b)}$$

and corresponding flexural parameter $\theta_m = m\theta$ i.e. the cross beams behave as if they are m times more flexible than under the load $p_1 \sin \frac{\pi x}{2a}$. Thus, the numerical values of coefficients K, μ and τ for fixed α, e, y are different for different terms and these vary according to $m\theta$.

From the principle of superposition the forces and moments in a bridge due to a concentrated load can be written as given below .

(i) Deflection w.

$$w(x,y) = \frac{8Pa^3}{b\rho_p\pi^4}\sum_{m=1}^{\infty}\frac{1}{m^4}K_{\alpha m}(e,y)\sin\frac{m\pi e}{2a}\sin\frac{m\pi x}{2a}$$

...(2.57a)

(ii) Bending moment in longitudinal beams.

$$M_x = \frac{2Pa}{b\pi^2}\sum_{m=1}^{\infty}\frac{1}{m^2}K_{\alpha m}(e,y)\sin\frac{m\pi x}{2a}\sin\frac{m\pi e}{2a}$$

... (2.57b)

(iii) Bending moment in the cross beams.

$$M_y = \frac{Pb}{a}\sum_{m=1}^{\infty}\mu_{\alpha m}(e,y)\sin\frac{m\pi e}{2a}\sin\frac{m\pi x}{2a}$$

... (2.57c)

(iv) Torsional moments in the bridge.

$$M_{xy} = \frac{2\gamma_P}{\gamma_P+\gamma_E}\cdot\frac{Pb}{a}\sum_{m=1}^{\infty}T_{\alpha m}(e,y)\sin\frac{m\pi e}{2a}\cos\frac{m\pi x}{2a}$$

$$M_{yx} = -\frac{\gamma_E}{\gamma_P}M_{xy}$$

... (2.57d)

e. **Calculation of Distribution Coefficients from graphs.**

From the equations derived in section 2.1 and 2.2, the distribution coefficients K, μ & τ can be evaluated for specific values of θ and if necessary for α. For simple presentation and use of the equations, curves have been plotted by dividing the width of the equivalent anisotropic plate, 2b, into eight equal parts and labelling the nine points thus obtained as $-b$, $-\frac{3b}{4}$, $-\frac{b}{2}$, 0, $\frac{b}{2}$, $\frac{b}{4}$ $\frac{3b}{4}$ and b. These points are occasionally referred to as the standard positions for e or occasionally, as the reference stations for y.

In the original papers of GUYON and MASSONNET[16] a limited number of values for K and μ are derived. However, in a later publication. MASSONNET[37] has presented some comprehensive tables giving the values of K_0 and K_1. These values are derived on electronic computer for intervals of 0.05 for θ varying from 0 to 1 and at intervals of 0.1 for values of θ between 1 and 2. The basic equations used are (2.14) for K_0 and (2.43) for K_1. The curves are then plotted for design office use. Graphs 1 to 6 given at the end are for K_0 for various reference stations, and load eccentricities. Similarly graph 7 to 11 show the values of K_1. Since the Maxwells' reciprocal theorem must be satisfied it follows that $K(\alpha, \theta, a, b) = K(\alpha, \theta, b, a)$ for any reference station say $\frac{b}{4}$ and load position say $-\frac{b}{2}$, K must be identical to K for reference station $-\frac{b}{2}$ and load position $\frac{b}{4}$.

Distribution coefficients μ_0 are calculated using eq. (2.17). As will be pointed out section 2.4.1, the Poisson's ratio has considerable effect on the coefficient μ_1, equation (2.75) is used with $\nu = 0.15$ which is applicable to reinforced and prestressed concrete. The values of μ_1 are presented by ROWE[23] and design curves for μ_0 and μ_1 are given in graphs 12 to 21.

f. Determination of parameters θ and α.

(i) Flexural parameter θ.

The value of θ can be written as

$$\theta = \frac{b}{2a}\sqrt[4]{\frac{\rho_P}{\rho_E}} = \frac{b}{2a}\sqrt[4]{\frac{i_L}{i_T}} \qquad \ldots (2.58)$$

where,

2b = width of equivalent anisotropic plate

2a = effective span.

i_L and i_T = equivalent distributed moment of inertias of longitudinals and transversals per unit width respectively.

In replacing an actual structure by an equivalent anisotropic plate the flexural stiffnesses of the actual longitudinal and transverse members are distributed according to their spacings. Examples of various types of structures are now considered.

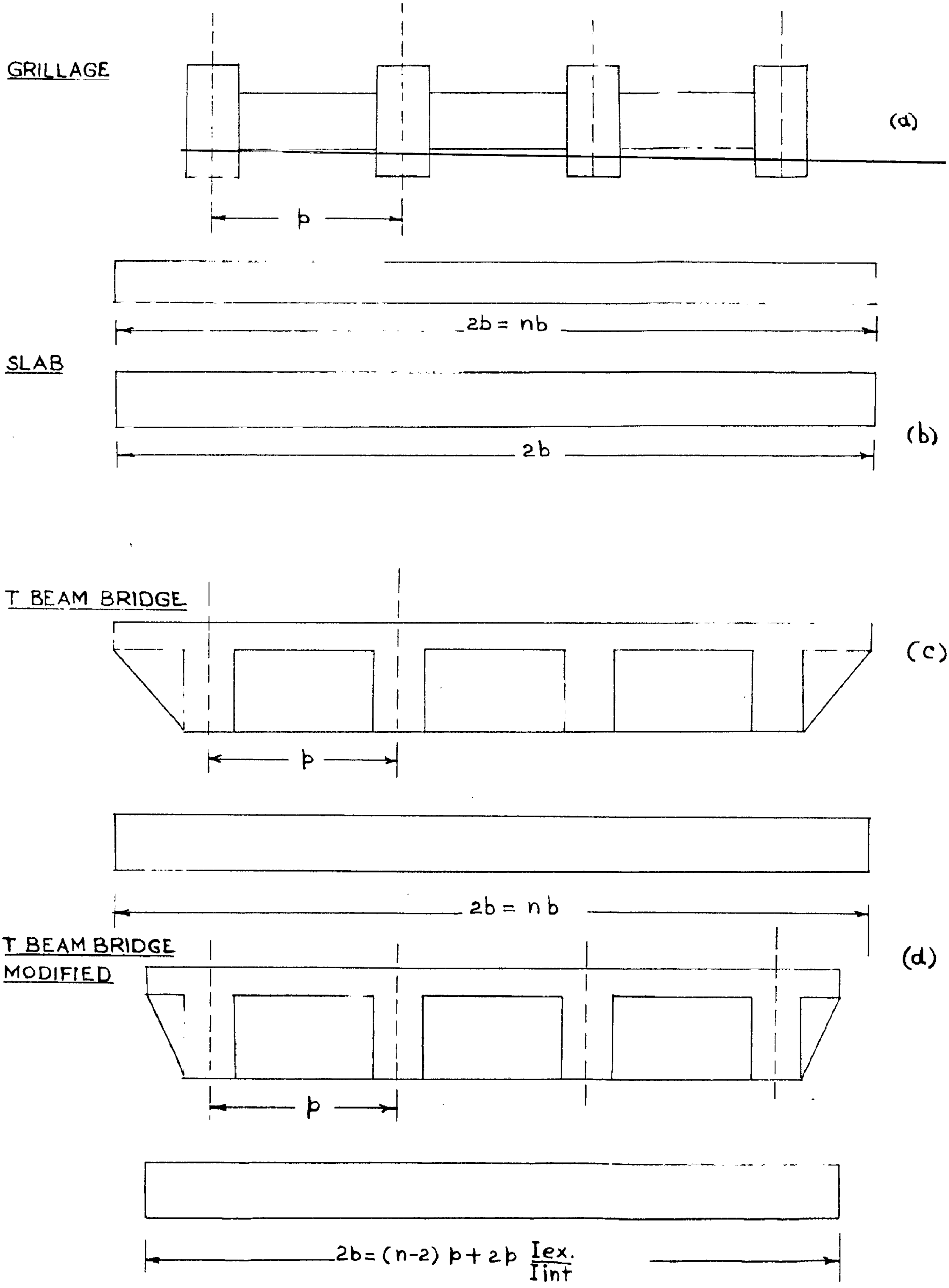

FIG 2·10 RELATION BETWEEN ACTUAL AND EQUIVALENT WIDTHS

(1) <u>Open grillage.</u> (Fig. 2.10a).

If I and I_T are the moment of inertias and p and q the spacings of individual longitudinal and cross beams, respectively then, if the moment of inertia is distributed, the equivalent anisotropic plate has an equivalent width 2b, given by $2b = np$ and $i_L = \frac{I}{p}$; $i_T = \frac{I_T}{q}$

(2) <u>Slab Bridge.</u> (Fig. 2.10 b)

The equivalent width obviously equals the actual width and $i_L = i_T = \frac{h^3}{12}$

(3) <u>T-Bea-m Bridge.</u> (Fig. 2.10c and d)

In a T-beam bridge , the equivalent width and the actual width are identical provided the edge members have flanges which cantilever out for half the beam spacing as shown in Fig. (2.10c). Where this is not the case, the effective width is simply deduced from the ratio of the moment of inertias of an edge and an internal member as given by

$$2b = (n-2)p + \frac{2\,I_{ex}}{I_{in}}\,p$$ and

$$i_L = I/p \ ; \qquad i_T = \frac{I_T}{q}$$ as for open grillage.

Where, I and I_T are moment of inertias of one of the T-beams with flange width s equal to the spacing p and q respectively.

In this connection, it should be noted that since the equivalent anisotropic plate is being derived, no restriction on flange width applies; further with regard to the cross-beams it should always be assumed that cross beams are provided at the supports. These support diaphrams are essential ensuring distribution of load and in sustaining the bearing stresses; the presence of these support beams is implied in the previous theoretical analysis.

Thus the flexural parameter θ is function of

1) the plan dimensions of the bridge i.e. b, c, p & q.
2) flexural stiffness in the longitudinal direction and
3) flexural stiffness in the transverse direction.

For most practical bridge structures in concrete the flexural parameter θ lies in the range 0.3 to 1.0. For a slab bridge θ is equal to $\frac{b}{2a}$ since $\frac{i_L}{i_T} = 1$. In a box section bridge θ also equals $\frac{b}{2a}$ since i_L and i_T are virtually equal.

(ii) <u>Torsional Parameter α :</u>

The torsional parameter α is given by

$$\alpha = \frac{\gamma_P + \gamma_E}{2\sqrt{\rho_P \rho_E}} = \frac{G}{2E} \frac{(j_L + j_T)}{\sqrt{i_L i_T}} \qquad (2.59)$$

where j_L and j_T = equivalent distributed torsional inertias of longitudinals and transversals per unit width respectively.

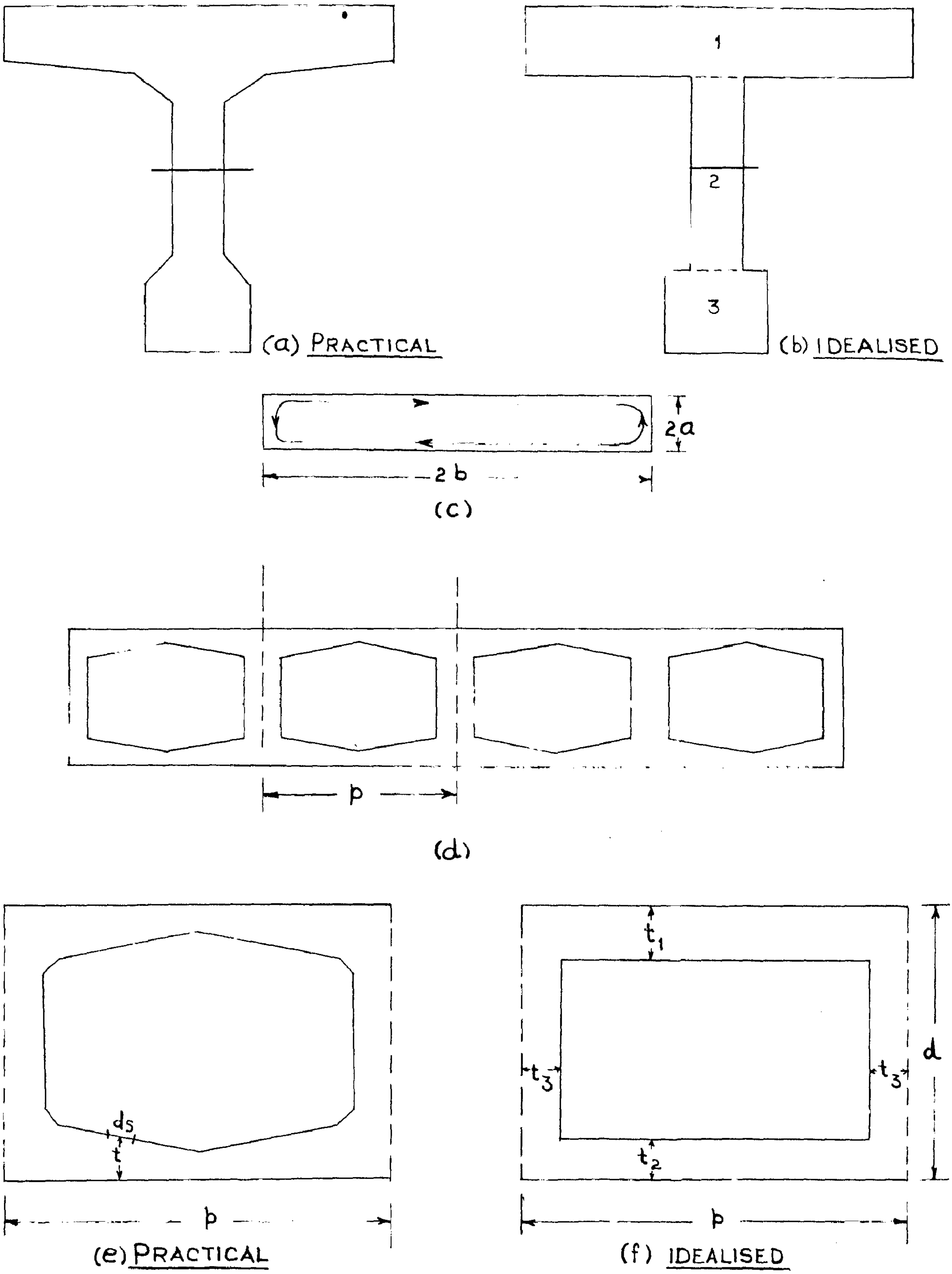

FIG. 2·11 - PRACTICAL & IDEALISED SECTIONS FOR DERIVATION OF TORSIONAL PARAMETER

For reinforced and prestressed concrete, Poisson's ratio is taken as 0.15; hence $\frac{G}{E} = 0.435$. If the torsional inertia of the longitudinal and transverse members are J and J_T respectively, then

$$j_L = \frac{J}{p} \; ; \qquad j_T = \frac{J_T}{q}$$

In determining the torsional parameter α the main problem lies in finding the values J and J_T and approximate values of α are used by using simplified theories. Examples of various types of sections are now considered.

(i) T-beam section. (Fig. 2.iia) shows a practical T-beam section and Fig. 2.iib shows an idealised section consisting of three rectangular areas. The torsional stiffness of a rectangular area of width 2a and length 2b is given by

$$\text{Torsional stiffness} = k\,(2a)^3 .\, 2b .\, G \quad \text{------}(2.60)$$

where k is a constant depending on the value of ratio $\frac{b}{a}$. The values of k are given in Table 2.1

Table No.21.

b/a	k	b/a	k	b/a	k
1.0	0.141	2.0	0.229	4.0	0.281
1.2	0.166	2.25	0.240	5.0	0.291
1.5	0.196	2.50	0.249	10.0	0.312
1.75	0.213	3.0	0.263	∞	0.333

In a section comprising of a number of rectangles it is logical that the overall torsional stiffness is equal to the sum of the torsional stiffnesses of individual rectangles. This is perfectly true but in load distribution procedure what is required is the equivalent torsional stiffness of anisotropic plate and torsional parameter α as function of this torsional stiffness. Hence, it is not correct to isolate an individual T-beam in a T-beam bridge and determine α in this way; if this is done the value α so derived will be greater than unity, which is impossible. This is due to the fact that the top flange of the T-beam , which is a part of continuous slab does not satisfy the equation (2.60) as equation (2.60) assumes the shear flow in the section as shown in Fig.(2.11c). If the shear stresses at ends of the rectangle which have a large lever arm are neglected the value of the torsional stiffness will be half of that given by eq.(2.60).

In a T-beam bridge, in each individual T-beam only the shear stresses parallel to the top surface can exist and if an individual T-beam is isolated, then top flange contributes only 50% of torsional stiffness or inertia found from equation (2.60). Thus torsional inertia is given by

$$J = \frac{1}{2} k_1 (2a_1)^3 2b_1 + K_2 (2a_2)^3 2b_2 + k_3 (2a_3)^3 2b_3$$

Further in reducing a practical section to idealised section, it is sufficiently accurate to make the concrete slab in two directions; let ρ_P and ρ_E are the flexural rigidities of an isotropic slab, increased in the ratio $l = \frac{\rho_P}{D}$ and $m = \frac{\rho_E}{D}$ respectively, where $D = \frac{Eh^3}{12(1-\nu^2)}$. Neglecting torsional rigidities of I beams, consider equation (2.30a)

$$(\gamma_P + \gamma_E) = 2(2\gamma + \rho_t) = 2\alpha\sqrt{\rho_P \rho_E} \qquad \text{where } \gamma = \frac{Gh^3}{12};$$

$$\rho_t = \frac{\nu Eh^3}{12(1-\nu^2)} \quad \text{and } \nu_x = \nu_y = \nu \text{ in case of isotropy.}$$

Substituting $G = \frac{E}{(2(1+\nu))}$ and $\rho_P = l_D$ and $\rho_E = mD$,

α is given by

$$\alpha = \frac{1}{\sqrt{lm}} \qquad \ldots\ldots (2.61)$$

Expression (2.61) also considers the effect of Poisson's ratio.

Apa-rt from the above three cases, for almost all practical sections equation (2.60) can be conveniently used.

The values of torsional parameters in a T-beam bridge are very less due to smaller torsional stiffness of T-section.The range of values of α is from 0.05 to 0.15. The behaviour of box section is similar to that of an isotropic slab and the values of α are usually in the range 0.5 to 0.8.

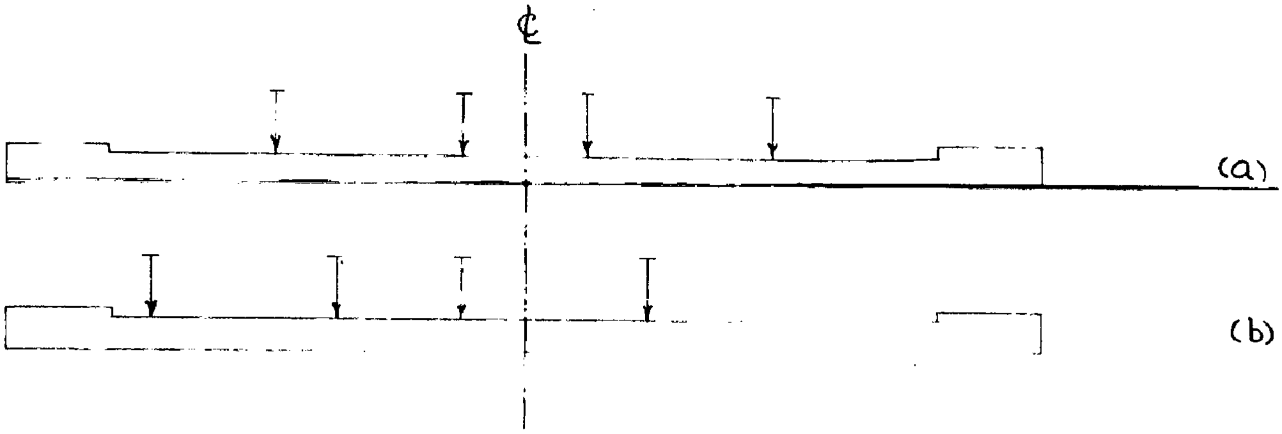

FIG. 2·12 LOADS ON A BRIDGE CROSS SECTION

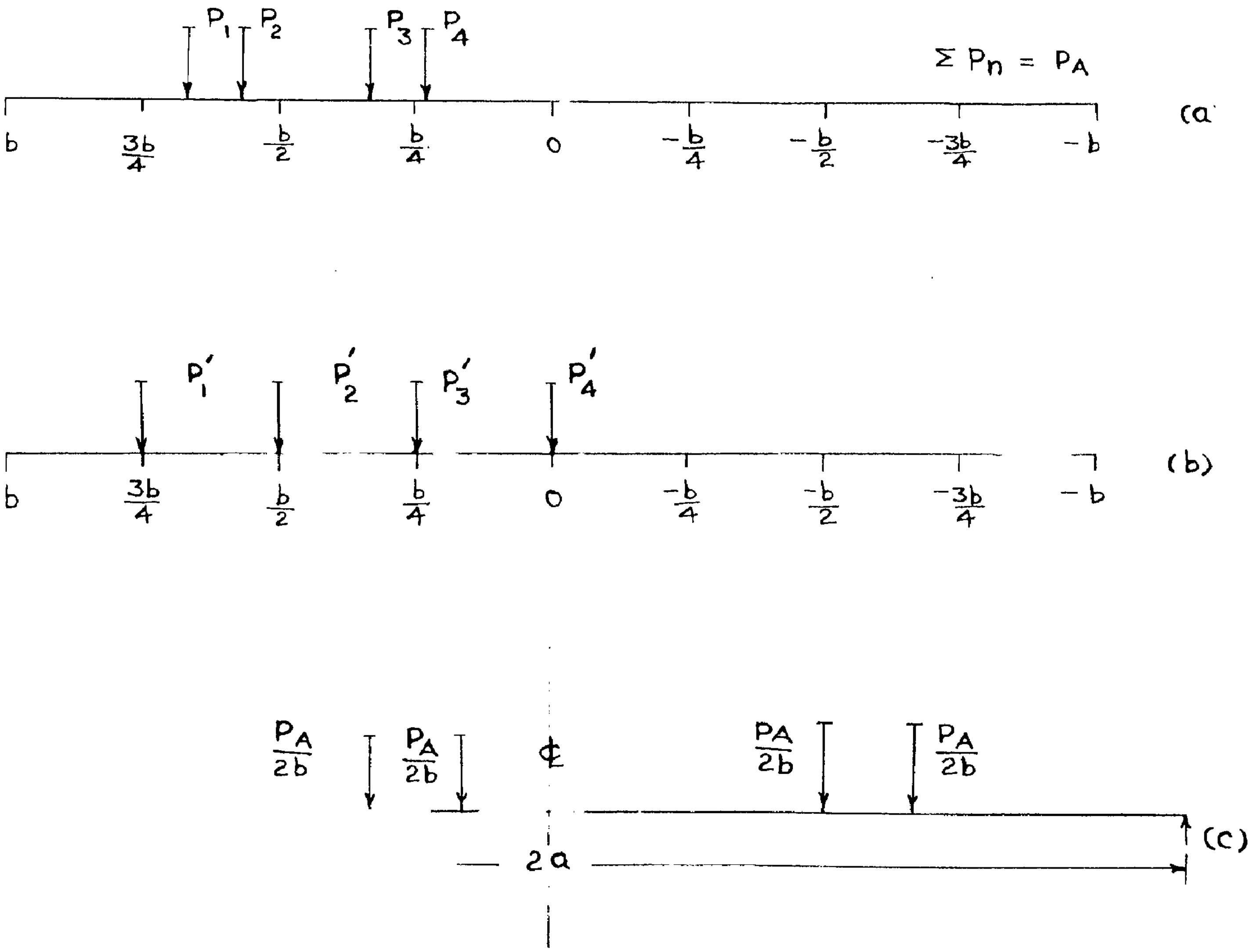

FIG. 2.13

2.2.8 Method of Calculation of the Deflections Bending Moments, Shear Forces and Reactions in a bridge due to Actual Vehicle Loads.

(1) Longitudinal Bending Moment and Deflection.

Consider a general case of a bridge loaded by a series of vehicles in a line, and call, P_1 , P_2 —— P_n. as the concentrated wheel loads of axles in the same file situated at definite transverse section of the abscissa ξ (Fig. 2.12). If m (x) is the bending moment at x in a simply supported beam of same span as bridge due to a unit load placed at the abscissa ξ , then the mean bending moment per unit width due a concentrated force $P(\xi,\eta)$ is equal to $\frac{m(x)\ P\ (\xi,\eta)}{2b}$ and the longitudinal bending moment at section x of beam at y with beam spacing p, is equal to $\frac{p}{2b}$ m(x) K(y, η) P (ξ, η). The group of loads P_1 to P_n in the same file at abscissa ξ will then produce a bending moment at x in a beam at y as

$$M_{x\,(y)} = \frac{p}{2b}\, m(x) \sum_{\eta=-b}^{\eta=+b} P(\xi,\eta)\, K(y,\eta) \qquad \text{....(2.62)}$$

For obtaining maximum bending moment, the group of loads must be placed transversely on the bridge in a definite position. Fig.(2.12 a) shows the position of loads which produce maximum bending moments in central beams and Fig.(2.12 b) shows the position of loads which produce the of vehicles are thus precisely defined and can be related to the equivalent width 2b as shown in Fig. (2.13a). The wheel loads do not, in general, coincide with the standard positions; they are, therefore, replaced by equivalent loads at the standard positions so that the values of K_0 and K_1 can be used conveniently. This is done by simple assumption; for each wheel load the equivalent loads at the adjacent standard positions are the reactions of simply supported beam of span $\frac{b}{4}$. The loads are thus P_1', P_2', P_3' and P_4' (Fig. 2.13b) where $\sum_{n=1}^{n} P_n = \sum_{n=1}^{n} P_n' = P_A$ and P_A is the total axle load.

In each of the two tables prepared for K_0 and K_1 for particular reference station, the rows appropriate to equivalent loads are multiplied by the loads P_1', P_2', P_3', P_4'. Since all these loads act simultaneously, the four rows of coefficients so derived are added up to obtain $\sum P_K$. The resulting coefficients are appropriate to a single axle with total load P_A. For unit axle load the resulting coefficients are divided by P_A. The interpolation formula (2.40) is then applied to the nine values of K_0 and K_1 resulting from this process to obtain distribution coefficients K_α for a single axle load.

If similar axle loads are acting along the longitudinal line of the bridge, the distribution profile remains constant along the span and it only remains to consider the mean effects caused by assuming that each axle load is replaced by a line load uniformly distributed the bridge in almost all the cases, and therefore those curves relevant to standard position O are required. The maximum value of My occurs when the load is applied near to the centre of the transverse section of the bridge. This is opposite to the case of the longitudinal moment which has its maximum value when the load is at a position of maximum eccentricity with respect to the longitudinal axis.

For a concentrated load P acting at C on a simply supported beam Fig. (2.14a) the load term $p_m = \frac{P}{a} \sin \frac{m\pi c}{2a}$. As the convergency in the case of transverse moments is not sufficient to allow an accurate assessment to be made with only one term, the expression for My used, is

$$M_y = \frac{Pb}{a}\left(\mu_{\alpha(1)} \sin\frac{\pi c}{2a} \sin\frac{\pi x}{2a} + \mu_{\alpha(2)} \sin\frac{2\pi c}{2a} \sin\frac{2\pi x}{2a} + \cdots\cdots + \mu_{\alpha}(m) \sin\frac{m\pi c}{2a} \sin\frac{m\pi x}{2a} + \cdots\cdots\right) \qquad \text{....(2.63a)}$$

The term $\sin \frac{m\pi x}{2a}$ refers to the transverse section at which the transverse moment is required. The critical section is at mid span i.e. x = a. Thus

$$M_y = \frac{Pb}{a}\left(\mu_{\alpha(1)} \sin\frac{\pi c}{2a} - \mu_{\alpha(3)} \sin\frac{3\pi c}{2a} + \mu_{\alpha(5)} \sin\frac{5\pi c}{2a} + \cdots\cdots\right) \qquad \text{....(2.63b)}$$

as even terms have cancelled out. Further the coefficients μ_α (m) is the value of μ_α for a bridge of flexural parameter mθ from graphs 12 to 31. Thus the transverse bending moment

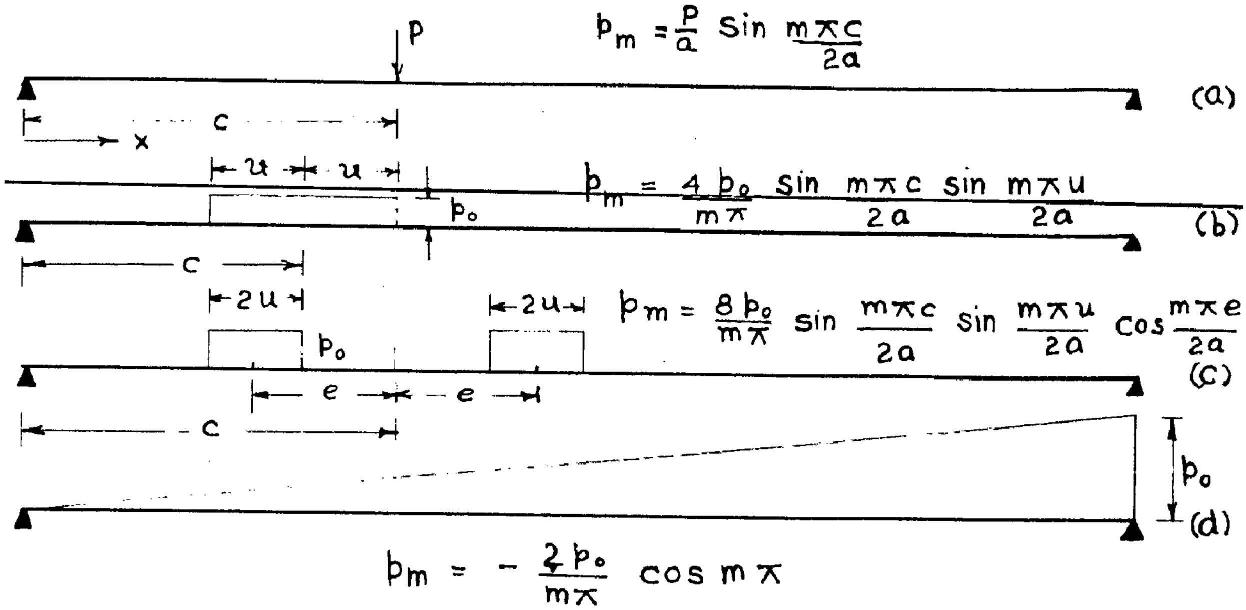

FIG. 2·14 FOURIER SERIES TERMS FOR VARIOUS LOADINGS.

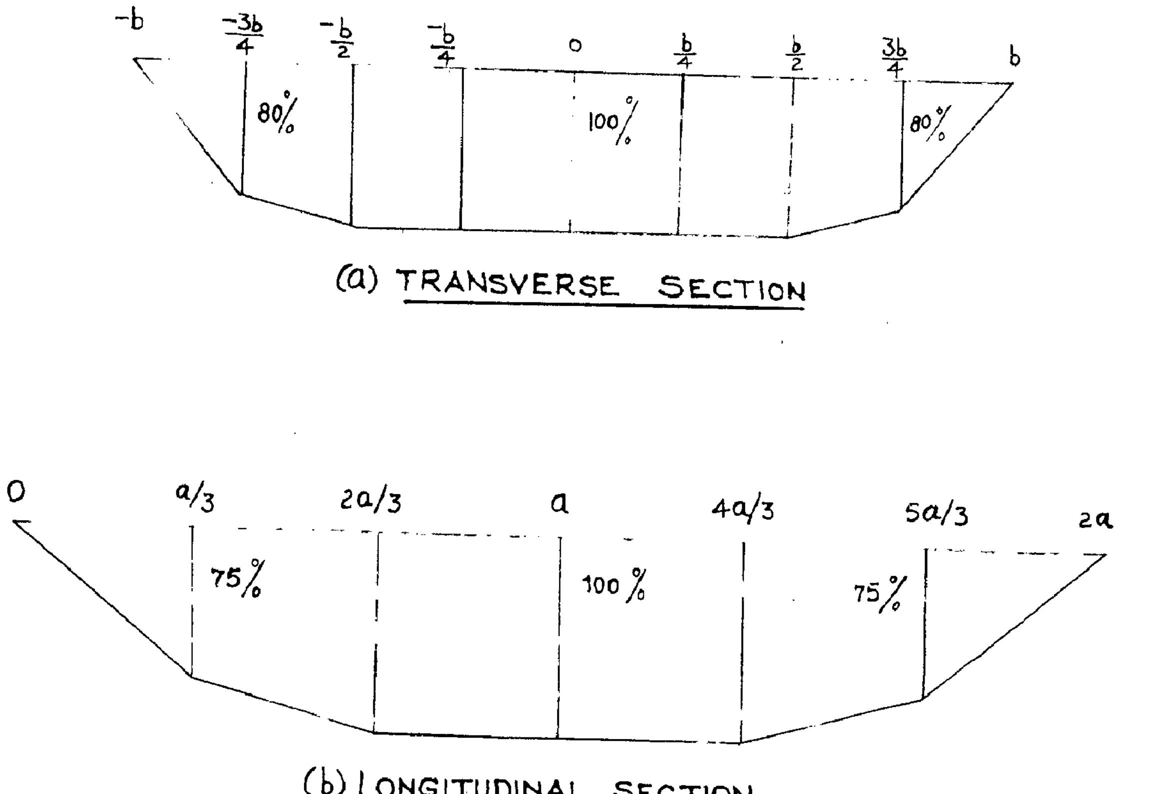

FIG. 2·15 APPROXIMATE TRANSVERSE AND LONGITUDINAL DISTRIBUTION OF (M_y) MAX.

at mid span due to a concentrated load can be rewritten as

$$M_y = \frac{Pb}{a}\left(\mu_{\alpha(\theta)} \sin\frac{\pi c}{2a} - \mu_{\alpha(3\theta)} \sin\frac{3\pi c}{2a} + \mu_{(\alpha)(5\theta)} \sin\frac{5\pi c}{2a} + \cdots\cdots \right) \qquad \ldots(2.63c)$$

It is sufficiently accurate to consider first three terms as for large values of θ, μ_α tends to zero.

If there are two lines of load moving having positions c' and c'', the resultant value of M_y is found by superposition. Thus

$$M_y = M_y(c') + M_y(c'') \qquad \ldots(2.64a)$$

For any value of α, using equations (2.53), (2.63) and (2.64a), the transverse bending moment is given by interpolation expression

$$M_{y\alpha} = M_{y_0} + (M_{y_1} - M_{y_0})\sqrt{\alpha} \qquad \ldots.(2.64b)$$

where M_{y_0} and M_{y_1} are calculated from the values of μ_0 and μ_1 in graphs 12 to 21.

For distributed loads the Fourier series terms for various types of loading are given in Fig. (2.14 b to d) and the calculations for these cases can be done in the same way as for concentrated loads.

The details of calculation for concentrated loads are given for I.R.C. class AA loading for wheeled vehicle in example 3 of section 2.3.

The procedure developed above is applicable only for the determination of maximum sagging transverse moment. The maximum hogging transverse moment occurs for the eccentric positions of the vehicle but their magnitudes are considerably less than the maximum sagging moment. Using all graphs 12 to 19 for μ , MORICE and LITTLE[27] have shown that for abnormal loading of Ministry of Transport England the max. hogging moment does not exceed the value of 10% of the maximum sagging moment. After carrying out a detailed analysis for transverse moment they have also shown for abnormal loading the approximate distribution of My along the transverse and longitudinal directions. For design purposes it is suggested that

(i) for varying positions of vehicles, the maximum sagging transverse moments in a transverse section approximately vary as shown in Fig(2.15a) and

(2) for varying position of section along longitudinal direction the maximum sagging transverse bending moments approximately vary as shown in Fig. 2.15b.

(iii) <u>Distribution of Shear Force and Reaction.</u>

Taking the expressions of T and T from eq. 2.29a and re-writing them as

$$\left.\begin{aligned} T_x &= -\rho_P \frac{\partial^3 w}{\partial x^3} + \alpha\sqrt{\frac{\rho_P}{\rho_E}}\;\frac{\partial}{\partial x}\left(-\rho_E \frac{\partial^2 w}{\partial y^2}\right) \\ T_y &= -\rho_E \frac{\partial^3 \omega}{\partial y^3} + \alpha\sqrt{\frac{\rho_P}{\rho_E}}\;\frac{\partial}{\partial y}\left(-\rho_P \frac{\partial^2 \omega}{\partial x^2}\right) \end{aligned}\right\} \quad ..(2.65)$$

Consider first term of the Fourier series for the load, the deflection and transverse moment are written as

$$w_1 = \frac{16a^4}{\pi^4 \rho_P} \frac{p_1}{2b} \sin\frac{\pi x}{2a} K_\alpha$$

$$M_{y_1} = -\rho_E \frac{\partial^2 \omega_1}{\partial y^2} = \mu'_\alpha \, b p_1 \sin\frac{\pi x}{2a}$$

Therefore, equation 2.65 can be written as

$$T_{x_1} = \frac{2a}{\pi} \frac{p_1}{2b} \left(K_{\alpha(1)} + 2\alpha \theta^2 \pi^2 \mu'_{\alpha(1)}\right) \cos\frac{\pi x}{2a}$$

$$T_{y_1} = \sqrt{\frac{\rho_E}{\rho_P}} \frac{4a^2}{\pi^2} \frac{p_1}{2b} \sin\frac{\pi x}{2a} \frac{\partial}{\partial y}\left(2\theta^2 \pi^2 \mu'_{\alpha(1)} + \alpha K_{\alpha(1)}\right) \quad \ldots (2.65a)$$

where μ'_α is the distribution coefficient for the transverse moments assuming Poisson's ratio as zero.

The complete expression for T_x is therefore

$$T_x = \sum_{m=1}^{\infty} \frac{2a}{m\pi} \frac{p_m}{2b} \cos\frac{m\pi x}{2a} \left\{K_{\alpha(m\theta)} + 2\alpha (m\theta)^2 \pi^2 \mu'_{\alpha(m\theta)}\right\}$$

$$\ldots (2.66)$$

For $\alpha = 0$

$$T_x = \sum_{m=1}^{\infty} \frac{2a}{m\pi} \frac{p_m}{2b} \cos\frac{m\pi x}{2a} K_0(m\theta).$$

At supports i.e. $x = 0$ and $x = 2a$, the reaction V_x is given by

$$V_x = T_x - \frac{\partial M_{xy}}{\partial y} \quad \text{where} \quad M_{xy} = \alpha\sqrt{\rho_P \rho_E} \frac{\partial^2 \omega}{\partial x \partial y}$$

For the first term of the load series

$$\frac{\partial M_{xy}}{\partial y} = -\alpha\sqrt{\frac{\rho_P}{\rho_E}}\ \frac{\partial}{\partial x}\left(-\rho_E\frac{\partial^2 \omega_1}{\partial y^2}\right) = -\alpha\sqrt{\frac{\rho_P}{\rho_E}}\ \frac{\pi}{2a}\ \mu'_\alpha$$

$$p_1 b \cos\frac{\pi x}{2a} \quad = -\frac{2a}{\pi}\ \frac{p_1}{2b}\left(2\alpha\theta^2\pi^2\mu'_\alpha\right)\cos\frac{\pi x}{2a}$$

and therefore,

$$V_{x_1\,(x=0 \text{ or } x=2a)} = \pm\ \frac{2a}{\pi}\ \frac{p_1}{2b}\left(K_\alpha + 4\alpha\theta^2\pi^2\mu'_\alpha\right)$$

....(2.67a)

The complete series for V_x is, therefore, given by

$$V_{x\,(x=0)} = \sum_{m=1}^{\infty}\frac{2a}{m\pi}\ \frac{p_m}{2b}\left\{K_\alpha(m\theta) + 4\alpha(m\theta)^2\pi^2\mu'_\alpha(m\theta)\right\}$$

$$V_{x\,(x=2a)} = \sum_{m=1}^{\infty}(-1)^m\frac{2a}{m\pi}\ \frac{p_m}{2b}\left\{K_\alpha(m\theta) + 4\alpha(m\theta)^2\pi^2\mu'_\alpha(m\theta)\right\}$$

...(2.67b)

For $\alpha = 0$

$$V_{x1} = \pm\ \frac{2a}{\pi}\ \frac{p_m}{2b}\ K_o$$

The calculation of the shear forces and reactions using the formulae derived above can be done for actual vehicle loads.

For shear T_x, the two positions producing the maximum longitudinal and transverse bending moments on a transverse section already discussed above are critical for concentrated load vehicle. From these two position distribution profile for K_α and μ'_α are obtained. For μ'_α the interpolation formula given by MASSONNET(10,37) for μ'

may be taken as $\mu'_\alpha = \mu_0 + (\mu'_1 - \mu_0)\sqrt{\alpha}$

Obviously a number of terms in the series given by equation (2.66) are considered.

The reaction V_x is derived directly from equation 2.67(b) using the two critical profiles for K and μ'_α. For V_x upto 3 terms of the load series are normally considered.

For shear T_y as equation (2.65a) shows, T_y cannot be obtained directly from the values of K_α and μ'_α but depends on the differential with respect to y of the distribution profiles for K_α and μ'_α. This differentiation is normally done graphically.

2.3. EXAMPLES OF GRID BEAM BRIDGES.

Numerical examples which are solved by using the graphs 1 to 21, indicate the validity and easy application of the anisotropic plate theory developed in sections 2.1 and 2.2. Considering the extreme cases of open bridge grillages, numerous examples for wide range of parameters are solved and a comparison of values thus obtained is made with exact values. In example 1 no torsion bridge grillages with three, four and six main beams and one cross beam for $\theta = 1$, $\theta = 0.5$ and $\theta = 0.25$, and unit load applications at different beams are solved. In example 2 torsionally resistant open grid beam bridges with four main beams and three cross beams for $\theta = 1.0$, $\theta = 0.5$, $\alpha = .04$, and $\alpha = 0.64$ are solved. Example 3

FIG. 2·16

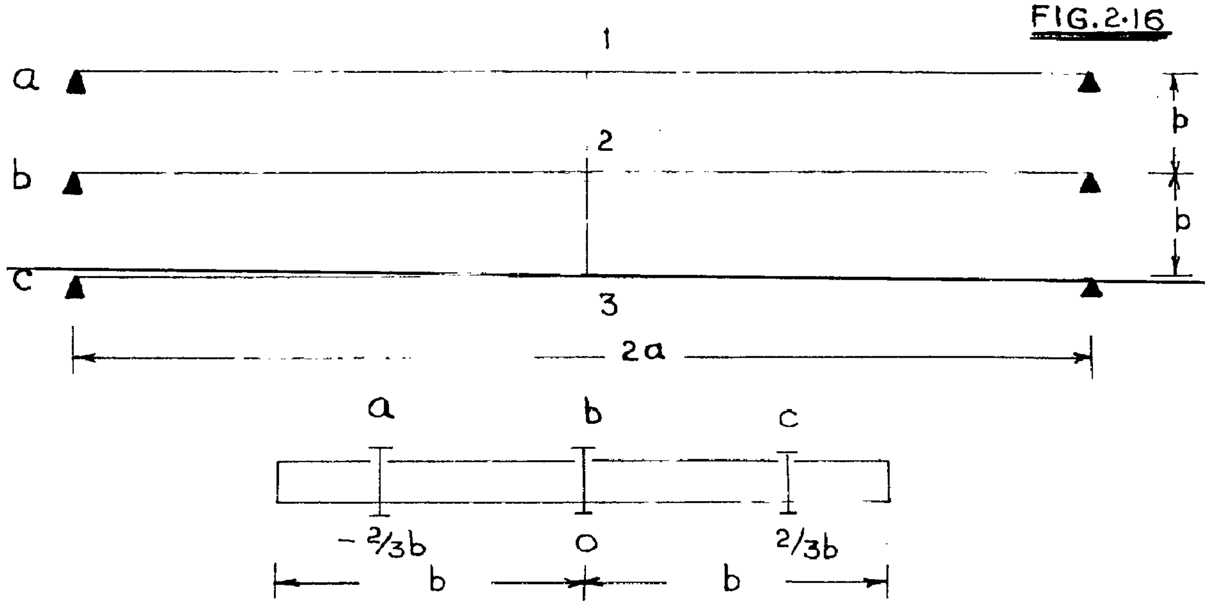

(a) THREE GIRDER BRIDGE

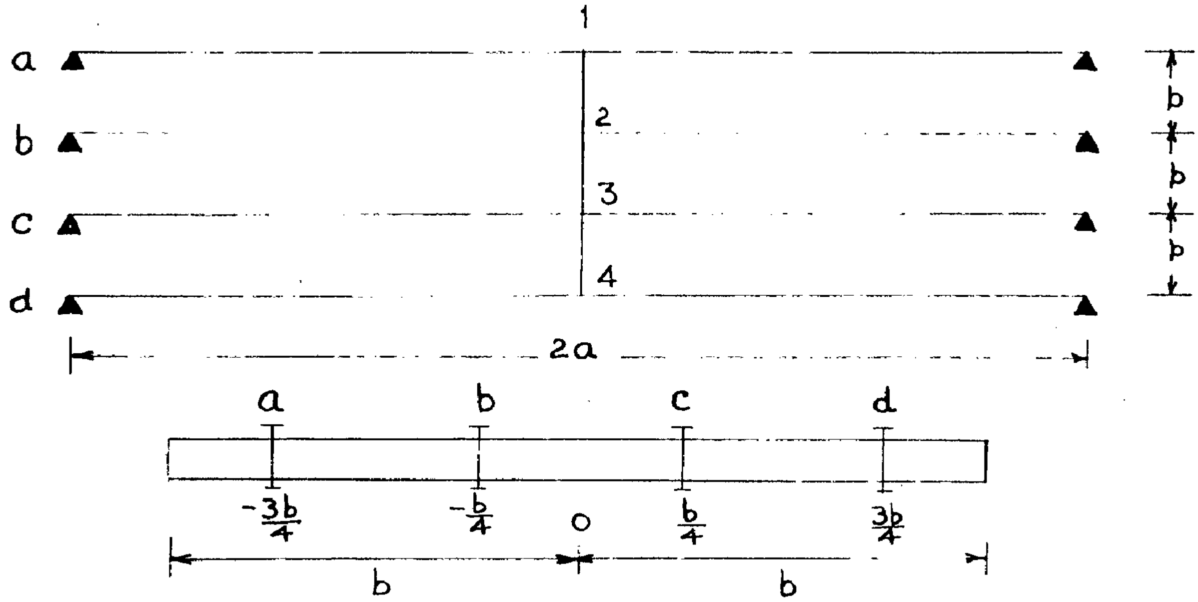

(b) FOUR GIRDER BRIDGE

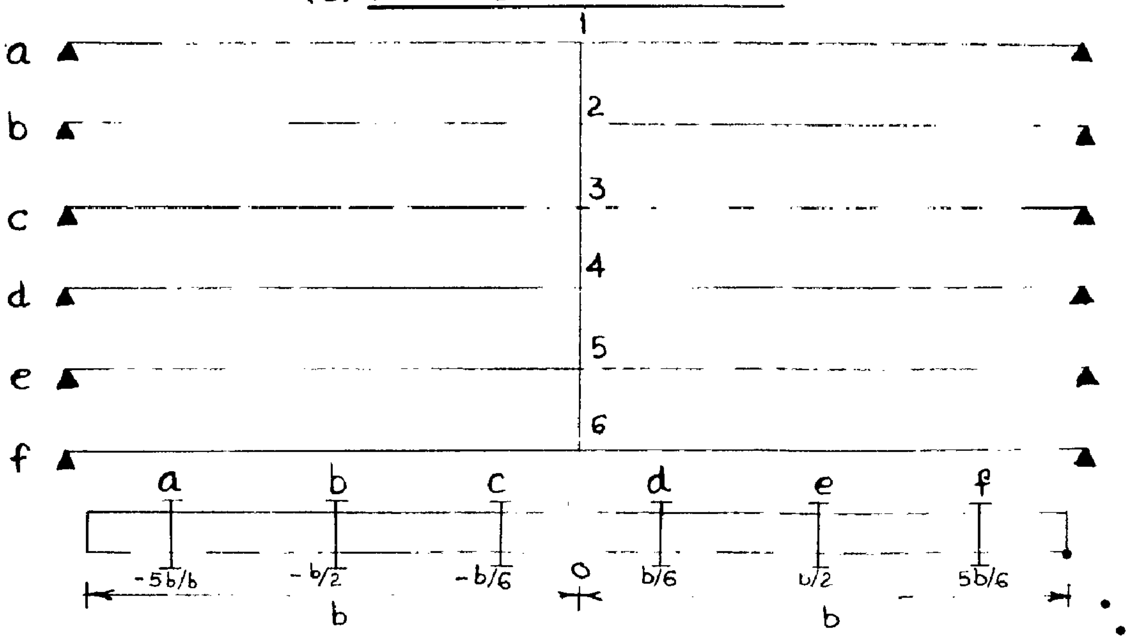

(C) SIX GIRDER BRIDGE

shows the method of calculation of bending moments in longitudinal and cross beams in a simply supported four girder bridge of 40' span and 22' roadway with three cross beams. The calculations are made for I.R.C. class AA loading wheeled vehicle of 40 tons and the critical positions for maximum longitudinal moment and maximum transverse moment are indicated.

2.3.1. Example on No Torsion Bridge Grillages ($\alpha = 0$)

Three cases of three, four and six girder bridge grillages with one cross beam are taken for analysis. Changing the relative stiffness of longitudinal and cross-beams adequately to obtain the flexural parameter θ defined by equation 2.58 as 1.0, 0.5, and 0.25, the ordinates of K_o are tabulated from graphs 1 to 6 for $\theta = 1.0$, $\theta = 0.5$ and $\theta = .25$ in tables 2.2 to 2.4. While tabulating the values of K_o, the Maxwell's theorem i.e. $K_{ij} = K_{ji}$ and $\int_{-b}^{+b} K_o dy = 2b$ are considered, to gaurd against any possible error in reading the graphs.

(a) Bridge grillage with three main beams.

Consider a bridge grillage with three main beams and one cross beam at the centre as shown in Fig.2.16(a), the dimensions taken are 2a = 54.0 ft. p = 12.0 ft.

$$\therefore 2b = np$$

$$= 36.0$$

$$q = 27.0 \text{ ft.}$$

Let I and I_T are the moment of inertias of longitudinal and cross beams respectively. When the unit load is applied at 1 (fig. 2.16a), the distribution of load for this open grillage is found out exactly in terms of parameter $\lambda = \left(\frac{b}{a}\right)^3 \frac{I}{I_T}$ by flexibility method and using symmetry and antisymmetry of the load and deformations. The complete results, thus obtained, are shown in Table 2.5(a).

While solving this problem of open grillage by approximate method of anisotropic plate theory, when θ given by $\frac{b}{2a}\sqrt[4]{\frac{I/p}{I_T/q}}$ is

$$\theta = 1.0 \; ; \; \frac{I}{I_T} = 36 \quad \text{and} \quad \lambda = \frac{256}{81}$$

$$\theta = 0.5 \; ; \; \frac{I}{I_T} = \frac{9}{4} \quad \text{and} \quad \lambda = \frac{16}{81}$$

$$\theta = 0.25 \; ; \; \frac{I}{I_T} = \frac{9}{64} \quad \text{and} \quad \lambda = \frac{1}{81}$$

It is interesting to note that for a case of one cross girder at the centre.

$$\lambda = \frac{256}{n^4} \times \theta^4 \qquad \ldots (2.68)$$

where,

n = Number of main beams

thus for $n = 3$,

$$\lambda = \frac{256}{81}\,\theta^4$$

Also if s denotes the ratio of span and equivalent width of anisotropic plate i.e. $\frac{a}{b}$, then for a case of one cross girder at the centre

$$\frac{I}{I_T} = \frac{32}{n}\, s^3\, \theta^4 \qquad \ldots (2.69)$$

TABLE 2.2

VALUES OF DISTRIBUTION COEFFICIENTS K_0 AND K_1 FOR $\theta = 1.0$

REFERENCE STATION		LOAD POSITION									
		-b	-3b/4	-b/2	-b/4	0	b/4	b/2	3b/4	b	Σ
K_0	0	-0.70	0.17	1.00	1.90	2.33	1.90	1.00	0.17	-0.70	0.993
	b/4	-0.52	-0.14	0.38	1.07	1.90	2.37	1.82	0.86	-0.24	1.003
	b/2	-0.35	-0.17	0.01	0.38	1.00	1.82	2.41	1.98	1.24	0.990
	3b/4	-0.07	-0.15	-0.17	-0.14	0.17	0.86	1.98	3.54	4.45	0.999
	b	0.16	-0.07	-0.35	-0.52	-0.70	-0.24	1.24	4.45	9.00	1.001
K_1	0	0.47	0.64	0.94	1.35	1.62	1.35	0.94	0.64	0.47	0.994
	b/4	0.24	0.36	0.56	0.89	1.35	1.67	1.45	1.10	0.85	0.995
	b/2	0.13	0.21	0.33	0.56	0.94	1.45	1.87	1.77	1.55	0.997
	3b/4	0.07	0.12	0.21	0.36	0.64	1.10	1.77	2.42	2.66	0.999
	b	0.03	0.07	0.13	0.24	0.47	0.85	1.55	2.66	4.20	0.992

TABLE 2.3

VALUES OF DISTRIBUTION COEFFICIENTS K_0 AND K_1 FOR $\theta = 0.5$

REFERENCE STATION		LOAD POSITION									
		-b	-3b/4	-b/2	-b/4	0	b/4	b/2	3b/4	b	Σ
K_0	0	0.55	0.785	1.01	1.22	1.325	1.22	1.01	0.785	0.55	0.993
	b/4	0.00	0.305	0.63	0.96	1.22	1.38	1.42	1.40	1.385	1.005
	b/2	-0.54	0.18	0.22	0.63	1.01	1.42	1.81	2.075	2.31	0.985
	3b/4	-0.96	0.55	-0.18	0.305	0.785	1.40	2.075	2.85	3.55	1.000
	b	-1.43	-0.96	-0.54	+0.00	0.55	1.385	2.31	3.55	4.70	0.992
K_1	0	0.86	0.93	1.00	1.08	1.13	1.08	1.00	0.93	0.86	1.003
	b/4	0.68	0.76	0.85	0.96	1.08	1.15	1.15	1.12	1.08	0.995
	b/2	0.55	0.63	0.73	0.85	1.00	1.15	1.29	1.35	1.38	0.995
	3b/4	0.45	0.54	0.63	0.76	0.93	1.12	1.35	1.58	1.75	1.009
	b	0.38	0.45	0.55	0.68	0.86	1.08	1.38	1.75	2.15	0.993

TABLE 2.4

VALUES OF DISTRIBUTION COEFFICIENT K_o FOR $\theta = 0.25$

REFERENCE STATION		LOAD POSITION -b	-3b/4	-b/2	-b/4	0	b/4	b/2	3b/4	b	Σ
K_o	0	0.90	0.96	0.97	1.05	1.08	1.05	0.97	0.96	0.90	0.997
	b/4	0.22	0.41	0.635	0.855	1.05	1.21	1.35	1.54	1.70	1.001
	b/2	-0.535	-0.155	0.245	0.635	0.97	1.55	1.73	2.10	2.48	0.982
	3b/4	-1.17	-0.64	-0.155	0.41	0.96	1.54	2.10	2.71	3.28	0.998
	b	-1.84	-1.17	-0.535	0.22	0.90	1.70	2.48	3.28	4.05	1.001

NOTE: $\Sigma = \frac{1}{3} \times \frac{b}{4} \times \frac{1}{2b} \left\{ K_{-b} + K_b + 2 (K_{-b/2} + K_o + K_{b/2}) + 4 (K_{-\frac{3b}{4}} + K_{-\frac{b}{4}} + K_{\frac{b}{4}} + K_{\frac{3b}{4}}) \right\}$

TABLE 2.5

(a) THREE GIRDER GRILLAGE

	k_a		k_b		k_c	
LOAD AT	SYMM.	ASYMM.	SYMM.	ASYMM.	SYMM.	ASYMM.
a (1)	$\frac{\lambda+1}{2\lambda+3}$	+0.50	$\frac{1.0}{2\lambda+3}$	0.0	$\frac{\lambda+1}{2\lambda+3}$	-0.50
b (2)	$\frac{1.0}{2\lambda+3}$	—	$\frac{2\lambda+1}{2\lambda+3}$	—	$\frac{1.0}{2\lambda+3}$	—

(b) FOUR GIRDER GRILLAGE

	k_a		k_b	
LOAD AT	SYMMETRICAL	ASYMMETRICAL	SYMMETRICAL	ASYMMETRICAL
a (1)	$\frac{2.5\lambda+0.5}{5\lambda+2}$	$\frac{1.5\lambda+4.5}{3\lambda+10}$	$\frac{0.5}{5\lambda+2}$	$\frac{1.5}{5\lambda+10}$
b (2)	$\frac{0.5}{5\lambda+2}$	$\frac{1.5}{3\lambda+10}$	$\frac{2.5\lambda+0.5}{5\lambda+2}$	$\frac{1.5\lambda+0.5}{3\lambda+10}$
	k_c		k_d	
a (1)	$\frac{0.5}{5\lambda+2}$	$\frac{-1.5}{3\lambda+10}$	$\frac{2.5\lambda+0.5}{5\lambda+2}$	$-\frac{1.5\lambda+4.5}{3\lambda+10}$
b (2)	$\frac{2.5\lambda+0.5}{5\lambda+2}$	$-\frac{1.5\lambda+0.5}{3\lambda+10}$	$\frac{0.5}{5\lambda+2}$	$-\frac{1.5}{3\lambda+10}$

TABLE 2·5 (c)

SIX GIRDER GRILLAGE

LOAD AT	K_a Symmetrical	K_a Asymmetrical	K_b Symmetrical	K_b Asymmetrical	K_c Symmetrical	K_c Asymmetrical
a(1)	$\frac{9.5\lambda^2+19.5\lambda+0.5}{19\lambda^2+44\lambda+3}$	$\frac{5.5\lambda^2+32.5\lambda+12.5}{11\lambda^2+68\lambda+35}$	$\frac{5.5\lambda+0.5}{19\lambda^2+44\lambda+3}$	$\frac{3.5\lambda+7.5}{11\lambda^2+68\lambda+35}$	$\frac{0.5-3\lambda}{19\lambda^2+44\lambda+3}$	$\frac{2.5-3\lambda}{11\lambda^2+68\lambda+35}$
b(2)	$\frac{5.5\lambda+0.5}{19\lambda^2+44\lambda+3}$	$\frac{5.5\lambda+7.5}{11\lambda^2+68\lambda+35}$	$\frac{9.5\lambda^2+8\lambda+0.5}{19\lambda^2+44\lambda+3}$	$\frac{5.5\lambda^2+24\lambda+4.5}{11\lambda^2+68\lambda+35}$	$\frac{8.5\lambda+0.5}{19\lambda^2+44\lambda+3}$	$\frac{12.5\lambda+1.5}{11\lambda^2+68\lambda+35}$
c(3)	$\frac{0.5-3\lambda}{19\lambda^2+44\lambda+3}$	$\frac{2.5-3\lambda}{11\lambda^2+68\lambda+35}$	$\frac{8.5\lambda+0.5}{19\lambda^2+44\lambda+3}$	$\frac{12.5\lambda+1.5}{11\lambda^2+68\lambda+35}$	$\frac{9.5\lambda^2+17.5\lambda+0.5}{19\lambda^2+44\lambda+3}$	$\frac{5.5\lambda^2+11.5\lambda+0.5}{11\lambda^2+68\lambda+35}$

LOAD AT	K_d Symmetrical	K_d Asymmetrical	K_e Symmetrical	K_e Asymmetrical	K_f Symmetrical	K_f Asymmetrical
a(1)	$\frac{0.5-3\lambda}{19\lambda^2+44\lambda+3}$	$\frac{2.5-3\lambda}{11\lambda^2+68\lambda+35}$	$\frac{5.5\lambda+0.5}{19\lambda^2+44\lambda+3}$	$\frac{3.5\lambda+7.5}{11\lambda^2+68\lambda+35}$	$\frac{9.5\lambda^2+19.5\lambda+0.5}{19\lambda^2+44\lambda+3}$	$\frac{5.5\lambda^2+32.5\lambda+12.5}{11\lambda^2+68\lambda+35}$
b(2)	$\frac{8.5\lambda+0.5}{19\lambda^2+44\lambda+3}$	$\frac{12.5\lambda+1.5}{11\lambda^2+68\lambda+35}$	$\frac{9.5\lambda^2+8\lambda+0.5}{19\lambda^2+44\lambda+3}$	$\frac{5.5\lambda^2+24\lambda+4.5}{11\lambda^2+68\lambda+35}$	$\frac{5.5\lambda+0.5}{19\lambda^2+44\lambda+3}$	$\frac{3.5\lambda+7.5}{11\lambda^2+68\lambda+35}$
c(3)	$\frac{9.5\lambda^2+17.5\lambda+0.5}{19\lambda^2+44\lambda+3}$	$\frac{5.5\lambda^2+11.5\lambda+0.5}{11\lambda^2+68\lambda+35}$	$\frac{8.5\lambda+0.5}{19\lambda^2+44\lambda+3}$	$\frac{12.5\lambda+1.5}{11\lambda^2+68\lambda+35}$	$\frac{0.5-3\lambda}{19\lambda^2+44\lambda+3}$	$\frac{2.5-3\lambda}{11\lambda^2+68\lambda+35}$

TABLE 2.6

(a) FOR $\theta = 1.0$

LOAD AT \ BEAM AT		$\frac{3}{4}$ b	$\frac{2}{3}$ b	$\frac{1}{2}$ b	0	$-\frac{1}{2}$ b	$-\frac{2}{3}$ b	$-\frac{3}{4}$ b
BEAM a	3/4 b	3.340	—	1.9800	0.1700	-0.17	—	-0.15
	1/2 b	1.9800	—	2.4100	1.0000	+0.01	—	-0.16
	2/3 b	2.8867	—	2.1233	0.4467	-0.1100	—	-0.1533
	2/3 b	—	2.6322	—	0.4467	—	-0.1389	—
BEAM b	0	0.17	—	1.00	2.33	1.00	—	0.17
	0	—	0.4467	—	2.33	—	0.4467	—

(b) FOR $\theta = 0.50$

LOAD AT \ BEAM AT		$\frac{3}{4}$ b	$\frac{2}{3}$ b	$\frac{1}{2}$ b	0	$-\frac{1}{2}$ b	$-\frac{2}{3}$ b	$-\frac{3}{4}$ b
BEAM a	3/4 b	2.84	—	2.075	0.785	-0.18	—	-0.53
	1/2 b	2.075	—	1.810	1.010	+0.22	—	-0.18
	2/3 b	2.5850	—	1.9867	0.860	-0.0467	—	-0.4133
	2/3 b	—	2.3856	—	0.860	—	-0.2911	—
BEAM b	0	0.785	—	1.010	1.325	1.01	—	0.785
	0	—	0.860	—	1.325	—	0.860	—

(c) FOR $\theta = 0.25$

LOAD AT \ BEAM AT		$\frac{3}{4}$ b	$\frac{2}{3}$ b	$\frac{1}{2}$ b	0	$-\frac{1}{2}$ b	$-\frac{2}{3}$ b	$-\frac{3}{4}$ b
BEAM a	3/4 b	2.71	—	2.10	0.96	-0.155	—	-0.64
	1/2 b	2.10	—	1.73	0.97	-0.245	—	-0.155
	2/3 b	2.51	—	1.9767	0.9633	-0.185	—	-0.4783
	2/3 b	—	2.3323	—	0.9633	—	-0.3806	—
BEAM b	0	0.960	—	0.97	1.08	0.97	—	0.96
	0	—	0.9633	—	1.08	—	0.9633	—

TABLE 2·7

THREE GIRDER GRILLAGE

LOAD AT	$k = \frac{K_c}{3}$	$\theta = 1.0$ $\lambda = 256/81$		$\theta = 0.50$ $\lambda = 16/81$		$\theta = 0.25$ $\lambda = 1/81$	
		BY GUYON'S METHOD	BY EXACT METHOD	BY GUYON'S METHOD	BY EXACT METHOD	BY GUYON'S METHOD	BY EXACT METHOD
BEAM a	k_{aa}	0·9023	0·9464	0·8123	0·8527	0·7877	0·8347
	k_{ba}	0·1453	0·1072	0·2868	0·2946	0·3225	0·3306
	k_{ca}	−0·0476	−0·0536	−0·0991	−0·1473	−0·1102	−0·1653
BEAM b	k_{ab}	0·1453	0·1072	0·2868	0·2946	0·3225	0·3306
	k_{bb}	0·7094	0·7856	0·4264	0·4108	0·3550	0·3388
	k_{cb}	0·1453	0·1072	0·2868	0·2946	0·3225	0·3306

TABLE 2·8

FOUR GIRDER GRILLAGE

LOAD AT	$k = \frac{K_o}{4}$	$\theta = 1.0$ $\lambda = 1.0$		$\theta = 0.50$ $\lambda = 1/16$		$\theta = 0.25$ $\lambda = 1/256$	
		BY GUYON'S METHOD	BY EXACT METHOD	BY GUYON'S METHOD	BY EXACT METHOD	BY GUYON'S METHOD	BY EXACT METHOD
BEAM a	R_{aa}	0·8600	0·8901	0·7091	0·7347	0·6737	0·7025
	R_{ba}	0·2133	0·1868	0·3474	0·3635	0·3834	0·3974
	R_{ca}	−0·0347	−0·0440	0·0758	0·0689	0·1020	0·0978
	R_{da}	−0·0386	−0·0529	−0·1323	−0·1671	−0·1591	−0·1977
BEAM b	R_{ab}	0·2133	0·1868	0·3474	0·3635	0·3834	0·3974
	R_{bb}	0·5659	0·5824	0·3402	0·3421	0·3016	0·3029
	R_{cb}	0·2555	0·2748	0·2366	0·2255	0·2130	0·2019
	R_{da}	−0·0347	−0·0440	0·0758	0·0689	0·1020	0·0978

for $n = 3$

and $\delta = \frac{54}{36}$

$= 1.5$,

equation 2.69 reduces to $I/I_T = 36\,\theta^4$.

Since in the plate solution the main beams are at $\pm 2/3b$ and 0, the values of K_o (from tables 2.2 to 2.4) for outer beams are linearly interpolated firstly for beam position $\pm \frac{2}{3}b$ from the values at $\pm 3/4b$ and $\pm b/2$ and subsequently once again the values obtained are linearly interpolated for load position $\frac{2}{3}b$ and 0. The calculations for $\theta = 1$, $\theta = 0.5$ and $= 0.25$ are shown in Tables 2.6 a, b and c. Dividing the values of K_o obtained in Tables 2.6 a, b and c by $n = 3 = \frac{2b}{p}$, the transverse distribution coefficient k_{ab}, k_{ba} etc. are obtained. The values thus obtained are tabulated in Table 2.7 and are compared with the exact values.

(b) Bridge grillage with four main beams.

Considering a bridge with four main beams and one cross beam at the centre as shown in fig. (2.16 b), the dimensions taken are $2a = 54.0'$

$p = 9.0'$

$\therefore \quad 2b = np$

$= 36.0$

$q = 27.0$ ft,

$\delta = 1.5$

For $n = 4$, $\lambda = \theta^4$ and $I/I_T = 8\delta^3\theta^4$

TABLE 2.9

(a) FOR θ = 1.0

Load at	Beam at →	b	5b/6	3b/4	b/2	b/4	b/6	0	−b/6	−b/4	−b/2	−3b/4	−5b/6	−b
BEAM a	b	9.00	—	4.45	1.24	−0.24	—	−0.70	—	−0.52	−0.35	−0.07	—	0.16
	3b/4	4.45	--	3.34	1.98	0.86	--	0.17	—	−0.14	−0.17	−0.15	—	−0.07
	5b/6	5.9667	—	3.7100	1.7333	0.4933	—	−0.12	—	−0.2667	−0.2300	−0.1233	—	+0.0067
	5b/6	—	4.4622	—	1.7333	—	0.2889	—	−0.2178	—	−0.2300	—	−0.0800	—
BEAM b	b/2	1.24	—	1.98	2.41	1.82	—	1.00	—	0.38	0.01	−0.17	—	−0.35
	b/2	—	1.7333		2.4100	—	1.5467	—	0.5667	—	0.0100	—	−0.2300	—
BEAM C	b/4	−0.24	—	0.86	1.82	2.37	—	1.90	—	1.07	0.38	−0.14	—	−0.52
	0	−0.70	—	0.17	1.00	1.90	—	2.33	—	1.90	1.00	+0.17	—	−0.70
	b/6	−0.3933	—	0.6300	1.5467	2.2133	—	2.0433	—	1.3467	0.5867	−0.0367	—	−0.5800
	b/6	—	0.2889	—	1.5467	—	2.1566	—	1.5789	—	0.5867	—	−0.2178	—

(b) FOR θ = 0.50

Load at	Beam at →	b	5b/6	3b/4	b/2	b/4	b/6	0	−b/6	−b/4	−b/2	−3b/4	−5b/6	−b
BEAM a	b	4.70	—	3.55	2.31	1.385	—	0.55	—	0.00	−0.54	−0.96	—	−1.43
	3b/4	3.55	—	2.84	2.075	1.40	—	0.785	—	0.305	−0.18	−0.53	—	−0.96
	5b/6	3.9333	—	3.0433	2.1533	1.395	—	0.7067	—	0.2033	−0.3000	−0.6733	—	−1.1167
	5b/6	—	3.3400	—	2.1533	—	1.1656	—	0.3711	—	−0.3000	--	−0.8211	--
BEAM b	b/2	2.31	—	2.075	1.81	1.42	—	1.01	—	0.63	0.22	−0.18	—	−0.54
	b/2		2.1533	—	1.8100	—	1.3167	—	0.7567	—	0.2200	—	−0.3000	—
BEAM C	b/4	1.385	—	1.40	1.42	1.38	—	1.22	—	0.96	0.63	0.305	—	0.00
	0	0.55	—	0.785	1.01	1.22	—	1.325	—	1.22	1.01	0.785	—	0.55
	b/6	1.1067	-	1.1950	1.2833	1.3267	—	1.2550	—	1.0467	0.7567	0.4650	—	0.1833
	b/6	—	1.1656	--	1.2833	—	1.3028	--	1.1161	—	0.7567	—	0.3711	—

(c) FOR θ = 0.25

Load at	Beam at →	b	5b/6	3b/4	b/2	b/4	b/6	0	−b/6	−b/4	−b/2	−3b/4	−5b/6	−b
BEAM a	b	4.05	—	3.28	2.48	1.70	--	0.30	—	0.22	−0.535	−1.17	—	−1.84
	3b/4	3.28	—	2.71	2.10	1.54	—	0.96	—	0.41	−0.155	−0.64	—	−1.17
	5b/6	3.5367	—	2.9000	2.2267	1.5933	—	0.94	—	0.3467	−0.2817	−0.8167	—	−1.3933
	5b/6	—	3.1122	—	2.2267	—	1.3755	—	0.5445	—	−0.2817	—	−1.0089	—
BEAM b	b/2	2.48	—	2.10	1.73	1.35	—	0.97	—	0.635	0.245	−0.155	—	−0.535
	b/2	--	2.2267	—	1.7300	—	1.2233	--	0.7467	—	0.2450	—	−0.2817	--
BEAM C	b/4	1.70	—	1.54	1.35	1.21	—	1.05	—	0.855	0.635	0.41	—	0.22
	0	0.90	—	0.96	0.97	1.05	—	1.08	—	1.05	0.97	0.96	—	0.90
	b/6	1.4333	—	1.3467	1.2233	1.1567	—	1.0600	—	0.9200	0.7467	0.5933	—	0.4467
	b/6	—	1.3756	—	1.2233	—	1.1245	—	0.9667	—	0.7467	—	0.5445	—

TABLE 2.10

SIX GIRDER GRILLAGE

LOAD AT	$k = \frac{K_0}{6}$	$\theta = 1.0$, $\lambda = 16/81$		$\theta = 0.50$, $\lambda = 1/81$		$\theta = 0.25$, $\lambda = 1/1286$	
		By Guyon's Method	By Exact Method	By Guyon's Method	By Exact Method	By Guyon's Method	By Exact Method
Beam a	k_{aa}	0.7511	0.7714	0.5694	0.5712	0.5184	0.5271
	k_{ba}	0.2866	0.2952	0.3630	0.3674	0.3756	0.3802
	k_{ca}	0.0486	0.0316	0.1958	0.1993	0.2303	0.2353
	k_{da}	-0.0366	-0.0464	0.0624	0.0619	0.0912	0.0927
	k_{ea}	-0.0383	-0.0400	0.0506	-0.0472	-0.0475	-0.0478
	k_{fa}	-0.0184	0.0118	0.1400	-0.1526	-0.1680	-0.1875
Beam b	k_{ab}	0.2866	0.2952	0.3630	0.3674	0.3756	0.3802
	k_{bb}	0.3923	0.3908	0.3061	0.3094	0.2977	0.2958
	k_{cb}	0.2579	0.2564	0.2176	0.2168	0.2061	0.2101
	k_{db}	0.0979	0.0940	0.1266	0.1244	0.1259	0.1239
	k_{eb}	0.0016	0.0036	0.0373	0.0292	0.0422	0.0378
	k_{fb}	-0.0383	0.0400	-0.0506	-0.0472	-0.0475	-0.0478
Beam c	k_{ac}	0.0486	0.0316	0.1958	0.1993	0.2303	0.2353
	k_{bc}	0.2579	0.2564	0.2176	0.2168	0.2061	0.2101
	k_{cc}	0.3650	0.3940	0.2142	0.2167	0.1864	0.1832
	k_{dc}	0.2672	0.2712	0.1834	0.1809	0.1601	0.1548
	k_{ec}	0.0979	0.0940	0.1266	0.1244	0.1259	0.1239
	k_{fc}	-0.0366	-0.0464	0.0624	0.0619	0.0912	0.0927

when

$$\theta = 1 \;;\; \frac{I}{I_T} = 27 \quad \text{and} \quad \lambda = 1$$

$$\theta = 0.5;\; \frac{I}{I_T} = \frac{27}{16} \quad \text{and} \quad \lambda = \frac{1}{16}$$

$$\theta = .25;\; \frac{I}{I_T} = \frac{27}{256} \quad \text{and} \quad \lambda = \frac{1}{256}$$

The values of K_o in this case can be directly obtained from tables 2.2 to 2.4 for beam positions $\pm \frac{3}{4}$ b and $\pm \frac{b}{4}$ and load positions $\frac{3}{4}$ b and $\frac{b}{4}$, multiplying the values of K_o by $\frac{p}{2b} = \frac{1}{4}$, the transverse distribution coefficients are obtained. The values are tabulated in Table 2.8 and compared with exact values calculated from results given in table 2.5 b.

(c) <u>Bridge grillage with six main beams.</u>

Consdering a bridge with six main beams and one cross beam at the centre as shown in fig. 2.16c, the dimensions taken are 2a = 54', p = 6.0'

$$\therefore \quad 2b = np$$

$$= 36.0$$

$$q = 27',$$

$$\delta = 1.5$$

For $\quad n = 6 \;;\; \lambda = \frac{16}{81}\theta^4$ and $I/I_T = 16\,\theta^4$

when $\quad \theta = 1;\frac{I}{I_T} = 16 \quad$ and $\quad \lambda = \frac{16}{81}$

$$\theta = 0.5;\; \frac{I}{I_T} = \frac{9}{8} \quad \text{and} \quad \lambda = \frac{1}{81}$$

$$\theta = .25;\; \frac{I}{I} = \frac{9}{128} \quad \text{and} \quad \lambda = \frac{1}{1296}$$

Again the K_o values are obtained using tables 2.2 to 2.4 by linear interpolations for beam positions $\pm \frac{5}{6} b$, $\pm \frac{b}{2}$ and $\pm \frac{b}{6}$ and load positions $\frac{5}{6} b$, $\frac{b}{2}$ and $\frac{b}{6}$. The interpolated values are shown in Table 2.9a, b and c. Finally the values are multiplied by $\frac{P}{2b} = \frac{1}{6}$ to obtain the distribution profile. The values thus obtained are compared with exact values in table 2.10.

Tables 2.7, 2.8 and 2.10 show the comparison of distribution coefficients for extreme cases of bridge grillages obtained, by anisotropic plate theory and exact analysis. The following observations can be made by comparing the values of the coefficients .

(1) The values of distribution coefficients obtained by anisotropic plate theory and exact analysis are very close to each other.

(2) Considering the absolute maximum values of distribution coefficients obtained by the methods, it is seen that the errors are 5.6% in three girder case, 3.4% in four girder case and 2.6% in six girder case. Thus, the assumption of anisotropic plate is better met with for a bridge with large number of longitudinals as it is evident from physical considerations.

(3). The distribution of load in a bridge improves with the increase in the stiffness of transverse medium i.e. decrease in the value of θ .

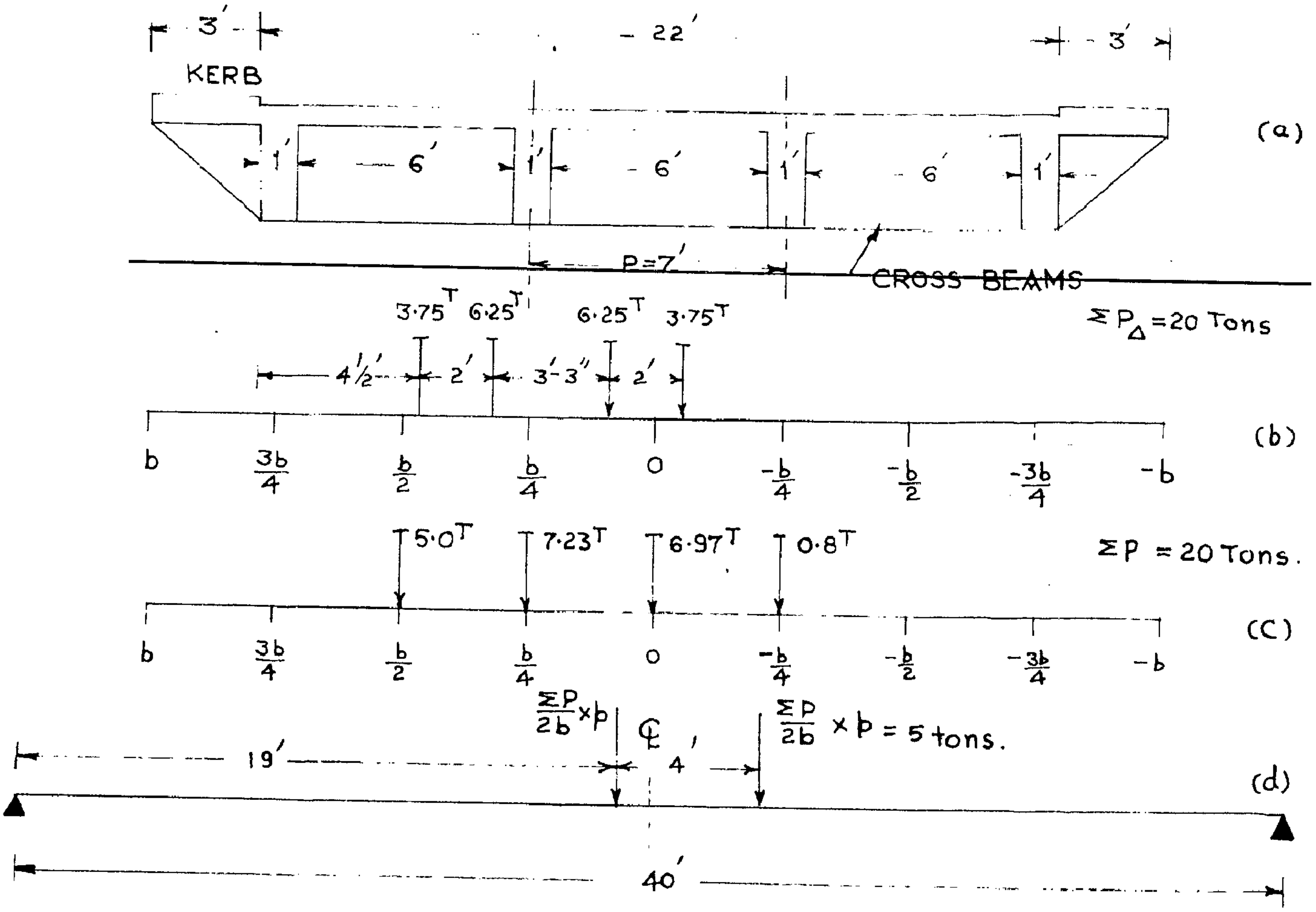

FIG. (2·17)

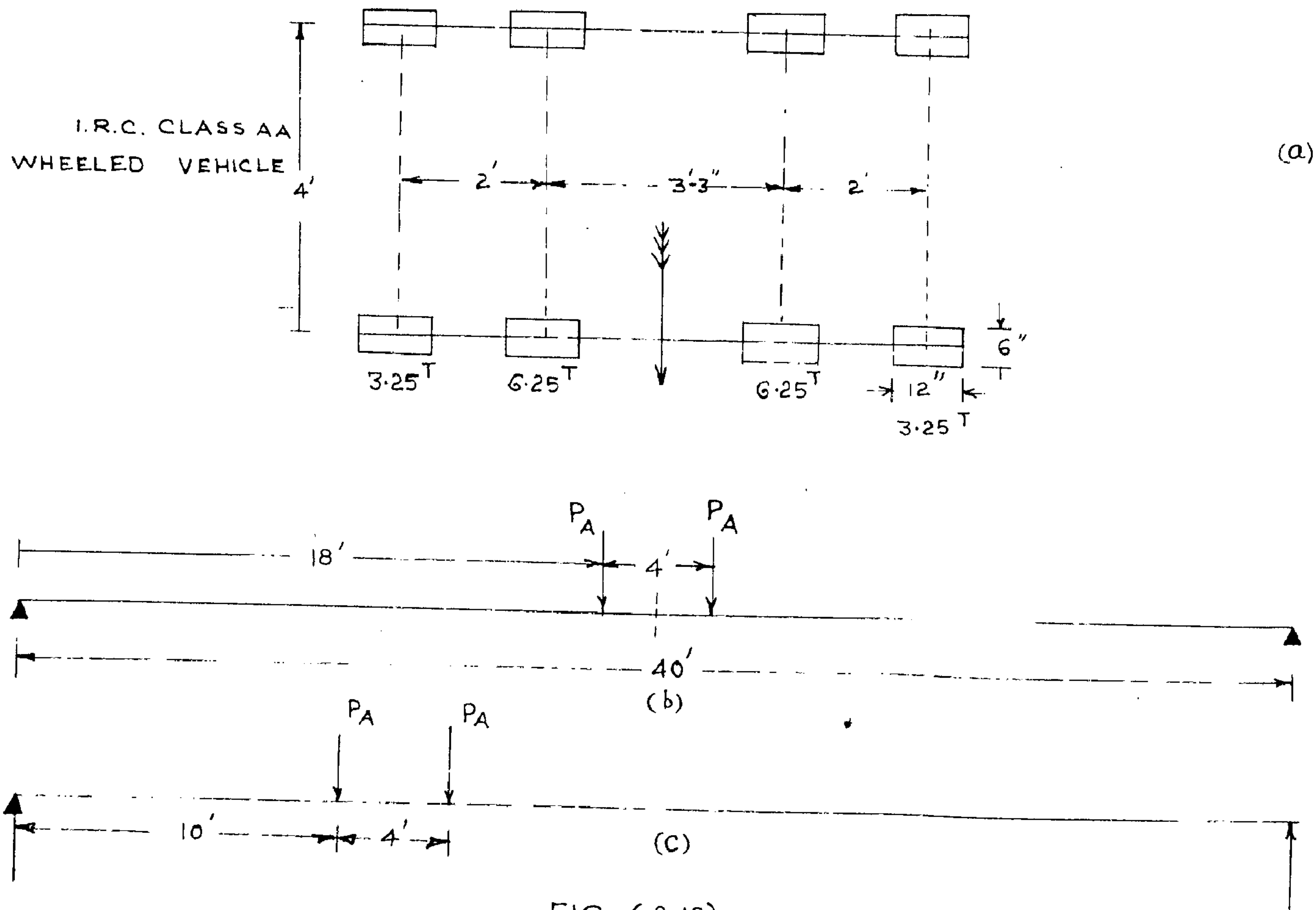

FIG. (2·18)

The negative distribution coefficients increase with the increase in the transverse stiffness and number of longitudinals. In the limit when the transverse stiffness becomes infinite it behaves as a rigid medium leading to linear variation distribution coefficients as in the case of plane transverse section of a beam in bending. With this condition prevailing the outer girders are more heavily loaded, than the case when the medium is flexible. In a six girder case the maximum negative value is about 35% of the maximum positive value for $\theta = 0.25$.

(4) The distribution of load obtained by anisotropic plate theory is better than by exact method. This is clear from the fact that unlike as in the open grillage analysis theory, the anisotropic plate theory assumes additional end cross beams and rotations of longitudinals at the supports as zero.

2.3.2 Torsionally Resistant Grid Beam Bridges.

A case of four girder torsionally resistant grid beam bridge is considered for flexural parameter $\theta = 1.0$ and $\theta = 0.5$. Considering the variation in torsional stiffness of the bridge two extreme values of torsional parameter $\alpha = 0.04$ and $\alpha = 0.64$ are used in the calculation. For comparison, the transverse distribution profile due unit load acting at the mid point of the longitudinal beam is derived for these cases by the method of 'Harmonic Analysis'[13]. In the analysis by anisotropic plate theory it is always assumed that the end cross beams are provided at the supports.

Four girder open grid beam bridge.

Considering a torsionally resistant four girder bridge with three cross beams equally spaced. The dimensions are

$$2a = 54' \quad p = 9.0'$$

$$q = 13.5 \quad 2b = np = 36.0.$$

For three cross beam case

$$\frac{I}{I_T} = \frac{64}{n}\,\theta^4 \delta^3 \qquad \ldots (2.70)$$

for $n = 4$ and $\delta = 1.5$,

$$\frac{I}{I_T} = 54, \quad \text{for} \quad \theta = 1$$

$$\frac{I}{I_T} = \frac{27}{8}, \quad \text{for} \quad \theta = \frac{1}{2}$$

Taking the torsional stiffness of the cross beams $J_T = 0$ and $\frac{G}{E} = 0.5$ the torsional parameter α is given by

$$\alpha = \frac{G}{2E} \frac{J/p}{\sqrt{\frac{I}{I_T}\frac{p}{q}}}$$

Substituting the value of I_T from equation(2.70)

$$\frac{J}{I} = \frac{\alpha}{\theta^2 \delta^2} \qquad .... (2.71)$$

$$\frac{J}{I_T} = \frac{64}{n} \alpha \theta^2 \delta$$

It is interesting to note that $J/_I$ is independent of number of main beams n. Thus for

$$\delta = 1.5$$

$$\frac{J}{I} = \frac{4}{9}\frac{\alpha}{\theta^2}$$

$$\frac{J}{I_T} = 24\,\alpha\,\theta^2$$

Hence for

$\theta = 1$; $\alpha = 0.04$; $\frac{J}{I} = \frac{16}{900}$ and $\frac{J}{I_T} = 0.96$

and $\alpha = 0.64$; $\frac{J}{I} = \frac{256}{900}$ and $\frac{J}{I_T} = 15.36$

for

$\theta = \frac{1}{2}$ $= 0.04$; $\frac{J}{I} = \frac{64}{900}$ and $\frac{J}{I_T} = 0.24$

and $\alpha = 0.64$; $\frac{J}{I} = \frac{1024}{900}$ and $\frac{J}{I_T} = 3.84$

Adopting the ratio $\frac{J}{I}$ as derived above for $\alpha = 0.04$ and $\alpha = 0.64$, the distribution coefficients K_1 for $\alpha = 1$ and K_0 for $\alpha = 0$ are obtained for beam positions $\pm 3b/_4$ and $\pm b/_4$ and load positions $3b/_4$ and $b/_4$ from tables 2.2 and 2.3. Subsequently the values of K_α are tabulated in table 2.11. Multiplying K_α values by $\frac{p}{2b} = \frac{1}{4}$, the distribution profiles are obtained for the two load positions.

The values thus obtained are compared with the values calculated by "Harmonic Analysis"(13) given in tables (2.13). In the method of 'Harmonic Analysis' given by HENDRY AND JAEGER, the parameter α_H is used to determine the ratio of span to spacing of longitudinals and the ratio of transverse and longitudinal flexural rigidities, and it is written as

$$\alpha_H = \frac{12}{\pi^4}\left(\frac{L}{h}\right)^3 \frac{nEI_T}{EI}$$ for the first

harmonic distribution, where,

L = the span of the bridge (=2a in case of plate theory)

h = spacing of the main girders (p in case of plate theory)

EI = flexural rigidity of one main girder.

EI_T = flexural rigidity of one cross girder.

and n = number of cross girder (say equal to m in plate theory)

The coefficient α_H of Harmonic Analysis can be correlated with the flexural parameter θ of plate theory by simple relation

$$\alpha_H = \frac{3}{4\pi^2}\,\frac{m}{(m-1)}\,\frac{n^4}{\theta^4} \qquad \text{.... (2.72)}$$

where, n = number of main girders.

Equation (2.72) assumes that in both cases there are end cross beams. Thus for m = 5 and n = 4, $\alpha_H = \dfrac{240}{\pi^4 \theta^4}$

The second parameter β used in harmonic analysis is given by

$$\beta = \frac{\pi^2}{2n} \left(\frac{h}{L}\right) \frac{GJ}{EI_T}$$

Thus parameter β is a measure of the relative torsional rigidity of longitudinals and neglecting the torsional rigidity of the transverse system, it can be correlated with the torsional parameter α of 'plate theory' by simple relation

$$\beta = \frac{16\pi^2}{mn^2} \alpha \theta^2 \qquad \text{.... (2.73)}$$

For m = 5 and n = 4 eq. 2.73 reduces to

$$\beta = \frac{\pi^2}{5} \alpha \theta^2 \qquad \text{.... (2.73a)}$$

The solution of a bridge for any value of by harmonic analysis can be easily obtained by using interpolation formula as the coefficient of transverse distribution ρ_0 and ρ_∞ are derived for two extreme cases as regards to torsional rigidity of longitudinals, namely zero and infinite torsional stiffness (i.e. $\beta = 0$ and $\beta = \infty$). These derived values are given in the book 'The Analysis of Grid frame-works and Related Structures' by HENDRY and JAEGER, appendix 18 table I. The interpolation formula used is

$$\rho_\beta = \rho_0 + (\rho_\infty - \rho_0)\sqrt{\frac{\beta \sqrt{\alpha_H}}{3 + \beta\sqrt{\alpha_H}}}$$

~~TABLE 2.11~~

LOAD AT	BEAM AT	θ = 1.0, 3b/4	θ = 1.0, b/4	θ = 1.0, −b/4	θ = 1.0, −3b/4	θ = 0.50, 3b/4	θ = 0.50, b/4	θ = 0.50, −b/4	θ = 0.50, −3b/4
3b/4	K_0	3.34	0.86	-0.14	-0.15	2.84	1.40	0.305	0.53
	K_1	2.42	1.10	0.36	0.12	1.58	1.12	0.76	0.54
	$(K_1 - K_0)$	-0.92	0.24	0.50	0.27	-1.26	-0.28	0.455	1.07
	$\sqrt{\alpha_1}(K_1 - K_0)$	-0.184	0.048	0.10	0.054	-0.252	-0.056	0.091	0.214
	$\sqrt{\alpha_2}(K_1 - K_0)$	-0.736	0.192	0.40	0.216	-1.008	-0.224	0.364	0.856
	K_{α_1}	3.156	0.908	-0.04	-0.096	2.588	1.344	0.396	-0.316
	$K_{\alpha_1}/4$	0.7890	0.2270	-0.0100	-0.0240	0.6470	0.3360	0.0990	-0.0790
	K_{α_2}	2.604	1.052	0.26	0.066	1.832	1.176	0.669	0.326
	$K_{\alpha_2}/4$	0.6510	0.2630	0.0650	0.0165	0.4580	0.2940	0.1673	0.0815
b/4	K_0	0.86	2.37	1.07	0.14	1.40	1.38	0.96	0.305
	K_1	1.10	1.67	0.89	0.36	1.12	1.15	0.96	0.76
	$(K_1 - K_0)$	0.24	-0.70	-0.18	0.50	-0.28	-0.23	0.00	0.455
	$\sqrt{\alpha_1}(K_1 - K_0)$	0.048	-0.14	-0.036	0.10	-0.056	-0.046	0.00	0.091
	$\sqrt{\alpha_2}(K_1 - K_0)$	0.192	-0.56	-0.144	0.40	-0.224	-0.184	0.00	0.364
	K_{α_1}	0.908	2.23	1.034	-0.04	1.344	1.334	0.96	0.396
	$K_{\alpha_1}/4$	0.2270	0.5575	0.2585	0.0100	0.3360	0.3335	0.2400	0.0990
	K_{α_2}	1.052	1.81	0.926	0.26	1.176	1.196	0.96	0.669
	$K_{\alpha_2}/4$	0.2630	0.4525	0.2315	0.0650	0.2940	0.2990	0.2400	0.1673

NOTE: $\alpha_1 = 0.04$; $\alpha_2 = 0.64$

Obtaining the multiplying factor $\sqrt{\dfrac{\beta\sqrt{\alpha_H}}{3+\beta\sqrt{\alpha_H}}} = X_\beta$ in terms of the parameters of plate theory, it is seen that

$$\beta\sqrt{\alpha_H} = \frac{8\sqrt{3}}{\sqrt{m(m-1)}}\,\alpha \qquad \text{.... (2.74)}$$

where,

α_H denotes the flexural parameter. of the Harmonic Analysis

and α denotes the torsional parameter of plate theory.

It is interesting to note that $\beta\sqrt{\alpha_H}$ is independent of number of main beams and θ and directly proportional to α. Putting $m = 5$ $\beta\sqrt{\alpha_H} = 3.095$ and the multiplying factor

$$X_\beta = \sqrt{\frac{3.095\alpha}{3+3.09\alpha}} \qquad \text{.... (2.74a)}$$

For comparison of numerical values of various coefficients used in 'Plate Theory' and 'Harmonic Analysis', table 2.12 is given.

Table 2.12.

S.No.	PLATE THEORY			HARMONIC ANALYSIS		
	θ	α	$\sqrt{\alpha}$	α_H	β	X_β
1	1.0	0.04	0.2	2.464	0.07896	0.1991
2.	1.0	0.04	0.8	2.464	1.2630	0.6306
3.	0.5	0.04	0.2	39.40	0.01974	0.1991
4.	0.5	0.04	0.8	39.40	0.3158	0.6306

TABLE 2·13

Distribution Coefficient	$\theta = 1.0$; $\alpha_H = 2.464$				$\theta = 0.50$; $\alpha_H = 39.4$			
	$\alpha = 0.04$ $\beta = 0.07896$		$\alpha = 0.64$ $\beta = 1.263$		$\alpha = 0.04$ $\beta = 0.01974$		$\alpha = 0.64$ $\beta = 0.3158$	
	By Guyon-Massonnet Method	By Hendry-Jaeger Method	By Guyon-Massonnet Method	By Hendry-Jaeger Method	By Guyon-Massonnet Method	By Hendry-Jaeger Method	By Guyon-Massonnet Method	By Hendry-Jaeger Method
K_{aa}	0·8090	0·8447	0·6565	0·7742	0·6465	0·6523	0·4576	0·4859
K_{ba}	0·2255	0·2105	0·2620	0·2263	0·3341	0·3490	0·2938	0·3042
K_{ca}	−0·0100	−0·0214	0·0648	0·0149	0·0984	0·1015	0·1672	0·1609
K_{da}	−0·0245	−0·0338	0·0167	−0·0154	−0·0790	−0·1028	0·0814	0·0490
K_{ab}	0·2255	0·2105	0·2620	0·2263	0·3341	0·3490	0·2938	0·3042
K_{bb}	0·5360	0·5398	0·4454	0·5055	0·3300	0·3234	0·2990	0·2985
K_{cb}	0·2485	0·2711	0·2278	0·2533	0·2375	0·2261	0·2400	0·2364
K_{db}	−0·0100	−0·0214	0·0648	0·0149	0·0984	0·1015	0·1672	0·1609

TABLE 2·14

(a) VALUES OF DISTRIBUTION COEFFICIENTS K_0 FOR $\theta = 0·60$

Ref. Station	Load Position								
	$-b$	$-\frac{3b}{4}$	$-\frac{b}{2}$	$-\frac{b}{4}$	0	$\frac{b}{4}$	$\frac{b}{2}$	$\frac{3b}{4}$	b
0	0·31	0·67	1·02	1·36	1·50	1·36	1·02	0·67	0·31
b/4	−0·18	0·21	0·62	1·02	1·36	1·53	1·48	1·31	1·07
b/2	−0·53	−0·18	0·21	0·62	1·02	1·48	1·88	2·06	2·20
3b/4	−0·80	−0·47	−0·18	0·21	0·67	1·31	2·06	2·92	3·75
b	−1·04	−0·80	−0·53	−0·18	0·31	1·07	2·20	3·75	5·45

(b) VALUES OF DISTRIBUTION COEFFICIENTS K_1 FOR $\theta = 0·60$

Ref. Station	Load Position								
	$-b$	$-\frac{3b}{4}$	$-\frac{b}{2}$	$-\frac{b}{4}$	0	$\frac{b}{4}$	$\frac{b}{2}$	$\frac{3b}{4}$	b
0	0·80	0·88	0·99	1·12	1·18	1·12	0·99	0·88	0·80
b/4	0·58	0·67	0·80	0·95	1·12	1·23	1·21	1·14	1·08
b/2	0·43	0·52	0·64	0·80	0·99	1·21	1·39	1·46	1·47
3b/4	0·33	0·41	0·52	0·67	0·88	1·14	1·46	1·76	1·96
b	0·28	0·33	0·43	0·58	0·80	1·08	1·47	1·96	2·50

Table 2.13 shows the comparison of distribution coefficients for the extreme cases of torsional and flexural parameters obtained by the two theories. It is seen from table 2.13 that the distribution of the load as calculated by anisotropic plate theory is always better. This is easily understandable when one compares the basic assumptions made in these two theories. While as in the anisotropic plate theory the torsional rotations of the longitudinals at the supports are assumed as zero; while as in harmonic analysis the torsional rotations of the longitudinals at the ends are permitted. However, by incorporating the assumption that the torsional rotations of the longitudinals at the ends are zero in the harmonic analysis, the distribution coefficients can be obtained, in which case they would compare better with the coefficients obtained by plate theory, the error being limited to the inherent errors of methods of approach.

2.3.3. Calculation Longitudinal and Transverse Bending Moment.

Consider a T-beam bridge with four main beams and three cross beams as shown in Fig. (2.17a.) The details of the bridge are

span = 2a =40' , p = 7' 2b = np = 28' q =10'

$$\theta = \frac{b}{2a} \sqrt[4]{\frac{i_L}{i_T}} = 0.6 \; ; \qquad \alpha = \frac{G}{2E} \frac{j_L + j_T}{\sqrt{i_L i_T}} = 0.09, \; \sqrt{\alpha} = 0.30$$

Loading: I.R.C. class AA wheeled vehicle.

(a) Maximum Longitudinal Bending Moment.

For load distribution analysis, the distribution coefficients K_0 and K_1 are tabulated in tables 2.14a and 2.14b from graphs 1-11, for $\theta = 0.60$. The arrangements of the wheeled vehicle on the transverse section of the bridge shown in fig. 2.17b is having maximum eccentricity from the longitudinal centre line. The clear distance C of outer wheel edge from the kerb has been kept as 4'- 0" according to I.R.C. Code. The distribution of wheel loads to standard positions is shown in fig. 2.17c. Table 2.15a gives the distribution of loads for the given transverse wheel positions and from this table the maximum bending moment taken by the beam are calculated. The maximum distribution coefficient for beam at b/4 is

$$K_{\alpha max} = 1.360$$

The maximum mean bending moment per beam is calculated from axle position shown in Fig.2.17d and is equal to

$$M_{(max)mean} = \frac{10 \times 19^2}{40} \text{ ton ft.}$$

$\therefore$ the maximum longitudinal bending moment $= 1.1\ K_{\alpha max}\ M_{(max)mean}$

$$= 135 \text{ ton ft.}$$

$$= 3630 \times 10^3 \text{ lb. in.}$$

If the eccentricity of the vehicle is increased and if the outerwheel is kept at 1' from the kerb it is seen from the table 2.15 b) that $K_{\alpha\ max} = 1.699$ for

TABLE. 2.15 a. CHART FOR DERIVATION OF DISTRIBUTION COEFFICIENT PROFILE OF LONGITUDINAL BENDING MOMENT FOR I.R.C. CLASS AA WHEELED VEHICLE. $\alpha = 0.09$; VEHICLE POSITION a

	POSITION ON SECTION		P	-b	-3b/4	-b/2	-b/4	0	+b/4	+b/2	+3b/4	+b
VALUES OF ΣPK_0	LOAD AT	b/2	5.0	-2.65	-0.90	+1.05	+3.10	+5.10	+7.40	+9.40	+10.30	+11.0
		b/4	7.23	-1.30	+1.52	+4.48	+7.37	+9.86	+11.07	+10.70	+9.47	+7.74
		0	6.97	+2.16	+4.67	+7.11	+9.49	+10.46	+9.49	+7.11	+4.67	+2.16
		-b/4	0.80	+0.86	+1.05	+1.18	+1.22	+1.09	+0.82	+0.50	+0.17	-0.14
	$\Sigma PK_0 \rightarrow$			-0.93	+6.34	+13.82	21.18	26.51	28.78	27.71	24.61	20.76
	$\Sigma PK_0 / \Sigma P \rightarrow$			-0.047	+0.317	+0.654	+1.059	+1.326	+1.439	1.386	1.231	1.038
VALUES OF ΣPK_1	LOAD AT	b/2	5.0	+2.15	+2.60	+3.20	+4.00	+4.95	+6.05	+6.95	+7.30	+7.35
		b/4	7.23	+4.19	+4.85	+5.79	+6.68	+8.11	+8.90	+8.76	+8.25	+7.82
		0	6.97	+5.57	+6.13	+6.90	+7.80	+8.22	+7.80	+6.90	+6.13	+5.57
		-b/4	0.80	+0.86	+0.91	+0.97	+0.98	+0.90	+0.76	+0.64	+0.54	+0.46
	$\Sigma PK_1 \rightarrow$			+12.77	+14.49	+16.86	18.46	+22.18	+23.51	+23.25	22.22	21.20
	$\Sigma PK_1 / \Sigma P \rightarrow$			+0.639	+0.725	+0.843	+0.923	+1.109	+1.176	1.163	1.111	1.050
$\frac{\Sigma PK_1}{\Sigma P} - \frac{\Sigma PK_0}{\Sigma P} \rightarrow$				0.686	0.408	0.189	-0.136	-0.217	-0.263	-0.223	-0.120	+0.022
$\left(\frac{\Sigma PK_1}{\Sigma P} - \frac{\Sigma PK_0}{\Sigma P}\right)\sqrt{\alpha} \rightarrow$				+0.206	+0.122	+0.057	-0.041	-0.065	-0.079	-0.067	-0.036	+0.007
$\frac{\Sigma PK_0}{\Sigma P} + \left(\frac{\Sigma PK_1}{\Sigma P} - \frac{\Sigma PK_0}{\Sigma P}\right)\sqrt{\alpha} \rightarrow$				0.159	0.439	0.711	+1.018	1.261	1.360	1.319	1.195	1.045

TABLE 2.15 C – CHART FOR DERIVATION OF DISTRIBUTION COEFFICIENT PROFILE OF LONGITUDINAL BENDING MOMENT FOR I.R.C. CLASS AA WHEELED VEHICLE. $\alpha = 0.09$; VEHICLE POSITION C

	POSITION ON SECTION		P	$-b$	$-3b/4$	$-b/2$	$-b/4$	0	$+b/4$	$+b/2$	$+3b/4$	$+b$
VALUES OF ΣPK_0	LOAD AT	$b/2$	1.61	-0.85	-0.29	0.34	1.00	1.64	2.38	3.03	3.32	3.54
		$b/4$	8.84	-1.59	+1.86	5.48	9.02	12.02	13.53	13.08	11.58	10.34
		0	7.67	2.38	+5.14	7.82	10.42	11.50	10.42	7.82	5.14	2.38
		$-b/4$	1.88	2.01	2.46	2.78	2.88	2.56	1.92	1.16	0.39	-0.34
	ΣPK_0 ⟶			1.95	9.17	16.42	23.32	27.72	28.25	25.09	20.43	15.92
	$\Sigma PK_0/\Sigma P$ ⟶			0.098	0.459	0.821	1.166	1.386	1.413	1.255	1.022	0.796
VALUES OF ΣPK_1	LOAD AT	$b/2$	1.61	0.69	0.84	1.03	1.29	1.60	1.95	2.24	2.35	2.37
		$b/4$	8.84	5.13	5.92	7.08	8.40	9.90	10.88	10.70	10.08	9.55
		0	7.67	6.13	6.74	7.58	8.58	9.04	8.58	7.58	6.74	6.13
		$-b/4$	1.88	2.03	2.14	2.28	2.31	2.11	1.78	1.50	1.26	1.09
	ΣPK_1 ⟶			13.98	15.64	17.97	20.58	22.65	23.19	22.02	20.43	19.14
	$\Sigma PK_1/\Sigma P$ ⟶			0.699	0.782	0.899	1.029	1.133	1.160	1.101	1.022	0.957
$\frac{\Sigma PK_1}{\Sigma P} - \frac{\Sigma PK_0}{\Sigma P}$ ⟶				0.601	0.323	0.078	-0.137	-0.253	-0.253	-0.154	0	+0.161
$\left(\frac{\Sigma PK_1}{\Sigma P} - \frac{\Sigma PK_0}{\Sigma P}\right)\sqrt{\alpha}$ ⟶				0.180	0.097	0.023	-0.041	-0.076	-0.076	-0.046	0	+0.048
$\frac{\Sigma PK_0}{\Sigma P} + \left(\frac{\Sigma PK_1}{\Sigma P} - \frac{\Sigma PK_0}{\Sigma P}\right)\sqrt{\alpha}$ ⟶				0.278	0.556	0.844	1.125	1.310	1.337	1.209	1.022	0.844

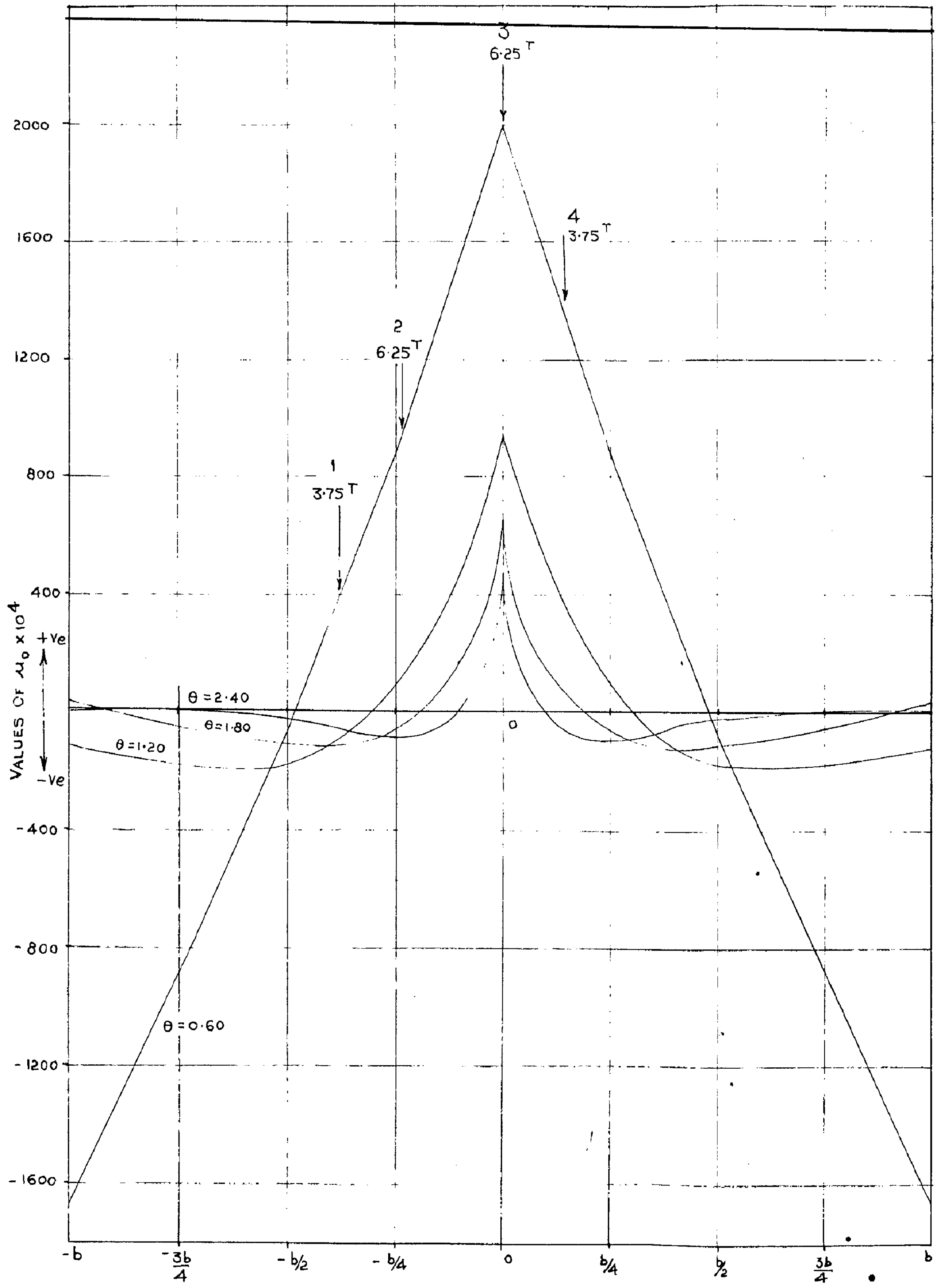

FIG. (2·19a) INFLUENCE CURVE FOR μ_0 FOR REFERENCE STATION 0

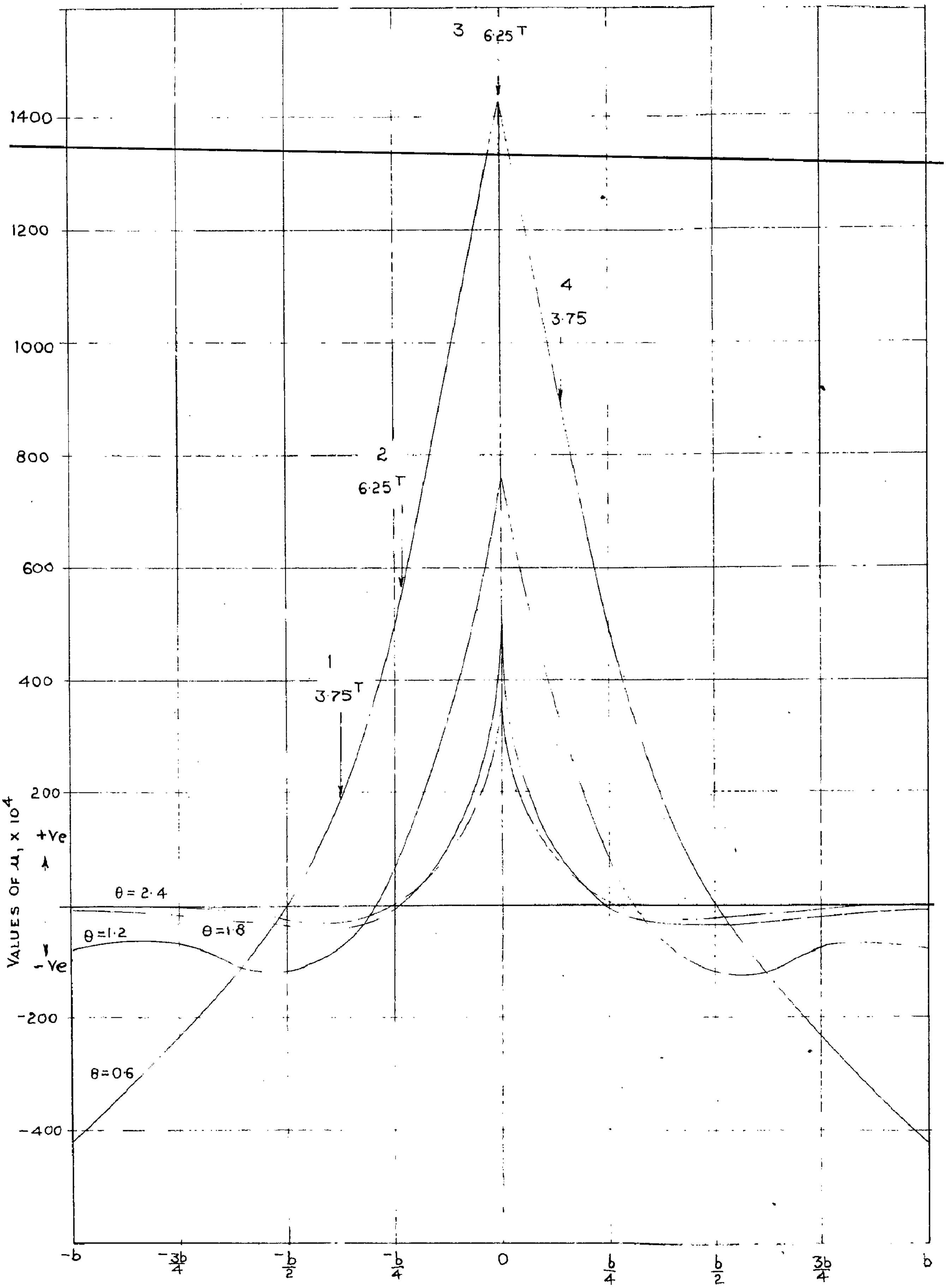

FIG. (2·19b) INFLUENCE CURVE FOR μ_1 FOR REFERENCE STATION O.

outer bea-m and for beam at b/4 K_α = 1.382. It can also be seen from table 2.15c that for beam at b/4 when one wheel load 6.25^T is kept on the beam $K_{\alpha max}$ for beam at b/4 is 1.337. Thus, it is not always true that for maximum longitudinal bending moment, one of the heaviest wheel loads should come on the beam. The critical position of the loads must be determined. Normally for design purposes the outermost beam is analysed for maximum eccentric position of the wheel loads from the longitudinal centre line.

(b) Transverse bending moment:

As indicated in section 2.2.2(ii) the coefficients of transverse bending moment μ_0 and μ_1 are tabulated in Table 2.16 for reference station 0, for θ = 0.6, 2θ =1.2, 3θ = 1.8 and 4θ = 2.4; from graphs 12 and 13. The influence curves for μ_0 and μ_1 are drawn in Figs. 2.19(a) and 2.19(b). The two axle I.R.C. class AA wheeled vehicle as shown in the fig. 2.18a is placed symmetrically about the mid-span as shown in Fig. 2.18 (b) forobtaining maximum transverse bending moment for mid-span cross beam. For 1/4 span cross beam the axle loads are arranged in Fig. (2.18c) so that the longitudinal bending moment induced is maximum. The transverse position of the loads for both cases is shown in fig. 2.19(a) and 2.19(b) in which one heavier inner load has zero eccentricity.

From figs. 2.19(a) and 2.19(b) for the wheel positions of an axle shown in those figures, the values

TABLE 2.16

VALUES OF μ_0 AND μ_1 FOR REFERENCE STATION O.

LOAD AT / θ	$\mu_0 \times 10^4$					$\mu_1 \times 10^4$				
	0	b/4	b/2	3b/4	b	0	b/4	b/2	3b/4	b
0·6	2000	870	−75	−890	−1670	1425	495	0	−235	−420
1·2	940	80	−190	−180	−120	760	80	−120	−70	−70
1·8	650	−70	−110	−50	30	495	−10	−35	−20	−10
2·4	480	−100	−30	5	10	370	0	−25	−5	0

TABLE 2.17

	θ	WHEEL POSITIONS				$\mu \times P \times 10^4$				
		1 (3·75T)	2 (6·25T)	3 (6·25T)	4 (3·75T)	1	2	3	4	Σ
μ_0	0·6	400	950	2000	1350	1500	5938	12500	5062	25000
	1·2	−110	120	940	370	−413	750	5875	1388	7600
	1·8	−120	−50	650	70	−450	−313	4063	263	3563
	2·4	−65	−100	480	−60	−294	−625	3000	−275	1806
μ_1	0·6	175	550	1425	880	656	3438	8906	3300	163000
	1·2	−75	105	760	300	−281	656	4750	1125	6250
	1·8	−40	0	495	80	−150	0	3090	300	3240
	2·4	−30	10	370	70	−113	63	2313	263	2526

TABLE 2.18

LOAD POSITION	C ft	$\frac{c}{2a}$	$\sin\frac{\pi c}{2a}$	$\sin\frac{2\pi c}{2a}$	$\sin\frac{3\pi c}{2a}$	$\sin\frac{4\pi c}{2a}$	$\sin\frac{5\pi c}{2a}$
C_1	18	0·450	0·9877	0·3090	−0·8910	0·5878	0·7071
C_2	22	0·550	0·9877	−0·3090	−0·8910	−0·5878	0·7071
		Σ	1·9754	0	−1·7820	0	1·4142
C_3	10	0·250	0·7071	1·0	0·7071	0	−0·7071
C_4	14	0·350	0·8912	0·8085	−0·1578	−0·9516	−0·7055
		Σ	1·5983	1·8085	0·5493	−0·9516	−1·4126

of ordinates μ_0 and μ_1 are tabulated in table 2.17; the ordinates are multiplied by corresponding loads and $\Sigma \mu P$ is finally obtained. The values for the sine functions for the axle positions shown in Fig. 2.18a and 2.18b are given in Table 2.18. Equation 2.63(a) for finding M_y at any point due to number of wheel loads acting in an axle can be re-written as

$$M_y = \frac{b}{a}\left(\Sigma \mu_{\alpha(\theta)} P_1 \sin\frac{\pi c}{2a} \sin\frac{\pi x}{2a} + \Sigma P_1 \mu_{\alpha(2\theta)} \sin\frac{2\pi c}{2a} \sin\frac{2\pi x}{2a} + \Sigma P_1 \mu_{\alpha(3\theta)} \sin\frac{3\pi c}{2a} \sin\frac{3\pi x}{2a} + \cdots\right)$$

The sign denotes the summation for all individual wheel loads in an axle positioned at C. If there are many axle loads on the span at C_1, C_2 ---- C_m then, the resultant value of M_y is found by superposition. Thus,

$$M_y = M_y(c_1) + M_y(c_2) + \cdots + M_y(c_m)$$

For mid span transverse section i.e. $x = a$ the even terms are zero and

$$M_y\Big]_{x=a} = \frac{b}{a}\left(\Sigma P_1 \mu_{\alpha(\theta)} \sin\frac{\pi c}{2a} + \Sigma P_1 \mu_{\alpha(3\theta)} \sin\frac{3\pi c}{2a} + \Sigma P_1 \mu_{\alpha(5\theta)} \sin\frac{5\pi c}{2a} + \cdots\right)$$

The total transverse bending for mid span beam is obtained by multiplying $M_y\Big]_{x=a}$ by q the spacing of the cross beam. Using Tables 2.17 and 2.18 the maximum transverse bending moments in the mid-span and 1/4 span cross beams are obtained. The details of calculation are given below:

Mid span cross beam:

$\frac{b}{a} = 0.70 \qquad q = 10'$

$M_{y_0} = 0.7 \times 10 \left[3.5 \times 1.0754\right] = 34.58$ ton ft.

$M_{y_1} = 0.7 \times 10 \left[1.63 \times 1.0754\right] = 22.54$ ton ft.

$M_{y_1} - M_{y_0} = -12.04$ ton ft.

$M_{y_\alpha} = M_{y_0} + (M_{y_1} - M_{y_0})\sqrt{\alpha} = 30.97$ ton feet

$\frac{1}{4}$ span cross beam:

Since $\quad x = \frac{a}{2} \qquad \sin\frac{\pi x}{2a} = 0.7071; \qquad \sin\frac{2\pi x}{2a} = 1.0$

$\sin\frac{3\pi x}{2a} = 0.7071 \qquad \sin\frac{4\pi x}{2a} = 0 \qquad \sin\frac{5\pi x}{2a} = -0.7071$

$M_{y_0} = 0.7 \times 10 \left[3.5 \times 1.5983 \times 0.7071 + 0.760 \times 1.8085 \times 1.0 + 0.3563 \times 0.5493 \times 0.7071\right] = 30.28$ ton ft

$M_{y_1} = 0.7 \times 10 \left[1.63 \times 1.5983 \times 0.7071 + 0.625 \times 1.8085 + 0.3240 \times 0.5493 \times 0.7071\right] = 21.71$ ton ft

$\therefore M_{y_\alpha} = 27.71$ ton.ft.

For the calculation of mid-span cross beam only first term of load series is used. If the third term is considered the maximum transverse moment reduces to 26.64 ton. ft. because it has a negative value. The fifth term has a positive value. There will, therefore, be a very slight reduction in the first term value of M_y if third and fifth terms are considered. For considering higher terms, the values of μ for large values of θ are required.

From the calculations given above, it is found that the maximum transverse bending moment is about 23% of the maximum longitudinal bending moment and the maximum transverse bending moment in the 1/4 span cross beam is about 90% of the maximum transverse bending moment of mid-span cross beam.

2.4 CONCLUDING REMARKS.

After considering some main points of a simply supported bridge-analysis in the sections 2.1 to 2.3, there are some secondary points, like effect of Poisson's ratio, effectiveness of transverse system and errors introduced by making the assumption that a bridge can be analysed as an equivalent anisotropic plate. These require a correct understanding .Further it is shown that the anisotropic plate theory is of particular advantage in the preliminary design of bridges. In the shortest possible time, the results can be obtained for the most varied designs by varying the number of main beams and cross beams, their dimensions, the type of construction etc. Hence the most economical design can be obtained rather easily.

2.4.1 Effect of Poisson's Ratio.

In the section 2.2 the distribution coefficients are derived for the limiting cases of $\alpha = 0$ and $\alpha = 1$. In the derivation of these coefficients the value of Poisson's ratio ν has been taken equal to zero. For a no-torsion grillage, it is clear from section 2.1 that Poisson's ratio has no effect on deflection or moments in the structure. In the limiting case where $\alpha = 1$ i.e. for full torsion slab, Poisson's ratio is of considerable importance in the case of distribution coefficient μ_1. A study on this subject has been carried out by ROWE[23] and the value μ_1 is derived as

$$\mu_1 = -\frac{1}{4\sigma \sinh^2\sigma}\left[\frac{\{[(1-\nu)\sigma\cosh\sigma - (1+\nu)\sinh\sigma]\cosh\theta\psi - (1-\nu)\sinh\sigma\,\theta\psi\sinh\theta\psi\}}{(3+\nu)\sinh\sigma\cosh\sigma - (1-\nu)\sigma}\right.$$

$$\times\left\{[(1-\nu)\sigma\cosh\sigma - (3+\nu)\sinh\sigma]\cosh\theta\beta - (1-\nu)\sinh\sigma\;\theta\beta\;\mathrm{sh}\,\theta\beta\right\}$$

$$+\frac{\{[(1-\nu)\sigma\cosh\sigma + 2\sinh\sigma]\sinh\theta\psi - (1-\nu)\sinh\sigma\,\theta\psi\cosh\theta\psi\}}{(3+\nu)\sinh\sigma\cosh\sigma + (1-\nu)\sigma}$$

$$\times\left\{\frac{(1-\nu)\sigma\cosh\sigma\sinh\theta\beta - (1-\nu)\sinh\sigma\;\theta\beta\;\cosh\theta\beta}{1}\right\}$$

$$\left.+\;[(1-\nu)\sigma\cosh\sigma - (1+\nu)\sinh\sigma]\cosh\theta\chi - (1-\nu)\sinh\sigma\;\theta\chi\sinh\theta\chi\right]$$

.....(2.75)

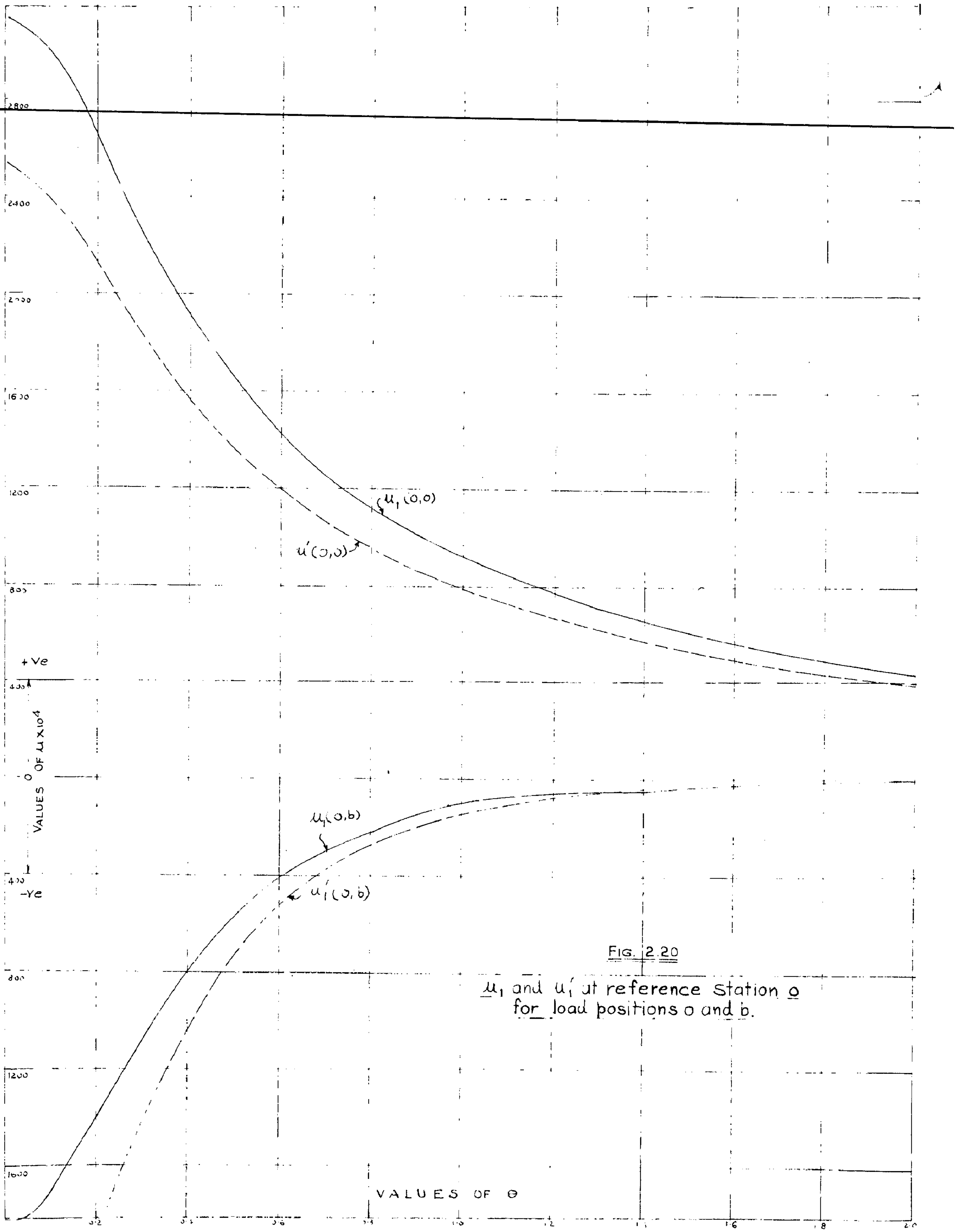

FIG. 2.20

u_1 and u_1' at reference station o for load positions o and b.

Equation(2.52) gives the value of transverse bending moment coefficient for full torsion slab when Poisson's ratio $\nu = 0$; denoting this value as μ_1' and for $\nu = 0.15$ as μ_1 , the governing values for reference station 0 are calculated for two extreme load positions 0 and b.

The difference in the values of μ_1' and μ_1 for various values of θ can be clearly seen from fig(2.20). For load position at 0, larger positive values are obtained if the Poisson's ratio is considered. For $\theta = 0.2$, $\theta = 0.6$ and $\theta = 1.2$, the increase in the values of μ_1 over μ_1' is about 25%, 20% and 13.5% respectively. For load position at b, lesser negative values are obtained with $\nu = 0.15$; the difference is shown in Fig(2.20).

The values of μ_1 in graphs 12 to 21 have been calculated using the equation(2.73) with $\nu = 0.15$ for concrete structures. The effect of torsional parameter α of the structure can be appropriately taken into consider-ation by using the same interpolation formula as suggested by MASSONNET i.e. $\mu_\alpha = \mu_0 + (\mu_1 - \mu_0)\sqrt{\alpha}$

2.4.2 Effectiveness of Transverse System.

The criterion of determining the optimum trans-verse stiffness is to find that value which produces the cheapest bridge. Such a criterion is difficult to specify since it will be influenced by many factors, such as per-missible structural depth and in certain cases the relativ costs of precast and cast in situ concrete. That the relative ease with which changes in both transverse stiffness and torsional stiffness can be investigated by anisotropic plate theory, should make the consideration of several trial schemes, a possibility. Theoretically, the best arrangement will be that which produces equal load distribution to all beams for all positions of load i.e. $K_{\alpha\,max} = 1$. This ideal load distribution is achieved when the bridge has the parameters $\theta = 0$ and $\alpha = 1$.

The value $\theta = 0$ corresponds to a bridge whose cross beams have infinitely large flexural rigidity or width 'b' is infinitely small.

A bridge possessing infinite transverse rigidity will linearly deform transversely and the deformation due to eccentric sinusoidal load $p = p_1 \sin\frac{\pi x}{2a}$ can be written as

$$\omega = (Ay+B)\sin\frac{\pi x}{2a}$$

and
$$\frac{\partial^2 \omega}{\partial x \partial y} = \frac{A\pi}{2a} \cos\frac{\pi x}{2a}$$

If the torsional rigidities γ_P and γ_E of the beams are infinitely large, then the amplitude A will be infinitely small and the bridge is deformed by uniform lowering of all the cross beams parallel to themselves; all the longitudinals beams have, therefore, equal deformations or $K_\alpha = 1$.

It is also known that torsionally rigid bridges with trough decking are economically used, closely correspond to a case of $\theta = 0$ and $\alpha = 1$. In an ordinary slab beam bridge this criterion is never achieved.

The load distribution in a grid beam bridge primarily depends upon the parameter θ which is also known as parameter of cross beam. For a particular value of θ, the ratio of flexural stiffness of longitudinal beam and cross beam can be written as

$$\frac{I}{I_T} = 16 \lambda^3 \theta^4 \frac{m+1}{n} \qquad \ldots(3.76)$$

where,

m = number of cross beams excluding the end cross beams.

Knowing the value of λ i.e. span/width ratio of a bridge, the amount of the transverse stiffness to be provided for a particular value of θ and any adopted number of longitudinals n and cross beams m, can be calculated easily from equation(3.76).It can be seen from equation (3.76) that the most effective position of the cross beam is at mid span and in general the effectiveness roughly corresponds to $\sin\frac{\pi x}{2a}$ where x is the distance of cross beam from one support.

When a required amount of transverse stiffness is to be provided, it is seen that the cross beam material performs as efficiently as possible.Thus, where possible, the full structural depth should be utilised; cross beams monolithic with top slab have obvious advantage of providing greater support to slab itself. It is also seen that the assumed transverse moment of resistance is not exceeded by the induced maximum bending moments.

2.4.3. Errors introduced by the assumption of continuous medium.

As some bridges have only a small number of longitudinal beams and cross beams, it is important to take into account the error introduced by considering an equivalent continuous medium along longitudinal as well as transverse direction.

Considering first the longitudinal beam, the flexural rigidity of which is distributed on either side of the beam equal to p/2 so that it covers the entire spacing p of the longitudinals. The total width of the bridge thus becomes 2b = np, where 2b is greater than the distance between the two outer beams of the actual bridge.

This case is analogous to cases of a beam on elastic foundation and of a beam on equidistant concentrated elastic supports. MASSONNET [40] has compared the results obtained for 3,4,5,6,7 spring supports with the equivalent continuous elastic support for two flexural parameters, $\theta = 0.069$ and $\theta = 1.495$. The variation in the results obtained by the two considerations are negligible. Therefore, the deformation of a beam on isolated elastic supports coincides practically with that of a beam placed on equivalent continuous elastic foundation, if it is assumed that the beam and the elastic foundation are extended by a length $p/2$ beyond the extreme supports.

For a single cross beam case MASSONNET (40) has shown that error is 1.4%.

In example 2.3.1 it is shown that for three girder open grillage with one cross beam at mid-span, the maximum error is 5.6%. Apart from theoretical results, the experimental results (34,35,36,50) obtained at various places have shown the validity of anisotropic plate theory. Therefore, it can be concluded that whatever may be the number of main beams and cross beams in a bridge, the error introduced is insignificant when a bridge is considered as an equivalent continuous medium.

2.4.4. <u>Preliminary Design Procedure.</u>

For preliminary bridge design it is useful to examine the range of values of flexural parameter θ and torsional parameter α, for various types of bridge structures. From this range of values one can always adopt the probable maximum distribution coefficient K_α and can determine the maximum longitudinal bending moment. In this way the initial structure which is analysed in full, can be proportioned very close to the final structure. Hence, the design time can be saved and most economical structure can be obtained rather easily. The following are the observations on the range of values for various types of bridge structures.

(c) <u>Box-section bridges.</u>

The behaviour of a box girder bridge is similar to slab bridges with torsional parameter usually lying between 0.3 to 0.8. The span lengths lie between 60 ft. to 130 ft. and from the studies carried out by Cement and Concrete Association $K_{\alpha max}$ lies between 1.4 to 2.0 for abnormal loading. It is, therefore, clear that for any type of loading, and any type of bridge, the following preliminary design procedure can be adopted.

(1) For the known span derive maximum bending moment any where in the span due to given loading.

(2) For the known width derive 'mean' bending moment.

(3) From the plan dimensions of the bridge and the type of bridge to be used estimate the value of θ and also the maximum value of K_{α} approximately.

(4) Select a suitable section on the basis of approximate maximum longitudinal bending moment obtained from steps 1,2,3.

(5) Analyse the bridge finally, using the theory developed in section 3.2.

CHAPTER 3

EDGE STIFFENED SIMPLY SUPPORTED BRIDGES.

In the previous chapter it is a pre-requisite for the use of graphs given by GUYON-MASSONNET that all longitudinal beams have the same moment of inertia. In many cases the beams on the free sides have increased moment of inertias and thus introduce the edge stiffening effect. The increase in stiffness of edge beams can be due to the following reasons.

1) Increase in depth of edge beams due to raising of footpaths.
2) Increase in depth due to the need to incorporate services of various types.
3) Provision of a parapet to prevent accidents.

The points raised against edge stiffening in the existing conventional design which does not consider the effect of edge stiffening can be guarded off and its structural advantage can be exploited. The various measures to make edge beams more effective are as follows:

1) The parapet is monolithically cast with the slab and cross beam.
2) The parapet wall is properly located as shown in Fig.3.2

3) The overhanging slabs, which are not included because it is a free edge, can be taken as part of edge beam if the cross beams are extended and the spacing of the cross beams is sufficiently close. (Fig.3.3b)

4) The local effects at the junction of edge beam and the main structure due to neutral axis of edge beam not coinciding with the theoretical axis are considered and suitable reinforcement and fillets are provided.

5) The edge beams are properly designed for its forces.

In view of all this the problems of edge stiffened bridge are investigated. However, such bridges have already been constructed. ROWE (60) has designed the bridges of the type shown inFig.(3.2) and slab bridges stiffened at its edges.

The problem of analysis is essentially one of determining the effect on an anisotropic plate of edge moments and edge shear forces; if this problem can be analysed then both the torsional and flexural stiffnesses of any edge member can be included.

MASSONNET (40) (1958) has given a solution for dge stiffening beams of negligible torsional stiffness.

The extension to cover this particular problem in general is given by LITTLE AND ROWE[30] (1956). However, SATTLER[41] (1959) develops an approximate method. To check the validity of the method suggested by SATTLER, example covering wide ranges of edge stiffening and bridge parameters has been solved here.

3.1 EXTENSION OF ANISOTROPIC PLATE THEORY TO SIMPLY SUPPORTED EDGE STIFFENED BEAM BRIDGE.

Considering a bridge with edge stiffening beams as shown in Fig. (3.1a), the bridge can be replaced by an equivalent anisotropic plate for bridge with all identical beams loaded by the sinusoidal load $p(x) = p_1 \sin \frac{\pi x}{2a}$ and acted upon by the edge shear forces and moments. The edge shear forces and edge moments can be assumed to be distributed sinusoidally as shown in Figs. (3.1 b) and (3.1 c). The solution of the bridge can be obtained by using the results of previous chapter and the unknown edge shear forces F_1 and F_2 and edge moments M_1 and M_2 are applied. These forces and moments are determined from compatibility equations for deflection and slopes at edges. The shear forces F_1 and F_2 can ordinarily be treated as applied loads and the deflection and slope at edges are written For finding deflection and slopes due to the edge moments at the

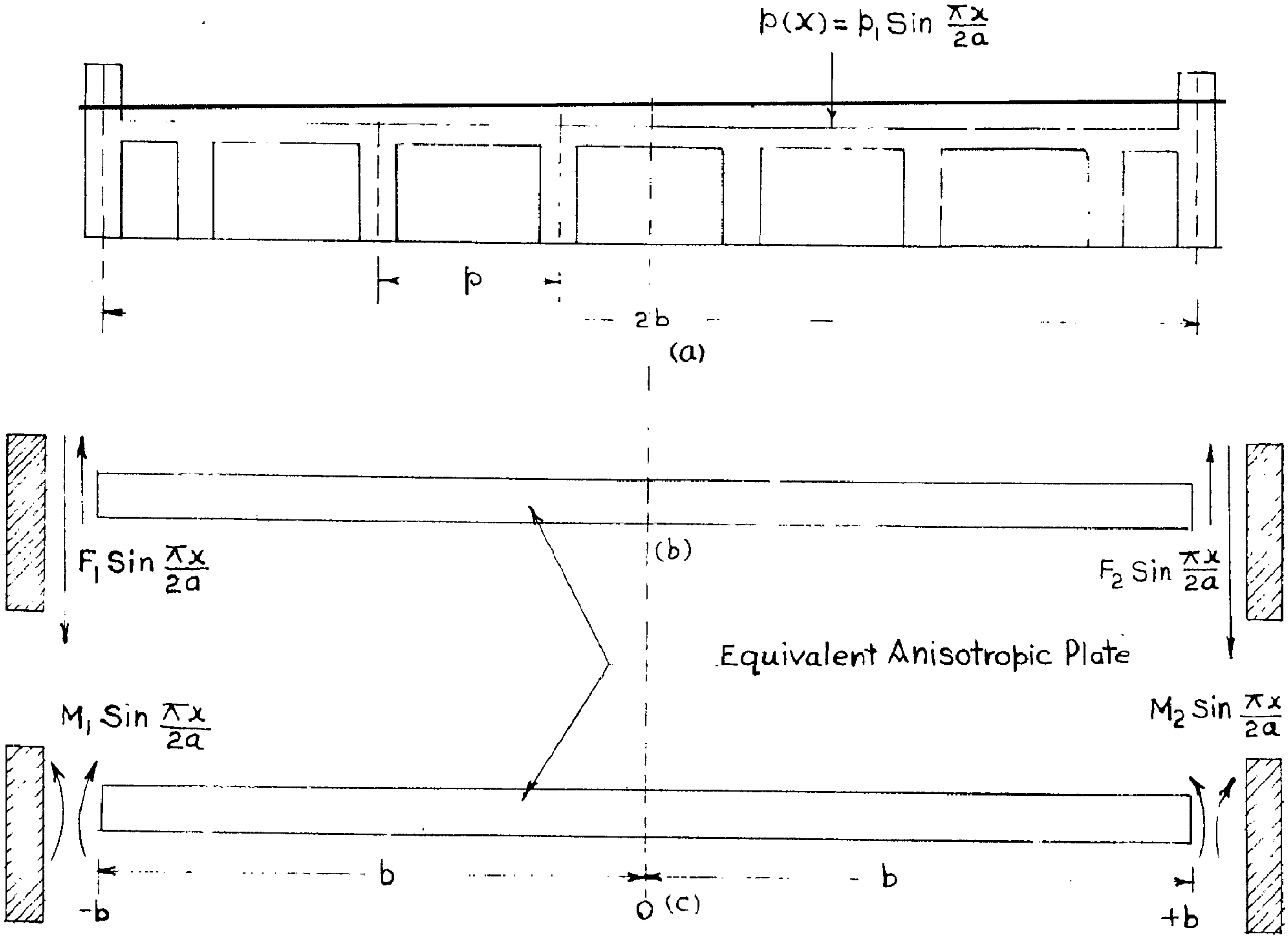

FIG. 3·1 FORCES AND MOMENTS ON EDGE STIFFENED BRIDGE

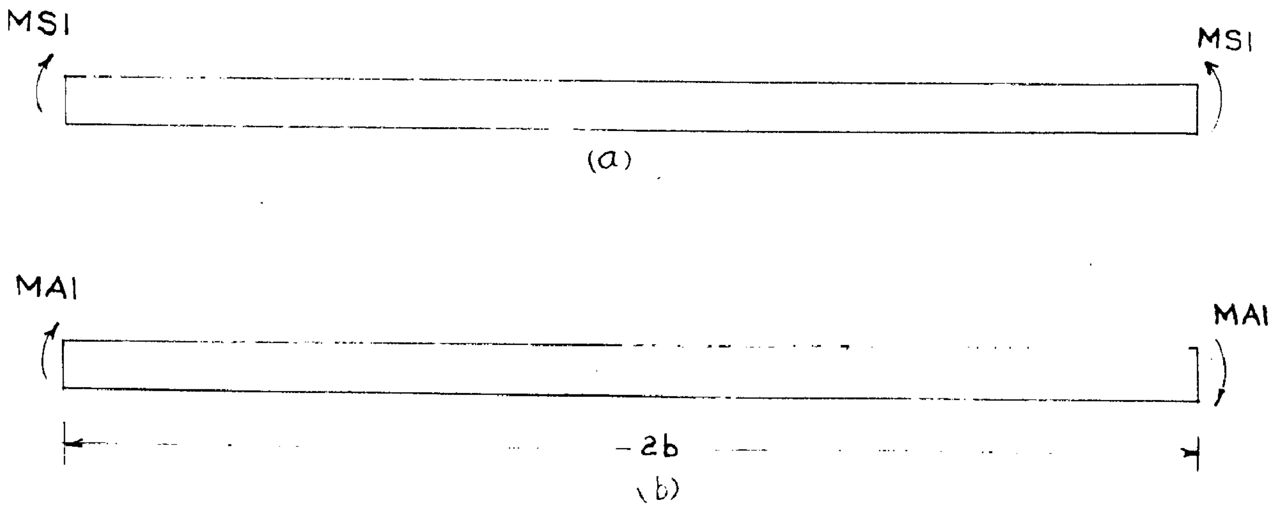

FIG. 3·2 SYMMETRICAL AND ASYMMETRICAL EDGE MOMENTS edges, the solution is given in section 3.1.1.

LITTLE AND ROWE[30] have written the compatibility equations for deflection and slope at the edges $y = \pm b$.

3.1.1. Edge moments on an anisotropic plate.

The basic equations of importance are only given in this section. The complete analysis has been given in ref.(30). The notation used in this chapter is the same as in chapter 2. In the analysis the edge moments are introduced as symmetrical and antisymmetrical components.

(a) Symmetrical edge Moments.

Consider the first harmonic component of the symmetrical edge moments M_{S_1} applied to the plate as shown in Fig. (3.2a). The deflection ω_{S_1} at any point is given by

$$\omega_{S_1} = -\frac{M_{S_1} b^2}{\rho_E} \sin\frac{\pi x}{2a}\, \Phi_\alpha \qquad \ldots (3.1)$$

where,

$$\Phi_\alpha = \frac{A}{\sigma^2}\left\{\cosh\theta\beta\sqrt{\tfrac{1+\alpha}{2}}\cos\theta\beta\sqrt{\tfrac{1-\alpha}{2}}\left(\sinh\sigma\sqrt{\tfrac{1+\alpha}{2}}\cos\sigma\sqrt{\tfrac{1-\alpha}{2}}\right.\right.$$

$$\left. -\sqrt{\tfrac{1+\alpha}{1-\alpha}}\cosh\sigma\sqrt{\tfrac{1+\alpha}{2}}\sin\sigma\sqrt{\tfrac{1-\alpha}{2}}\right) + \sinh\theta\beta\sqrt{\tfrac{1+\alpha}{2}}\sin\theta\beta\sqrt{\tfrac{1-\alpha}{2}}$$

$$\left.\left(\sqrt{\tfrac{1+\alpha}{1-\alpha}}\sinh\sigma\sqrt{\tfrac{1+\alpha}{2}}\cos\sigma\sqrt{\tfrac{1-\alpha}{2}} + \cosh\sigma\sqrt{\tfrac{1+\alpha}{2}}\sin\sigma\sqrt{\tfrac{1-\alpha}{2}}\right)\right\}$$

$$\ldots (3.2)$$

and

$$A = \frac{1}{\left[(2\alpha+1)\sinh\sigma\sqrt{\frac{1+\alpha}{2}}\cosh\sigma\sqrt{\frac{1+\alpha}{2}} - (2\alpha-1)\sqrt{\frac{1+\alpha}{1-\alpha}}\sin\sigma\sqrt{\frac{1-\alpha}{2}}\cos\sigma\sqrt{\frac{1-\alpha}{2}}\right]}$$

The slope at the edge y = b is given by

$$\left(\frac{\partial w_{s1}}{\partial y}\right)_{y=b} = -\frac{M_{s1} b}{P_E}\sin\frac{\pi x}{2a}\,Y_\alpha \qquad \text{... (3.3)}$$

where

$$Y_\alpha = \frac{A}{\sigma}\left\{\sinh\sigma\sqrt{\frac{1+\alpha}{2}}\cos\sigma\sqrt{\frac{1-\alpha}{2}}\left[\sqrt{2(1+\alpha)}\sinh\sigma\sqrt{\frac{1+\alpha}{2}}\cos\sigma\sqrt{\frac{1-\alpha}{2}}\right.\right.$$

$$\left. - \frac{2\alpha}{\sqrt{2(1-\alpha)}}\cosh\sigma\sqrt{\frac{1+\alpha}{2}}\sin\sigma\sqrt{\frac{1-\alpha}{2}}\right] + \cosh\sigma\sqrt{\frac{1+\alpha}{2}}\sin\sigma\sqrt{\frac{1-\alpha}{2}}$$

$$\left[\frac{2\alpha}{\sqrt{2(1-\alpha)}}\sinh\sigma\sqrt{\frac{1+\alpha}{2}}\cos\sigma\sqrt{\frac{1-\alpha}{2}} + \sqrt{2(1+\alpha)}\cosh\sigma\sqrt{\frac{1+\alpha}{2}}\right.$$

$$\left.\times\sin\sigma\sqrt{\frac{1-\alpha}{2}}\right]$$

... (3.4)

The transverse bending moment, My, is given by

$$M_y = M_{s1}\sin\frac{\pi x}{2a}\,\psi_\alpha \qquad \text{... (3.5)}$$

where,

$$\psi_\alpha = A\left\{\cosh\theta\beta\sqrt{\frac{1+\alpha}{2}}\cos\theta\beta\sqrt{\frac{1-\alpha}{2}}\left[(2\alpha+1)\sinh\sigma\sqrt{\frac{1+\alpha}{2}}\cos\sigma\sqrt{\frac{1-\alpha}{2}}\right.\right.$$

$$\left.-(2\alpha-1)\sqrt{\frac{1+\alpha}{1-\alpha}}\cosh\sigma\sqrt{\frac{1+\alpha}{2}}\sin\sigma\sqrt{\frac{1-\alpha}{2}}\right]+\sinh\theta\beta\sqrt{\frac{1+\alpha}{2}}$$

$$\sin\theta\beta\sqrt{\frac{1-\alpha}{2}}\left[(2\alpha-1)\sqrt{\frac{1+\alpha}{1-\alpha}}\sinh\sigma\sqrt{\frac{1+\alpha}{2}}\cos\sigma\sqrt{\frac{1-\alpha}{2}}\right.$$

$$\left.\left.+(2\alpha+1)\cosh\sigma\sqrt{\frac{1+\alpha}{2}}\sin\sigma\sqrt{\frac{1-\alpha}{2}}\right]\right\} \quad \ldots. \; (3.6)$$

The longitudinal bending moment, M_x, is given by

$$M_x = \sqrt{\frac{\rho_P}{\rho_E}}\, M_{s_1} \sin\frac{\pi x}{2a}\,\eta_\alpha \quad \ldots. \; (3.7)$$

where,

$$\eta_\alpha = A\left\{\cosh\theta\beta\sqrt{\frac{1+\alpha}{2}}\cos\theta\beta\sqrt{\frac{1-\alpha}{2}}\left[\sqrt{\frac{1+\alpha}{1-\alpha}}\cosh\sigma\sqrt{\frac{1+\alpha}{2}}\right.\right.$$

$$\left.\sin\sigma\sqrt{\frac{1-\alpha}{2}}-\sinh\sigma\sqrt{\frac{1+\alpha}{2}}\cos\sigma\sqrt{\frac{1-\alpha}{2}}\right]-\sinh\theta\beta\sqrt{\frac{1+\alpha}{2}}$$

$$\sin\theta\beta\sqrt{\frac{1-\alpha}{2}}\left[\sqrt{\frac{1+\alpha}{1-\alpha}}\sinh\sigma\sqrt{\frac{1+\alpha}{2}}\cos\sigma\sqrt{\frac{1-\alpha}{2}}\right.$$

$$\left.\left.+\cosh\sigma\sqrt{\frac{1+\alpha}{2}}\sin\sigma\sqrt{\frac{1-\alpha}{2}}\right]\right\} \quad \ldots. \; (3.8)$$

Using equations (3.2), (3.4) , (3.6) and (3.8) to calculate the values of ϕ_α , γ_α , ψ_α and η_α corresponding to the first harmonic edge moment, for various values of torsional parameter α , LITTLE and ROWE[30] have shown that, as in the case of the distribution coefficients K and μ, an interpolation formula was sufficiently accurate for design purposes provided that for an isotropic slab a Poisson's ratio of 0.15 was included for reinforced and prestressed concrete. For the intermediate values of α the interpolation formula (3.9) holds good

$$Y_\alpha = Y_0 + (Y_1 - Y_0)\sqrt{\alpha} \qquad \ldots\ldots \quad (3.9)$$

where Y is representative of ϕ, γ, ψ and η.

Y_0 = the values of (ϕ, γ, ψ and η for $\alpha = 0$

and Y_1 = the values of (ϕ, γ, ψ and η for $\alpha = 1$ with

$\nu = 0.15$

From the equations above it follows that for $\alpha = 0$

$$\phi_0 = \frac{B}{2\lambda^2\pi^2}\Big\{\cosh\lambda\beta\cos\lambda\beta(\sinh\lambda\pi\cos\pi\lambda - \cos\pi\lambda\sin\pi\lambda)$$

$$+ \sinh\lambda\beta\sin\lambda\beta(\sinh\pi\lambda\cos\lambda\pi + \cosh\pi\lambda\sin\pi\lambda)\Big\}$$

where

$$B = \frac{1}{\sinh\pi\lambda\cosh\pi\lambda + \cos\pi\lambda\sin\pi\lambda} \qquad \ldots \quad (3.10)$$

$$Y_0 = \frac{B}{\lambda\pi}\Big\{\sinh^2\pi\lambda\cos^2\pi\lambda + \cosh^2\pi\lambda\sinh^2\pi\lambda\Big\} \qquad \ldots \quad (3.11)$$

... (..1..)

$$\psi_0 = B\Big\{\cosh\lambda\beta\cos\lambda\beta\,(\sinh\pi\lambda\cos\pi\lambda + \cosh\pi\lambda\,\sin\pi\lambda)$$

$$+ \sinh\lambda\beta\,\sin\lambda\beta\,(\cosh\pi\lambda\,\sin\pi\lambda - \sinh\pi\lambda\cos\pi\lambda)\Big\}$$

...(3.12)

$$\eta_0 = B\Big\{\cosh\lambda\beta\,\cos\lambda\beta\,(\cosh\pi\lambda\,\sin\pi\lambda - \sinh\pi\lambda\cos\pi\lambda)$$

$$- \sinh\lambda\beta\,\sin\lambda\beta\,(\cos\lambda\pi\,\sinh\pi\lambda + \cosh\pi\lambda\,\sin\pi\lambda)\Big\}$$

...(3.13)

where, $\lambda = \dfrac{\theta}{\sqrt{2}}$.

For $\alpha = 1$

$$\phi_1 = \frac{Q}{(1-\nu)\sigma^2}\Big\{\big[(1+\nu)\sinh\sigma - (1-\nu)\sigma\cosh\sigma\big]\cosh\sigma\beta$$

$$+ (1-\nu)\sinh\sigma\;\sigma\beta\;\sinh\sigma\beta\Big\}$$

... (3.14)

where

$$Q = \frac{1}{\big[(3+\nu)\sinh\sigma\cosh\sigma - (1-\nu)\sigma\big]}$$

$$\gamma_1 = \frac{Q}{(1-\nu)\sigma}\;2\sinh^2\sigma$$

....(3.15)

$$\psi_1 = Q\left\{\left[(3+\nu)\sinh\sigma - (1-\nu)\sigma\cosh\sigma\right]\cosh\theta\beta + (1-\nu)\sinh\sigma\cdot\theta\beta\sinh\theta\beta\right\}$$

....(3.16)

$$\eta_1 = Q(1-\nu)\left\{\left[(\sigma\cosh\sigma - \sinh\sigma)\cosh\theta\beta - \sinh\sigma\cdot\theta\beta\sinh\theta\beta\right]\right\}$$

....(3.17)

(b) **Asymmetrical edge moments.**

Consider the asymmetrical edge moments M_{A1} applied to plate as shown in Fig. (3.2b). As for symmetrical edge moments, the interpolation formula given by equation (3.9) is applicable , therefore the equations for torsional parameter = 0 and = 1 are considered.

Thus

$$(\omega A_1)_{\alpha=0} = -\frac{M_{A1}b^2}{P_E}\sin\frac{\pi x}{2a}\phi_0' \qquad \text{.... (3.18)}$$

and $$(\omega A_1)_{\alpha=1} = -\frac{M_{A1}b^2}{P_E}\sin\frac{\pi x}{2a}\phi_1'$$

where,

$$\phi_0' = \frac{D}{2\lambda^2\pi^2}\left\{\sinh\lambda\beta\cos\lambda\beta(\cosh\pi\lambda\cos\pi\lambda - \sinh\pi\lambda\sin\pi\lambda) + \cosh\lambda\beta\sin\lambda\beta(\cosh\pi\lambda\cos\pi\lambda + \sinh\pi\lambda\sin\pi\lambda)\right\}$$

.... (3.19)

and $$D = \frac{1}{\sinh \pi\lambda \cosh \pi\lambda - \sin \pi\lambda \cos \pi\lambda}$$

$$\Phi_1' = \frac{R}{(1-\nu)\sigma^2}\left\{\left[(1+\nu)\cosh\sigma - (1-\nu)\sigma\sinh\sigma\right]\sinh\sigma\beta + (1-\nu)\cosh\sigma \cdot \sigma\beta \cosh\sigma\beta\right\}$$

where

$$R = \frac{1}{\left[(3+\nu)\sinh\sigma\cosh\sigma + (1-\nu)\sigma\right]} \qquad \text{....(3.20)}$$

$$\left.\begin{aligned} \left(\frac{\partial w_1}{\partial y}\right)_{y=b} \text{ for } \alpha=0 &= \frac{-M_{A_1} b}{P_E} \sin\frac{\pi x}{2a}\,\gamma_0' \\ \left(\frac{\partial w_{A_1}}{\partial y}\right)_{y=b} \text{ for } \alpha=1 &= \frac{-M_{A_1} b}{P_E} \sin\frac{\pi x}{2a}\,\gamma_1' \end{aligned}\right\} \qquad \text{... (3.21)}$$

where,

$$\gamma_0' = \frac{D}{\lambda\pi}\left\{\cosh^2\lambda\pi \cos^2\lambda\pi + \sinh^2\lambda\pi \sin^2\lambda\pi\right\} \qquad \text{.... (3.22)}$$

$$\gamma_1' = \frac{R}{(1-\nu)\sigma^2}\, 2\cosh^2\sigma$$

$$\text{.... (3.23)}$$

The transverse bending moment

$$\left.\begin{aligned} M_y\Big]_{\alpha=0} &= M_{A_1}\sin\frac{\pi x}{2a}\,\psi_0' \\ \text{and}\quad M_y\Big]_{\alpha=1} &= M_{A_1}\sin\frac{\pi x}{2a}\,\psi_1' \end{aligned}\right\} \qquad \text{... (3.24)}$$

where,

$$\psi_o' = D\Big\{\sinh\lambda\beta\cos\lambda\beta\,(\cosh\pi\lambda + \sinh\pi\lambda\,\sin\pi\lambda)$$

$$- \cosh\lambda\beta\,\sin\lambda\beta\,(\cosh\pi\lambda\,\cos\pi\lambda - \sinh\pi\lambda\,\sin\pi\lambda)\Big\}$$

... (3.25)

$$\psi_1' = R\Big\{\big[(3+\nu)\cosh\sigma + (1-\nu)\,\sigma\sinh\sigma\big]\sinh\Theta\beta \; +$$

$$(1-\nu)\cosh\sigma\,.\,\Theta\beta\,\cosh\Theta\beta\Big\}$$

... (3.26)

The longitudinal bending moment

$$M_x\Big]_{\alpha=0} = \sqrt{\frac{\rho_P}{\rho_E}}\; M_{A_1}\,\sin\frac{\pi x}{2a}\,\eta_o'$$

and $$M_x\Big]_{\alpha=1} = \sqrt{\frac{\rho_P}{\rho_E}}\; M_{A_1}\,\sin\frac{\pi x}{2a}\,\eta_1'$$

... (3.27)

where,

$$\eta_o' = D\Big\{\sinh\lambda\beta\cos\lambda\beta\,(\sinh\pi\lambda\,\sin\pi\lambda$$

$$- \cosh\pi\lambda\,\cos\pi\lambda) - \cosh\lambda\beta\,\sin\lambda\beta$$

$$(\cosh\pi\lambda\,\cos\pi\lambda + \sinh\pi\lambda\,\sin\pi\lambda)$$

... (3.28)

and

$$\eta_1' = R(1-\nu)\left\{\left[(\sigma \sinh\sigma - \cosh\sigma)\sinh\theta\beta \right.\right.$$

$$\left.\left. - \cosh\sigma . \theta\beta \cosh\theta\beta\right]\right\} \qquad \ldots (3.29)$$

3.1.2. Slope at edge of an Anisotropic Plate due to Applied Load.

The deflection at any point in an anisotropic plate due to applied load $p(x) = p_1 \sin \frac{\pi x}{2a}$ is given by

$$\omega_1 = \frac{16a^4}{\pi^4 \rho_p} \cdot \frac{p_1}{2b} \sin\frac{\pi x}{2a} K_\alpha$$

Then the slope at the edge of the plate, $y = b$ is given by

$$\left(\frac{\partial \omega_1}{\partial y}\right)_{y=b} = \frac{16a^4}{\pi^4 \rho_p} \frac{p_1}{2b} \sin\frac{\pi x}{2a} \frac{dK_\alpha}{dy}$$

By differentiation of eq. (3.42) the slope at the edge $y = b$ can be derived; thus

$$\left(\frac{\partial \omega_1}{\partial y}\right)_{y=b} = \frac{p_1 a^2}{\sqrt{\rho_p \rho_E}} \sin\frac{\pi x}{2a} K_\alpha'$$

$$\ldots . (3.30)$$

Again K_α' is found to comply with the interpolation formula given by equation (3.9) atleast to a sufficient degree of accuracy for practical design purposes. Therefore, only the values for K_0' for $\alpha = 0$ and K_1' for $\alpha = 1$ need be considered; these are given by

$$K_0' = \frac{\cosh\lambda\pi - \sinh\lambda\pi}{2}\left(\left\{\left[\cosh\lambda\psi\cos\lambda\psi\,(\sin\lambda\pi - \cos\lambda\pi) - \right.\right.\right.$$

$$\sinh\lambda\psi\sin\lambda\psi\,(\sin\lambda\pi+\cos\lambda\pi)\Big]\Big[-\big(\sinh^2\lambda\pi\cos^2\lambda\pi +$$

$$\cosh^2\lambda\pi\ \sin^2\lambda\pi\big)\Big] + \Big[\cosh\lambda\psi\cos\lambda\psi\cos\lambda\pi + \sinh\lambda\psi$$

$$\sin\lambda\psi\sin\lambda\pi\Big]\Big[\sinh\lambda\pi\cosh\lambda\pi - \sin\lambda\pi\cos\lambda\pi\Big]\Big\}$$

$$\times\frac{1}{\sinh\lambda\pi\cosh\lambda\pi + \sin\lambda\pi\cos\lambda\pi} + \Big\{\Big[\sinh\lambda\psi$$

$$\cos\lambda\psi\,(\sin\lambda\pi - \cos\lambda\pi) - \cosh\lambda\psi\sin\lambda\psi\,(\sin\lambda\pi+\cos\lambda\pi)\Big]$$

$$\Big[-\big(\cosh^2\lambda\pi\cos^2\lambda\pi + \sinh^2\lambda\pi\sin^2\lambda\pi\big)\Big] + \Big[\sinh\lambda\psi\cos\lambda\psi$$

$$\cdot\cos\lambda\pi + \cosh\lambda\psi\ \sin\lambda\psi\sin\lambda\pi\Big]\Big[\sinh\lambda\pi\ \cosh\lambda\pi + \sin\lambda\pi\cos\lambda\pi\Big]\Big\}$$

$$\times\frac{1}{\sinh\lambda\pi\ \cosh\lambda\pi - \sin\lambda\pi\cos\lambda\pi}$$

$$\left. + \big(\sinh\lambda\pi + \cosh\lambda\pi\big)\Big[\sinh\lambda|\pi-\psi| - \cosh\lambda|\pi-\psi|\Big]\sin\lambda|\pi-\psi|\right)$$

$$\ldots\ldots (3.31)$$

$$K_1' = \frac{1}{\pi^2\sinh^2\sigma}\left(-2\sinh^2\sigma\frac{\{[(1-\nu)\sigma\cosh\sigma - (1+\nu)\sinh\sigma]\cosh\theta\psi - (1-\nu)\sinh\sigma\,\theta\psi\,\sinh\theta\psi\}}{[(3+\nu)\sinh\sigma\cosh\sigma - (1-\nu)\sigma]\,(1-\nu)}\right.$$

$$+\Big[(1-\nu)\sigma + (1+\nu)\sinh\sigma\cosh\sigma\Big]$$

$$\times\left\{\frac{[(1-\nu)\sigma\cosh\sigma + 2\sinh\sigma]\sinh\theta\psi - (1-\nu)\sinh\sigma\,\theta\psi\cosh\theta\psi}{[(3+\nu)\sinh\sigma\cosh\sigma + (1-\nu)\sigma]\,(1-\nu)}\right\}$$

$$\left. - \sigma\cosh\sigma\sinh\theta\psi + \sinh\sigma.\,\theta\psi\ \cosh\theta\psi\right)$$

$$\ldots (3.32)$$

3.1.3. Application to Edge Stiffened Bridges.

Let the span of the bridge be 2a, the width of uniform section of equivalent anisotropic plate of the bridge (i.e. excluding width of edge beams) be 2b, the stiffness of transverse and longitudinal section per unit length of the sections be ρ_p and ρ_E respectively and the flexural and torsional rigidities of edge be EI_E and GJ_E respectively.

The bridge can be analysed using the results of previous sections and the unknown shear forces F_1 and F_2 and edge moments M_1 and M_2 determined from the compatibility equations for deflection and slope at the edges $y = \pm b$.

The shear forces F_1 and F_2 can be treated as applied loads on the bridge and hence the deflection at the edge $y = b$ due to all applied loads can be written

$$\omega_1\Big]_{y=b} = \frac{16a^4}{\pi^4\,\rho_p}\,\frac{1}{2b}\,\sin\frac{\pi x}{2a}\left[\left(\Sigma\, p_1 K_b\right) - \left(F_1 K_b + F_2 K_{-b}\right)\right]$$

......(3.33)

where p_1 is the amplitude of first term of Fourier series for the applied loads.

The edge moment M_1 and M_2 can be considered by superposing symmetrical and asymmetrical edge moments and thus enabling the use of the coefficients ϕ. Thus the deflection at the edge $y = b$ due to the edge moments can be written:

$$w_1\Big]_{y=b} = -\frac{b^2}{\rho_E}\sin\frac{\pi x}{2a}\left(\frac{M_1+M_2}{2}\phi_b + \frac{M_1-M_2}{2}\phi'_b\right)$$

... (3.34)

The total deflection then must be equal tothat of the edge beam at y = b under the action of $F_1 \sin\frac{\pi x}{2a}$. Writing the compatibility equation:

$$\frac{16a^4}{\pi^4 EI_E}F_1 = \frac{16a^4}{\pi^4\rho_p}\times\frac{1}{2b}\Big[(\Sigma p_1 K_b) - (F_1 K_b + F_2 K_b)\Big] - \frac{b^2}{2\rho_E}\Big[(M_1+M_2)\phi_b + (M_1-M_2)\phi'_b\Big]$$

... (3.35)

Similarly at y = -b

$$\frac{16a^4}{\pi^4 EI_E}F_2 = \frac{16a^4}{\pi^4 \rho_p}\times\frac{1}{2b}\Big[(\Sigma p_1 K_b) - (F_1 K_{-b} + F_2 K_b)\Big] - \frac{b^2}{2\rho_E}\Big[(M_1+M_2)\phi_b + (M_2-M_1)\phi'_b\Big]$$ ... (3.36)

The total slope at edge y = b is given as

$$\left(\frac{\partial w_1}{\partial y}\right)_{y=b} = \frac{a^2}{\sqrt{\rho_p\rho_E}}\sin\frac{\pi x}{2a}\Big[(\Sigma p_1 K'_b) - (F_1 K'_b + F_2 K'_{-b})\Big] - \frac{b}{2\rho_E}\sin\frac{\pi x}{2a}\Big[(M_1+M_2)\gamma_b + (M_1-M_2)\gamma'_b\Big]$$

... (3.37)

Considering the torsion of the edge beam subjected to a twisting moment varying simusoidally over the span, the angle of twist at any point may be determined by considering the equilibrium condition of the edge beam with restraining couples applied at its junction with the support diaphrams. Thus the rotation at a distance x from the support can be equated with slope at y = b

$$\frac{M_1}{GJ_E}\left(\frac{2a}{\pi}\right)^2 = \frac{a^2}{\sqrt{\rho_p\rho_E}}\left[\left(\Sigma p_1 K'_b\right)-\left(F_1 K'_b + F_2 K'_{-b}\right)\right] - \frac{b}{2\rho_E}\left[(M_1+M_2)\gamma_b + (M_1-M_2)\gamma'_b\right]$$

.... (3.38)

Similarly at y = -b

$$\frac{M_2}{GJ_E}\left(\frac{2a}{\pi}\right)^2 = \frac{a^2}{\sqrt{\rho_p\rho_E}}\left[\left(\Sigma p_1 K'_{-b}\right)-\left(F_1 K'_{-b} + F_2 K'_b\right) - \frac{b}{2\rho_E}\left[(M_1+M_2)\gamma_p + (M_2-M_1)\gamma'_p\right]\right.$$

.... (3.39)

The unknown edge effects F_1, F_2, M_1 and M_2 for any given position of the loads can be determined by solving equations (3.35), (3.36), (3.38) and (3.39). For this purpose it is sufficient to consider the mid-span section of the bridge i.e. $x = a$. The values of the deflections, the longitudinal transverse bending moment at any point of the bridge , and the bending and torsional moments at any point of the edge beam can then be determined by superposing the various effects.

To obtain a fully rigorous solution it would be necessary to consider the various terms in the Fourier series for the load; this would imply using values of coefficients K, K', ϕ , ϕ', γ , γ' , ψ and ψ' appropriate to values of the flexural parameter θ , 2θ , 3θ etc. This involves solving the compatibility equation for each term. However, sufficient accuracy can be obtained by considering only the first termof the Fourier series and by applying correcting factors.The curves for Φ_0 , Φ_1 , Φ_0' , Φ_1', γ_0 , γ_1 γ_0' , γ_1' , ψ_0 , ψ_1 , ψ_0' , ψ_1' , k_0' & k_1' using equations (3.10), (3.14) (3.19), (3.20), (3.11), (3.15), (3.22), (3.23) (3.12), (3.16), (3.25), (3.26), (3.31) and (3.32 respectively have been given by LITTLE and ROWE (24, 30, 33) for various values of θ and reference stations or load positions as the case may be. The coefficients for $\alpha = 1$ have been plotted with Poisson's ratio $\nu = 0.15$ for reinforced and prestressed concrete bridges.

If the effect of edge moments is neglected then only two compatibility equations are required to find the edge forces F_1 and F_2. Thus rewriting equations (3.35) and (3.36) for the deflections at the edges with $M_1 = M_2 = 0$ it is obtained that

$$F_1 = \frac{E I_E}{2b \rho_p}\left[\left(\sum p_1 k_b\right) - \left(F_1 K_b + F_2 K_{-b}\right)\right] \quad \ldots\ldots (3.40a)$$

$$F_2 = \frac{E I_E}{2b \rho_p}\left[\left(\sum p_1 K_{-b}\right) - \left(F_1 K_{-b} + F_2 K_b\right)\right] \quad \ldots\ldots (3.40b)$$

Equations (3.35, 3.36, 3.38, 3.39, 3.40) have been derived for edge beams at $\pm$ b; therefore, these equations are valid only for the case of a bridge having edge beams located at $\pm$ b of equivalent anisotropic plate. It is thus seen that these equations can only be used for the edge stiffened slab bridges or the bridges of the type shown in Fig. (3.1a).

For the construction of the type shown in Fig. (3.3a 3.3b) the equations (3.40a) and (3.40b) are to be modified if the edge beams are at $\pm$ b' from the centre line of the bridge. Thus neglecting the edge moments again the equations for edge forces F_1 and F_2 are obtained as

$$F_1 = \frac{1}{R}\left[\left(\sum p_1 K(e,b')\right) - \left(F_1 K_{(b',b')} + F_2 K_{(-b',b')}\right)\right] \quad \ldots\ldots (3.41a)$$

$$F_2 = \frac{1}{R}\left[\left(\sum p_i K_{(e,-b')} - \left(F_1 K_{(b',-b')} + F_2 K_{(b',b')}\right)\right)\right]$$

.... (3.41b)

where

$$R = \frac{2b\,P_p}{(\gamma-1)EI} = \frac{n}{(\gamma-1)}$$ .... (3.42)

and γ = $\frac{\text{flexural rigidity of edge beam}}{\text{flexural rigidity of inner beam}} = \frac{EI_E}{EI}$

For sinusoidal load $1 \sin\frac{\pi x}{2a}$ at an eccentricity e (fig.3.3c), the influence coefficient for edge forces F_1 and F_2 can be obtained from equations (3.43a) and (3.43b).

$$F_1 = \frac{K_{(e,b')}\left\{R + K_{(b',b')}\right\} - K_{(e,-b')}\,K_{(b',-b')}}{\left[R + K_{(b',b')}\right]^2 - K^2_{(b',-b')}}$$

....(3.43a)

$$F_2 = \frac{K_{(e,-b')}\left\{R + K_{(b',b')}\right\} - K_{(e,b')}\,K_{(b',-b')}}{\left[R + K_{(b',b')}\right]^2 - K^2_{(b',-b')}}$$

... (3.43b)

Knowing F_1 and F_2 the transverse distribution coefficient of an edge stiffened bridge can be written as

$$\overline{K}_{(e,y)} = \frac{R}{R+2}\left[K_{(e,y)} - \left(F_1 K_{(b',y)} + F_2 K_{(-b',y)}\right)\right]$$ ... (3.44)

3.2 APPROXIMATE METHOD OF CALCULATIONS OF EDGE STIFFENED BRIDGE.

The solution given in Section 3.1 is though general

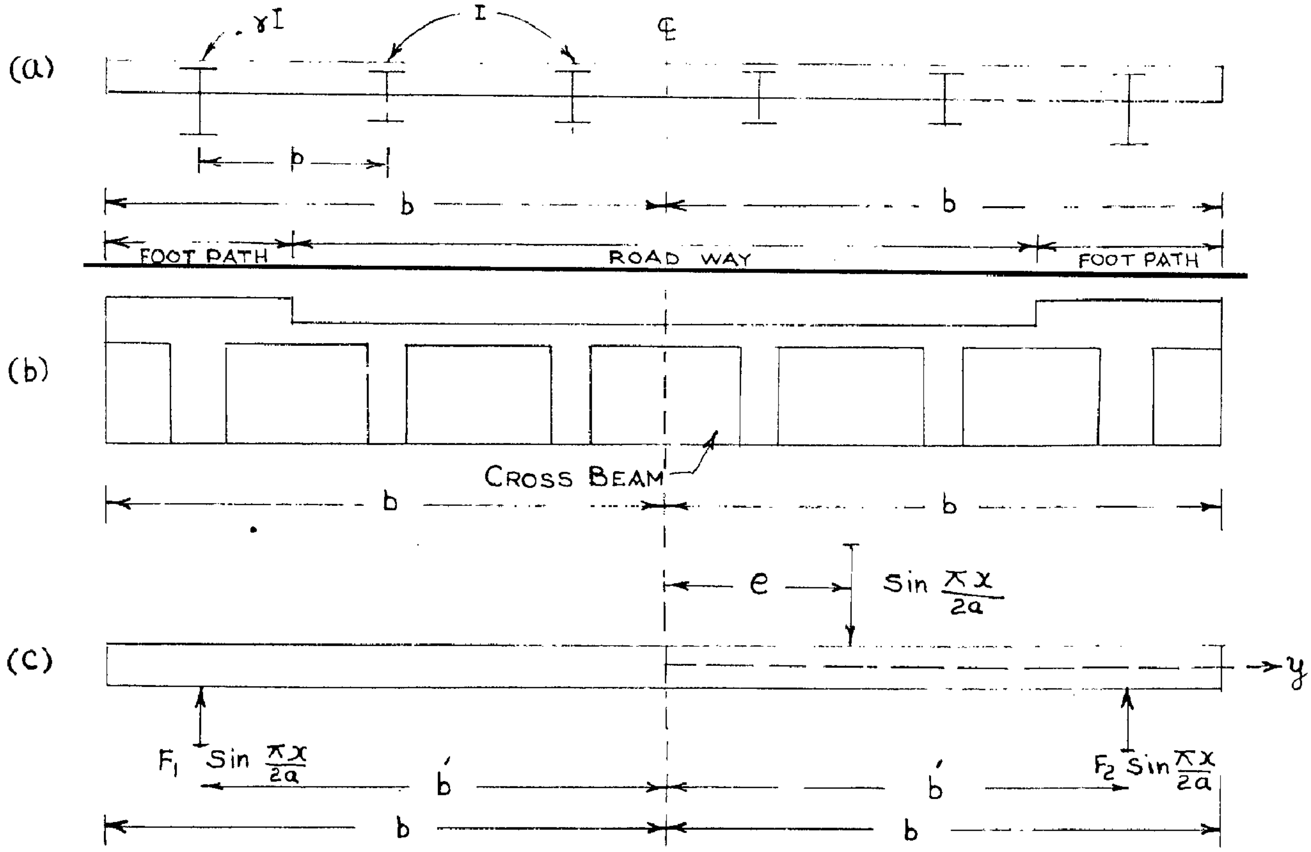

(a)
γI
I
℄
b
b
b
FOOT PATH
ROAD WAY
FOOT PATH
(b)
CROSS BEAM
b
b
(c)
e
sin πx/2a
y
F1 sin πx/2a
b'
b'
F2 sin πx/2a
b
b

FIG. 3·3

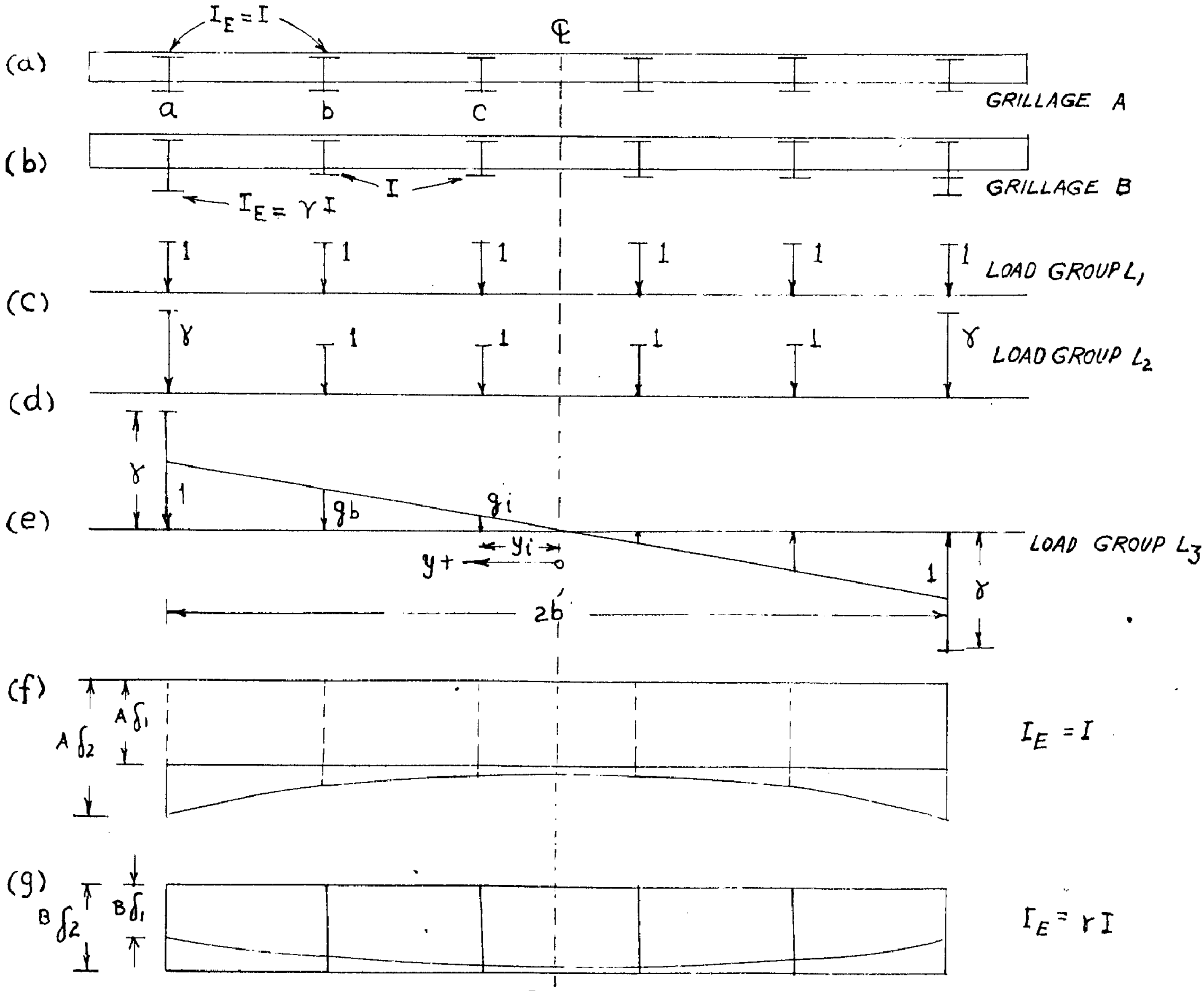

(a)
IE = I
℄
a
b
c
GRILLAGE A
(b)
I
IE = γI
GRILLAGE B
(c)
1
1
1
1
1
1
LOAD GROUP L1
γ
1
1
1
1
γ
LOAD GROUP L2
(d)
(e)
γ
1
gb
gi
yi
y+
LOAD GROUP L3
1
γ
2b'
(f)
Aδ1
Aδ2
IE = I
(g)
Bδ2
Bδ1
IE = γI

FIG. 3.4

in approach but require four compatibility equations to be framed for obtaining the edge forces for a particular position of load; then superpose the effects of edge forces and loads on the equivalent anisotropic plate to obtain the forces in the edge stiffened bridge. In general for solving a moving load problem, distribution profiles or influence line for a particular girder are required to be calculated. The calculation of each influence line is a problem in itself as the values can not be obtained directly either by tables or graphs. If any how, the critical load positions are known then the problem can be solved in one cycle of calculation of simultaneous equations and superposition of different effects. By solving the problem in this manner one is unable to understand the physical behaviour of the bridge.

Using the results obtained in Chapter 2 an approximate method is derived which is simple in use and is based on elementary principles of structural analysis.

In this analysis the ordinates $k = \frac{K}{n}$ of the transverse distribution influence lines are used instead of the distribution coefficient K, where n is the number of longitudinal beams.

3.2.1. <u>No-torsion edge Stiffened Grillages ($\alpha = 0$)</u>

Considering Fig.(3.4), it is a established fact that for the grillage A with $I_g = I$, the load group

L_1 acting at mid-span cross section produces equal deflections $A\delta_1 = c$ of all beams. For the grillage B with $I_B = \gamma I$, with load group L_2 similar equal deflections $B\delta_2 = c$ are obtained and the cross beam remains horizontal. Besides this, for the grillage B, the load group L_3 with $g_i = \frac{y_i}{b'}$, a sloping position of cross beam is obtained and the cross beam remains entirely straight. These are the elementary basic principles used as starting point for the following derivation.

If the load group L_2 acts on the grillage A, the deflection $A\delta_2$ as shown in Fig. (3.4 f) is obtained for edge beam a. If the load group L_1 acts on grillage B the deflection $B\delta_1$ is obtained.

As per MAXWELL BETTI Theorem

$$\frac{A\delta_1}{A\delta_2} = \frac{B\delta_1}{B\delta_2} \qquad \text{......(3.45)}$$

(a) Transverse distribution influence line for edge beam a:

In Fig. (3.5a) the ordinates of transverse distribution influence line of the edge beam a, for grillage A (K_{ai}) and grillage $B(\bar{k}_{ai})$ are shown. If the load group L_1 is acting on grillage A then

$$A\delta_1 = c \sum_{r+m} k_{ai} = c \qquad \text{since } \sum_{r+m} k_{ai} = 1$$

If the load group L_2 is acting on grillage A then

$$A\delta_2 = c\left[\gamma \sum_{\gamma} k_{ai} + \sum_{m} k_{ai}\right]$$

where, $\sum_{\gamma} k_{ai}$ represents the sumof the ordinates of the two edge beam load positions (i.e. k_{aa} & k_{ae}) and $\sum_{m} k_{ai}$ represents the sum of the ordinates of all inner beam load positions. $\sum_{\gamma+m} k_{ai}$ is used to express the sum of the ordinate of all beam load positions. Similarly by using the influence lines for grillage B

$$B\delta_1 = \frac{c}{\gamma} \sum_{\gamma+m} \bar{k}_{ai} \quad \text{and.}$$

$$B\delta_2 = \frac{c}{\gamma}\left[\gamma \sum_{\gamma} \bar{k}_{ai} + \sum_{m} \bar{k}_{ai}\right] = c$$

Therefore,

$$\gamma \sum_{\gamma} \bar{k}_{ai} + \sum_{m} \bar{k}_{ai} = \gamma \qquad \text{....(3.46a)}$$

From equation (3.45) it follows that

$$\sum_{\gamma+m} \bar{k}_{ai} = \frac{\gamma}{\gamma \sum_{\gamma} k_{ai} + \sum k_{ai}} = Z_a \qquad \text{.... (3.46)}$$

Therefore the sum of all the ordinates for the edge beam a of the grillage B (Z_a) can be calculated from equation (3.46), if the ordinates for grillage A ($\gamma = 1$) are known. Thus, it only remains to find the form of the line $\bar{k}_{ai}$. For determining this all the ordinates of the known k_{ai} line are resolved into a symmetrical component ζ'_{ai} and asymmetric component ζ''_{ai} . Referring to fig.(3.5b) and (3.5c) it is obtained that

$$\gamma'_{aa} = \tfrac{1}{2}(k_{aa}+k_{af}); \qquad \gamma''_{aa} = \tfrac{1}{2}(k_{aa}-k_{af})$$
$$\gamma'_{ab} = \tfrac{1}{2}(k_{ab}+k_{ae}); \qquad \gamma''_{ab} = \tfrac{1}{2}(k_{ab}-k_{ae})$$
$$\bar{\gamma}_{aa} = \tfrac{1}{2}(\bar{k}_{aa}+\bar{k}_{af}); \qquad \bar{\gamma}''_{aa} = \tfrac{1}{2}(\bar{k}_{aa}-\bar{k}_{af}).$$
$$\bar{\gamma}_{ab} = \tfrac{1}{2}(\bar{k}_{ab}+\bar{k}_{ae}); \qquad \bar{\gamma}_{ab} = \tfrac{1}{2}(\bar{k}_{ab}-\bar{k}_{ae}) \qquad \text{(3.47a)}$$

$$\sum_{r+m} \bar{\gamma}'_{ai} = \sum_{r+m} \bar{k}_{ai} = Z_a; \quad \sum_{r+m} \gamma'_{ai} = \sum_{r+m} k_{ai} = 1$$

$$\sum_{r+m} \bar{\gamma}''_{ai} = \sum_{r+m} \gamma''_{ai} = 0$$

It is found that the symmetrical component $\bar{\gamma}'_{ai}$ of the grillage B are linearly related to those of grillage A i.e.

$$\bar{\gamma}'_{ai} = u_a \gamma'_{ai} \qquad \text{(3.47b)}$$

If the load group L_1 acts on the grillage B then

$$u_a \sum_{r+m} \gamma'_{ai} = \sum_{r+m} \bar{k}_{ai} = Z_a$$

since $\sum_{r+m} \bar{\gamma}_{ai} = 1 \qquad u_a = Z_a$ (3.47)

For the asymmetric component it is found that according to Fig. 3.5e the following holds good

$$\left.\begin{aligned} \bar{\gamma}''_{ai} &= \gamma''_{ai} + x_i v_a \\ \bar{\gamma}''_{aa} &= \gamma''_{aa} + v_a \quad \text{where} \quad x_i = \frac{\gamma''_{ai}}{\gamma''_{aa}}. \end{aligned}\right\} \qquad \text{(3.48)}$$

If the load group L_3 is acting on grillage B (Fig.3.4) the component of load shared by edge beam 'a' must be . Therefore v_a is determined from equation (3.49)

$$2\gamma\left(z''_{aa}+v_a\right)+2\left[\sum_{g_0}^{g'_b} g_i\left(z''_{ai}+x_i v_a\right)\right]=\gamma$$

....(3.49)

After determining the only unknown v_a from equation (3.49) the ordinates $\bar{k}_{ai}$ can be calculated Thus,

$$\bar{k}_{aa} = u_a z'_{aa} + z''_{aa} + v_a \quad \text{and}$$
$$\bar{k}_{ai} = u_a z'_{ai} + z''_{ai} + x_i v_a$$

(b) <u>Transverse distribution influence line for inner beams</u>

According to MAXWELL'S reciprocal theorem

$$\bar{k}_{ia} = \frac{1}{\gamma}\bar{k}_{ai}\,; \quad \bar{z}'_{ia} = \frac{1}{\gamma}\bar{z}'_{ai}\,; \quad \bar{z}''_{ia} = \frac{1}{\gamma}\bar{z}''_{ai}$$

...(3.50)

From eq.(3.50) the two edge ordinates can be determined for any inner beam. Taking beam b, as $\bar{k}_{ab}$ and $\bar{k}_{ae}$ are already known, the edge ordinates are obtained as

$$\bar{k}_{ba} = \frac{1}{\gamma}\bar{k}_{ab}\,; \qquad \bar{k}_{bf} = \frac{1}{\gamma}\bar{k}_{ae}\,.$$

$$\bar{z}'_{ba} = \frac{1}{\gamma}\bar{z}'_{ab}\,; \qquad \bar{z}''_{ba} = \frac{1}{\gamma}\bar{z}''_{ab}\,.$$

If the load group L_3 is acting on grillage B, the load taken up by beam b must be 1. Therefore,

$$2r\,\bar{\zeta}'_{ba} + \sum_{m} \bar{\zeta}'_{bj} = 1 \qquad \text{..(3.51a)}$$

where the suffix j denotes the load position.

Similarly for load group L_1 acting on grillage B

$$2\,\bar{\zeta}'_{ba} + \sum_{m} \bar{\zeta}'_{bj} = \sum_{r+m} \bar{k}_{bj} = Z_b \qquad \text{...(3.51b)}$$

From eqs.(3.51a) and (3.51b) the sum of all the ordinates for beam b, Z_b can be calculated. Thus

$$Z_b = \sum_{r+m} \bar{k}_{bj} = 1 - 2(r-1)\,\bar{\zeta}'_{ba}$$

$$Z_i = \sum_{r+m} \bar{k}_{ij} = 1 - 2(r-1)\,\bar{\zeta}'_{ia} \qquad \text{...(3.52)}$$

Knowing Z_i, for the 3 main beam grillage and 4 main beam grillage the ordinates $\bar{\zeta}'_{bb}$ can be easily determined from eqs (3.52) and (3.50)

For n = 3 $\qquad \bar{\zeta}'_{bb} = 1 - 2\,\bar{\zeta}'_{ab}$

For n = 4 $\qquad \bar{\zeta}'_{bb} = 0.5\,(1 - 2\,\bar{\zeta}'_{ab})$

For n main beams, after finding the sum of the ordinates Z_i, the symmetrical component for inner beams can be taken as parabolic in shape as shown in Fig. (3.6a). Thus

$$\bar{\zeta}'_{bj} = \bar{\zeta}'_{ba} + u_b\,(1 - g_j^2) \qquad \text{...(3.53)}$$

The value of the unknown U_b can be evaluated from the equation (3.54) when the load group L_1 is acting on grillage B. Thus

$$\sum_{r+m} \bar{\zeta}'_{bj} = Z_b = n\bar{\zeta}'_{ba} + U_b \sum_{m} (1-g_j^2)$$

$$= n\bar{\zeta}'_{ba} + U_b\Big[(n-2) - 2\sum_{g_0}^{g_b} g_j^2\Big] \qquad \ldots (3.54)$$

For determining asymmetric components the emperical relation (3.55) holds good.

$$\bar{\zeta}''_{bj} = \zeta''_{bj} + \Big[\bar{\zeta}''_{ba}\, g_j + 0.45\,\theta^3 (g_j - g_j^2) - \zeta''_{bj}\Big] \times \frac{\gamma-1}{\gamma} \times 1.10 \qquad \ldots (3.55)$$

Then the ordinates are finally obtained as

$$\bar{k}_{bj} = \bar{\zeta}'_{bj} + \bar{\zeta}''_{bj} \;; \qquad \bar{k}_{ij} = \bar{\zeta}'_{ij} + \bar{\zeta}''_{ij} \qquad \ldots (3.56)$$

3.2.3 Torsionally Resistant Edge Stiffened Bridges.

For torsionally resistant bridge ($\alpha \neq 0$) with $\gamma \neq 1$, the equations become more complicated since the elementary basic equations developed in section 3.2.1 are either no more valid or are only valid approximately. If one assumes that for the edge beams, the torsional stiffness J_E follows the relation

$$\frac{J_E}{I_E} = \frac{J}{I}$$

then the following approximate formulae can be used for wide range of values $0 \leq \alpha \leq 1{\cdot}0$, $0 \leq \theta \leq 1{\cdot}0$, $1 \leq \gamma \leq 10$ upto 10 girder bridge.

(a) Transverse Distribution Influence Line for Edge beam a

For the bridge having equal beams ($\gamma = 1$) and the parameter θ and α, the ordinates $k_{ai\alpha}$ can be easily calculated as illustrated in examples 3.3.3. These ordinates are resolved corresponding to equation (3.47a) into their symmetrical and asymmetrical components, $\gamma'_{ai\alpha}$ and $\gamma''_{ai\alpha}$

Corresponding to equations 3.46 and 3.47 the value

$$u_{a\alpha} = \frac{\gamma}{\gamma \sum_{\gamma} k_{ai\alpha} + \sum_{m} k_{ai\alpha}} = \frac{\gamma}{\gamma \sum_{\gamma} \gamma'_{ai\alpha} + \sum_{m} \gamma'_{ai\alpha}} \qquad (3.57)$$

is determined and thereby the value

$$\Delta_a = (\mu_{a\alpha} - 1)\, \gamma_{aa\alpha} \qquad \ldots\ldots (3.58)$$

For an edge stiffened bridge for n equal to (3. to 5)

$$\Delta_a \approx \Delta_m.$$

and for n > 5. $\Delta_m \approx \Delta_a \sqrt{\frac{5}{n}}$ ... (3.59)

Using the values of Δ_a and Δ_m the symmetrical components of the ordinates can be determined from the following equations $\bar{\mathfrak{z}}'_{aa\alpha} = \bar{\mathfrak{z}}_{aa\alpha} + \Delta_a = u_{a\alpha}\bar{\mathfrak{z}}_{aa\alpha}.$

and $\bar{\mathfrak{z}}'_{ai\alpha} = \mathfrak{z}'_{ai\alpha} + \Delta m.$ ..(3.60)

For determining the asymmetrical components of the ordinates $\bar{\mathfrak{z}}''_{ai\alpha}$. the values of $x_{i\alpha}$ and $v_{a\alpha}$ are determined from equation (3.61)

$$x_{i\alpha} = \frac{\mathfrak{z}''_{ai\alpha}}{\mathfrak{z}''_{aa\alpha}} \quad \text{and}$$

$$v_{a\alpha} = 1 + \left[(1.1 + 1.8\alpha^{2/3} e^{-2\theta^2})(0.6 + 0.1\eta) - 1\right]\frac{\gamma - 1}{\gamma} \times 1.1$$

..(3.61)

Thus the asymmetrical components are given by

$$\bar{\mathfrak{z}}''_{aa\alpha} = v_{a\alpha}\,\mathfrak{z}''_{aa\alpha}\ ; \quad \bar{\mathfrak{z}}''_{ai\alpha} = x_{i\alpha}\,\bar{\mathfrak{z}}''_{aa\alpha}.$$

.. (3.62)

(b) <u>Transverse Distribution Line for Inner Beams</u>

The edge ordinates of the transverse distribution influence line for the inner beams can be determined by MAXWELL'S Theorem. Thus,

$$\bar{k}_{ia\alpha} = \frac{1}{\gamma}\bar{k}_{ai\alpha};\quad \bar{\mathfrak{z}}'_{ia\alpha} = \frac{1}{\gamma}\bar{\mathfrak{z}}'_{ai\alpha}\ ;\ \bar{\mathfrak{z}}''_{ia\alpha} = \frac{1}{\gamma}\bar{\mathfrak{z}}''_{ai\alpha}$$ ...(3.63)

<u>Symmetrical Components of the Ordinates</u>

Corresponding to equation (3.52) the values

$$\left.\begin{aligned} Z_{b\alpha} &= 1 - 2(\gamma-1)\,\bar{\mathfrak{z}}'_{ba\alpha}. \\ Z_{i\alpha} &= 1 - 2(\gamma-1)\,\bar{\mathfrak{z}}'_{ia\alpha} \end{aligned}\right\}$$ ...(3.64a)

are determined.

Although $z_{b\alpha}$ can not be sum of the ordinates as determined in Section 3.2.1 there yet continues to exist for the internal beams approximately the same ratio of the individual sums between each other. Thus,

$$\beta_i = \frac{Z_i}{\sum_m Z_j} \approx \frac{z_i'}{\sum_m z_j'} \qquad \text{.... (3.64b)}$$

where, z_i' is the actual sum of the ordinates for beam i and z_γ' for the beam j. If the load group L_1 is acting on the bridge then sum of all ordinates must yield the value n. Consequently,

$$\eta = 2 \sum_{\gamma+m} \bar{z}'_{ai\alpha} + \sum_m z'_j \qquad \text{... (3.64c)}$$

and from equation (3.64b)

$$z_i' = \beta_i \left(\eta - 2 \sum_{\gamma+m} \bar{z}_{ai\alpha} \right) \qquad \text{... (3.64)}$$

If again a parabola is assumed for the shape of influence line $\bar{z}_{ij\alpha}$ of the internal beam then for the beam b similar to equation (3.54)

$$n \bar{z}'_{ba\alpha} + u_{b\alpha} \sum_m (1 - g_j^2) = z_b' \qquad \text{... (3.64)}$$

from which $u_{b\alpha}$ can be determined.

TABLE 3.1 – SYMMETRICAL AND ASYMMETRICAL COMPONENTS OF LOAD DISTRIBUTION COEFFICIENTS FOR SIX GIRDER EDGE STIFFENED GRILLAGE.

Beam \ Load At	a(1) Symmetrical	a(1) Asymmetrical	b(2) Symmetrical	b(2) Asymmetrical	c(3) Symmetrical	c(3) Asymmetrical
a	$\frac{19\lambda^2\gamma+39\lambda\gamma+\gamma}{D_1}$	$\frac{11\lambda^2\gamma+65\lambda\gamma+25\gamma}{D_2}$	$\frac{\gamma(11\lambda+1)}{D_1}$	$\frac{\gamma(7\lambda+15)}{D_2}$	$\frac{\gamma(1-6\lambda)}{D_1}$	$\frac{\gamma(5-6\lambda)}{D_2}$
b	$\frac{(11\lambda+1)}{D_1}$	$\frac{(7\lambda+15)}{D_2}$	$\frac{19\lambda^2\gamma+11\lambda\gamma+5\lambda+1}{D_1}$	$\frac{11\lambda^2\gamma+45\lambda\gamma+3\lambda+9}{D_2}$	$\frac{(17\lambda\gamma+1)}{D_1}$	$\frac{(25\lambda\gamma+3)}{D_2}$
c	$\frac{(1-6\lambda)}{D_1}$	$\frac{(5-6\lambda)}{D_2}$	$\frac{(17\lambda\gamma+1)}{D_1}$	$\frac{(25\lambda\gamma+3)}{D_2}$	$\frac{19\lambda^2\gamma+28\lambda\gamma+5\lambda+1}{D_1}$	$\frac{11\lambda^2\gamma+20\lambda\gamma+3\lambda+1}{D_2}$
	$D_1 = 2(19\lambda^2\gamma+39\lambda\gamma+5\lambda+\gamma+2)$;			$D_2 = 2(11\lambda^2\gamma+65\lambda\gamma+3\lambda+25\gamma+10)$		

TABLE – 3.2

Load at		$\lambda = 16/81$, $\theta = 1.0$				$\lambda = 1/81$, $\theta = 0.50$				$\lambda = 1/1296$, $\theta = 0.25$			
		$\gamma=1$	$\gamma=3$	$\gamma=5$	$\gamma=10$	$\gamma=1$	$\gamma=3$	$\gamma=5$	$\gamma=10$	$\gamma=1$	$\gamma=3$	$\gamma=5$	$\gamma=10$
a	$\bar{k}_{aa}$	0.7714	0.9101	0.9437	0.9712	0.5712	0.7844	0.8552	0.9203	0.5271	0.7446	0.8229	0.8993
	$\bar{k}_{ba}$	0.2952	0.1159	0.0722	0.0371	0.3674	0.1735	0.1141	0.0617	0.3802	0.1871	0.1260	0.0698
	$\bar{k}_{ca}$	0.0316	0.0123	0.0079	0.0039	0.1993	0.0992	0.0665	0.0366	0.2353	0.1270	0.0881	0.0501
	$\bar{k}_{da}$	-0.0464	-0.0181	-0.0112	-0.0059	0.0619	0.0428	0.0311	0.0182	0.0927	0.0684	0.0511	0.0309
	$\bar{k}_{ea}$	-0.0400	-0.0147	-0.0090	-0.0045	-0.0472	+0.0009	0.0057	0.0055	-0.0478	0.0109	0.0150	0.0122
	$\bar{k}_{fa}$	-0.0118	-0.0055	-0.0033	-0.0018	-0.1526	-0.1008	-0.0726	-0.0423	-0.1875	-0.1380	-0.1031	-0.0625
b	$\bar{k}_{ab}$	0.2952	0.3479	0.3608	0.3711	0.3674	0.5203	0.5706	0.6173	0.3802	0.5613	0.6298	0.6978
	$\bar{k}_{bb}$	0.3908	0.3210	0.3040	0.2904	0.3094	0.1746	0.1342	0.0997	0.2958	0.1545	0.1070	0.0621
	$\bar{k}_{cb}$	0.2564	0.2478	0.2457	0.2441	0.2168	0.1475	0.1243	0.1030	0.2101	0.1200	0.0859	0.0521
	$\bar{k}_{db}$	0.0940	0.1058	0.1085	0.1109	0.1244	0.1027	0.0917	0.0802	0.1239	0.0840	0.0631	0.0599
	$\bar{k}_{eb}$	0.0036	0.0216	0.0258	0.0290	0.0292	0.0522	0.0509	0.0453	0.0378	0.0475	0.0392	0.0265
	$\bar{k}_{fb}$	-0.0400	-0.0441	-0.0448	-0.0455	-0.0472	0.0027	0.0282	0.0545	-0.0478	0.0327	0.0750	0.1218
c	$\bar{k}_{ac}$	0.0316	0.0367	0.0380	0.0390	0.1993	0.2977	0.3327	0.3658	0.2353	0.3811	0.4401	0.5004
	$\bar{k}_{bc}$	0.2564	0.2478	0.2457	0.2441	0.2168	0.1475	0.1243	0.1030	0.2101	0.1200	0.0859	0.0521
	$\bar{k}_{cc}$	0.3940	0.3908	0.3903	0.3897	0.2167	0.1719	0.1561	0.1411	0.1832	0.1111	0.0817	0.0517
	$\bar{k}_{dc}$	+0.2712	0.2734	0.2739	0.2743	0.1809	0.1515	0.1397	0.1279	0.1548	0.0987	0.0737	0.0473
	$\bar{k}_{ec}$	0.0940	0.1058	0.1085	0.1109	0.1244	0.1027	0.0917	0.0802	0.1239	0.0840	0.0631	0.0399
	$\bar{k}_{fc}$	-0.0464	-0.0545	-0.0564	-0.0580	0.0619	0.1287	0.1555	0.1820	0.0927	0.2051	0.2555	0.3086

Asymmetric Component $\bar{z}''_{ij\alpha}$

The end ordinates of the influence line can be determined from MAXWELL's Theorem i.e.

$$\bar{z}''_{ia\alpha} = \frac{1}{\gamma}\bar{z}''_{ai\alpha}$$

For the inner ordinates an emporical equation similar to equation (3.55) can be used. Thus,

$$\bar{z}''_{bj\alpha} = z''_{bj\alpha} + \left[\bar{z}''_{ba\alpha}\cdot g_j + 0.45\,\theta^3 (g_j - g_j^2) - z''_{bj\alpha}\right]\frac{\gamma-1}{\gamma}\times 1.10$$

$$\bar{k}_{bj\alpha} = \bar{z}'_{bj\alpha} + \bar{z}''_{bj\alpha} \qquad \ldots.(3.65)$$

Finally,

$$\bar{k}_{bj\alpha} = \bar{z}'_{bj\alpha} + \bar{z}''_{bj\alpha}$$

3.3 EXAMPLE: SIX GIRDER EDGE STIFFENED GRILLAGE.

To study the application of the approximate method developed in section 3.2, a six-girder edge stiffened open grillage with one cross beam at the mid-span is considered. The grillage is also analysed by flexibility method and the symmetrical and asymmetrical components of the load distributed on each girder are tabulated in Table 3.1 for unit load application at mid-span point of the beams a, b, and c (Fig. 3.4 b). The analysis is general and the values are given in terms of $\lambda = \left(\frac{b}{a}\right)^3 \frac{EI}{EI_T}$ and $\gamma = \frac{EI_E}{EI}$

LOAD AT		θ = 1·0			θ = 0·5			θ = 0·25		
		K	ζ'	ζ''	K	ζ'	ζ''	K	ζ'	ζ''
a	aa	0·7511	0·36885	0·38225	0·5694	0·2147	0·3547	0·5184	0·1752	0·3432
	ab	0·2886	0·12515	+0·16345	0·3630	0·1562	0·2068	0·3756	0·16405	0·21155
	ac	0·0486	0·00600	0·04260	0·1958	0·1291	0·0667	0·2303	0·16075	0·06955
	ad	−0·0366	0·00600	−0·04260	0·0624	0·1291	−0·0667	0·0912	0·16075	−0·06955
	ae	−0·0383	0·12515	−0·16345	−0·0506	0·1562	−0·2068	−0·0475	0·16405	−0·21155
	af	−0·0134	0·36885	−0·38225	−0·1400	0·2147	−0·3547	−0·1680	0·1752	−0·3432
b	ba	0·2886	0·12515	0·16345	0·3630	0·1562	0·2068	0·3756	0·16405	0·21155
	bb	0·3923	0·19695	0·19535	0·3061	0·1717	0·1344	0·2977	0·16995	0·12775
	bc	0·2579	0·1779	0·0800	0·2176	0·1721	0·0455	0·2061	0·1660	0·0401
	bd	0·0979	0·1779	−0·0800	0·1266	0·1721	−0·0455	0·1259	0·1660	−0·0401
	be	0·0016	0·19695	−0·19535	0·0373	0·1717	0·1344	0·0422	0·16995	−0·12775
	bf	−0·0383	0·12515	−0·16345	−0·0506	0·1562	−0·2068	−0·0475	0·16405	−0·21155
c	ca	+0·0486	0·0600	0·0426	0·1958	0·1291	0·0667	0·2303	0·16075	0·06955
	cb	0·2579	0·1779	0·0800	0·2176	0·1721	0·0455	0·2061	0·1660	+0·0401
	cc	0·3650	0·3161	0·0489	0·2142	0·1988	0·0154	0·1864	0·17325	0·01315
	cd	0·2672	0·3161	−0·0489	0·1834	0·1988	−0·0154	0·1601	0·17325	−0·01315
	ce	0·0979	0·1779	−0·0800	0·1266	0·1721	−0·0455	0·1259	0·1660	−0·0401
	cf	−0·0366	0·0600	−0·0426	0·0624	0·1291	−0·0667	0·0912	0·16075	−0·06955

TABLE 3.3 - SYMMETRICAL AND ASYMMETRICAL COMPONENT FOR $\gamma = 1$

where,

p = Spacing the main beams,

$2a$ = span length.

EI = Flexural rigidity of inner beam.

EI = Flexural rigidity of cross beam.

EI_E = Flexural rigidity of edge beam.

Using the results obtained in table 3.1, the numerical values of various distribution coefficients are tabulated in table 3.2 for $r = 1$, $r = 3$, $r = 5$ and $r = 10$ and $\lambda = \frac{16}{81}$ and $\lambda = \frac{1}{81}$ and $\lambda = \frac{1}{1296}$. The values of λ correspond to the values of flexural parameter θ of equivalent anisotropic plate equal to 1.0, 0.5 and 0.25 respectively.

For analysing the grillage by approximate method developed in section 3.2, the distribution coefficients $k = \frac{K}{n}$ obtained from graphs 1 to 6 and their symmetric components g' and asymmetric components g'' are tabulated in table 3.3 for $\theta = 1.0$, $\theta = 0.5$ and $\theta = 0.25$. Using equations (3.46) to (3.56) of section 3.2 the influence line ordinates for transverse distribution of loads for edge beam and inner beams b and c are calculated for $r = 3$, $r = 5$ and $r = 10$ and the values are tabulated in Table 3.4.

A comparison of values obtained by the two methods is given table 3.5. It is seen from the table 3.5 that the

TABLE 3·5

FOR BEAM	DIST. COEFF.	$\beta = 1·0$						$\beta = 0·50$						$\beta = 0·25$					
		$\gamma = 3$		$\gamma = 5$		$\gamma = 10$		$\gamma = 3$		$\gamma = 5$		$\gamma = 10$		$\gamma = 3$		$\gamma = 5$		$\gamma = 10$	
		APPROX.	EXACT	APPROX.	EXACT	APPROX.	EXACT	APPROX.	EXACT	APPROX.	EXACT	APPROX.	EXACT	APPROX.	EXACT	APPROX.	EXACT	APPROX.	EXACT
a	$\bar{k}_{aa}$	0·9045	0·9101	0·9404	0·9437	0·9693	0·9712	0·7893	0·7844	0·8591	0·8552	0·9228	0·9203	0·7518	0·7446	0·8269	0·8229	0·9021	0·8993
	$\bar{k}_{ab}$	0·3473	0·3479	0·3609	0·3608	0·3718	0·3711	0·5103	0·5203	0·5580	0·5706	0·6018	0·6173	0·5623	0·5615	0·6263	0·6298	0·6911	0·6978
	$\bar{k}_{ac}$	0·0583	0·0367	0·0604	0·0380	0·0621	0·0390	0·2417	0·2977	0·3248	0·3527	0·3559	0·3658	0·3733	0·3811	0·4283	0·4461	0·4843	0·5004
	$\bar{k}_{ad}$	-0·0437	-0·0545	-0·0452	-0·0564	-0·0463	-0·0580	0·1251	0·1287	0·1502	0·1555	0·1749	0·1820	0·1939	0·2051	0·2411	0·2555	0·2897	0·3086
	$\bar{k}_{ae}$	-0·0439	-0·0441	-0·0441	-0·0448	-0·0442	-0·0455	-0·0061	0·0027	0·0168	0·0282	0·0404	0·0545	0·0165	0·0327	0·0567	0·0750	0·0989	0·1280
	$\bar{k}_{af}$	-0·0105	-0·0055	-0·0068	-0·0033	-0·0037	-0·0018	-0·0963	-0·1008	-0·0651	-0·0726	-0·0400	-0·0425	-0·1338	-0·1380	-0·0975	-0·1031	-0·0585	-0·0623
b	$\bar{k}_{ba}$	0·1158	0·1159	0·0722	0·0722	0·0372	0·0371	0·1701	0·1735	0·1116	0·1141	0·0602	0·0617	0·1874	0·1871	0·1252	0·1260	0·0691	0·0698
	$\bar{k}_{bb}$	0·3093	0·3210	0·2823	0·3040	0·2590	0·2904	0·1996	0·1746	0·1523	0·1342	0·1093	0·0997	0·1788	0·1545	0·1233	0·1070	0·0705	0·0621
	$\bar{k}_{bc}$	0·2824	0·2478	0·2787	0·2457	0·2747	0·2441	0·1633	0·1475	0·1387	0·1243	0·1157	0·1050	0·1319	0·1200	0·0973	0·0859	0·0625	0·0521
	$\bar{k}_{bd}$	0·1150	0·1058	0·1185	0·1085	0·1223	0·1109	0·1006	0·1027	0·0934	0·0917	0·0860	0·0802	0·0822	0·0840	0·0662	0·0631	0·0478	0·0399
	$\bar{k}_{be}$	0·0187	0·0216	0·0236	0·0258	0·0166	0·0290	0·0324	0·0522	0·0407	0·0509	0·0466	0·0453	0·0272	0·0475	0·0312	0·0392	0·0294	0·0263
	$\bar{k}_{bf}$	-0·0146	-0·0147	-0·0088	-0·0090	-0·0044	-0·0045	-0·0020	+0·0009	0·0034	0·0057	0·0040	0·0056	0·0055	0·0109	0·0113	0·0150	0·0099	0·0122
c	$\bar{k}_{ca}$	0·0194	0·0125	0·0121	0·0076	0·0062	0·0039	0·0972	0·0992	0·0650	0·0665	0·0356	0·0366	0·1244	0·1270	0·0867	0·0881	0·0484	0·0501
	$\bar{k}_{cb}$	0·3056	0·2478	0·3078	0·2457	0·3079	0·2441	0·1648	0·1475	0·1410	0·1243	0·1184	0·1030	0·1306	0·1200	0·0955	0·0859	0·0608	0·0521
	$\bar{k}_{cc}$	0·3635	0·3908	0·3664	0·3903	0·3686	0·3897	0·1757	0·1719	0·1608	0·1561	0·1464	0·1411	0·1197	0·1111	0·0916	0·0817	0·0632	0·0517
	$\bar{k}_{cd}$	0·2268	0·2734	0·2238	0·2739	0·2223	0·2743	0·1462	0·1515	0·1552	0·1597	0·1246	0·1279	0·1022	0·0987	0·0801	0·0757	0·0568	0·0473
	$\bar{k}_{ce}$	0·0896	0·1058	0·0867	0·1085	0·0861	0·1109	0·0963	0·1027	0·0881	0·0917	0·0800	0·0802	0·0804	0·0840	0·0636	0·0651	0·0430	0·0399
	$\bar{k}_{cf}$	-0·0146	-0·0181	-0·0090	-0·0112	-0·0046	-0·0059	+0·0417	0·0428	0·0300	0·0311	0·0175	0·0182	0·0646	0·0684	0·0452	0·0511	0·0290	0·0309

values obtained by approximate method are very close to the values obtained by exact method. The variation is due to the assumption made in plate theory. If the values of k in table 3.2 for r = 1, instead of the values given in table 3.3, are considered in the analysis of section 3.2 then the influence ordinates for beam a exactly coincide with the exact values. A small amount of error is introduced in case influence ordinates for inner beams b and c because of the assumption made in shape of influence diagrams for symmetric and assymmetric components according to equations (3.53) and (3.58). Also it is evident that due to assumptions made in the shape of influence diagrams the MAXWELL's reciprocal theorem is violated at some points but the difference is very small.

The above example, therefore, proves the utility of approx. method for wide range of values. Moreover, the method is also applicable for certain cases of bridges with torsional resistance. Considering the further advantage of the method of section 3.2 it is seen that in the intermediate steps of calculations of influence lines, the values of Z_a and Z_i are determined according to equations (3.46) and (3.53). These values of Z_a and Z_i correspond to dead load distribution coefficients of edge stiffened bridges when equal loads are applied on all beams. The values of Z calculated in the above example for $\theta = 1.0$, $\theta = 0.5$, $\theta = 0.25$,

TABLE 3.4 - DISTRIBUTION COEFFICIENTS FOR SIX GIRDER EDGE STIFFENED BRIDGE.

I.L. FOR BEAM	DIST. COEFF.	θ = 1.0			θ = 0.5			θ = .25		
		γ = 3	γ = 5	γ = 10	γ = 3	γ = 5	γ = 10	γ = 3	γ = 5	γ = 10
a	$\bar{k}_{aa}$	0.9045	0.9404	0.9693	0.7893	0.8591	0.9228	0.7518	0.8269	0.9021
	$\bar{k}_{ab}$	0.3473	0.3609	0.3718	0.5103	0.5580	0.6018	0.5623	0.6263	0.6911
	$\bar{k}_{ac}$	0.0583	0.0604	0.0621	0.2917	0.3248	0.3559	0.3733	0.4283	0.4843
	$\bar{k}_{ad}$	-0.0437	-0.0452	-0.0463	0.1251	0.1502	0.1749	0.1939	0.2411	0.2897
	$\bar{k}_{ae}$	-0.0439	-0.0441	-0.0442	-0.0061	0.0168	0.0404	0.0165	0.0567	0.0987
	$\bar{k}_{af}$	-0.0105	-0.0068	-0.0037	-0.0963	-0.0691	-0.0400	-0.1338	-0.0973	-0.0585
b	$\bar{k}_{ba}$	0.1158	0.0722	+0.0372	0.1701	0.1116	0.0602	0.1874	0.1252	0.0691
	$\bar{k}_{bb}$	0.3093	0.2823	0.2590	0.1996	0.1523	0.1093	0.1788	0.1233	0.0705
	$\bar{k}_{bc}$	0.2824	0.2787	0.2747	0.1633	0.1387	0.1157	0.1319	0.0973	0.0625
	$\bar{k}_{bd}$	0.1150	0.1185	0.1223	0.1006	0.0934	0.0860	0.0822	0.0662	0.0478
	$\bar{k}_{be}$	-0.0107	0.0036	0.0166	0.0324	0.0407	0.0466	0.0272	0.0312	0.0294
	$\bar{k}_{bf}$	-0.0146	-0.0088	-0.0044	-0.0020	0.0034	0.0040	0.0055	0.0113	0.0099
c	$\bar{k}_{ca}$	0.0194	0.0121	0.0062	0.0972	0.0650	0.0356	0.1244	0.0857	0.0484
	$\bar{k}_{cb}$	0.3056	0.3078	0.3079	0.1648	0.1410	0.1184	0.1306	0.0955	0.0608
	$\bar{k}_{cc}$	0.3635	0.3664	0.3680	0.1757	0.1608	0.1464	0.1197	0.0916	0.0632
	$\bar{k}_{cd}$	0.2268	0.2238	0.2223	0.1462	0.1352	0.1246	0.1022	0.0801	0.0568
	$\bar{k}_{ce}$	0.0896	0.0867	0.0861	0.0963	0.0881	0.0800	0.0804	0.0636	0.0450
	$\bar{k}_{cf}$	-0.0146	-0.0090	-0.0046	0.0417	0.0300	0.0175	0.0646	0.0482	0.0290

TABLE 3.6 - DEAD LOAD DISTRIBUTION IN A SIX GIRDER EDGE STIFFENED BRIDGE.

BEAM	DIST. COEFF.	θ = 1.0			θ = 0.5			θ = 0.25		
		γ = 3	γ = 5	γ = 10	γ = 3	γ = 5	γ = 10	γ = 3	γ = 5	γ = 10
a	Z_a	1.2119	1.2656	1.3090	1.6139	1.8399	2.0557	1.7639	2.0819	2.4076
b	Z_b	0.7978	0.7466	0.7052	0.6639	0.5401	0.4220	0.6142	0.4541	0.2890
c	Z_c	0.9903	0.9878	0.9858	0.7222	0.6200	0.5223	0.6219	0.4640	0.3034

and $\gamma = 3$, $r = 5$, $r = 10$ are tabulated in Table 3.6 from which load distribution for dead load can be obtained. It is thus seen that in case of edge stiffened bridges , the inner beams are relieved by as much as 70% of its dead load for $r = 10$ and $\theta = 0.25$.

Considering the live load effects on edge stiffened bridges it is seen that the influence line ordinates for inner beams are considerably less than that of an ordinary bridge whereas the ordinates for edge beams are considerably more. The values of influence ordinates for inner beams go on decreasing with increase in the stiffness of edge beams and for edge beams those values increase with the increase in the stiffness. Also the transverse bending moments in cross beams increase with the increase in stiffness of edge beams. It is, therefore, realised that there is always an optimum edge stiffening. The optimum edge stiffening primarily depends upon width of the bridge and the loads coming on it. However, it is difficult to arrive at the optimum ratio of the moment of inertia of edge beam to inner beam since it depends upon many variables.

CHAPTER 4

CONTINUOUS GRID BEAM BRIDGES

Load distribution analysis of right bridges with simple support conditions, has been derived in Chapters 2 and 3 employing Fourier series for various loads, shear forces, moments and deflections. The basic functions are employed by ROWE [26] to derive a load distribution analysis for bridges with various support conditions. The general equations of deformation, longitudinal bending moment and transverse bending moment are derived for no-torsion bridges with prismatic longitudinal and transverse beams. No analytical method is available for finding the distribution properties of a bridge with indeterminate support conditions and considering the effect of torsional stiffness of various members.

Approximate method of analysis is developed for continuous bridges; analysing the equivalent simply supported span between points of contra-flexure for the mean effects which are known from moment distribution analysis. An approximate analysis is also developed for continuous bridges with prismatic and non-prismatic main beams on the basis of equivalent longitudinal stiffness of simply supported bridge for the derivation of flexural and torsional parameters. The bridge is then analysed as a simply span having derived equivalent stiffness. The equivalent stiffness for various cases of continuous bridges has been derived by using moment distribution analysis.

4.1 LOAD DISTRIBUTION IN NO-TORSION GRILLAGES WITH VARIOUS SUPPORT CONDITIONS.

As the deflection of a beam with various support conditions can be expressed in terms of Basic function series for any loading on the beam, the problem can be treated in a manner similar to the Fourier Series analysis. The load p(x) per unit length of a beam is expressed in the form

$$p(x) = \sum_{m=1}^{\infty} A_m F_m(x) \qquad \ldots\ldots (4.1a)$$

where, the general numerical coefficient A_m is found similar to Fourier series analysis and $F_m(x)$ is the Basic function given by

$$F_m(x) = f_m\left[\cosh k_m x - \cos k_m x\right] - \left[\sinh k_m x - \sin k_m x\right] \qquad (4.1b)$$

where, f_m and k_m are constants determined from the support conditions of the beam.

Considering a particular case of a load P at any given section $x = c$, $0 < x < l$, the loading can be expressed in terms of Basic function series

$$p(x) = \frac{P}{l} \sum_{m=1}^{\infty} \frac{F_m(c)\; F_m(x)}{\int_0^l \left[F_m(x)\right]^2 dx} \qquad \text{-----}(4.1c)$$

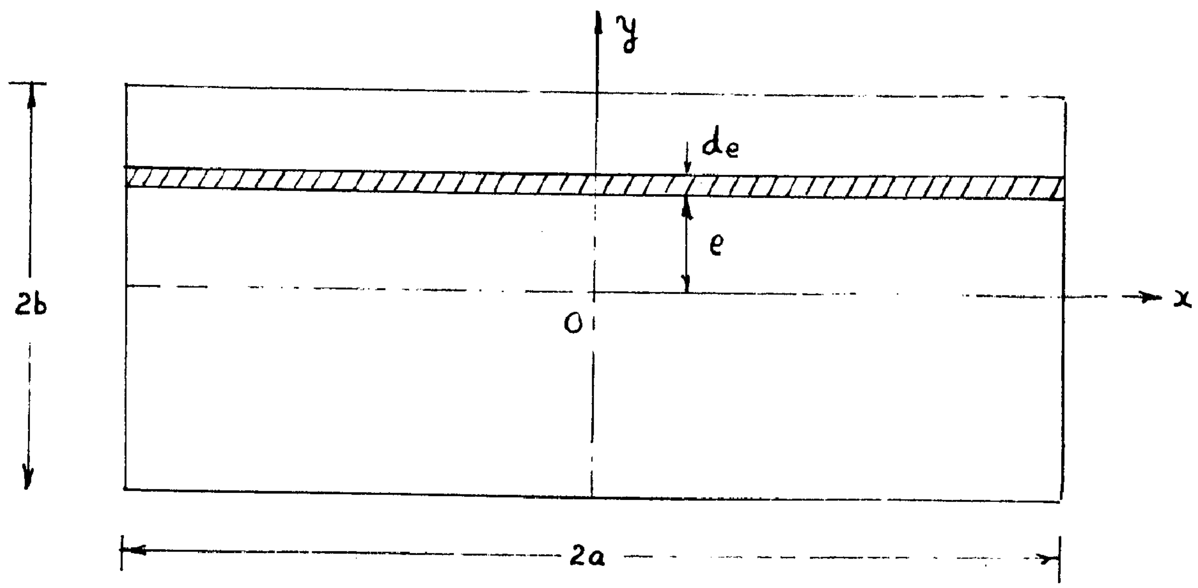

FIG. 4·1

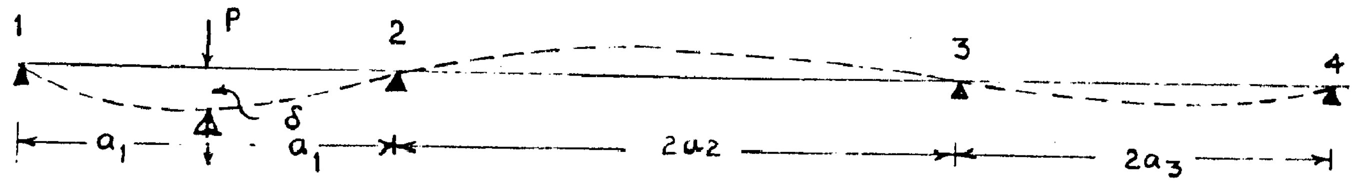

CASE 3: OUTER SPAN LOADED $\gamma_{12} = \frac{C_{12}}{6} = 1.328$

$a_1 : a_2 : a_3$

$2 : 3 : 2$

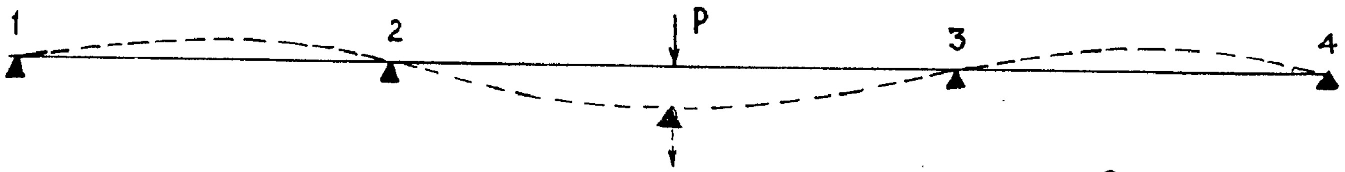

CASE 4: MIDDLE SPAN LOADED $\gamma_{23} = \frac{C_{23}}{6} = 2.080$

FIG. 4·2

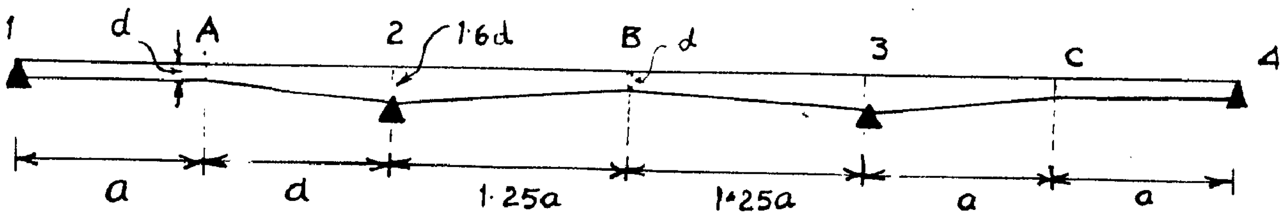

FIG. 4·3

For a beam fixed at both ends, the denominators are given as (58)

$$\int_0^1 [F_1(x)]^2 dx = 1.0359 \quad ; \quad \int_0^l [F_2(x)]^2 dx = 0.9984$$

$$\int_0^1 [F_3(x)]^2 dx = 1.0001$$ and the Basic function series for a concentrated load on fixed beam is

$$p = \frac{P}{l}\left\{ \frac{F_1(e)F_1(x)}{1.0359} + \frac{F_2(e)F_2(x)}{0.9984} + \frac{F_3(x)\,F_3(e)}{1.0001} + \cdots \right\}$$

.... (4.1)

The values of the Basic functions $F_m(x)$ and $F_m(e)$ can be evaluated from the tables given in ref. (25). Similarly Basic function series can be derived for various support conditions.

Considering a no-torsion grillage represented by an anisotropic plate (fig. 4.1) with the effective width $2b = np$, length $2a$, $i_L = I/p$, $i_T = I_T/q$, the longitudinal and transverse flexural rigidities ρ_p and ρ_E respectively.

With the coordinate axes as shown in Fig. (4.1) the load $p(x) = \sum_{m=1}^{\infty} A_m F_m(x)$ is applied on the elementary strip, de, at an eccentricity e. The load intensity is given by

$$p(x) = \frac{P(x)}{de} = \pi \sum_{m=1}^{\infty} \frac{A_m F_m(x)}{b\,d\varphi} \quad \text{if} \quad \varphi = \frac{\pi e}{b}$$

Writing $\beta = \frac{\pi y}{b}$ the governing differential equation of flexural of no-torsion anisotropic plate is written as

$$\rho_P \frac{\partial^4 w}{\partial x^4} + \rho_E \frac{\partial^4 w}{\partial y^4} = \sum_{m=1}^{\infty} \frac{A_m f_m(x)}{2b} \left\{ 1 + 2\sum_{n=1}^{\infty} \cos n(\beta - \psi) \right\} \qquad \text{.... (4.2)}$$

The solution of differential equation (4.2) has been obtained in two parts (a) and (b) as given below.

(a) For $\rho_P \frac{\partial^4 w}{\partial x^4} + \rho_E \frac{\partial^4 w}{\partial y^4} = \sum_{m=1}^{\infty} \frac{A_m f_m(x)}{2b}$

The solution is

$$W_m = \frac{A_m f_m(x)}{2b\, \rho_P\, k_m^4} \qquad \text{... (4.3)}$$

where, W_m is the mean deflection corresponding to m^{th} term of the basic function load series and k_m is the m^{th} root multiplier depending upon the type of support conditions.

(b) For $\rho_P \frac{\partial^4 w}{\partial x^4} + \rho_E \frac{\partial^4 w}{\partial y^4} = \sum_{m=1}^{\infty} \frac{A_m f_m(x)}{b} \sum_{n=1}^{\infty} \cos n(\beta - \psi)$

the solution is of the form $w_m = X_m Y_m$ where, X_m is the function of x satisfying the support condition and Y_m is the function of y satisfying the boundary conditions at the free edges. Thus solving the equation, it is obtained that

$$X_m = \frac{A_m f_m(x)}{b\ \rho_E} \frac{b^4}{\bar{\lambda}^4} \qquad \text{and}$$

$$Y_m = \cosh \lambda_m \beta \, (C \sin \lambda_m \beta + D \cos \lambda_m \beta) + \sinh \lambda_m \beta \times (F \sin \lambda_m \beta + G \cos \lambda_m \beta) + \sum_{n=1}^{\infty} \frac{\cos n(\beta - \psi)}{(n^4 + \theta_m'^4)}$$

where C, D, F, G are arbitrary constants which are evaluated from the boundary conditions at the free edges and

$$\lambda_m = \frac{\theta_m'}{\sqrt{2}} \quad ;$$

$$\theta_m' = \frac{2ak_m}{\pi} \left(\frac{b}{2a} \sqrt[4]{\frac{\rho_P}{\rho_E}} \right) \qquad \ldots (4.4)$$

Thus θ_m' is a parameter defining the relative flexural stiffness and the support conditions. θ_m' can be considered as the flexural parameter θ used in the load distribution analysis of right simply supported bridges multiplied by a factor $\frac{2a\,k_m}{\pi}$ which depends on the actual support conditions of the bridge. The appropriate value of k_m is found from Basic functions for deflection of a beam with various support conditions.(25, 26). Combining the solutions (a) and (b) and applying the boundary conditions at the free edges the deflection at any point can be written in the form

$$w = \frac{A\,F(x)}{2b\,\rho_P\,k^4} K \qquad \ldots (4.5)$$

where K is distribution coefficient and is given by

$$K = \left\{ 1 + \left[\frac{(\cosh\lambda\beta \sin\lambda\beta \cosh\lambda\pi \sin\lambda\pi + \sinh\lambda\beta \cos\lambda\beta \sinh\lambda\pi \cos\lambda\pi}{(\cosh\lambda\pi \sinh\lambda\pi - \cos\lambda\pi \sin\lambda\pi)} \right.\right.$$

$$\times 2\sqrt{2}\ \theta' \sum_{n=1}^{\infty} n^3 (-1)^{n+1} \frac{\sin n\psi}{(n^4+\theta'^4)} + \frac{2\theta'^2 \sum_{n=1}^{\infty} n^2 (-1)^{n+1} \frac{\cos n\psi}{(n^4+\theta'^4)}}{(\cosh\lambda\pi \sinh\lambda\pi + \cos\lambda\pi \sin\lambda\pi)}$$

$$\{ \cosh\lambda\beta \cos\lambda\beta\ (\cosh\lambda\pi \sin\lambda\pi - \sinh\lambda\pi \cos\lambda\pi) - \sinh\lambda\beta \sin\lambda\beta$$

$$\left.\left. (\cosh\lambda\pi \sin\lambda\pi + \sinh\lambda\pi \cos\lambda\pi) \} + 2\theta'^4 \sum_{n=1}^{\infty} \frac{\cos n(\beta-\psi)}{(n^4+\theta'^4)} \right] \right\} \qquad \ldots\ldots (4.6)$$

Thus,

$$K = f(\theta', y/b, e/b)$$

The complete series for the deflection is given by

$$\omega = \frac{1}{2b\rho_p} \left\{ \frac{A_1 F_1(x)}{k_1^4} K_1 + \frac{A_2 F_2(x)}{k_2^4} K_2 + \frac{A_3 F_3(x)}{k_3^4} K_3 + \cdots \right\} \qquad \ldots\ldots (4.7)$$

For each individual term there is a unique value of k and hence, the flexural parameter θ' and distribution coefficient K. However, for deflections the 1st term of equation (4.7) gives an accuracy of about 3% and for 3 terms the accuracy is within 0.6%.

<u>Longitudinal bending moments M_x</u>

Since $$M_x = -\rho_p \frac{\partial^2 \omega}{\partial x^2}$$

From equation (4.7) the value of $\frac{\partial^2 \omega}{\partial x^2}$ is derived and M_x can be written as

$$M_x = -\frac{1}{2b} \left\{ \frac{A_1 \Phi_1(x)}{k_1^2} K_1 + \frac{A_2 \Phi_2(x)}{k_2^2} K_2 + \frac{A_3 \Phi_3(x)}{k_3^2} K_3 + \cdots \right\} \qquad \ldots (4.8)$$

where, $\phi_1(x)$, $\phi_2(x)$ etc. are complementary basic functions to $F_1(x)$, $F_2(x)$ etc. given by $k_m^2 \phi_m(x) = \dfrac{d^2 F_m(x)}{dx^2}$ and K_1 , K_2 etc. are the distribution coefficients for deflection written in eq.4.7 For calculating M_x the first three terms give sufficient accuracy.

Transverse Bending Moment.

$$\text{Since} \quad M_y = -\rho_E \frac{\partial^2 w}{\partial y^2}$$

From equation (4.5) M_y can be written in the form

$$M_y = \frac{A\ F(x)}{4b\ k^2} \sqrt{\frac{\rho_E}{\rho_P}} \quad \mu$$

where μ is distribution coefficient for transverse bending moment and is equal to

$$\mu = \Bigg\{ - \frac{(\cosh\lambda\pi \sin\lambda\pi \sinh\pi\beta \cos\lambda\beta - \sinh\lambda\pi \cos\lambda\pi \cosh\lambda\beta \sin\lambda\beta)}{\cosh\lambda\pi \sinh\lambda\pi - \cos\lambda\pi \sin\lambda\pi}$$

$$\times 4\sqrt{2}\,\theta' \sum_{n=1}^{\infty} n^3 (-1)^{n+1} \frac{\sin n\psi}{(n^4+\theta'^4)} + \frac{4\theta'^2 \sum_{n=1}^{\infty} n^2 (-1)^{n+1} \dfrac{\cos n\psi}{(n^4+\theta'^4)}}{\cosh\lambda\pi \sinh\lambda\pi + \cos\lambda\pi \sin\lambda\pi}$$

$$\Big[\sinh\lambda\beta \sin\lambda\beta (\cosh\lambda\pi \sin\lambda\pi - \sinh\lambda\pi \cos\lambda\pi)$$

$$- \cosh\lambda\beta \cos\lambda\beta (\cosh\lambda\pi \sin\lambda\pi + \sinh\lambda\pi \cos\lambda\pi) \Big]$$

$$+ 4\theta'^2 \sum_{n=1}^{\infty} n^2 \frac{\cosh(\beta-\psi)}{(n^4+\theta'^4)} \Bigg\} \qquad \ldots (4.9)$$

The complete expression for the transverse bending moment, M_y, is thus

$$M_y = \frac{1}{4b}\sqrt{\frac{\rho_E}{\rho_P}}\left\{ \frac{A_1 F_1(x)}{K_1^2}\mu_1 + \frac{A_2 F_2(x)}{K_2^2}\mu_2 + \frac{A_3 F_3(x)}{K_3^2}\mu_3 + \cdots \right\} \qquad (4.10)$$

The calculation of transverse bending moment is carried out in the same way as for deflections and longitudinal bending moments. The first three terms in equation (4.10) give sufficiently accurate value of M_y.

The values of distribution coefficients K and μ for various values of flexural parameter θ' are given by ROWE)[25] in the form of design curves for no-torsion grillage similar to curves of Chapter 2. The application of the analysis is shown in example 4.3.1.

4.2. APPROXIMATE METHOD OF ANALYSIS.

Since no rigorous analysis is available for torsionally resistant continuous bridges; some form of approximate analysis based upon the theory developed in previous chapters is necessary. Two approximate methods have been developed by the author. These have been named as follows:

1) Equivalent Stiffness method.

2) Equivalent simply supported span method.

4.2.1 EQUIVALENT STIFFNESS METHOD

The deflections on loading a span of a continuous beam, are lesser than that of a simply supported span of same moment of inertia and span length. The continuity of main beams thus stiffens the bridge in longitudinal direction and produces a different load distribution than that of a simply supported bridge. Taking the deflection of a continuous beam into consideration, an equivalent stiff simply supported span can be derived and the use of distribution coefficients as obtained in Chapter 2 can be made.

A continuous prismatic beam of moment of inertia I is subjected to a concentrated load P at the middle of the span 2a causing a deflection δ at the point of application of the load. Let

$$\delta = \frac{Pa^3}{EI} \times \frac{1}{c}$$

Let I_o be the moment of inertia of equivalent simply supported beam of span 2a. When load P is applied at mid-span , the mid-span deflection δ_o is equal to δ or

$$\delta_o = \frac{Pa^3}{6EI_o} = \frac{Pa^3}{c\,EI}$$

If $I_o = \gamma I$ then $\gamma = \frac{c}{6}$ .....(4.11)

For determining the load distribution in the loaded span 2a of the continuous bridge, the new value $I_o = \gamma I$ is substituted instead of in the equation (2.58), for finding the flexural parameter θ^{o}. Thus

$$\theta^{o} = \frac{b}{2a} \sqrt[4]{\frac{I_o}{I_T} \cdot \frac{q}{p}} = \theta \sqrt[4]{\gamma} \quad ..(4.12)$$

where,

$$\theta = \frac{b}{2a} \sqrt[4]{\frac{I}{I_T} \cdot \frac{q}{p}}$$

Knowing the value of θ^{o} the coefficients of transverse distribution can be obtained using graphs i to ii. In case of no-torsion bridges the distribution of load in unloaded span at any time can be taken approximately the same as for the loaded span in which the corresponding loads are present. The distribution coefficients, thus obtained, are then used with the influence line for mean effects on one continuous main beam.

For torsionally resistant continuous bridge, the value of $\theta^{o} = \theta \sqrt[4]{\gamma}$ is firstly determined. The equivalent value of $I_o = \gamma I$ is then used to determine the new torsional parameter α^{o} given by equation (2.59). Thus

$$\alpha^{o} = \frac{G \left(\frac{J}{p} + \frac{J_T}{q} \right)}{2E \sqrt{I_o/p \times I_T/q}} = \frac{\alpha}{\sqrt{\gamma}} \quad ...(4.13)$$

The parameters θ^{o} and α^{o} are used in the same manner as indicated in Chapter 2 and the interpolation formula (2.49) is considered as valid. Thus, the values of K_{α}^{o} can be easily obtained for loaded span. For the load distribution in the unloaded span it has been shown experimentally by MORICE AND LITTLE (22) that all the beams share loads equally. This can be explained by the action of torsionally resistant cross beams present over the continuous supports. It can, therefore, be assumed that for unloaded spans, in case of torsionally resistant continuous bridges with cross beams over the supports, all the main beams share loads equally, whether the loading in the loaded spans is central or eccentric to the longitudinal axis of the bridge.

From above, it is clear that knowing θ° and α° the problem can be easily solved using the results of Chapter 2. For the determination of θ° and α°, the additional value γ is determined by ordinary methods of finding deflection in a continuous beam. For continuous bridges with prismatic or non-prismatic main beams and varying span lengths, it is obvious that there will be separate values of γ, θ, θ° and α° for each span. The additional values of γ, $\sqrt[4]{\gamma}$ and $\sqrt{\gamma}$ are, therefore, calculated for continuous bridges with (a) prismatic main beams and (b) non-prismatic main beams. The number of spans and the ratios between the different spans are also varied according to practical cases of construction.

TABLE - 4.1

S. NO.	SYSTEM	RELATIVE DIMENSIONS	C	γ	$4\sqrt{\gamma}$	$\sqrt{\gamma}$
1	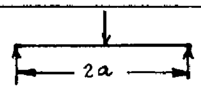	–	6	1·0	1·0	1·0
2		$a_1 : a_2$ 1 : 1	8·349	1·3915	1·0861	1·180
3	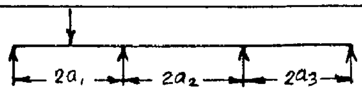	$a_1 : a_2 : a_1$ 2 : 3 : 2	7·970	1·328	1·0736	1·152
4	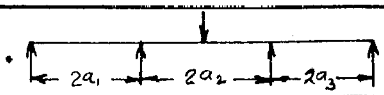	$a_1 : a_2 : a_3$ 2 : 3 : 2	12·48	2·080	1·201	1·442
5	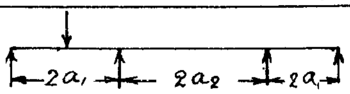	$a_1 : a_2 : a_3$ 2 : 2·5 : 2	8·228	1·371	1·082	1·171
6	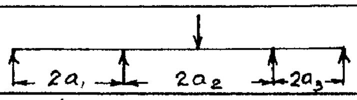	$a_1 : a_2 : a_3$ 2 : 2·5 : 2	11·744	1·957	1·183	1·399
7	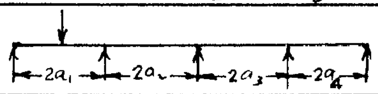	$a_1 : a_2 : a_3 : a_4$ 2 : 2 : 2 : 2	8·590	1·432	1·094	1·197
8	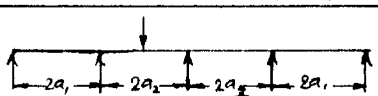	$a_1 : a_2 : a_3 : a_4$ 2 : 2 : 2 : 2	11·228	1·871	1·170	1·368
9	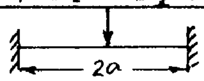	–	24	4·0	1·414	2·0

TABLE - 4.2.

S.NO.	SYSTEM	RELATIVE DIMENSIONS	$2a_0$	$\gamma' = \frac{a}{a_0}$	
1	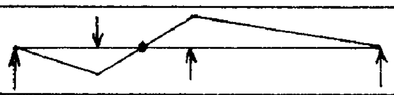	2 : 2	$\frac{32}{19}a$	1·1875	
2	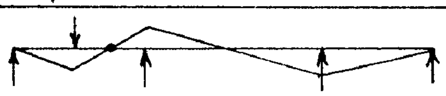	2 : 2·5 : 2	1·695a	1·179	
3	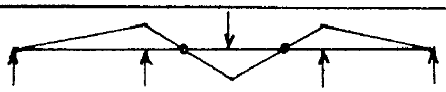	2 : 2·5 : 2	1·348 a	1·483	
4	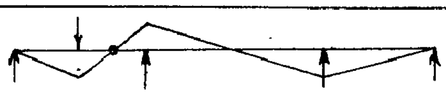	2 : 3 : 2	1·717 a	1·165	
5	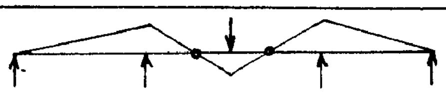	2 : 3 : 2	1·308 a	1·53	
6	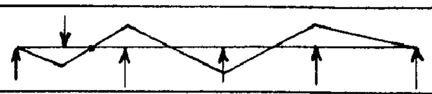	2 : 2 : 2 : 2	1·661 a	1·203	
7	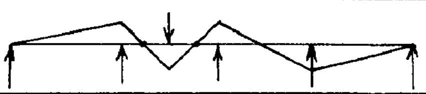	2 : 2 : 2 : 2	1·3850a	1·443	
8	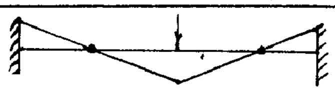	–	a	2·0	

(a) Prismatic main beams.

The evaluation of value r according to eq.(4.11) is carried out by moment distribution method and the values γ, $\sqrt[4]{\gamma}$ and $\sqrt{\gamma}$ are tabulated in table 4.1 for various cases. For example, according to Fig.(4.2) of a continuous beam with the span length ratio $a_1 : a_2 : a_3$ as 2:3:2, for outer span and middle span $r_{12} = 1.328$ and $r_{23} = 2.080$ have been calculated and are shown in Table 4.1 for cases 3 and 4. In case 3, the loaded mid point of the outer span is given an unknown displacement δ and by introducing a temporary support the moment distribution for the induced displacement effect is carried out; then the reaction value at the temporary support is equated to the applied load P to obtain c_{12} from $\delta = \frac{Pa_1^3}{c_{12}EI}$. Similarly for case 4, C_{23} is determined. Amongst the nine cases tabulated in Table 4.1, the maximum value of $\gamma = 4.0$ for the fixed beam of case 9.

(b) Non-Prismatic main beams:

A particular case of three span continuous beam having varying moment of inertia as shown in Fig.4.3 is considered. The results are used for the load distribution analysis of model of 5.3.

The depth of the continuous beam as shown in Fig.4.3 has straight line variation with d as depth at A, B, and C and 1.8 d as maximum depth at supports 2 and 3. If I is the moment of inertia at A, B and C, then the deflection at A due to a concentrated load P applied at A is calculated by moment distribution method; the deflection being equal to $\frac{Pa^3}{11.126\,EI}$. Similarly the deflection at B due to load P at B is equal to $\frac{P(1.25a)^3}{18.9\,EI}$.

Therefore,

$c_{12} = 11.126 \qquad r_{12} = 1.854 \qquad \sqrt[4]{r_{12}} = 1.167$

$c_{23} = 18.9 \qquad r_{23} = 3.15 \qquad \sqrt[4]{r_{23}} = 1.332$

The stiffnesses and carry-over factors for members with varying moment of inertias are obtained from Table 3 and Table 4 of the book[54] " Analysis of Statically Indeterminate Structures" by PARCEL and MOORMAN pp. 278-280.

4.2.2 Equivalent Simply supported span Method.

In a continuous bridge structure it is possible to use the moment distribution method or slope-deflection method to determine the mean bending moment diagrams produced by any loading. Thus certain points of contra-flexure can be located in the primary deck structure. Assuming that the longitudinal deflection and bending moment profiles due to distribution of load remain of the same form for all longitudinal sections, it follows that the points of contra-flexure form lines in the plan parallel to the supports. Although these lines of contraflexure will in fact have some transverse curvature, they can, for the purpose of an approximate analysis, be considered as simple supports. Hence it is possible to analyse that portion of the structure between the points of contraflexure as a simply supported span of appropriate length and width and with a flexural parameter and torsional parameter determined according to equations (2.58) and (2.59).

For the equivalent simply supported spanbetween points of contraflexure the mean effects are known from moment distribution analysis and the distribution coefficients K are derived according to theory developed in Chapter 2. Thus, a solution to a specific portion of the continuous bridge can be obtained. For points outside the equivalent simply supported span analysed as above, it is reasonable to assume that the distribution of moment will be same as that in the equivalent simply supported span in case of bridges having negligible torsional resistance and equal load distribution in case of torsionally resistant bridges with heavy torsionally resistant transverse beam at the continuous supports.

The transverse moments can be derived in the same way as for a simply supported bridge. The Fourier series for loads on the equivalent span are then derived and the analysis of section 2.2. can be applied. If the equivalent simply supported span is $2a_0$ and the loaded span is $2a$ then for deriving the distribution coefficients K and μ the modified flexural parameter $\theta_0' = \gamma' \theta$ where $\gamma' = \frac{a}{a_0}$

and $\theta = \frac{b}{2a} \sqrt[4]{\frac{i}{i_T}}$ ...(4.14)

The values of γ' for various cases of continuous beams are tabulated in Table 4.2 for a concentrated load applied at middle point of the loaded span.

4.3 EXAMPLES

To examine the accuracy of the approximate methods developed in Section 4.2 , two examples of four girder grillage are considered. In example 4.3.1 a four girder grillage (fig. 4.4) fixed at its two supports is analysed by theory developed in section 4.1 and a comparison of values thus obtained is made with the values obtained by approximate method of analysis developed in sections 4.2.1 and 4.22. Accuracy obtained by using 3 terms of basic function series is also shown. In example 4.3.2 a two span continuous open bridge grillage (Fig.4.5) is analysed exactly and a comparison of values thus obtained is made with the values obtained by approximate method of analysis developed in sections 4.2.1 and 4.2.3.

4.3.1 Four Girder Grillage Fixed at Two Ends.

A four girder grillage fixed at two supports with three cross beams, is considered. The dimensions are

$2a = 54'$; $p = 9'$; $2b = 36'$; $q = 13.5'$; $I/I_T = \frac{27}{8}$

According to equation (2.58) $\theta = 0.5$

Basic function series for unit concentrated load:

When the unit load is at $x = a$ from table 4.3 the series is written as

$$p(x) = \frac{1}{54}\left[\frac{1.6165}{1.0359} F_1(x) - \frac{1.4059}{1.0001} F_3(x) + --\right]$$

$$\text{Hence, } A_1 = \frac{1.6165}{54 \times 1.0359};\ A_2 = 0;\ A_3 = \frac{-1.4059}{1.0001}.$$

..... (4.15a)

when the unit load is at $x = a/2$

$$p(x) = \frac{1}{54}\left[\frac{0.8634}{1.0359} F_1(x) + \frac{1.4439}{0.9984} F_2(x) + \frac{1.3709}{1.0001} F_3(x) + -\right]$$

$$\text{Hence } A_1 = \frac{0.8634}{1.0359 \times 54};\ A_2 = \frac{1.4439}{.9984 \times 54};\ A_3 = \frac{1.3709}{1.0001 \times 54}.$$

........(4.15b)

For fixed end condition, the first three roots of Basic function series are

$2ak_1 = 4.73004$ hence $k_1 = \dfrac{4.73004}{54}$ ft. units.

TABLE 4·3 - BASIC FUNCTION VALUES FOR FIXED BEAM

$x \rightarrow$	0	$a/2$	a	$3a/2$	$2a$
$F_1(x)$	0	0·8634	1·6165	0·8634	0
$F_2(x)$	0	1·4439	0	-1·4439	0
$F_3(x)$	0	1·3709	-1·4059	1·3709	0
$\phi_1(x)$	2·0356	-0·2119	-1·2374	-0·2119	2·0356
$\phi_2(x)$	1·9984	-1·1685	0	1·1685	-1·9984
$\phi_3(x)$	2·0001	-1·2424	1·4426	-1·2424	2·0001

TABLE 4·4 - DISTRIBUTION COEFFICIENTS FOR VARIOUS VALUES OF θ'

	K_1 ; $\theta_1' = 0·753$		K_2 $\theta_2' = 1·25$		K_3 $\theta_3' = 1·75$	
	$b/4$	$3b/4$	$b/4$	$3b/4$	$b/4$	$3b/4$
$-3b/4$	0·04	-0·34	-0·18	-0·04	-0·12	0
$-b/4$	1·09	0·04	0·85	-0·18	0·30	-0·12
$b/4$	1·82	1·12	2·97	0·64	3·91	0·26
$3b/4$	1·12	3·09	0·64	3·59	0·26	4·26
Σ	1·0175	0·9775	1·0700	1·0025	1·0875	1·1000

TABLE - 4·5

IT AD T	DIST. COEFF.	LOAD AT $x = a$			LOAD AT $x = a/2$				APPROX. THEORY	
		DEFLECTION AT $x = a$	B.M. AT $x = a$	B.M. AT $x = 2a$ or 0	DEFLECTION AT $x = a/2$	B.M. AT $x = a$	B.M. AT $x = 0$	B.M. AT $x = 2a$	$\theta^\circ = 0·707$ EQ. STIFFNESS METHOD	$\theta_0' = 1·0$ EQ. S.S. SPAN METHOD
EAM a	k_{aa}	0·8013	0·8244	0·7631	0·8338	0·7027	0·8564	0·7794	0·7726	0·8600
	k_{ba}	0·2750	0·2451	0·3243	0·2345	0·4025	0·2056	0·2981	0·2997	0·2133
	k_{ca}	0·0090	0·0040	0·0174	-0·0062	0·0306	-0·0131	0·0420	0·0250	-0·0347
	k_{da}	-0·0853	-0·0735	-0·1048	-0·0621	-0·1358	-0·0489	-0·1195	-0·0973	-0·0386
AM b	k_{ab}	0·2750	0·2451	0·3243	0·2345	0·4025	0·2056	0·2981	0·2997	0·2133
	k_{bb}	0·4555	0·5169	0·3540	0·5357	0·1931	0·5944	0·4191	0·4154	0·5659
	k_{cb}	0·2605	0·2340	0·3043	0·2360	0·3738	0·2131	0·2408	0·2609	0·2555
	k_{db}	0·0090	0·0040	0·0174	-0·0062	0·0306	-0·0131	0·0420	0·0250	-0·0347
ERROR DUE THREE RMS OF B.E		-0·65%	-17·8 %	-5·1%	-3·6%	-4·8%	+3·4%	+10·2%	—	—

$$2ak_2 = 7.8540 \qquad \text{hence} \quad k_2 = \frac{7.8540}{54} \text{ ft. units.}$$

$$2ak_3 = 10.9956 \qquad \text{hence} \quad k_3 = \frac{10.9956}{54} \text{ ft. units.}$$

and the corresponding first three term flexural parameters given by eq. (4.4) are:

$$\left.\begin{aligned} \theta_1' &= \frac{2a\,k_1}{\pi}\,\theta = 0.753 \\ \theta_2' &= \frac{2a\,k_2}{\pi}\,\theta = 1.25 \\ \theta_3' &= \frac{2a\,k_3}{\pi}\,\theta = 1.75 \end{aligned}\right\} \qquad \ldots\ldots(4.16)$$

The distribution coefficient K for various values of obtained from graphs (25) are tabulated in table 4.4 for load positions $\frac{3b}{4}$ and $\frac{b}{4}$ and beam positions $\pm\frac{3b}{4}$ and $\pm\frac{b}{4}$.

Using equations (4.7) and (4.8) the distribution factors for load at x = a and x = a/2 are derived for longitudinal deflections and bending moments and the values are tabulated in Table 4.5. The errors introduced by using first three terms of Basic function series are also tabulated in Table 4.5.

Considering the approximate method of analysis the modified flexural parameters θ_0' and θ° are derived from

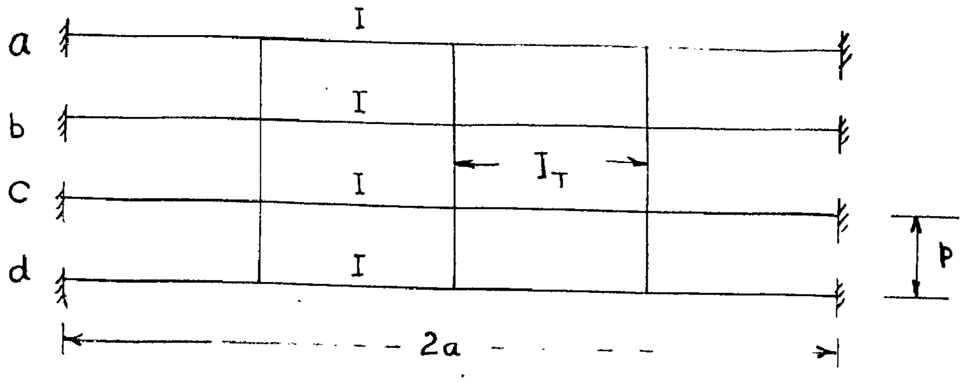

FIG. 4.4 FOUR GIRDER GRILLAGE FIXED AT BOTH ENDS.

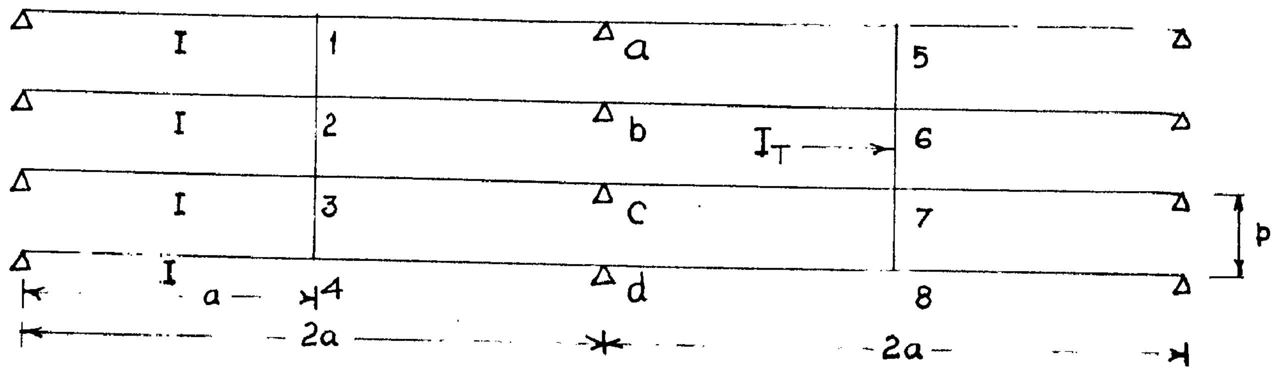

(a)

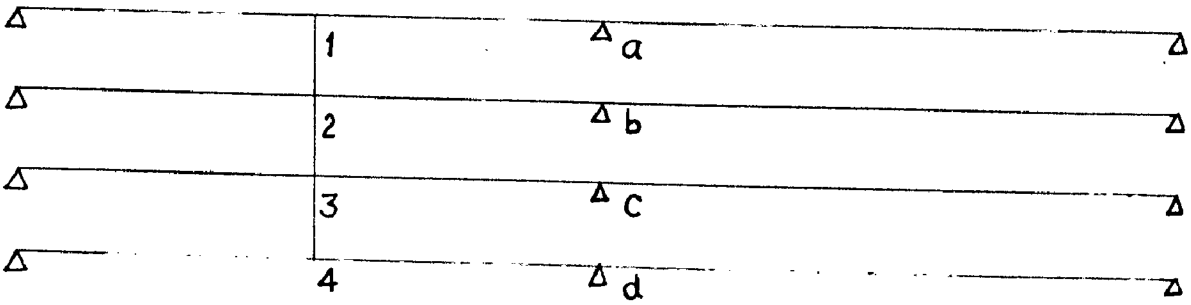

(b)

FIG. 4.5 TWO SPAN FOUR GIRDER CONTINUOUS BRIDGE GRILLAGE

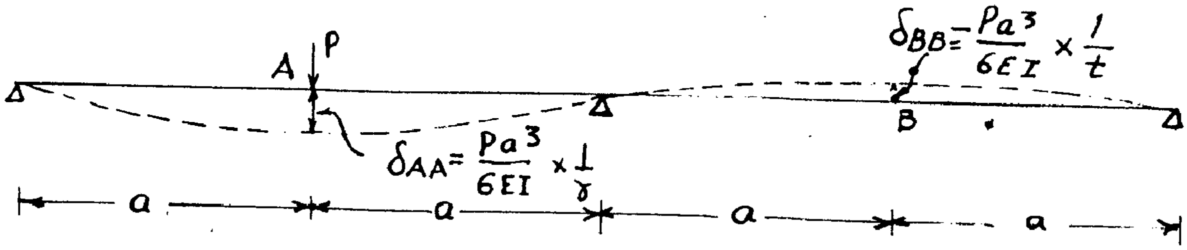

FIG. 4.6

equations 4.12 and 4.14 and using the values of γ' and γ' from tables 4.1 and 4.3 . They are θ^{0} = 0.707 and θ_0' = 1.0. From graphs 1 to 6 the distribution of loads for unit load applied at beam a and b are calculated and tabulated in Table 4.5.

After comparing the results obtained in Table 4.5 the following observations can be made.

1. The values of distribution coefficients obtained by equivalent stiffness method are very close in most of the cases of loading and transverse section to those obtained by theory of 4.1. The wide difference in the values obtained by equivalent simply supported span method from theory of 4.1 is due to the transverse curvature at the points of contraflexure.

2. The difference is also due to the consideration of only first term of sine series in approximate theory and 3 terms of Basic function series in theory of 4.1.

3. The errors admitted in the bending moments by Basic functions are sufficiently high as indicated in the Table 4.5. Suitable corrections are therefore necessary when the bending moments are calculated by using Basic function series.

TABLE 4.6. LOAD DISTRIBUTION COEFFICIENTS FOR TWO SPAN BRIDGE GRILLAGE BY FLEXIBILITY METHOD

UNIT LOAD AT	WITH MEMBER 5678 (FIG. 4.5a)						WITHOUT MEMBER 5678 (FIG. 4.5b)		
		SYMM. z'	ASYMM. z''		SYMM. z'	ASYMM. z''		SYMM. z'	ASYMM. z''
1	11	$\frac{(0.5+2.5\lambda\gamma)-\frac{\gamma^2}{t^2 D_1}}{D_3}$	$\frac{(4.5+1.5\lambda\gamma)-\frac{45\gamma^2}{t^2 D_2}}{D_4}$	51	$\frac{\gamma}{t}\,\frac{2.5\lambda\gamma}{D_1 D_3}$	$\frac{\gamma}{t}\,\frac{1.5\lambda\gamma}{D_2 D_4}$	11	$\frac{0.5+2.5\lambda\gamma}{D_1}$	$\frac{4.5+1.5\lambda\gamma}{D_2}$
	21	$\frac{0.5-\frac{\gamma^2}{t^2 D_1}}{D_3}$	$\frac{1.5-\frac{15\gamma^2}{t^2 D_2}}{D_4}$	61	$= -z'_{51}$	$= -3z''_{51}$	21	$0.5/D_1$	$1.5/D_2$
	31	$= z'_{21}$	$= -z''_{21}$	71	$= -z'_{51}$	$= +3z''_{51}$	31	$= z'_{21}$	$= -z''_{21}$
	41	$= z'_{11}$	$= -z''_{11}$	81	$= z'_{51}$	$= -z''_{51}$	41	$= z'_{11}$	$= -z''_{11}$
	$D_1 = (2+5\lambda\gamma)$		$D_2 = (10+3\lambda\gamma)$			$D_3 = D_1 - 4\gamma^2/t^2 D_1$		$D_4 = D_2 - 100\gamma^2/t^2 D_2$	
2	12	$= z'_{21}$	$= z''_{21}$	52	$= -z'_{62}$	$-\frac{\gamma}{t}\,\frac{4.5\lambda\gamma}{D_2 D_4}$	12	$0.5/D_1$	$1.5/D_2$
	22	$\frac{(0.5+2.5\lambda\gamma)-\frac{\gamma^2}{t^2 D_1}}{D_3}$	$\frac{(0.5+1.5\lambda\gamma)-\frac{5\gamma^2}{t^2 D_2}}{D_4}$	62	$\frac{\gamma}{t}\cdot\frac{2.5\lambda\gamma}{D_1 D_3}$	$= -3z''_{52}$	22	$\frac{0.5+2.5\lambda\gamma}{D_1}$	$\frac{0.5+1.5\lambda\gamma}{D_2}$
	32	$= z'_{22}$	$= -z''_{22}$	72	$= z'_{62}$	$= +3z''_{52}$	32	$= z'_{22}$	$= -z''_{22}$
	42	$= z'_{12}$	$= -z''_{12}$	82	$= -z'_{62}$	$= -z''_{52}$	42	$= z'_{12}$	$= -z''_{12}$

TABLE 4.7 - LOAD DISTRIBUTION COEFFICIENTS

UNIT LOAD AT	WITH MEMBER 5678								WITHOUT MEMBER 5678			
	D.C.	$\lambda = 1$	$\lambda = 1/16$	$\lambda = 1/256$	D.C.	$\lambda = 1$	$\lambda = 1/16$	$\lambda = 1/256$	D.C.	$\lambda = 1$	$\lambda = 1/16$	$\lambda = 1/256$
1	k_{11}	0.9116	0.7513	0.7040	k_{51}	0.0215	0.0166	0.0016	k_{11}	0.9089	0.7459	0.7035
	k_{21}	0.1565	0.3457	0.3958	k_{61}	-0.0303	-0.0177	-0.0016	k_{21}	0.1616	0.3516	0.3964
	k_{31}	-0.0479	+0.0547	0.0964	k_{71}	-0.0039	-0.0143	-0.0014	k_{31}	-0.0500	0.0592	0.0968
	k_{41}	-0.0202	-0.1517	-0.1962	k_{81}	+0.0127	0.0154	0.0014	k_{41}	-0.0205	-0.1567	-0.1967
2	k_{12}	0.1565	0.3457	0.3958	k_{52}	-0.0303	-0.0177	-0.0016	k_{12}	0.1616	0.3516	0.3964
	k_{22}	0.6391	0.3632	0.3054	k_{62}	0.0567	0.0211	0.0018	k_{22}	0.6267	0.3560	0.3041
	k_{32}	0.2523	0.2364	0.2024	k_{72}	-0.0225	0.0109	0.0012	k_{32}	0.2617	0.2332	0.2027
	k_{42}	-0.0479	0.0547	0.0964	k_{82}	-0.0039	-0.0143	-0.0014	k_{42}	-0.0500	0.0592	0.0968

4.3.2. Four Girder Two Span Continuous Bridge Grillage.

The continuous bridge grillages shown in Fig. 4.5a and 4.5b are analysed by flexibility method. The symmetrical and asymmetrical components of loads distributed at different junctions of cross beams and longitudinals, due to unit load applied at points 1 and 2 are tabulated in Table 4.6 in terms of parameters λ and influence coefficients γ and t. The parameter λ is equal to $(\frac{b}{a})^3 \frac{I}{I_T}$; r and t are such that when a load P is applied at A (Fig. 4.6), the deflections are

$$\delta_{AA} = \frac{Pa^3}{6\gamma EI} \quad \text{and} \quad \delta_{BA} = -\frac{Pa^3}{6t\,EI}$$

For two equal span continuous beam shown in Fig.4.6 r = 1.3913 and t = 3.5555.

Numerical values of loads distributed at different joints due to unit load applied at points 1 and 2 are tabulated in table 4.7 for $\lambda = 1$, $\lambda = 1/16$ and $\lambda = 1/256$ the values correspond to the values of flexural parameters $\theta = 1.0$, $\theta = 0.5$ and $\theta = 0.25$ respectively of equivalent anisotropic plate when loaded span is treated simply supported. To find the effect of cross beam 5678 in the unloaded span the grillage shown in fig.4.5(b) without member 5678 is also analysed.

TABLE 4.8

DISTRIBUTION COEFFICIENTS FOR TWO SPAN CONTINUOUS BRIDGE

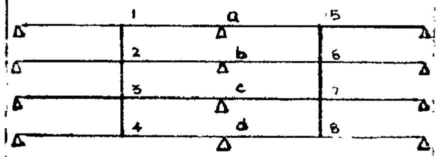

UNIT LOAD AT	D.C.	DEFLECTION AT SECTION 1234 $\lambda = 1$	$\lambda = 1/16$	$\lambda = 1/256$	D.C.	B.M. AT SECTION 1234 $\lambda = 1$	$\lambda = 1/16$	$\lambda = 1/256$	D.C.	B.M. AT SECTION abcd $\lambda = 1$	$\lambda = 1/16$	$\lambda = 1/256$
1	$\overset{d}{k}_{11}$	0.9032	0.7448	0.7034	$\overset{m}{k}_{11}$	0.9066	0.7475	0.7036	$\overset{m}{k}_{a1}$	0.9331	0.7679	0.7056
	$\overset{d}{k}_{21}$	0.1684	0.3526	0.3964	$\overset{m}{k}_{21}$	0.1635	0.3498	0.3962	$\overset{m}{k}_{b1}$	0.1262	0.3280	0.3942
	$\overset{d}{k}_{31}$	−0.0464	0.0603	0.0969	$\overset{m}{k}_{31}$	−0.0470	0.0580	0.0967	$\overset{m}{k}_{c1}$	−0.0518	0.0404	0.0950
	$\overset{d}{k}_{41}$	−0.0252	−0.1577	−0.1967	$\overset{m}{k}_{41}$	−0.0231	−0.1553	−0.1965	$\overset{m}{k}_{d1}$	−0.0075	−0.1363	−0.1948
2	$\overset{d}{k}_{12}$	0.1684	0.3526	0.3964	$\overset{m}{k}_{12}$	0.1635	0.3498	0.3962	$\overset{m}{k}_{a2}$	0.1262	0.3280	0.3942
	$\overset{d}{k}_{22}$	0.6169	0.3550	0.3047	$\overset{m}{k}_{22}$	0.6260	0.3583	0.3049	$\overset{m}{k}_{b2}$	0.6958	0.3843	0.3072
	$\overset{d}{k}_{32}$	0.2611	0.2321	0.2020	$\overset{m}{k}_{32}$	0.2575	0.2339	0.2022	$\overset{m}{k}_{c2}$	0.2298	0.2473	0.2036
	$\overset{d}{k}_{42}$	−0.0464	0.0603	0.0969	$\overset{m}{k}_{42}$	−0.0470	+0.0580	0.0967	$\overset{m}{k}_{d2}$	−0.0518	0.0404	0.0950

UNIT LOAD AT	D.C.	DEFLECTION AT SECTION 5678 $\lambda = 1$	$\lambda = 1/16$	$\lambda = 1/256$	D.C.	B.M. AT SECTION 5678 $\lambda = 1$	$\lambda = 1/16$	$\lambda = 1/256$	D.C.	EQUIVALENT STIFFNESS METHOD $\theta^{\circ} = 1.086$	$\theta^{\circ} = 0.543$	$\theta^{\circ} = 0.272$	EQ. SIMPLY SUPPORTED SPAN METHOD $\theta_o' = 1.188$	$\theta_o' = 0.594$	$\theta_o' = 0.297$
1	$\overset{d}{k}_{51}$	0.8517	0.7052	0.7000	$\overset{m}{k}_{51}$	0.8184	0.6795	0.6972	$\overset{\circ}{k}_{11}$	0.8747	0.7261	0.6737	0.8919	0.7435	0.6754
	$\overset{d}{k}_{61}$	0.2409	0.3950	0.4000	$\overset{m}{k}_{61}$	0.2878	0.4224	0.4029	$\overset{\circ}{k}_{21}$	0.1903	0.3383	0.3829	0.1700	0.3292	0.3799
	$\overset{d}{k}_{71}$	−0.0370	0.0945	0.1000	$\overset{m}{k}_{71}$	−0.0310	0.1167	0.1025	$\overset{\circ}{k}_{31}$	−0.0395	0.0646	0.1007	−0.0493	0.0503	0.0993
	$\overset{d}{k}_{81}$	−0.0556	−0.1947	−0.2000	$\overset{m}{k}_{81}$	−0.0752	−0.2186	−0.2026	$\overset{\circ}{k}_{41}$	−0.0255	−0.1290	−0.1573	−0.0126	−0.1230	−0.1546
2	$\overset{d}{k}_{52}$	0.2409	0.3950	0.4000	$\overset{m}{k}_{52}$	0.2878	0.4224	0.4029	$\overset{\circ}{k}_{12}$	0.1903	0.3383	0.3829	−0.1700	0.3292	0.3799
	$\overset{d}{k}_{62}$	0.4811	0.3044	0.3006	$\overset{m}{k}_{62}$	0.3934	0.2717	0.2973	$\overset{\circ}{k}_{22}$	0.6076	0.3573	0.3019	0.6686	0.3743	0.3040
	$\overset{d}{k}_{72}$	0.3150	0.2061	0.1994	$\overset{m}{k}_{72}$	0.3498	0.1892	0.1973	$\overset{\circ}{k}_{32}$	0.2416	0.2398	0.2145	0.2187	0.2462	0.6168
	$\overset{d}{k}_{82}$	−0.0370	0.0945	0.1000	$\overset{m}{k}_{82}$	−0.0310	0.1167	0.1025	$\overset{\circ}{k}_{42}$	−0.0395	0.0646	0.1007	−0.0493	0.0503	0.0993

(1) when $\lambda = 1$; $\theta = 1.0$; $\theta^{\circ} = 1.086$; $\theta_0' = 1.188$

(2) when $\lambda = \frac{1}{16}$; $\theta = 0.5$; $\theta^{\circ} = 0.543$; $\theta_0' = 0.594$

(3) when $\lambda = \frac{1}{256}$; $\theta = 0.25$; $\theta^{\circ} = 0.272$; $\theta_0' = 0.297$

From graphs 1 to 6 the distribution coefficients $\frac{K_0}{4}$ for beam positions $\pm$ 3/4 b and $\pm$ b/4 and load position 3/4 b and b/4 are calculated and the values are tabulated in Table 4.8.

After comparing the results obtained in Table 4.8 the following observations can be made.

1. The difference in the values of distribution coefficients by the two approximate methods is not much. The errors due to transverse curvature at the point contra-flexure is little because the point contra-flexure is near to the middle support.

2. The values of distribution coefficients calculated by approximate methods are close to values by exact method The difference is due to open grillage analysis and assumed equivalent plate analysis as it has already been indicated in Chapter. 2.

3. The effect of transversal 5678 on distribution coefficients is small and is due to the factor $\frac{\gamma^2}{t^2 D_1}$. The predominant effect of transversal 5678 is seen on the distribution coefficients for support moments; the distribution

is poorer with member 5678. To account for this poor distribution at the continuous support the values of θ° should be increased by about 10% in the approximate method of analysis and a different set of distribution coefficients should be obtained for support moment.

4) It is easily understandable that the equivalent stiffness method is better and can be adopted for continuous bridges with non-prismatic main beams.

PART II

EXPERIMENTAL WORK

CHAPTER 5

EXPERIMENTAL WORK

As various approximate theories have been proposed in Chapters 3 and 4 for edge stiffened and continuous bridges, it is intended here to verify the errors introduced by these approximate calculations. Models of no-torsion bridge grillages have been constructed and deflection measurements are taken to obtain transverse distribution profiles of various systems. Following models have been tested;

5.1.1 Steel model of six girder edge stiffened grillage with $\theta = 0.656$ and $\Upsilon = 2.2$.

5.1.2. Perspex model of six girder edge stiffened grillage with $\theta = 0.85$ $\Upsilon = 8.0$

5.2. Steel model of four girder two span continuous bridge grillage with prismatic main beams and four sets of cross beams.

5.3. Perspex model of four girder three span bridge grillage with non-prismatic main beams and two sets of cross beams.

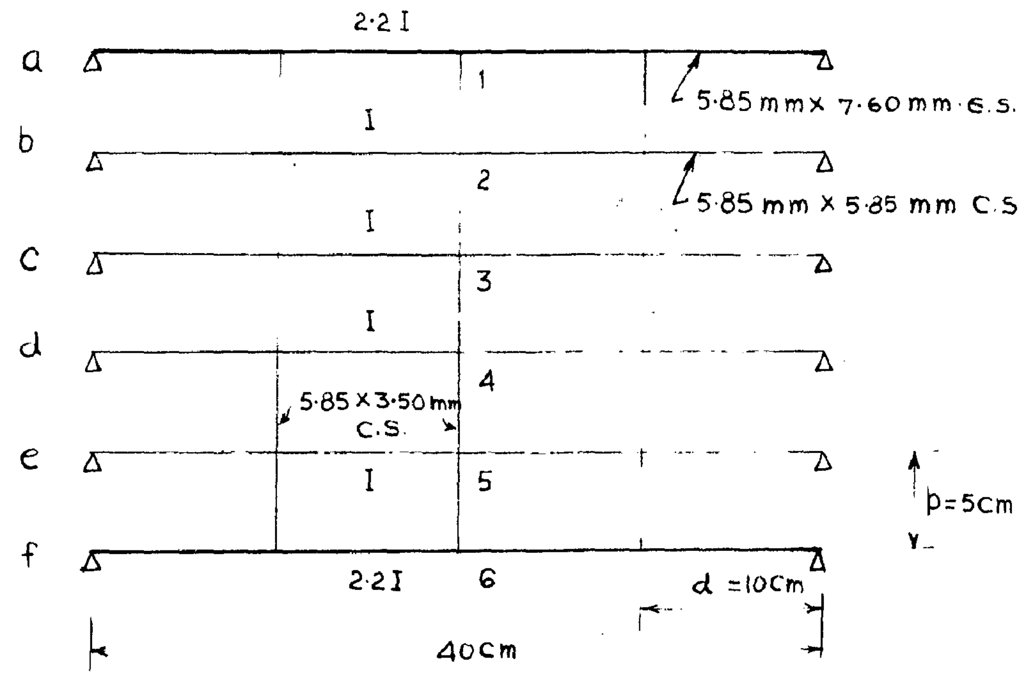

(a) STEEL MODEL OF SIX GIRDER GRILLAGE

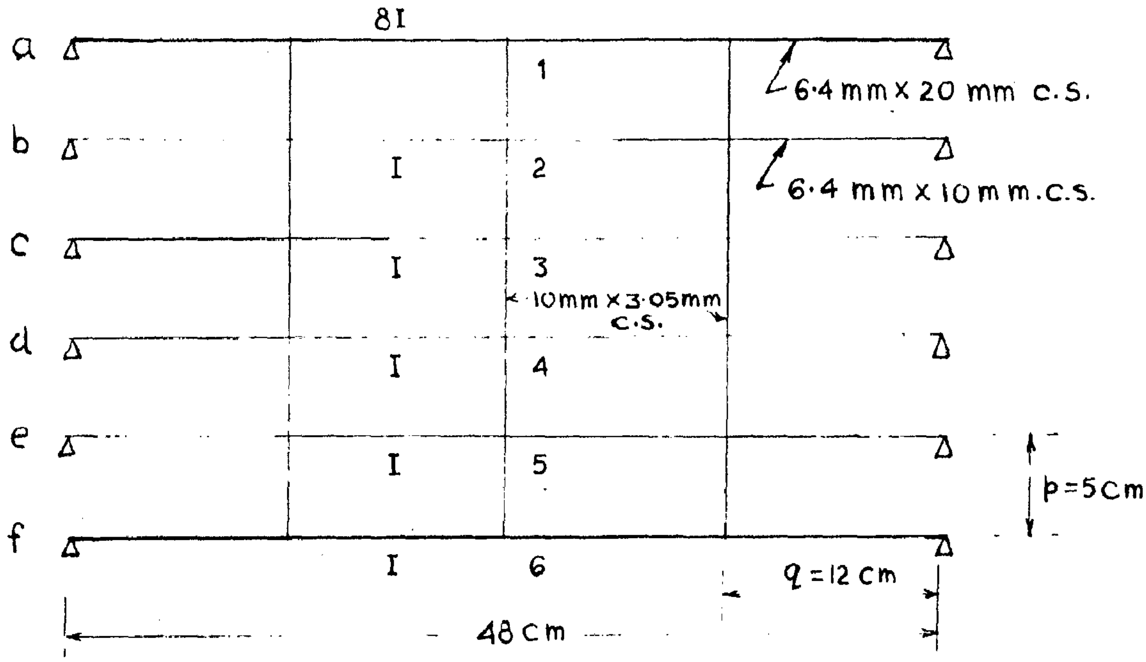

(b) PERSPEX MODEL OF SIX GIRDER GRILLAGE.

FIG. 5·1

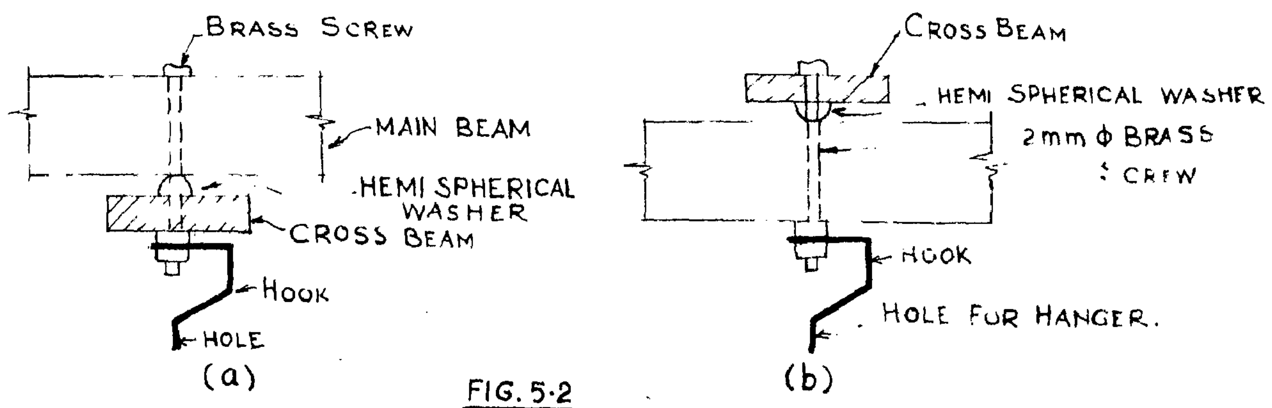

FIG. 5·2

5.1. EDGE STIFFENED SIX GIRDER GRILLAGES.

Two grillages have been tested. The flexural parameter θ of the steel grillage as shown in Fig. (5.1a) is 0.656 and $\gamma = 2.2$. The flexural parameter θ of perspex grillage as shown in Fig. (5.1 b) is 0.65 and $r = 8.0$.

5.1.1. Steel Grillage.

The grillage consisted of 6 main beams of 40 cm. span, 4 inner main beams of 5.85 m.m. x 5.85 m.m. and the two edge beams of 5.85 m.m. x 7.60 m.m. mild steel section and spaced at 5 c.m. centres.(Fig. 5.1a). The variation of $\pm$ 0.05 m.m. in the sectional dimensions was permitted. Three cross beams of the size 5.85 m.m. x 3.50 m.m were used and placed as shown in Fig. (5.1a)

To ensure that the grillage was free from torsion, the cross beams in the span were connected to main beams at the bottom face, by means of a join shown in Fig.(5.2a). In this joint a 2 m.m. dia. brass screw passes through a hole drilled centrally through the cross beam and main beam with a hemispherical washer inserted in between these two. A bracket type hook with a hole for the suspending loading hanger, is fitted at bottomof the screw.

The deflections at points 1,2,3,4,5, and 6 were measured by dial gauges of 0.0001" least count. A 3 kg load

load was applied at different points. To avoid lifting of the beams each beam was initially loaded by 1.0 lbs. weights . For every loading the initial and final readings were noted and the reading were taken at an interval of 30 minutes to minimise creep effects. The experimental set up is shown in photograph 1.

The observed deflections are tabulated in table 5.1, after taking the average of the two readings obtained by loading two symmetrical points.

<u>Calculations:</u>

The dimensions and other elements of the grillage are

$$2a = 40 \text{ cm}; \quad q = 10 \text{ cm} \quad ; \quad p = 5 \text{ cm}; \quad n = 6$$

$$1/I_T = \left(\frac{5.85}{3.50}\right)^3 = 4.67 \quad ; \quad 2b = np = 30 \text{ cm}.$$

$\therefore$ The flexural parameter $\theta = \frac{15}{40}\sqrt[4]{4.67 \times \frac{10}{5}} = 0.656$

The ratio $\gamma = \frac{I_E}{I} = \left(\frac{7.60}{5.85}\right)^3 = 2.2.$

The values of distribution coefficients $k = \frac{K_0}{6}$ for beam positions $\pm\frac{5b}{6}$, $\pm\frac{b}{2}$ and $\pm\frac{b}{6}$ and load positions $\frac{5b}{6}$, $\frac{b}{2}$ and $\frac{b}{6}$ for $\theta = 0.656$ have been tabulated in table 5.2 (as per example 2.3.1c) and the symmetric and asymmetric components z' and z'' are determined according to equation (3.47a).

Using equations (3.46) and (3.47) and (3.47b) the symmetrical components $\bar{z}'$ are obtained as

$$Z_a = u_a = \frac{2.2}{2.2(0.6299 - 0.0993) + 0.4694} = 1.3442$$

$$\left.\begin{aligned} \bar{z}'_{aa} &= \bar{z}'_{af} = 0.3566 \\ \bar{z}'_{ab} &= \bar{z}'_{ae} = 0.1991 \\ \bar{z}'_{ac} &= \bar{z}'_{ad} = 0.1163 \end{aligned}\right\} \qquad (5.1)$$

As per equations (3.48) and (3.49), $x_a = -x_f = 1.0$;

$$x_b = -x_e = \frac{0.19755}{0.3646} = 0.5418 \ ; \ x_c = -x_d = \frac{0.06315}{0.3646} = 0.1732$$

$$g_b = 3/5 \ ; \quad g_c = 1/5 \qquad \text{and}$$

$$2 \times 2.2\,(0.3646 + v_a) + 2\left[\tfrac{3}{5}(0.19755 + 0.5418 v_a) + \tfrac{1}{5}(0.06315 + 0.1732 v_a)\right] = 2.2$$

$$\therefore \ v_a = 0.0651$$

and the asymmetrical components are

$$\left.\begin{aligned} \bar{z}''_{aa} &= -\bar{z}''_{af} = 0.4297 \\ \bar{z}''_{ab} &= -\bar{z}''_{ae} = 0.2328 \\ \bar{z}''_{ac} &= -\bar{z}''_{ad} = 0.0744 \end{aligned}\right\} \quad --- \quad (5.2)$$

Adding symmetric and asymmetric components as obtained from equations (5.1) and (5.2) the ordinates for edge beam a are tabulated in table 5.3.

For inner beams b and c the edge ordinates as per equation (3.50) are obtained as

$$\left.\begin{aligned} \bar{\zeta}'_{ba} = \bar{\zeta}'_{bf} &= 0.09050 \; ; \quad \bar{\zeta}'_{ca} = \bar{\zeta}'_{cf} = 0.05286 \\ \bar{\zeta}''_{ba} = -\bar{\zeta}''_{bf} &= 0.10582 \; ; \quad \bar{\zeta}''_{ca} = -\bar{\zeta}''_{cf} = 0.03382 \end{aligned}\right\} \quad \ldots(5.3)$$

As per equation (3.52) Z_b = 0.7828 and Z_c = 0.8731. Using equation (3.54) the values of u_b and u_c are determined from

$$0.7828 = 6 \times 0.0905 + u_b\left[4 - 2\left\{\left(\frac{3}{5}\right)^2 + \left(\frac{1}{5}\right)^2\right\}\right]$$

$$0.8731 = 6 \times 0.05286 + u_c\left[4 - 2\left\{\left(\frac{3}{5}\right)^2 + \left(\frac{1}{5}\right)^2\right\}\right]$$

Therefore, u_b = 0.07496 and u_c = 0.17373. As per equation (3.53) the symmetrical

$$\bar{\zeta}'_{bb} = \bar{\zeta}'_{be} = 0.13846 \; ; \quad \bar{\zeta}'_{cb} = \bar{\zeta}'_{ce} = 0.16404$$

$$\bar{\zeta}'_{bc} = \bar{\zeta}'_{bd} = 0.16244 \; ; \quad \bar{\zeta}'_{cc} = \bar{\zeta}'_{cd} = 0.21963 \quad (5.4)$$

The asymmetrical components as per equation (3.55) are obtained as

$$\left.\begin{aligned} \bar{\zeta}''_{bb} = -\bar{\zeta}''_{be} &= 0.11244 \; ; \quad \bar{\zeta}''_{cb} = -\bar{\zeta}''_{ce} = 0.05548 \\ \bar{\zeta}''_{bc} = -\bar{\zeta}''_{bd} &= 0.04305 \; ; \quad \bar{\zeta}''_{cc} = -\bar{\zeta}''_{cd} = 0.02695 \end{aligned}\right\} \quad \ldots(5.5)$$

Adding the symmetric and asymmetric components as obtained from equations (5.3), (5.4) and (5.5) the

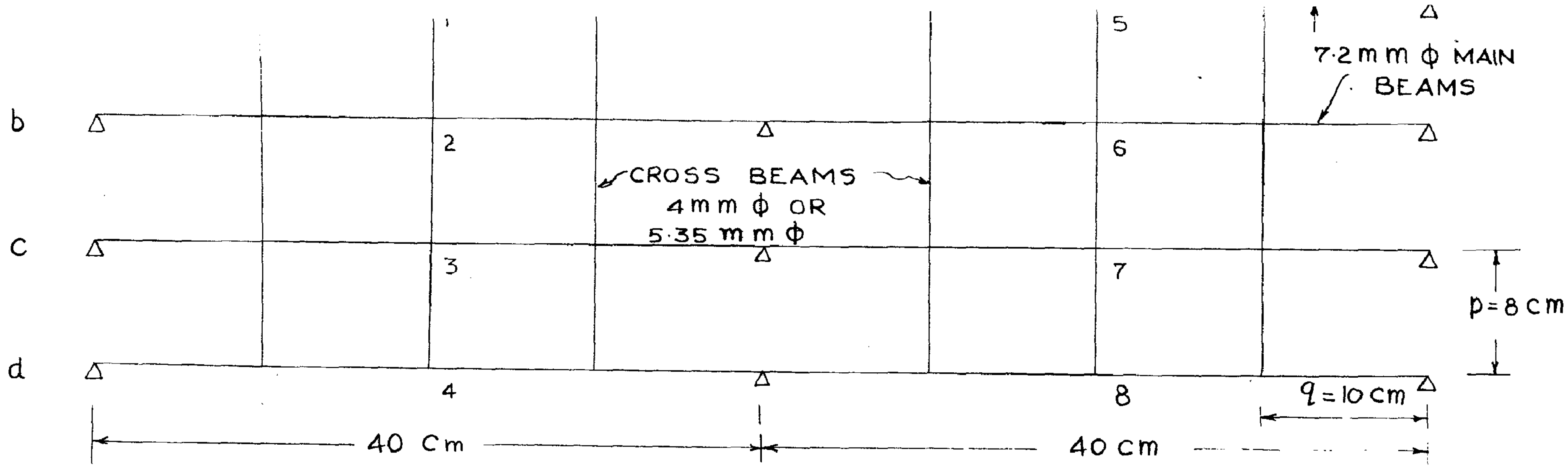

FIG. 5·3 STEEL MODEL OF TWO SPAN CONTINUOUS BRIDGE GRILLAGE

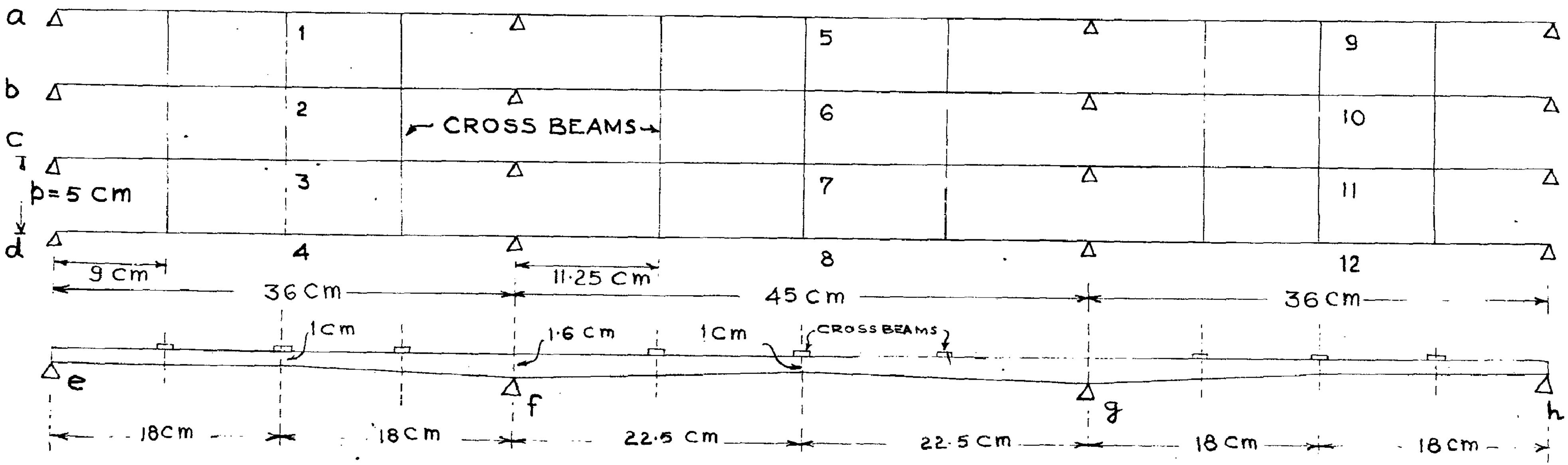

FIG. 5·4 PERSPEX MODEL OF THREE SPAN CONTINUOUS BRIDGE GRILLAGE WITH NON PRISMATIC MAIN BEAMS.

The experimental set-up was similar to one of 5.1.1. All girders were initially loaded by 1/4 lb. weights and the deflections were measured by applying 1.0 lb load at different points. Average values of deflections from two symmetrical loading are recorded in table 5.1.

Using similar calculation procedure as given in 5.1.1, the values in the tables 5.2, 5.3 and 5.4 are recorded. A comparison between the theoretical and experimental values is made. As per table 5.4 a good agreement between theoretical and experimental values is obtained. From tables 5.1 and 5.4 it can also be seen that the behaviour steel grillage is better than perspex grillage. Creep affects in perspex grillage are predominant as the variation in the total deflections is more when different beams are loaded. Also the negative values at the edges of the bridge are not in very good accord. Little discrepancies in the MAXWELL's reciprocal theorem are due to creep effects, though the readings were taken at an interval of 30 minutes.

5.2 TWO SPAN CONTINUOUS BRIDGE GRILLAGE:

The grillage consisted of four main beams, continuous over two equal spans of 40 cm. each and spaced at 8.0 cm. (Fig. 5.3). Main beams were made of

7.2 m.m. dia. mild steel bars. Following four sets of cross beams made of mild steel bars were used to test the grillage having wide range of parameters.

I- Six cross beams of 5.35 mm. dia., three in each span placed at equal spacing ; q = 10 cm

II- Two cross beams of 5.35 m.m. dia., one in each span placed in the middle; q = 20 cm.

III- Six cross beams of 4.0 mm dia., three in each span placed at equal spacings ; q = 10 cm.

IV- Two cross beams of 4.0 mm. dia., one in each span placed in the middle ; q = 20 cm.

To ensure that the grillage was free from torsion the joint shown in Fig. (5.2b) was used to connect the cross beams and main beams. The deflections at points 1 to 8 (Fig. 5.3) were measured by applying 2 kg and 3 kg loads at different points . All points 1 to 8 were initially loaded by 1.0 lb. weights to avoid lifting of beams.

The experimental set up is shown in photograph 2.

The initial and final readings were taken at an interval of 30 minutes to minimise the creep effects. The average of four readings is obtained by loading four symmetrical points i.e. 1,4,5 and 8 and 2,3,6 and 7 and the observed deflections are tabulated for four sets of cross beams.

Calculations:

Full dimensions and the flexural parameters for four sets of cross beams are given in table 5.6. The parameters , according to equivalent stiffness method of 4.2.1 (Table 4.1) for the four cases are determined. Using graphs 1 to 6 the distribution coefficients, for loaded span for four values of θ° are determined. The values are tabulated in table 5.7 and the theoretical values are compared with the experimental values obtained from table 5.5. A very good agreement between theoretical and experimental values is obtained especially since the negative values at the edges of the bridge are in accord.

5.3 THREE SPAN CONTINUOUS BRIDGE WITH NON-PRISMATIC MAIN BEAMS:

The four main beams of the grillage having depth varying according to Fig. (5.4) were cut out from a perspex sheet of 6.3 mm. thickness .The depth increases linearly from 10 mm. at mid-span to 16 m.m. at the inner supports f and g . The lengths of the outer spans and inner span were kept as 36.0 cm and 45.0 cm. The main beams were spaced at 5.0 cm. and the following two sets of cross beams were connected by means of joint shown in Fig. 5.2.

TABLE 5·8 OBSERVED MEAN DEFLECTIONS FOR THREE SPAN CONTINUOUS PERSPEX BRIDGE MODEL

CASE I						CASE II					
	LOAD AT 1	LOAD AT 2		LOAD AT 5	LOAD AT 6		LOAD AT 1	LOAD AT 2		LOAD AT 5	LOAD AT 6
1	770	259	5	701	241	1	831	245	5	742	241
2	254	437	6	253	429	2	239	508	6	244	436
3	54	225	7	54	189	3	4	247	7	−15	207
4	−17	48	8	−13	38	4	−11	8	8	−29	−13
Σ	1061	969	Σ	995	897	Σ	1063	1008	Σ	942	871

TABLE 5·9 – BRIDGE PARAMETERS

CASE	SPAN	θ	$\sqrt[4]{\gamma}$	θ°
I	ef	0·664	1·167	0·775
	fg	0·56	1·332	0·746
II	ef	0·789	1·167	0·92
	fg	0·667	1·332	0·889

TABLE 5·10 – THEORETICAL AND EXPERIMENTAL VALUES OF DISTRIBUTION COEFFICIENTS

CASE I						CASE II					
θ°_{ef} = 0·775			θ°_{fg} = 0·746			θ°_{ef} = 0·92			θ°_{fg} = 0·889		
	EXPT.	THEORY		EXPT.	THEORY		EXPT.	THEORY		EXPT.	THEORY
k_{11}	0·7257	0·7951	k_{55}	0·7045	0·7855	k_{11}	0·7817	0·8348	k_{55}	0·7876	0·8274
k_{21}	0·2394	0·2826	k_{65}	0·2543	0·2898	k_{21}	0·2248	0·2368	k_{65}	0·2590	0·2471
k_{31}	0·0509	0·0075	k_{75}	0·0543	0·0175	k_{31}	0·0038	−0·0200	k_{75}	−0·0159	−0·0150
k_{41}	−0·0160	−0·0852	k_{85}	−0·0131	−0·0928	k_{41}	−0·0103	−0·0516	k_{85}	−0·0308	−0·0595
k_{12}	0·2673	0·2826	k_{56}	0·2687	0·2898	k_{12}	0·2431	0·2368	k_{56}	0·2767	0·2471
k_{22}	0·4510	0·4458	k_{66}	0·4783	0·4336	k_{22}	0·5040	0·5181	k_{66}	0·5006	0·5032
k_{32}	0·2322	0·2641	k_{76}	0·2107	0·2591	k_{32}	0·2450	0·2651	k_{76}	0·2376	0·2648
k_{42}	0·0495	0·0075	k_{86}	0·0423	0·0175	k_{42}	0·0079	−0·0200	k_{86}	−0·0149	−0·0150

I- Nine cross beams of cross section 10 mm wide x 3.25 mm deep, three in each span placed at equal spacing;

q_{ef} = 9.0 cm and q_{fg} = 11.25 cm.

II- Three cross beam of cross section 10 mm x 3.25 mm one in each span placed in the middle; q_{ef} = 18.0 cm a nd q_{fg} = 22.5 cm.

The deflections at points 1 to 12 (Fig.5.4) were measured by applying a 2 lb. load at different points. All points were initially loaded by 1/4 lb. weights. The experimental set up is shown in photograph 3.

The average values of the observed deflections of the outer and middle spans are tabulated in table 5.8.

The flexural parameters θ for two sets of cross beams and two spans ef and fg are tabulated in table 5.9. The parameters θ°, according to equivalent stiffness method 4.2.1 (b) for these cases are determined. Using graph 1 to 6 the distribution coefficients $k = \frac{K_0}{4}$ for loaded spans ef and fg are obtained for various values of θ°. These theoretical values of the distribution coefficients are tabulated in table 5.10 for comparison with the values obtained from table 5.8.

A single main beam of the grillage was tested alone to find the total deflections due to a 2 lb.

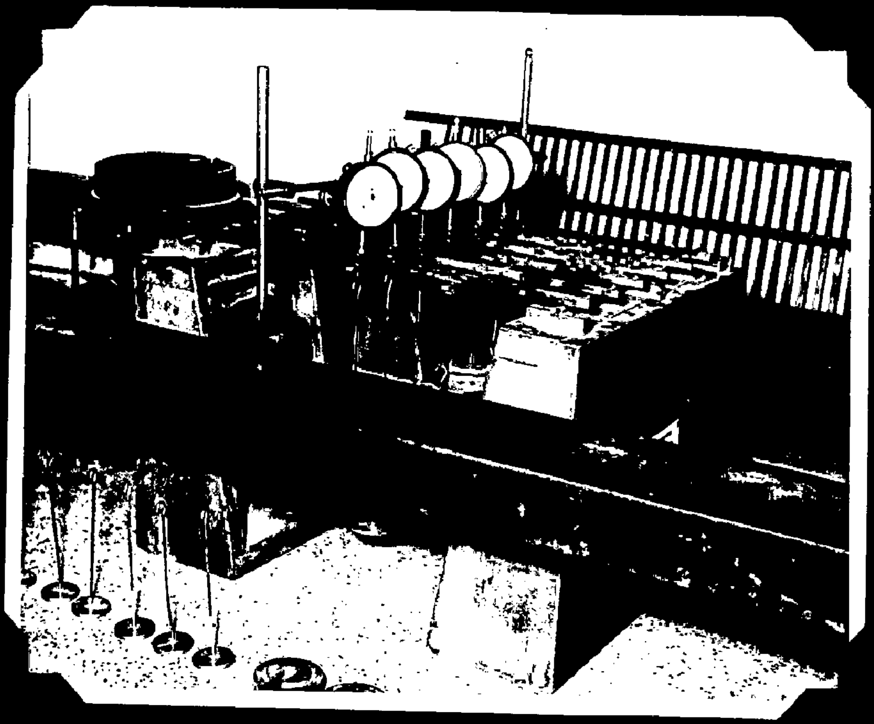

1: Steel Grillage Model.

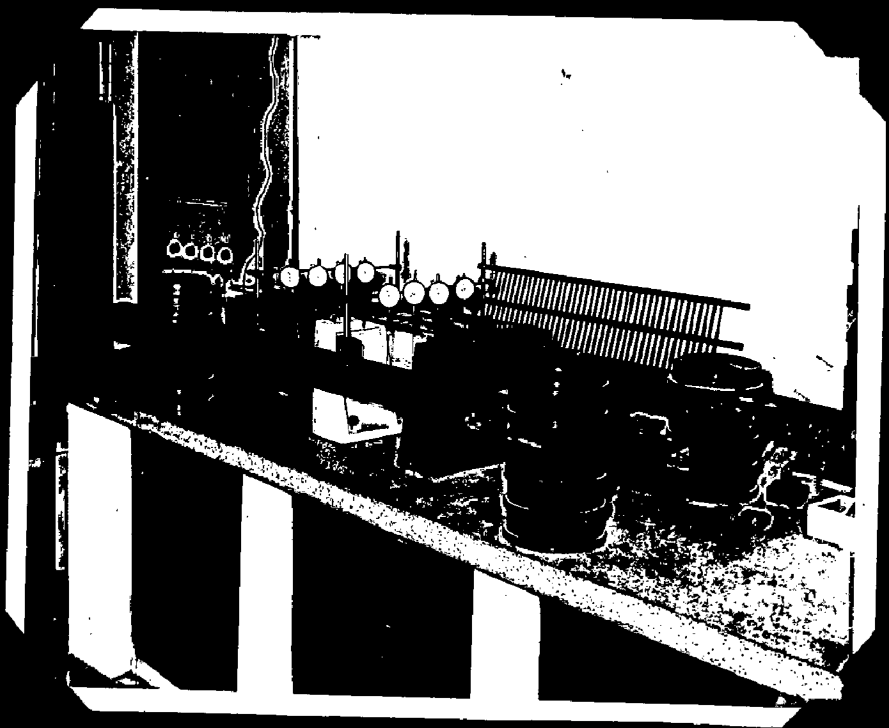

2: Two Span Continuous Steel Bridge Model

: Three Span Continuous Perspex Bridge Model.

load applied at different points. The beam was tested to check the total deflection of the grillage at a transverse section.

It is seen that the creep effects are more in the middle span as the residual upward deflections could not be removed.

From table 5.10 it is seen that the theoretical values are quite close to experimental values except the negative values at the edges of the bridge.

CONCLUSIONS

It is seen that the load distribution analysis based on the anisotropic plate theory is elegant and versatile tool to evolve design charts and curves. It permits convenient parameter variation study so that with the help of a computer suitable design charts can be developed. One may note that this method has been accepted and adopted by most of the continental Bridge Design Organisations.

Of course, the analytical expressions are highly involved and without the aid of computing machines their applications may not be possible. The merit of the method can only be appreciated if this facility is available else, other loads distribution theories may work better. The real merit lies in as much as it permits design charts and tables evolved once for all and subsequently used in the routine design work.

REFERENCES

1. LAZARIDES, T.O.

'The Design and Analysis of openwork prestressed concrete beam grillages' , Civil Engineering and Public Works Review, Vols. 47 and 48, June, 1952. page 471 etc.

2. LIGHTFOOT AND SAWKO,

'The analysis of grid frame works and floor systems by the electronic computer', Structural Engineer, March 1960 page 79.

3. MARTIN, I and HERNADEZ, J.

'Orthogonal gridworks loaded normally to their planes' Proc. Am. Soc. of Civil Engg.Vol. 86, Jan. 1960, pp 1-12.

4. JANSSONIUS, G.F.

'Nieuwe Vereffeningsmethoden Voor het Berekenen Van Balkroosters'. Prvefschrift, Techn. Hogeschool 1948.

5. EWELL, W.W., OKUBO, S. and ABRAMS J.I.

'Deflections in gridworks and Slabs' Trans. Am. Soc. of Civil Engg. Vol. 117, 1952, page. 869.

6. BEER, H. and RESINGER, F.

'Nachr. d. Osterr. Betonvereins', 14, 1954 S.13 Beilg. 2. Osterr. Bauzeitschrift (1954) H.3.

7. RAY, K.C.

'Analysis of grid floors' (Treated partly as orthotropic plate and partly as space frame) Indian Concrete Journal, Vol. 34, June 1960. pp. 227-232.

8. LEONHARDT, F.

'Bautechnik 16 1938 S. 535.

9. LEONHARDT, F. and ANDRA, W.

'Die Vereinfachte tragerrostberechnung' Julius Hoffman Press, Stuttgart, 1950-Book.

10. MALTER.

'Numerical solution for interconnected bridge girders' Proc.Am. Soc. of Civil Engr. Oct. 1958, 1815.

11. PIPPARD, A.J.S. & de WAELE, J.P.A.

'The Loading of interconnected bridge girders' J. Inst. C.E. London Vol. 10, No.1. 1938.

12. HETENYI, M.

' A method for calculating grillage beams', S. Timoshenko, 60th Anniversary volume, Newyork, 1938 pp. 60-72.

13. HENDRY, A.W. and JAEGER, L.G.

'The analysis of grid frameworks and related structures' Chatto and Windus London 1958-Book.

14. GUYON, Y.

'Calcul des ponts larges a poutres multiples solidarisees par des entretoises' Annales des Ponts et Chaussees, France No.24. Sept.-Oct.1946. pp. 533-612.

15. GUYON, Y.

Calcul des ponts dalles'. Annales des Ponts et Chaussees. Vol. 119. France No.29. 1949. pp.555-589 No.36. pp. 683-718.

16. MASSONNET, C.

'Methode de Calcul des ponts a pourtres multiples tenant compte de leur resistance a la torsion' (Method of calculation of bridges with several longitudinal beams, taking into consideration their torsional resistance). Zurich, International Association for Bridge and Structural Engineering. Publications. Vol. 10, 1950. pp. 147-182.

17. BALOG.L.

'Grid Bridge Design' Civil Engineering (A.S.C.E.), Vol. 40, Jan 1957 pp. 8-12.

18. GUPTA , B.K.

' A Critical Study of Load Distribution Theory on Interconnected girder bridges'. M.E. Thesis, University of Roorkee, Roorkee. 1962.

19. HEYMAN, J.

'Plastic design of grillages', Engineering, 1953. page. 804.

20. REYNOLDS, G.C.

'The strength of prestressed concrete grillage bridges'. Cement and Concrete Association, London. Technical Report TRA/263. June 1957.

21. GRANHOLM, C. and ROWE, R.E.,

'The ultimate load of skew slab bridges'. Cement and Concrete Association, London. Research Report. Nr.12.

22. MORICE, P.B. and LITTLE, G.

'Load distribution in prestressed Concrete bridge systems'. The Structural Engineer. Vol.32. No.3. March, 1954. pp. 83-111.

23. ROWE, R.E.

'A load distribution theory for bridge slabs allowing for the effect of Poisson's ratio. Magazine of Concrete Research. Vol. 7. No.20. July 1955. pp. 69-78.

24. LITTLE, G. and ROWE, R.E.

'The effect of edge stiffening and eccentric transverse in bridges'. Cement and Concrete Association. Technical Report. TRA/279. Nov., 1957.

25. ROWE, R.E.

'Load distribution in no-torsion bridge grillages with various support conditions. Cement and Concrete Association, Technical Report, TRA/247. March, 1957.

26. ROWE, R.E.

'A load distribution theory for no-torsion bridge grillages with various support conditions. Cement and Concrete Association, Technical Report, TRA/244 Feb. 1957.

27. MORICE, P.B. and LITTLE, G.

'Analysis of right bridge decks subjected to abnormal loading.' London, Cement and Concrete Association , July 1956. pp. 43.Db 11.

28. MORICE, P.B., LITTLE, G. and ROW, R.E.

'Design curves for the effects of concentrated loads on concrete bridge decks. London, Cement and Concrete Association, July 1956, pp. 24. Db 11a.

29. ROWE, R.E.

'The Design of right concrete slab bridges for abnormal loading. Cement and Concrete Association, London. Db 12.Sept., 1958 pp.8.

30. LITTLE, G. and ROWE, R.E.

'The effect of edge stiffening beams on bridges. Cement and Concrete Association Technical Report. TRA/221 Feb. 1956.

31. ROW, R.E.

'Load distribution in bridge slabs (with special reference to transverse bending moments determined from tests on three prestressed concrete slabs)' Magazine of Concrete Research, vol. 9, No.27 Nov.1957. pp. 151-160.

32. LITTLE, G. and ROWE, R.E.,

'Load distribution in multi-webbed bridge Structures from tests on plastic models.' Magazine of Concrete Research, vol.7, No.21 Nov.1955 pp.133-142.

33. LITTLE, G and ROWE, R.E.

'The effects of edge stiffening and eccentric transverse prestress in bridges! Zurich. International Association for Bridge and Structural Engineering. Publications. Vol. 19. 1959. pp.169-200.

34. MORICE , P.B. and LITTLE, G.

' Load tests on a small prestressed concrete highway bridge'. Proc. of the Conference on the correlation between calculated and observed stresses and displacements in structures.' Inst. of Civil Engineers. Sept. 1955.

35. ROWE, R.E.

' Loading tests on two prestressed concrete highway bridges'. Proc. Inst. of C.E. Vol. 13.Aug.1959. pp. 477-498.

36. ROWE, R.E.

' The analysis and testing of a type of bridge suitable for medium right span subjected to abnormal loading'. Cement and Concrete Association, Research Report No.8. Nov. 1958.

37. MASSONNET, C.

' Complements a la methode de calcul des ponts a poutres multiples.' Annales des Travaux Publics de Belgique , Oct, 1954. 68 pp.

38. HOFFMAN, J.W. and VLUGT

' Design of grid frame and flat slab bridges.' Cement (Amster dam) No.19-20 Augu. 1956 pp.479-486.

39. SATTLER, K.

'Betrachtungen zum Berechnungsverfahren von Guyon-Massonnet fur freiaufliegende Tragerroste and Erweiterung dieses Verfahrens auf beliebige Systeme. Der Bauingenieur, Vol.30, 1955.pp.77-89.

'Thoughts on the Guyon-Massonnet method of analysis for simply supported grid frame works and extension of this method to any system.

40. MASSONNET, C.

'Le Dimensionnement Pratique des ponts a poutres multiples et des ponts-dalles en Tenant compte de Leur Rigidite Torsionnelle.

'Practical design of multiple girder bridges taking into account torsional rigidity' PUB.DEL CORSO DI PER. 8, 77-114 April 1955.

41. SATTLER, K.

'Betrachtungen uber Tragerroste mit Steifigkeit-Suntersonieden zwischen Rand-und Innentragern'. 'Reflections on grillage beams with stiffness variations between outer and inner beams'. Der Bauingenieur Vol.34 Jan.-Feb 1959.pp 1-9 , 53-59.

42. NARUOKA , M. And OMURA, H.

'Digitial computer analysis of influence coefficients for deflections and bending moments of orthotropic parallelogram plates.' Memoirs of the Faculty of Engineering. Kyoto University, Japan, Vol.XXI part 2 April 1959.pp 103-137.

43. NARUOKA, M. and OMURA, H.

' On the analysis of a skew girder bridge by theory of orthotropic parallelogram plates. Zurich, International Association for Bridge and Structural Engineering. Publications Vol.19, 1959 pp.231-256.

44. JENSEN, V.P.

'Analysis of skew slabs'. The Engineering Experiment Station, Univ. of Illinois. Bull. Series No.332 Vol. XXXIX Sept. 1941. No.3.

45. ROBINSON, K.E.,

'The behaviour of simply supported skew bridge slabs under concentrated loads.' Cement and Concrete Association , Research Report No.8 Nov. 1959.

46. HETENYI, M.

'Beams on elastic foundation' University of Michigan, Studies Scientific Series Volume XVI 1955.

47. BEST, B.C. and ROWE R.E.

'Abnormal loading on composite slab bridges.' Cement and Concrete Association, Research Report No.7 Oct. 1959.

48. TIMOSHENKO, S. and WOINOWSKY- KRIEGER,S.

'Theory of Plates and Shells'. McGraw Hill 1959. pp. 364-371.

49. MASSONNET, C.

'Contribution au calcul des ponts a poutres multiples.' Ann. Trav. Publ. Belgique. June, Oct. and Sept. 1950.

50. DEHAN, E. MASSONNET, C. and SEYVERT, J.

'Recherches experimentales sur les ponts a poutres multiples'Ann. Trav. Publ. Belgique No.2. 1955.p.33.

51. LITTLE, G.

'Tests for load distribution in a two span prestressed concrete grillage'. Cement and Concrete Association. Technical Report TRA/178 Feb.1955.18pages

52. MORICE, P.B. and REYNOLDS G.C.

'Strength of Simply Supported Slab Bridges subjected to concentrated loads'. Proc. ofSymposium on the strength of concrete struct'. Cement and Concrete Association London, 1958. pp. 557-575.

53. BEER, H and RESINGER, F.

'Exact analysis of Skew grid (Girder and floor beam) with the aid of influence line'. Der Bauingenieur. Vol. 30 Dec. 1955.

54. HENDRY, A.W. and JAEGER, L.G.

'The analysis of certain interconnected skew bridge girders'. J. Inst. of C.E. London. 6055, 1955. pp. 939.

55. HOMBERG, H.

'Forschungshefte aus dem Gebiete des Stahlbaues' H.8. Kreuzwerke. Berlin. 1951.

56. KACHURIN, V.K.

'Nekotorye voprosy rascheta kosyleh mostor'. Some problems on calculations of skew bridges.' Sb. Lennigrad. intaush. zh-dtrausp. no.146.1958. pp. 283-290.

57. TIMOSHENKO, S.

'Theory of Elasticity' McGraw Hill 1934-book.

58. INGLIS, C.E.

The determination of Critical Speeds, natural frequencies and modes of vibration by means of Basic functions. Transactions of the North East Coast Inst. of Engrs. and Ship builders- 1944. Vol. 61 pp. 111-136.

59. PARCEL, J.I. and MOORMAN, R.B.B.

Analysis of Statically indeterminate Structures -book.pp. 279-282. J.W. 1957.

60. ROWE, R.E.

'Concrete Bridge Design'- book pp. 124-141 J.W. 1962.

61. I.R.C. CODE

Standard Specification and Code of Practice for Road Bridges Section II Loads and Stresses. 1958.

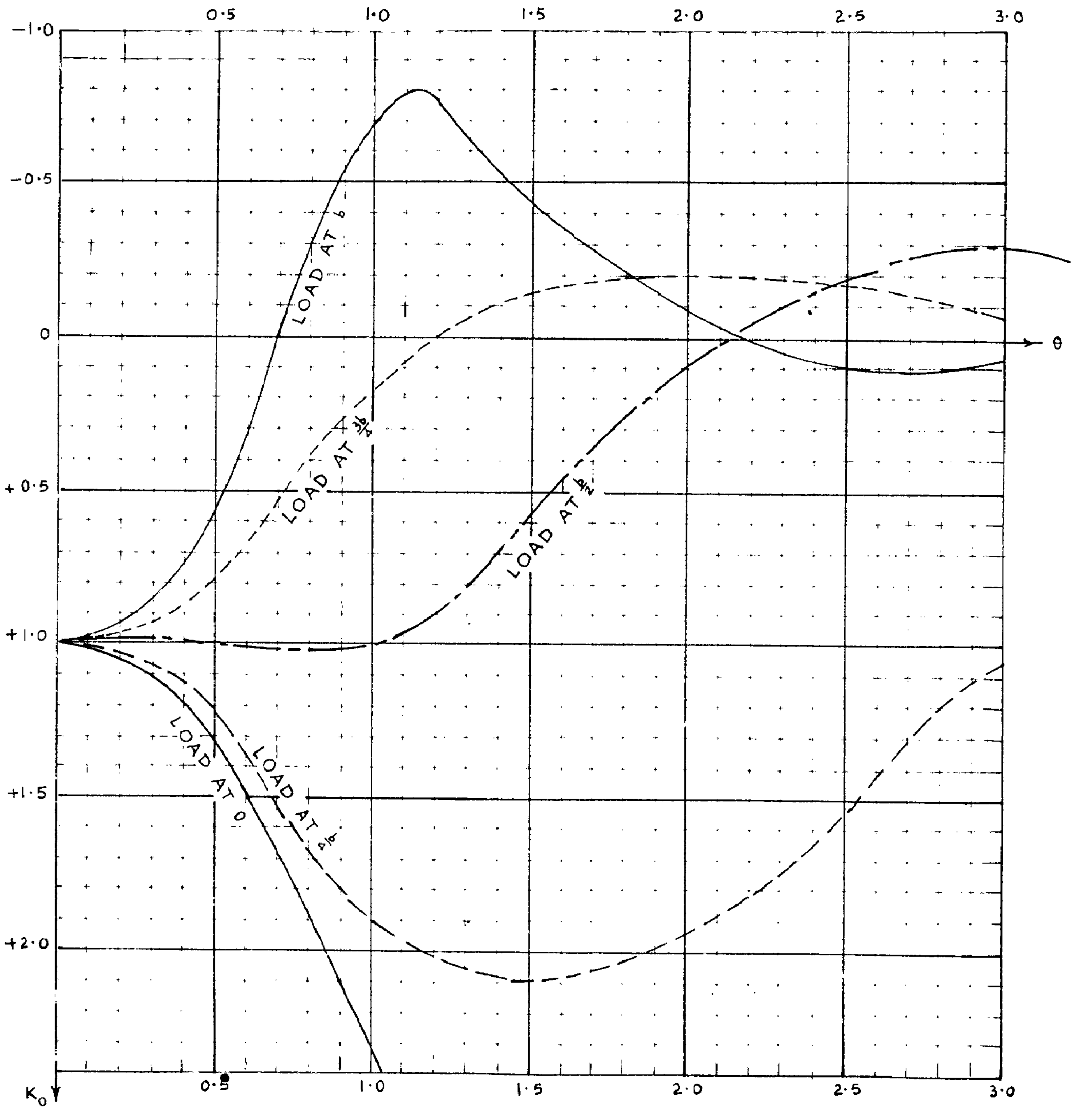

0·5
1·0
1·5
2·0
2·5
3·0
−1·0
−0·5
0
+0·5
+1·0
+1·5
+2·0
θ
K₀
LOAD AT b
LOAD AT 3b/4
LOAD AT b/2
LOAD AT b/4
LOAD AT 0

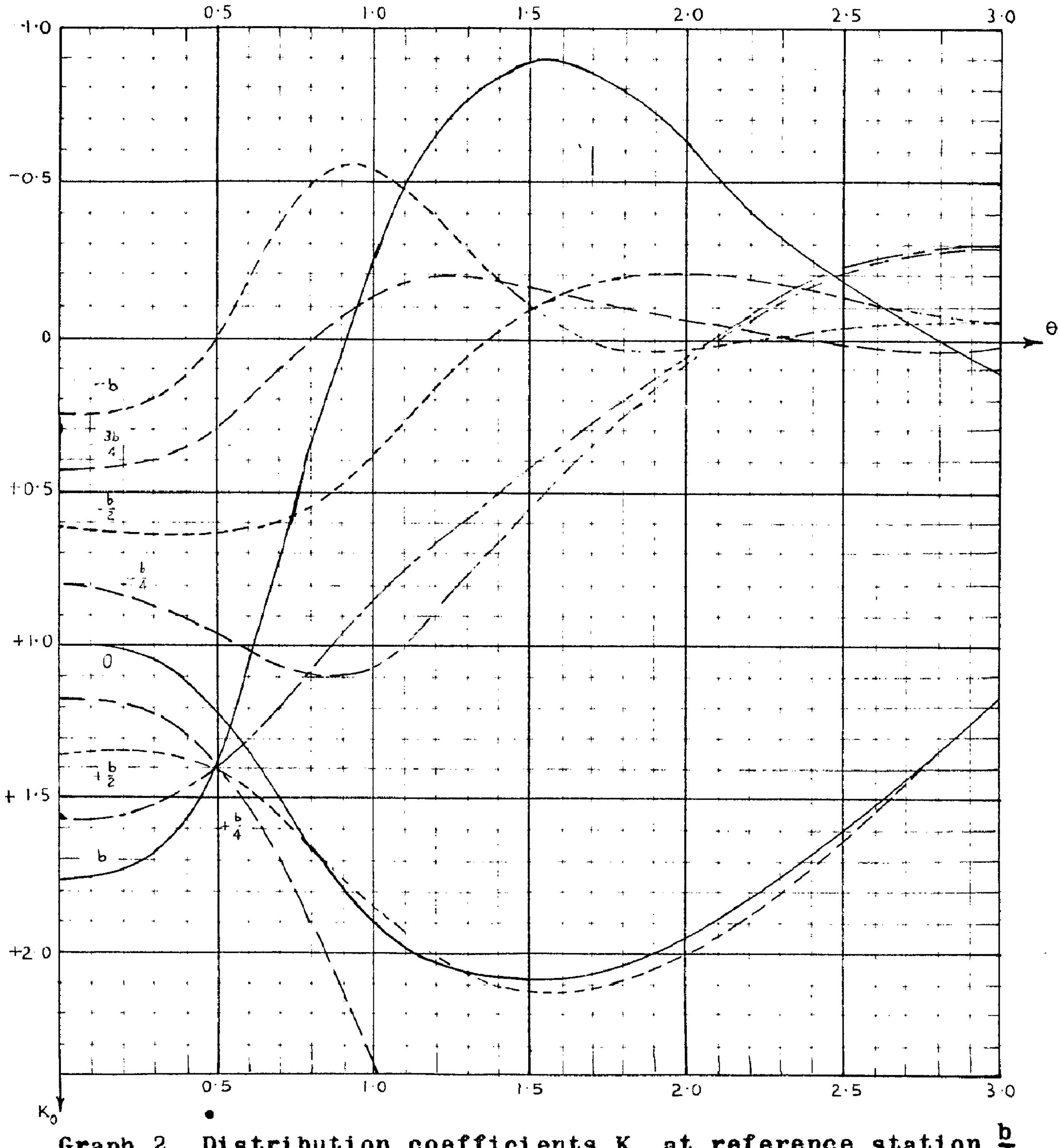

Graph 2. Distribution coefficients K_0 at reference station $\frac{b}{4}$ for various load eccentricities.

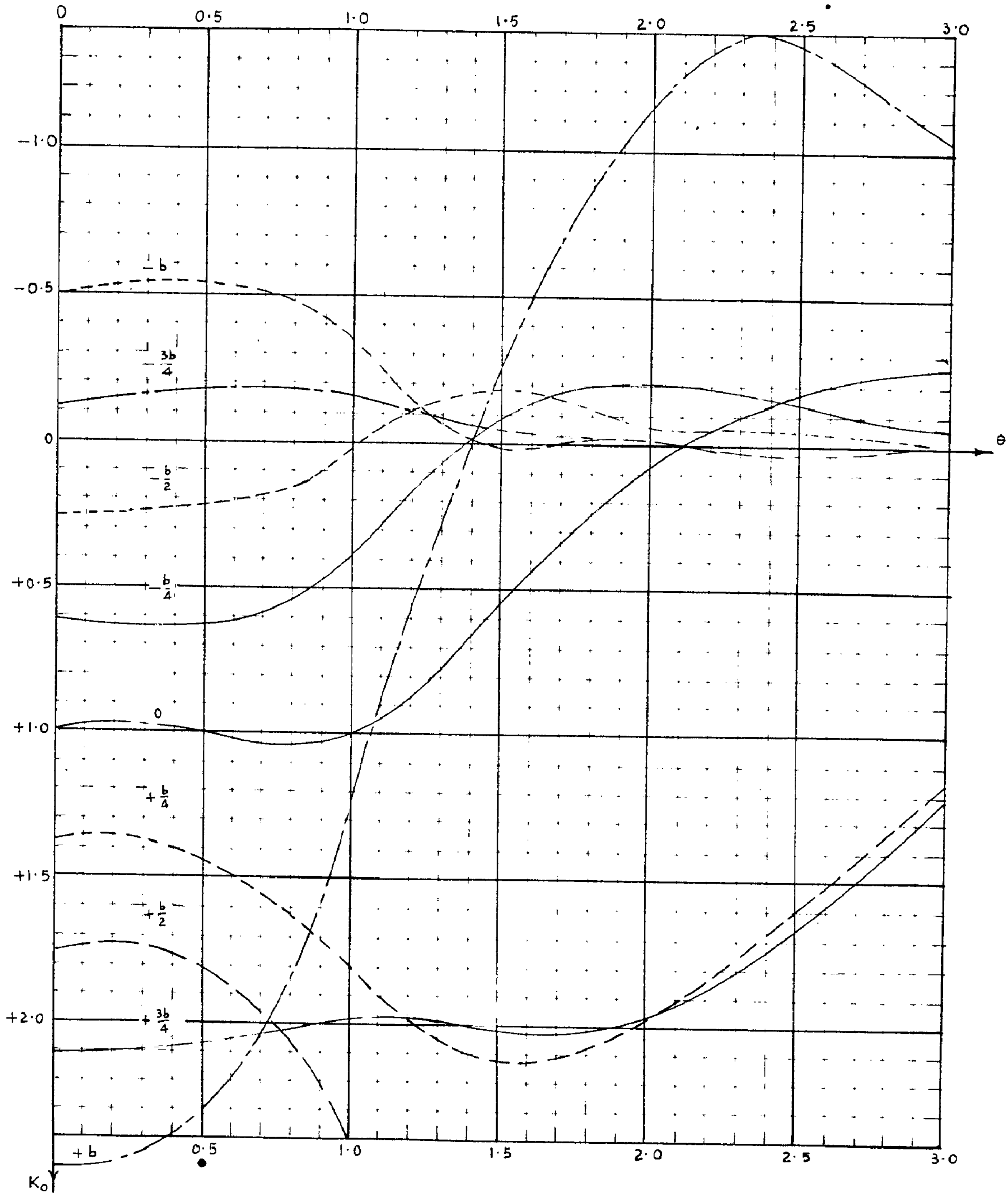

Graph 3. Distribution coefficients K_0 at reference station $\frac{b}{2}$ for various load eccentricities.

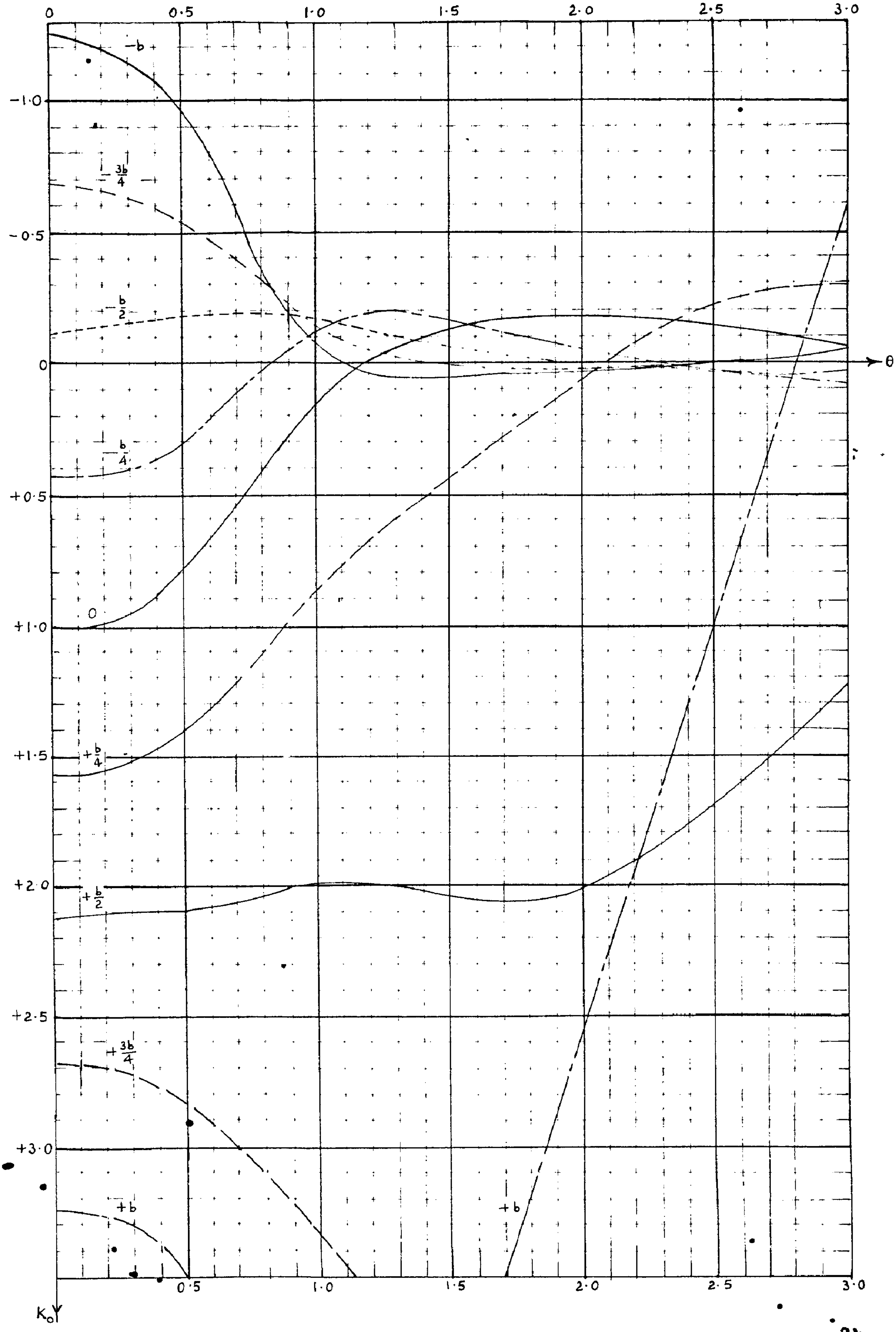

Graph 4. Distribution coefficients K_o at reference station $\frac{3b}{4}$ for various load eccentricities.

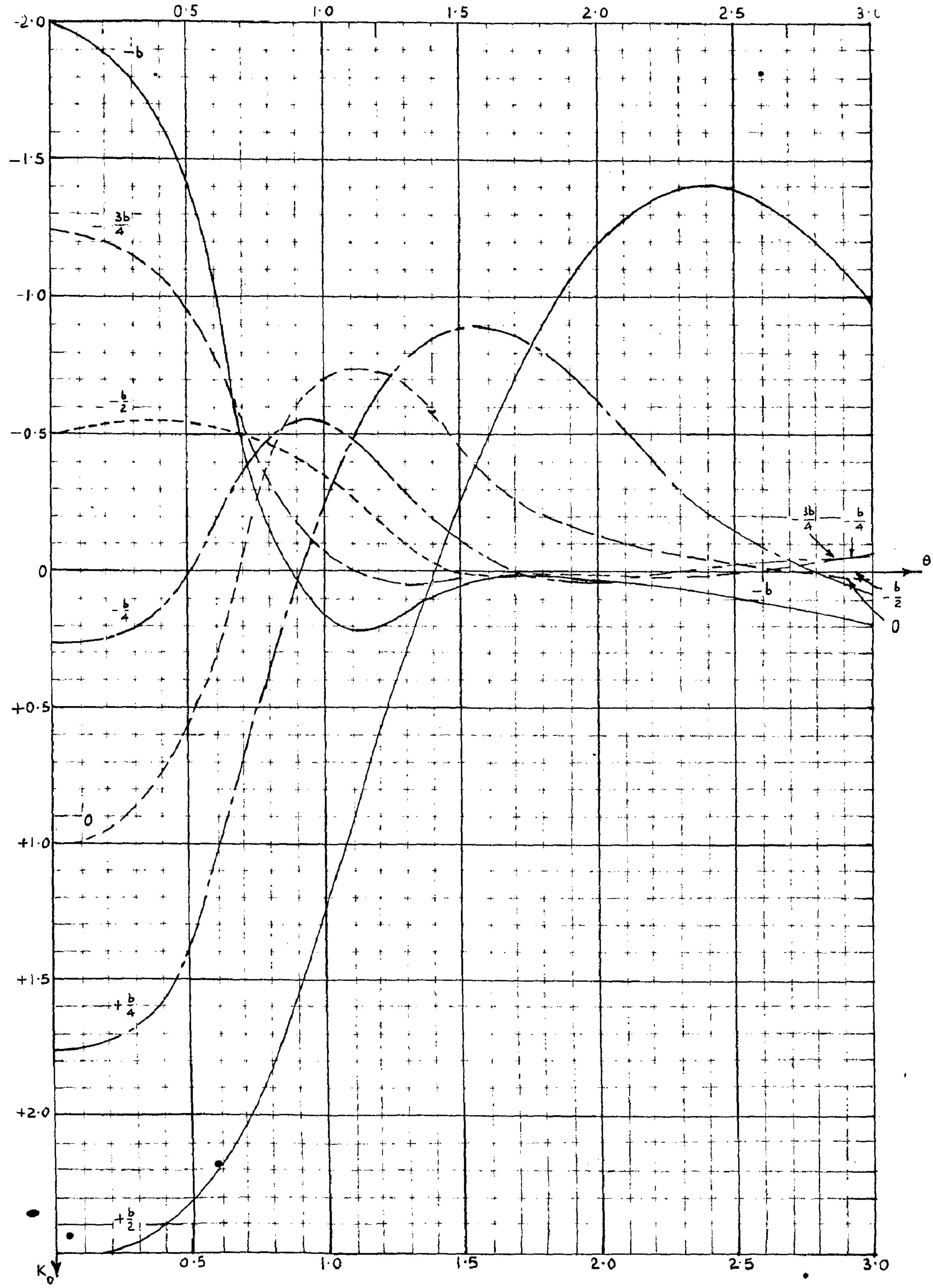

Graph 5. Distribution coefficients K_0 at reference station b for various load eccentricities.

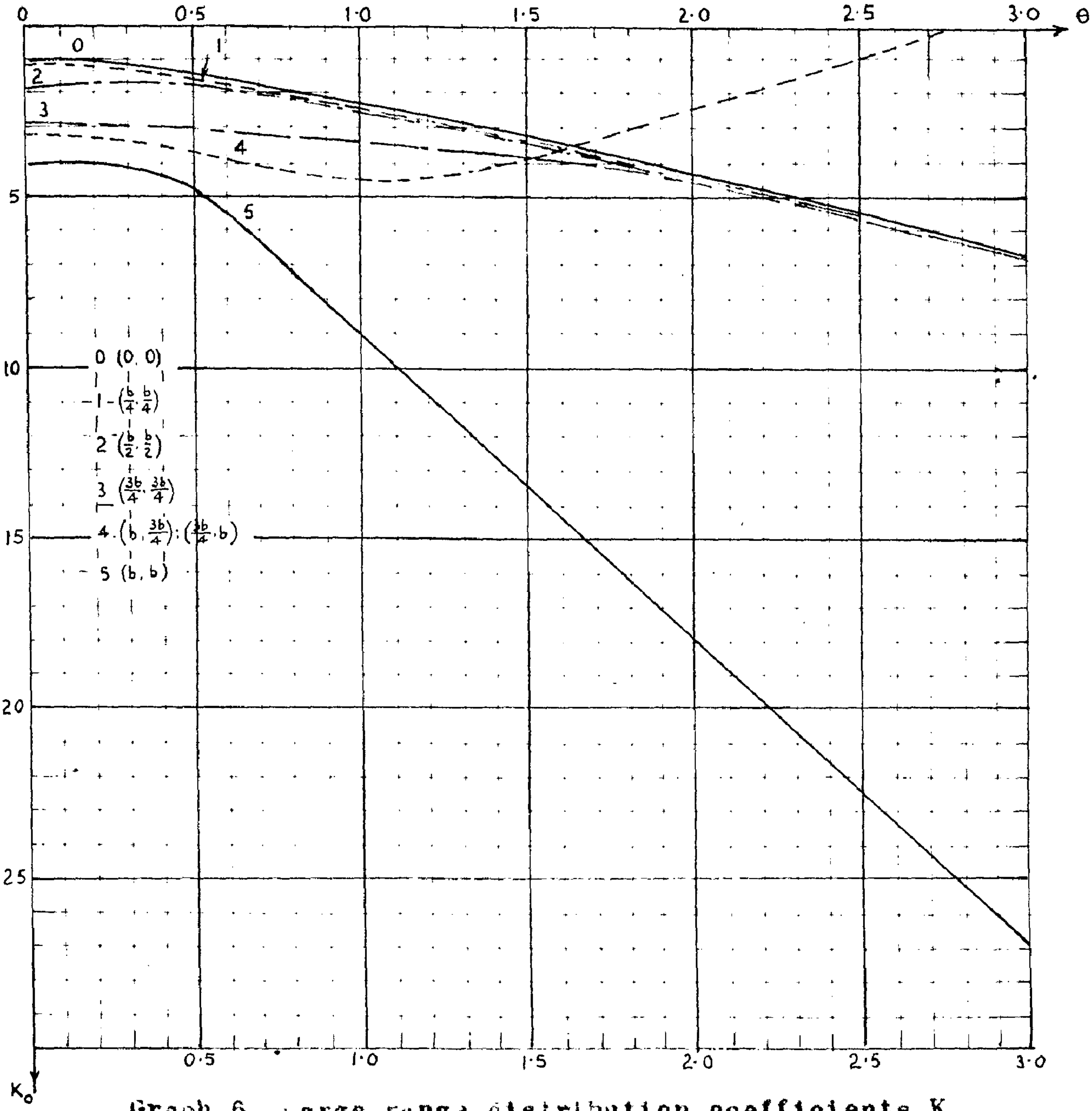

Graph 6. Large range distribution coefficients K_0

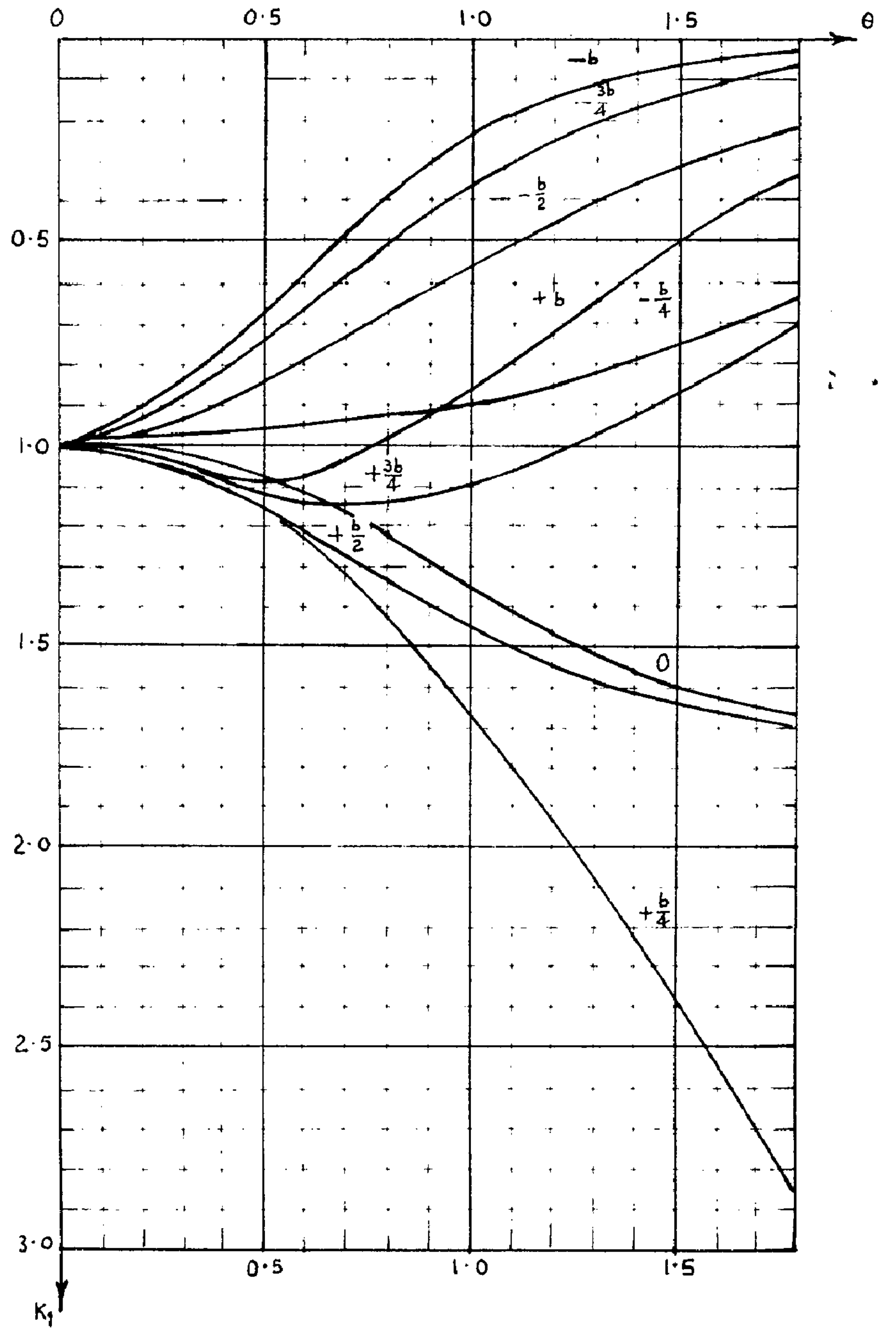

Graph 8. Distribution coefficients K_1 at reference station $\frac{b}{4}$ for various load eccentricities.

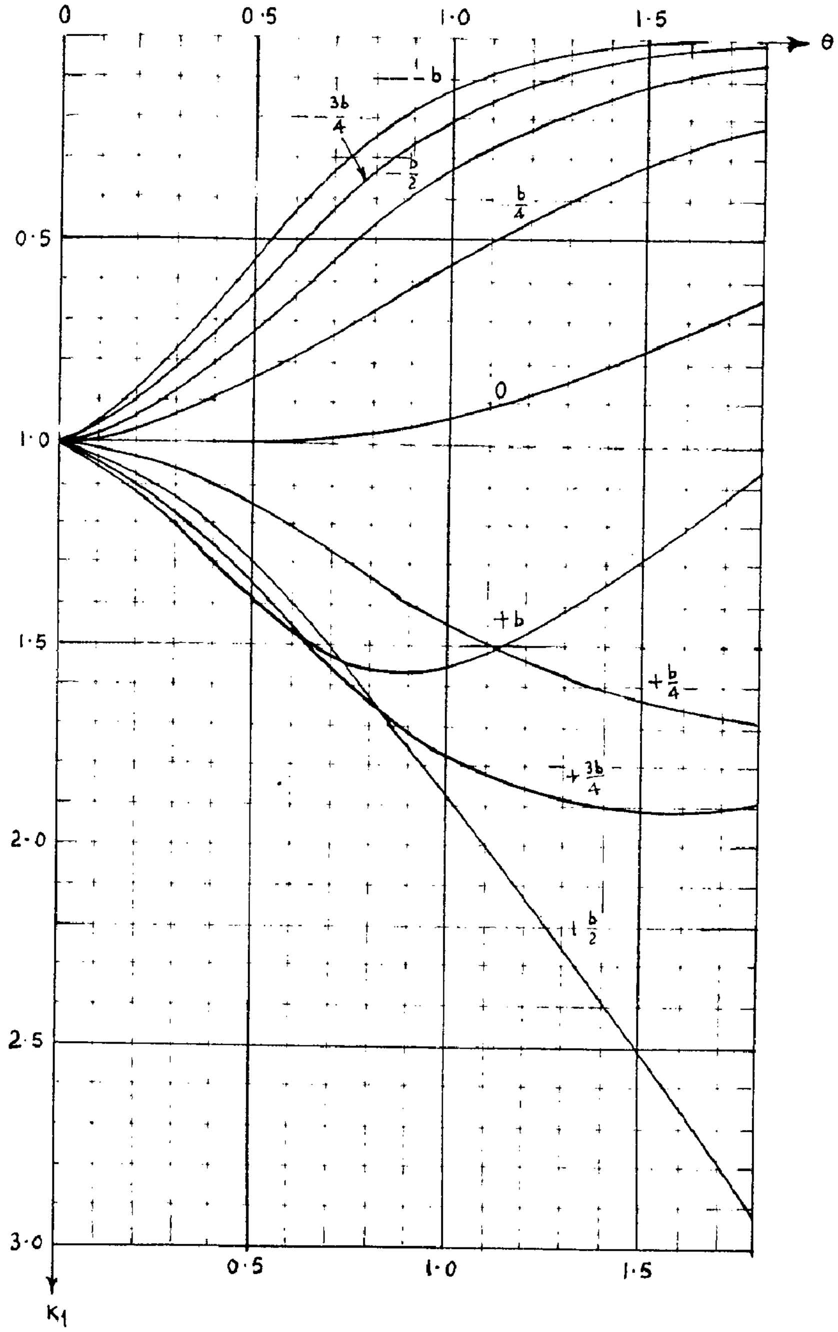

Graph 9. Distribution coefficients K_1 at reference station $\frac{b}{2}$ for various load eccentricities.

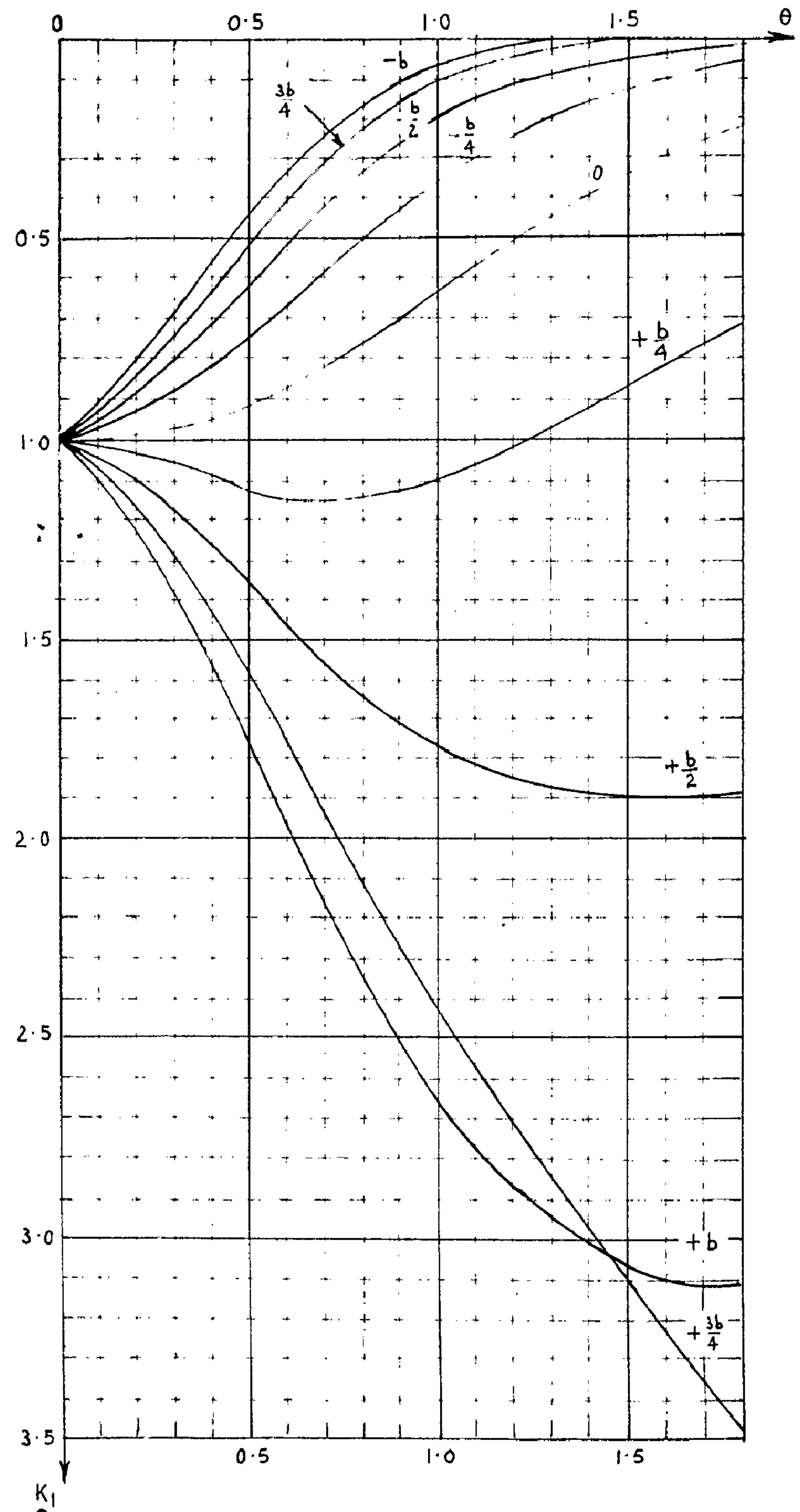

Graph 10. Distribution coefficients K_1 at reference station $\frac{3b}{4}$ for various load eccentricities.

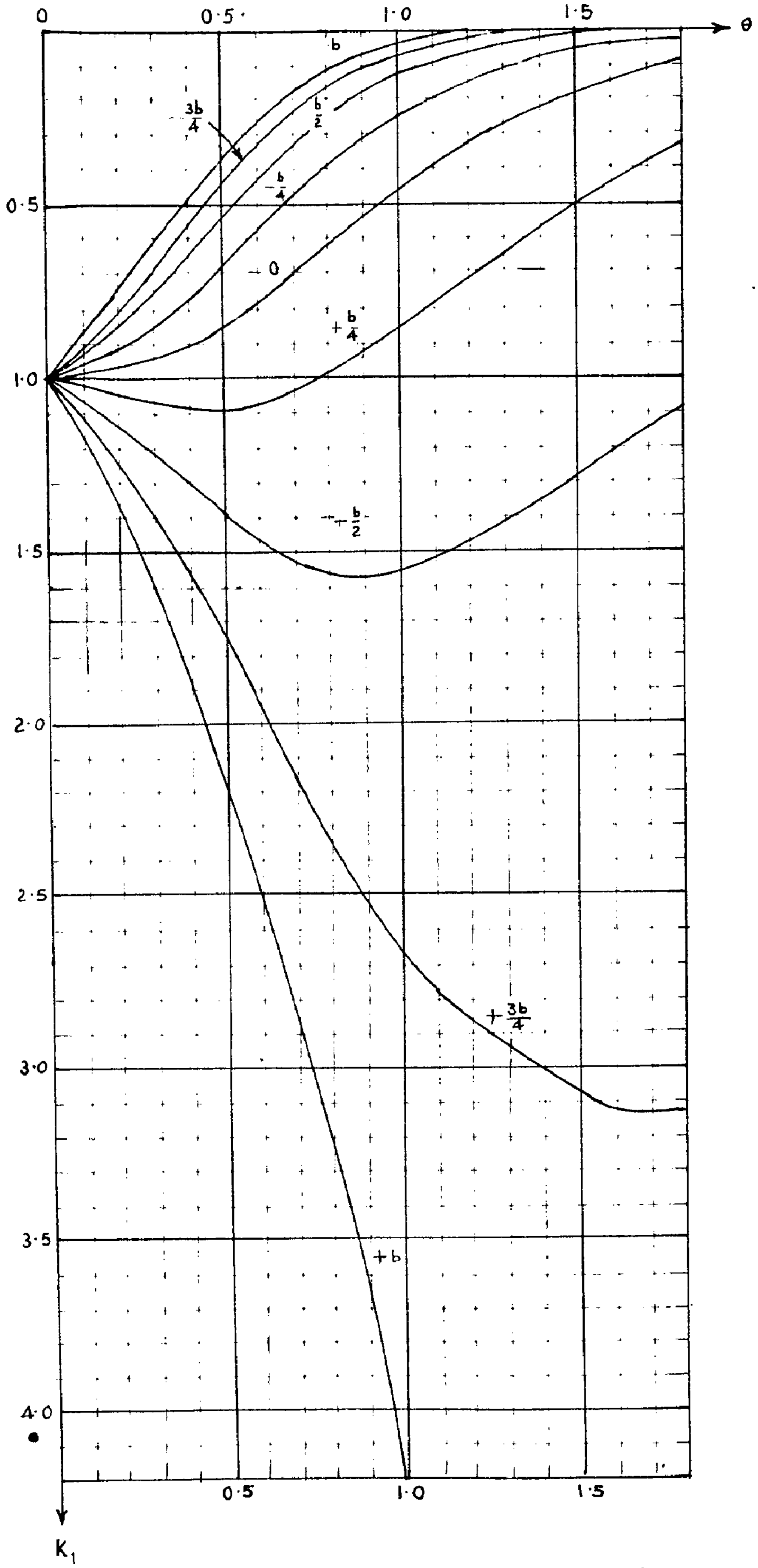

Graph 11. Distribution coefficients K_1 at reference station b for various load eccentricities.

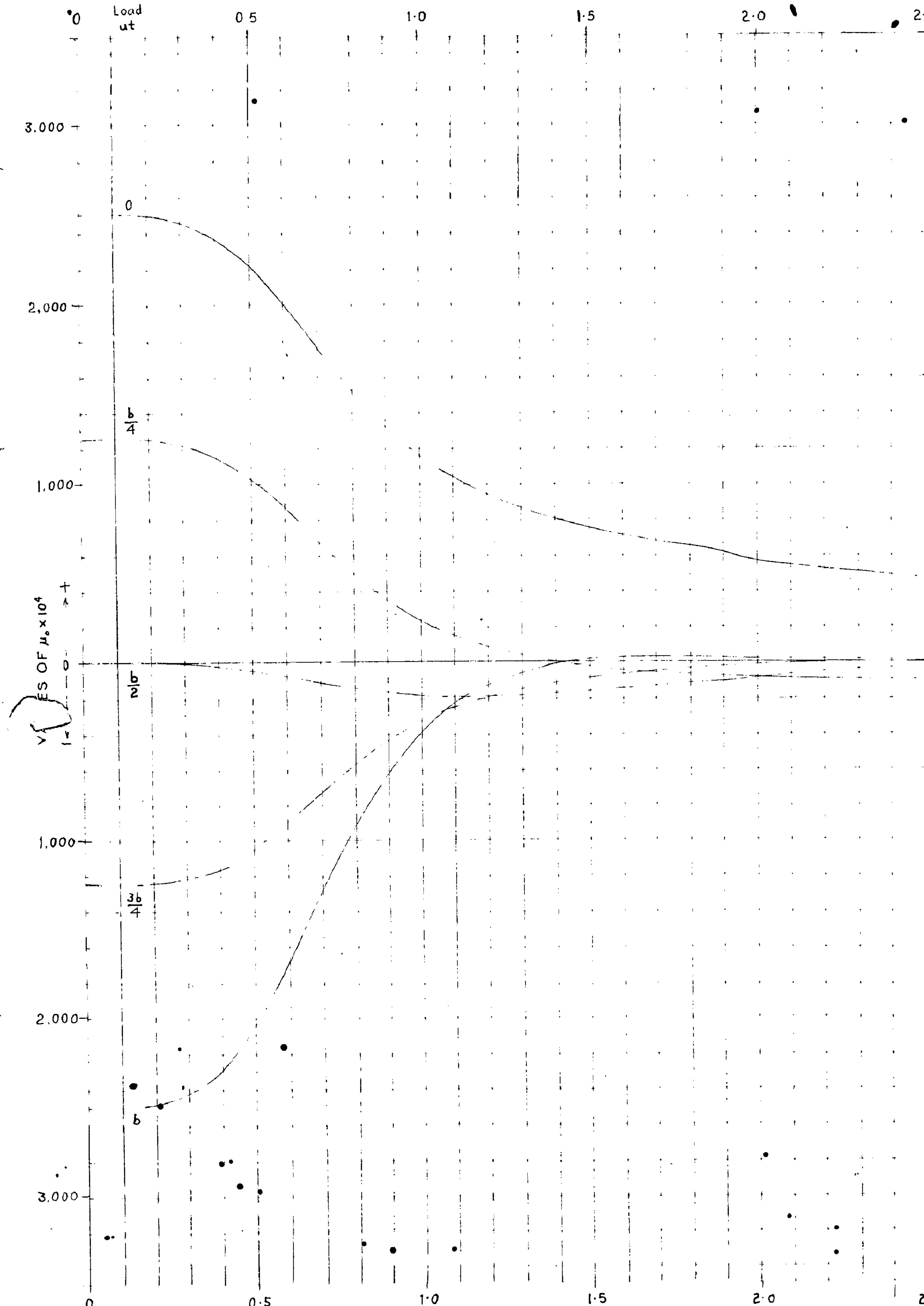

Load ut
0
0.5
1·0
1·5
2·0
3,000
2,000
1,000
0
$\frac{b}{4}$
$\frac{b}{2}$
$\frac{3b}{4}$
b
VALUES OF $\mu_o \times 10^4$

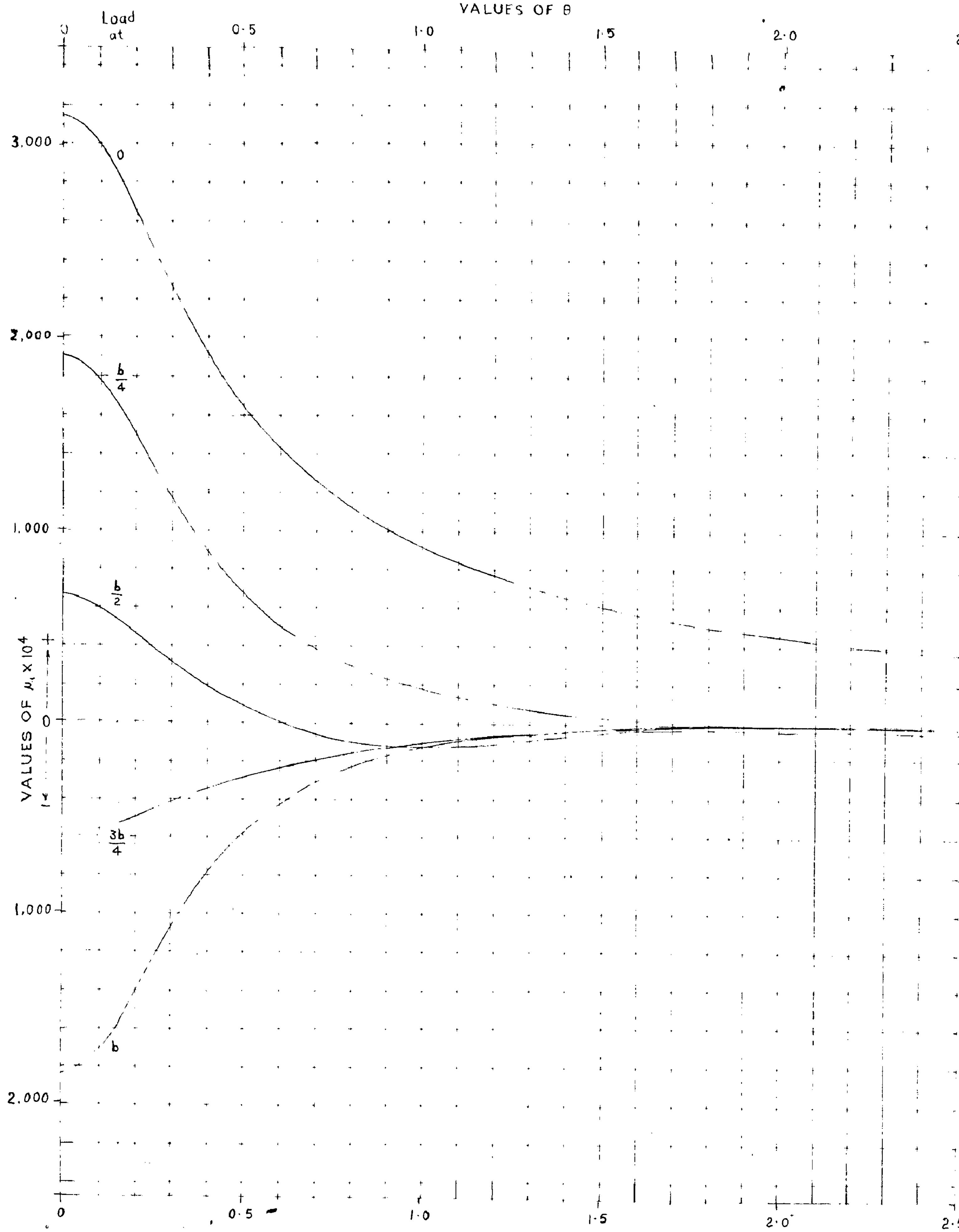

Graph 13: Transverse moment coefficients, μ_1, at reference station o for various load eccentricities.

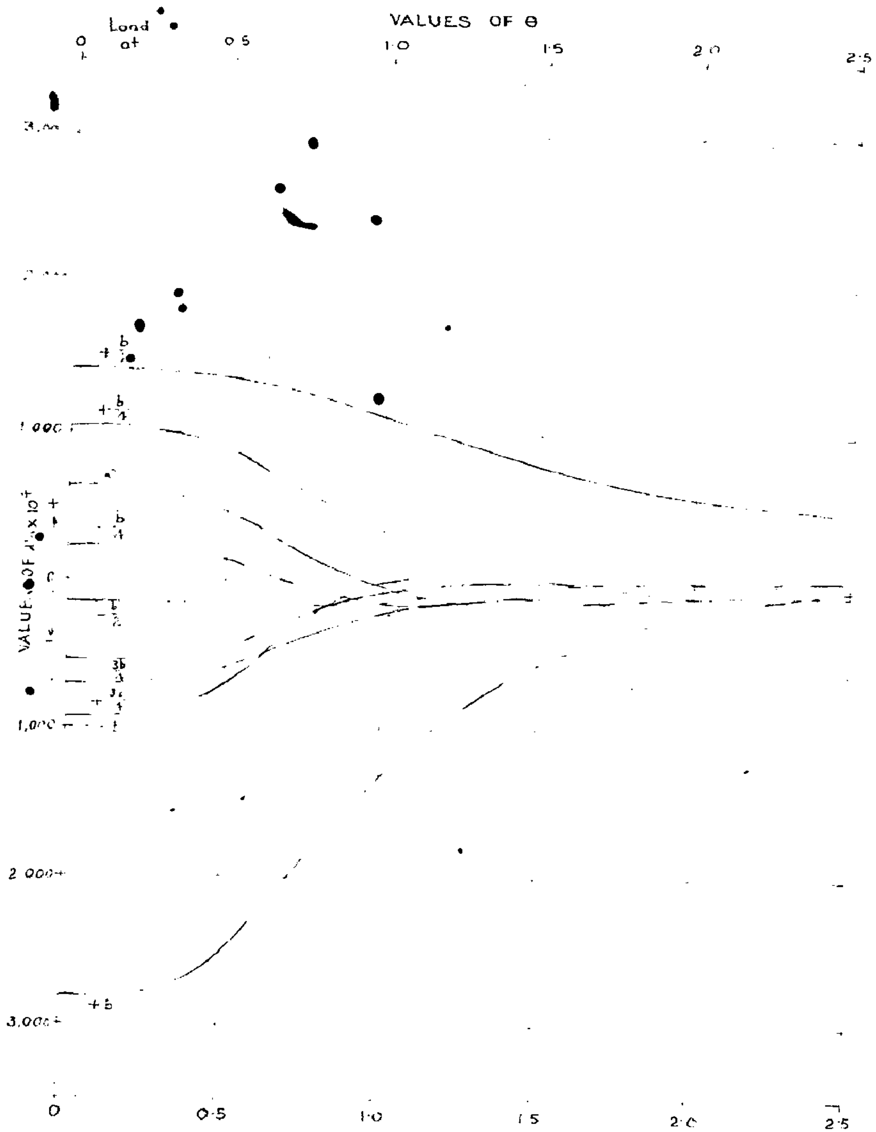

Graph 16: Transverse moment coefficients, μ_o, at reference station $\frac{b}{2}$ for various load eccentricities.

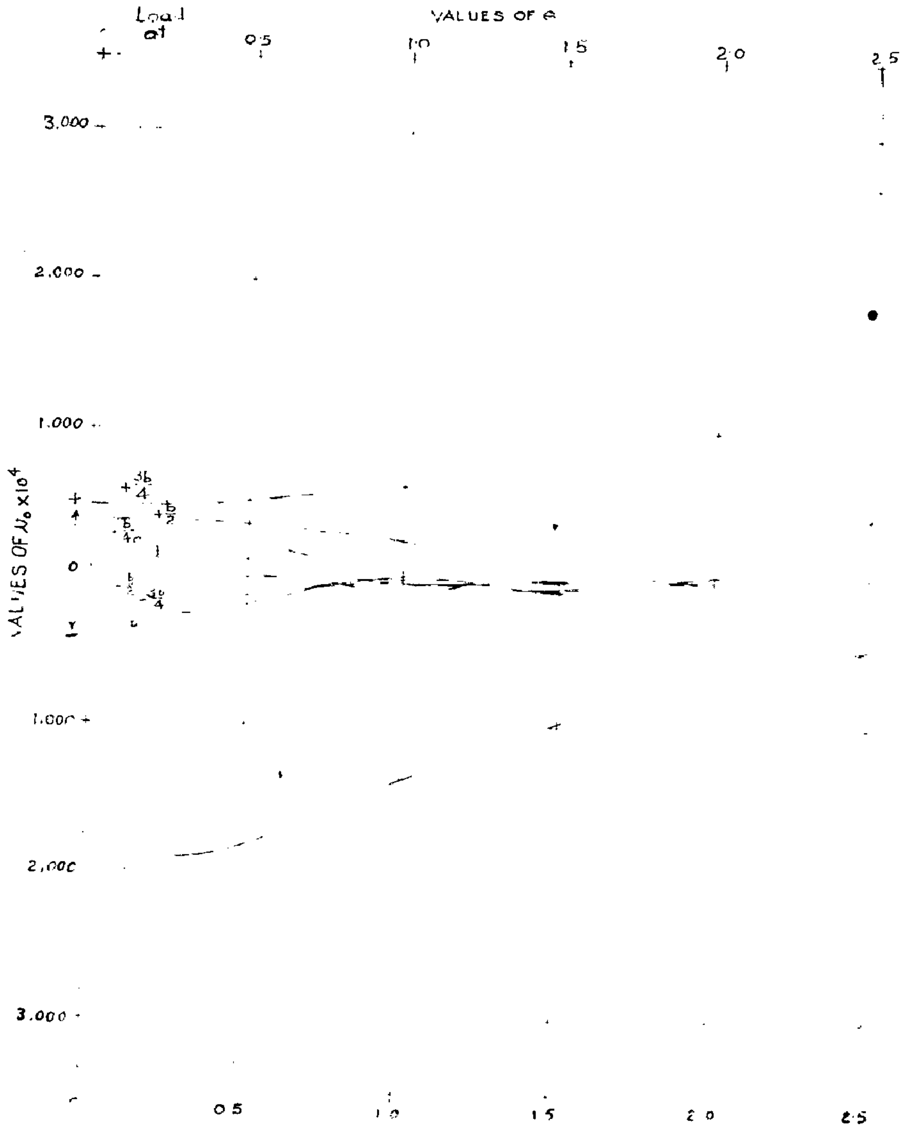

Graph 17: Transverse moment coefficients, μ_o, at reference station $\frac{3b}{4}$ for various load eccentricities

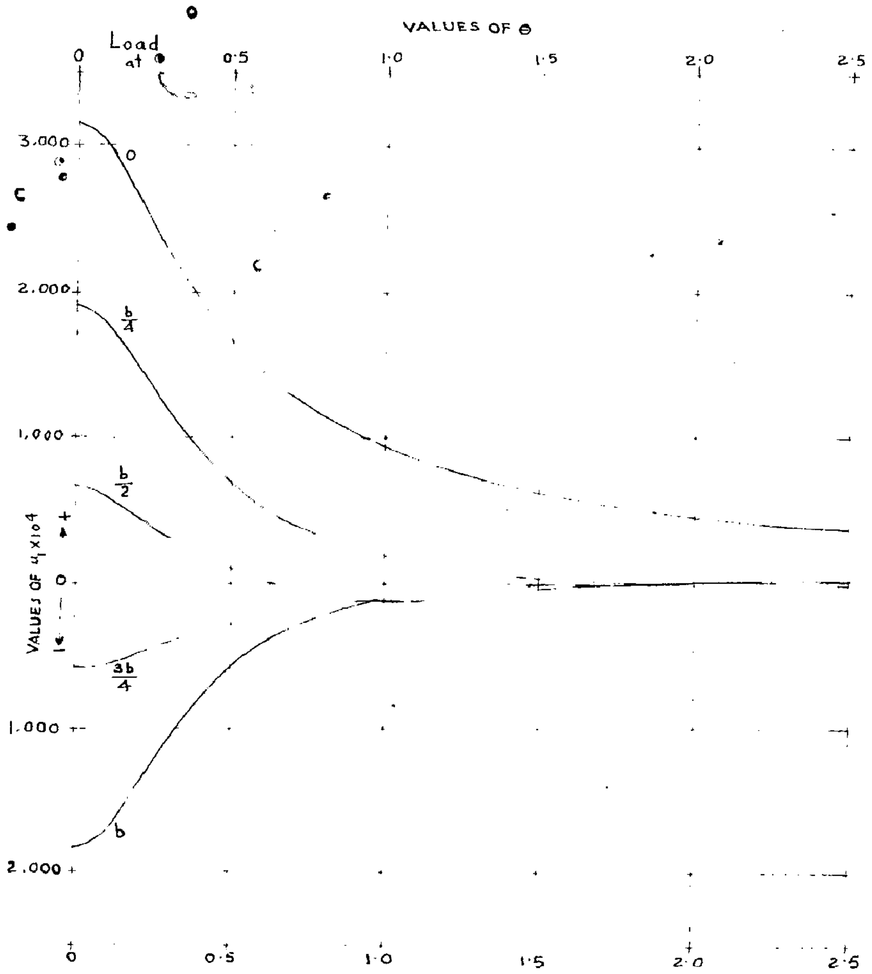

Graph 18: Transverse moment coefficients, μ_1, at reference station 0 for various load eccentricities.

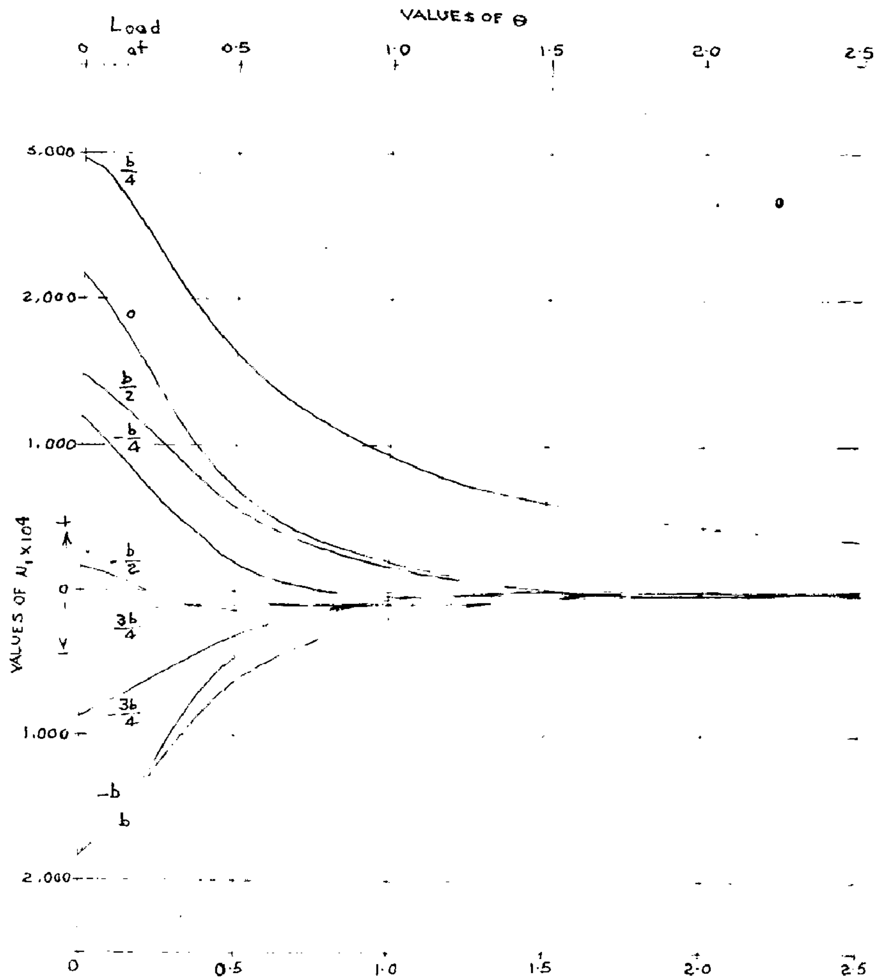

Graph 19: Transverse moment coefficients, μ_1, at reference station $\frac{b}{4}$ for various load eccentricities.

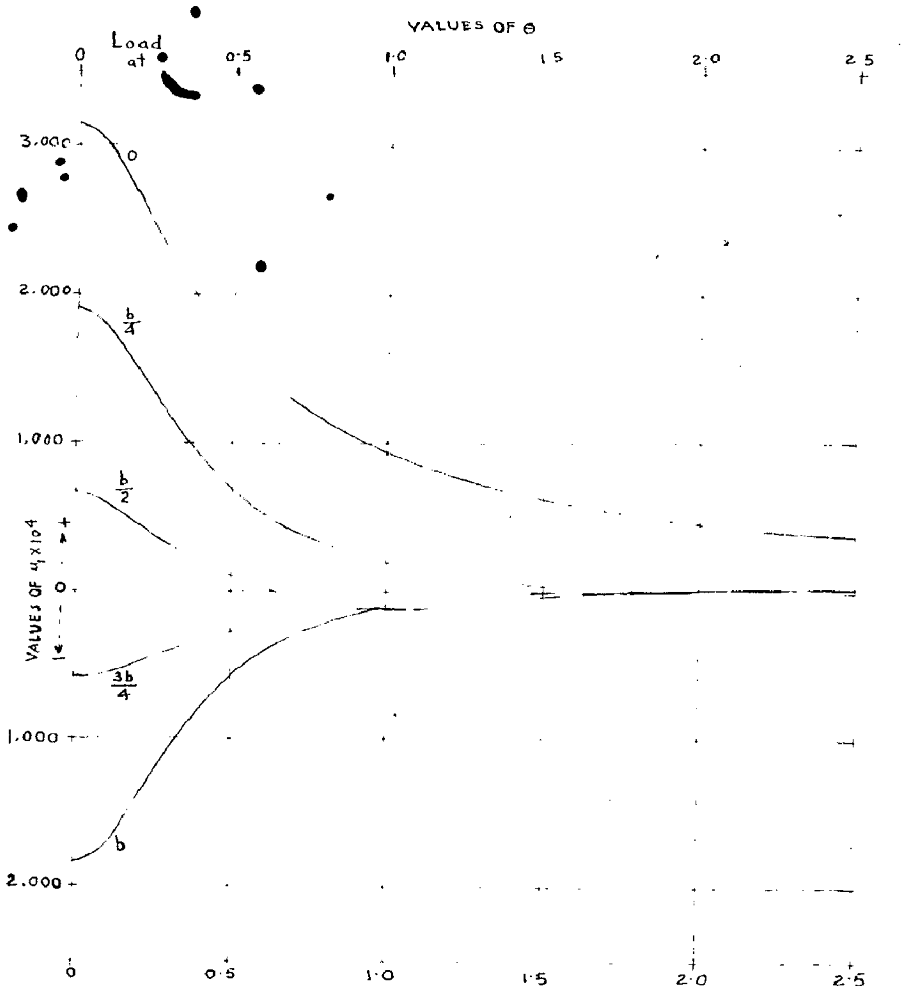

Graph 18: Transverse moment coefficients, μ_1, at reference station 0 for various load eccentricities.

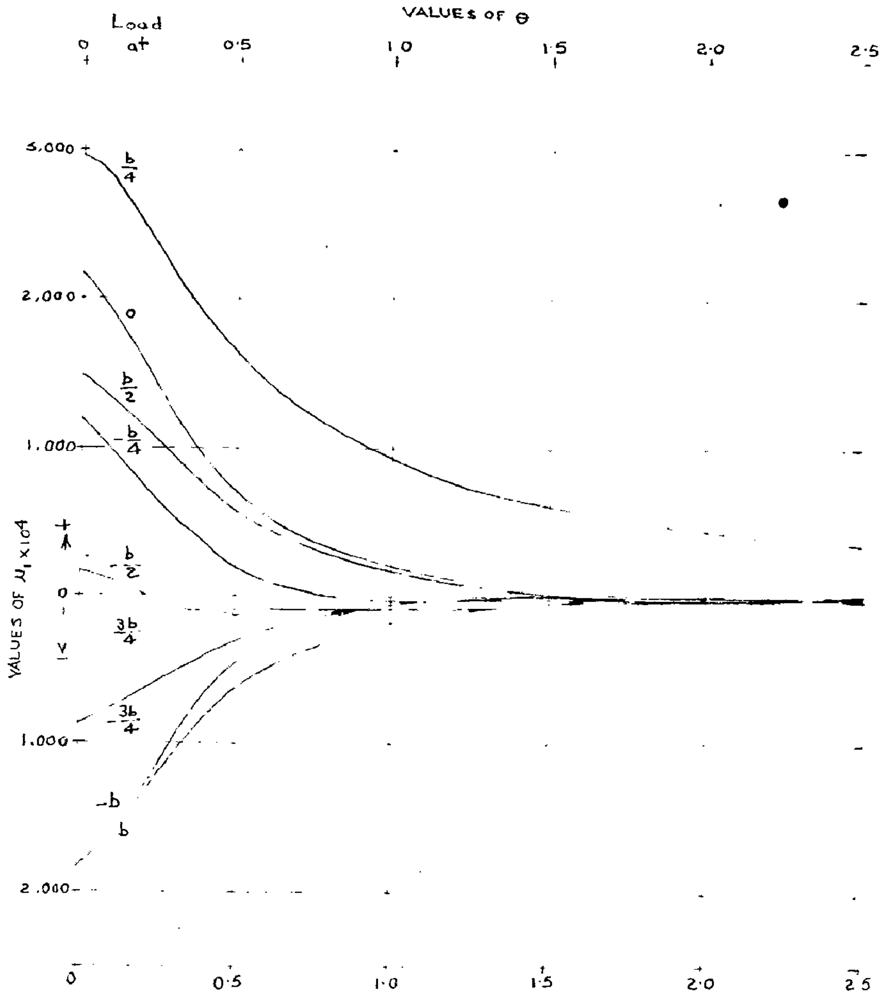

Graph 19: Transverse moment coefficients, μ_1, at reference station $\frac{b}{4}$ for various load eccentricities.

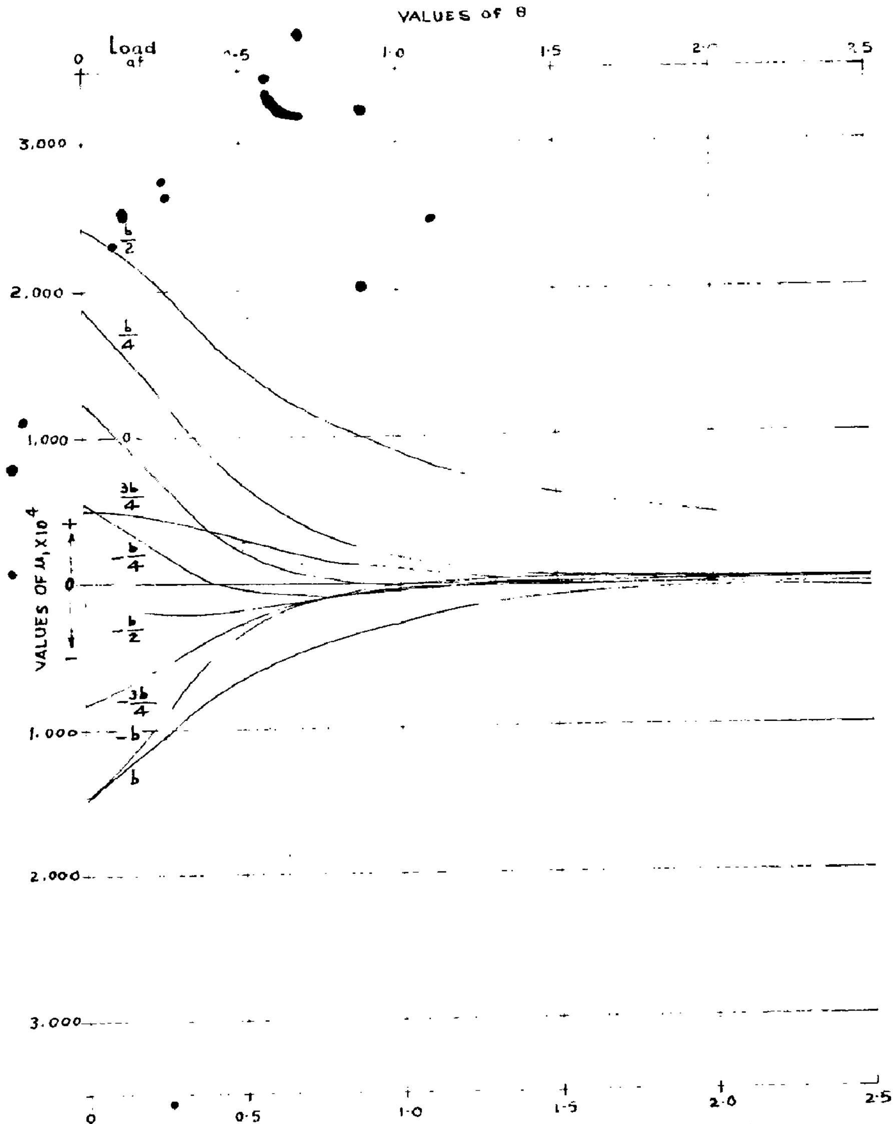

Graph 20: Transverse moment coefficients, μ_1, at reference station $\frac{b}{2}$ for various load eccentr ities.

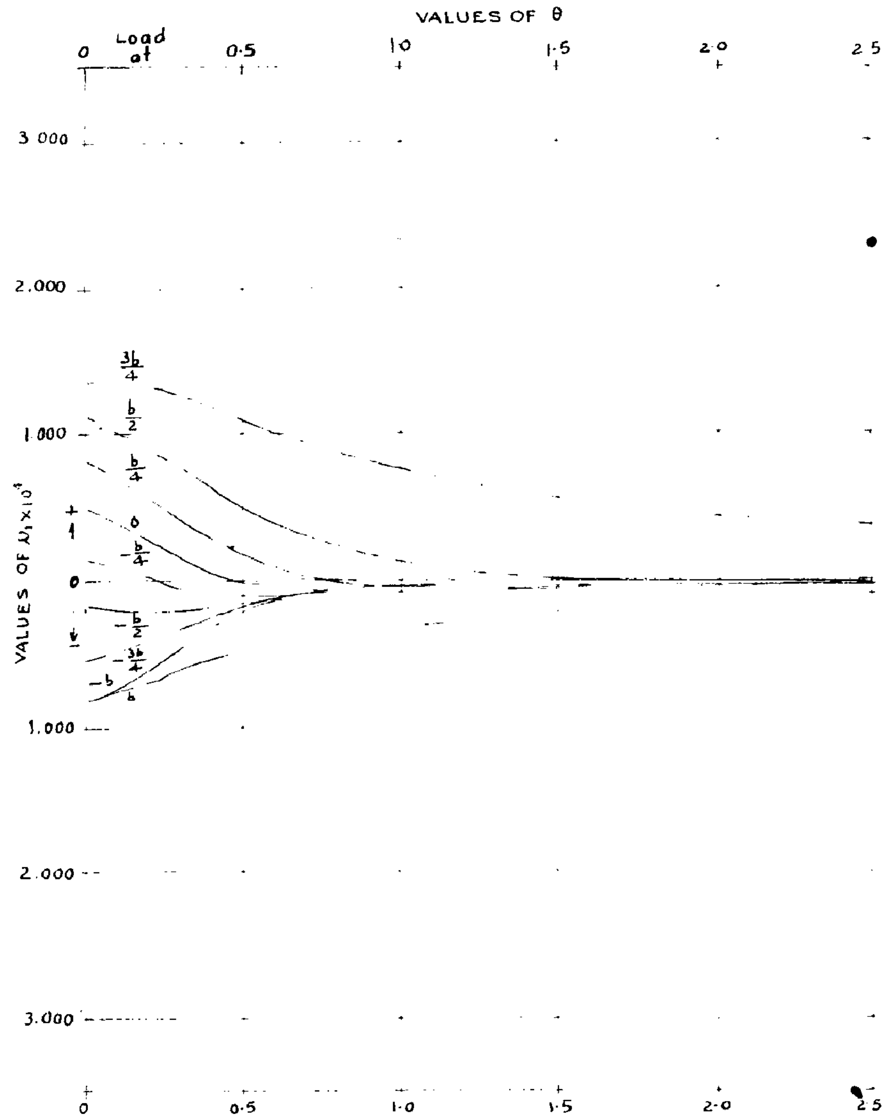

Graph 21: Transverse moment coefficients, μ_1, at reference station $\frac{3b}{4}$ for various load eccentricities.